Characterisation of Dynamics associated with Skeletal Muscle Contraction Initiated by Acetylcholine Injection

Ghabiba Modak

December 2011

Supervisors:

Professor L. Kellaway

Dr N.A. Sachs

Dissertation submitted in partial fulfillment for the degree of Master of Science in Biomedical Engineering

Department of Human Biology

University of Cape Town

The financial assistance of the National Research Foundation (NRF) towards this research is hereby acknowledged. Opinions expressed and conclusions arrived at, are those of the author and are not necessarily to be attributed to the NRF.

Abstract

Lower motor neuron damage often results in flaccid paralysis in which the affected muscles are unable to be stimulated artificially via the supplying nerve. Such damage is common in patients who suffer from spinal cord injury and Multiple Sclerosis. Current practice for artificial recovery of muscle function involves stimulating the muscles directly by means of Functional Electrical Stimulation (FES), which requires 100-1000 times more current than that required for nerve stimulation, thus presenting the risk of pain receptor activation. A potential alternative exists in chemical stimulation by means of administration of the neurotransmitter, Acetylcholine (ACh). This study investigates the potential of this possibility by examining the response of two muscle types to extracellular administration of ACh. Peak forces and times taken to reach peak forces were recorded for gastrocnemii (predominantly fast twitch) and solei (predominantly slow twitch) for 2 ranges of concentrations (low 4μg/ml-550μg/ml and high 1.6g/ml-6.3g/ml). Muscles were denervated for 4 different periods namely 7 days, 14 days, 50-55 days and 204-208 days. Novel application of Empirical Mode Decomposition (EMD), Hilbert Spectral Analysis (HSA) and Marginal Hilbert Spectra (MHS) were applied to stochastic force-time data and allowed for visual depictions of energy-frequency-time distributions. Additional alternate chemical and electrical stimulation was used to determine the effect of ACh in comparison to a known stimulus.

Post-denervation fibre type changes occurred sooner in gastrocnemii than solei. In order of decreasing sensitivity, and taking both slow contractures and contractions into account, muscles were ranked as follows: denervated solei (DS), innervated solei (IS), denervated gastrocnemii (DG) and innervated gastrocnemii (IG). In general, denervated muscles were more sensitive to ACh and produced more measurable responses than their innervated contralaterals, except for short term DG at high concentrations. This was attributed to receptor proliferation. The suggestion of a lower concentration threshold to produce the same response for denervated muscles than their innervated contralaterals is made. Moreover, this observation is first visible in fast twitch muscles, reasoned by preferential phenotypical changes of fast twitch fibres post-denervation. It is further suggested that fibre type changes (as opposed to receptor proliferation) is the governing factor of long term denervated muscles. The largest difference in response between DS and IS was observed at 14 days post-denervation.

Long term DS were found to lose all potential for slow contracture for all tested concentrations of ACh. This was not the case for long term DG. Additionally, fast twitch responses were still visible in long term DG. These observations were attributed to a decrease in sensitivity of long term denervated slow twitch fibres such that they are less sensitive to ACh stimulation than both orginally slow twitch fibres as well as slow twitch fibres which appear post-denervation in originally fast twitch muscles. Results are supportive of a threshold denervation period for slow twitch muscles, beyond which an increase in concentration corresponds to an increase in output force. In addition, times taken to contraction could be grouped according to short and long term denervation periods, where the short term periods (7 and 14 days) and followed the same trends (which were different between solei and gastrocnemii) and a

similar observation was made for long term denervation periods (50-55 days and 204-208 days). Concentration threshold dependencies were observed at different denervation periods such that denervated slow twitch muscles reacted faster than their innervated contralaterals. IG displayed an increase in fast twitch fibre sensitivity, attributed to increased activity necessitated by denervation of the contralateral limb.

DG were slower to reach peak force than IG. The opposite was true for DS. DG contracted sooner than IG at combinations of long term denervation periods (50-55 days and 204-208 days) and low concentrations (4-550μg/ml); as well as short term denervation periods (7 days and 14 days) and high concentrations (1.6-6.3g/ml).

IS produced larger contractions than DS when stimulated chemically if first primed by electrical stimulation. Combined EMD, HSA and MHS analysis revealed high energy outputs from fibre bundles contracting within a wider frequency range for denervated muscles compared to their innervated contralaterals. It was suggested that this be attributed to larger fibre type variation in denervated muscles than innervated muscles. Denervated muscles stimulated with large concentrations of ACh post electrical stimulation, produced a reduced energy output from the contracting fibres and a shift in frequency of contraction. This was probably due to either preferential fibre type saturation and or fatigue of fast twitch fibres. Fast twitch fibre fatigue was further noted by reduced energy output of muscle contraction whilst the frequency of contraction remained unchanged. This was observed in IG subjected to alternate stimulation (ACh-electrical-ACh). Low energy output from muscle fibres contracting at low frequencies when stimulated with high concentrations of ACh post electrical stimulation were considered to be responses from slow twitch fibres thus indicating slow fibre predominance, potential fatigue and block of fast twitch fibre conduction ability.

Based on the results obtained, it was concluded that direct muscle stimulation by ACh in the manner conducted in this study would be less effective than the current use of electrical stimulation.

Recommendations for future studies include the use of larger testing groups to verify statistical significance; *in vivo* testing of the investigated parameters by i.a. ACh administration; set rate stimulation by ACh administration for a finite period (comparable to like FES testing) and conduction of presented experiments for shorter denervation periods with the aim of determining the optimal time period and concentrations required for denervated muscles to behave as close as possible in functionality as innervated muscles. Additionally, application of intra arterial (i.a.) or micro fluidic administration of ACh could potentially benefit from implementation of the broad results documented herein.

Plagiarism declaration

1. I know that plagiarism is wrong. Plagiarism is to use another's work and pretend that it is ones own.

2. I have used the Harvard referencing style for citation and referencing. Each contribution to, and quotation in this dissertation from the work(s) of other people, has been cited and referenced.

3. This dissertation is my own work.

Signature: Date:

Acknowledgements

I would like to extend my heartfelt thanks to each one of the inspirators who have contributed in part to the successful completion of my thesis.

To my supervisors, Professor Lauriston Kellaway and Dr Nicholas Sachs for their valuable advice, precious time, kind encouragement and invaluable guidance.

To Morea Peterson for help with cryosectioning, slide preparation, allowing me the use of her laboratory and for always having a kind word and offering good advice; Gabi De Bie for her help with histological ATPase staining and for taking the time to teach and mentor me through the laboratory process despite her busy schedule; Professor Vivienne Russell for use of her laboratory facilities; Iekraam Fakier for working overtime to fix the laboratory amplifier so that my experiments could remain on track; and to Hiram Arendse and Rodney Lucas for help with post-operative animal care and for their kindness and sound advice.

To Nielen Venter for being a good sport with all those long hours in the lab - early mornings, late nights and long weekends! And to Matthew Proxenos for his kindness and willingness to help out with delivering my administration forms when I was out of the country.

To my best friend, Gameema Salie, for sharing those endless nights with me in "the passage", living off three minute noodles, cremora and Joshua Radin. You turned the worst of times into the best of times.

To Kwame-Boachie Yiadom, for keeping me together when it all felt like it was coming apart, and for encouraging me and believing in me.

To Cynthia Cheung for being so supportive and kind, for looking out for me, not only as my dive buddy, but as my friend; and to Faatiema Salie, Gadija Ebrahim, Laura Rowe and Maria Carvounes for being great friends.

To my parents, Saleem and Soraya Modak and my sister Safia Modak, for being so supportive and caring, for coming in to campus on weekends to help me when I needed an extra set of hands and for believing in me and always guiding me to be the best that I can be. You taught me to live, love and learn by example, always encouraging me to seek knowledge and understanding. You were my cheerleaders, my defenders and my motivators. Thank you for being there through it all.

And finally, to Reyan Mikail Weston, for being the most incredible and supportive partner and the best of friends. Thank you for your inspiring talks when I felt like I was losing ground, for your witty sense of humour that kept me laughing through the final stretch, for the coding "competitions" and for teaching and helping me document my large amount of data. You taught me the value of stepping back and learning to crawl, and motivated me to see things from different perspectives. Thank you for being my voice of reason and, most of all, for being my home away from home.

Contents

List of Figures

List of Tables

Glossary of Terms

Term	Definition
a posteriori	Derived from empirical observation.
cholinergic	Denoting nerve endings, that when stimulated, release acetylcholine as a neurotransmitter, such as those of the parasympathetic system.
	Releasing or activated by acetylcholine or a related compound.
concentration lag	Initiation at a higher concentration of a pattern or trend similar to that of a different muscle.
contracture	A reversible and prolonged contraction, not characterised by short bursts of propagated contractile activity along the muscle fibre.
endoplasmic reticulum	A network of membranous tubules within the cytoplasm of a cell, responsible for the production of the protein and lipid components of most of the cell's organelles.
exocytosis	The process of cellular secretion in which the secretory products are contained within a membrane-enclosed vesicle. The vesicle fuses with the cell membrane so that the lumen of the vesicle is open to the extracellular environment
fibrillation	Fine, rapid twitching of individual muscle fibers with little or no movement of the muscle as a whole.
frequency modulation	Modulation in which the instantaneous frequency of a sine wave carrier is caused to depart from the center frequency by an amount proportional to the instantaneous value of the modulating signal.
Gibbs phenomenon	The Gibbs phenomenon is an overshoot (or "ringing") of Fourier series and other eigenfunction series occurring at simple discontinuities.
isometric contraction	Muscular contraction during which muscle fibre length remains unchanged.
ligand	A smaller molecule that binds chemically to a larger molecule, which is usually a protein. Neurotransmitters can be the ligands for specific membrane proteins (ACh is thus considered a ligand).
lower motor neuron	A motor neuron that has its cell body in the grey matter of the spinal cord and that contributes axons to peripheral nerves. This neuron innervates muscles and glands.

Term	Definition
motor neuron	An efferent neuron that conducts muscle action potentials away from the central nervous system to effector organs (muscles and glands). It forms the ventral root of spinal nerves.
motor unit	A lower motor neuron and all the skeletal muscle fibres stimulated by branches of its axon. Larger motor units (more muscle fibres per axon) produce more force when the unit is activated, but smaller motor units afford a finer degree of neural control over muscle contraction. A set of muscle fibres innervated by a motor neuron.
physostigmine	A compound used for its anti-cholinergic activity.
sensitivity	Skeletal muscle sensitivity to Acetylcholine. No attempt is made at quantifying the this term, but it is rather used as a comparative measure of the muscle's reaction to ACh. For instance, if one of two muscles tested at the same concentration were to produce a larger contractile output than the other, it would considered more sensitive than the other to ACh in terms of contractility. If one were to contract sooner than the other, it would be considered more sensitive to ACh in its' time to contraction response than the other.
somatic motor neuron	A motor neuron in the spinal cord that innervates skeletal muscles. Somatic motor neurons may be categorized as alpha and gamma motoneurons. Alpha motoneurons stimulate extrafusal skeletal muscle fibers and gamma motoneurons stimulate intrafusal fibers within the muscle spindle.
tetanus	Denotes a smooth, sustained contraction of a muscle (as opposed to muscle twitching), caused by rapidly repeated stimuli.
upper motor neuron	Cell bodies of interneurons located in the precentral gyrus of the frontal lobe of the brain (involved in motor control). Upper motor neurons play a role in muscle regulation.

Nomenclature

ACh Acetylcholine

AChCl Acetylcholine Chloride

AChE Acetylcholinesterase

ADP Adenosine diphosphate

AEC Animal ethics committee

ATP Adenosine triphosphate

ATPase Adenosine triphosphatase

CNS Central Nervous System

CSA Cross sectional area

D Constant of diffusion

DG Deneravated Gastrocnemius/Gastrocnemii

DS Denervated Soleus/Solei

EC Excitation contraction

EMD Empirical mode decomposition

EPSP Excitatory post-synaptic potential

F-t Force-time

FA Fourier analysis

FES Functional electrical stimulation

FSA Fourier spectral analysis

FT Fourier transform

HHT Hilbert-Huang transform

HS Hilbert spectrum

HT Hilbert transform

i.a. intra arterial(ly)

IG Innervated Gastrocnemius/Gastrocnemii

IMFs Intrinsic mode functions

IS Innervated Soleus/Solei

LG Lateral gastrocnemius

LMN Lower motor neuron

MG Medial gastrocnemius

MS Multiple sclerosis

nAChr nicotinic Acetylcholine receptor

NCAM Neural cell adhesion molecule

NMJ Neuromuscular junction

Q Dose (of ACh administered)

SCh Succinylcholine

SCI Spinal Cord Injury

SD Standard deviation

SR Sarcoplasmic reticulum

STFT Short time fourier transform

T Rise time

UMN Upper motor neuron

VAChT Vesicular Acetylcholine transporter

WA Wavelet analysis

1 Introduction

Nervous system damage may result from spinal cord injury (SCI), stroke or neurological disorders (such as multiple sclerosis (MS)) which may all have severe impacts on muscle tone and contraction. In 2007, the number of Americans living with SCI was 255,702 on average; with a further 12,000 incidences occurring per year. Less than 1% of patients experience full neurological recovery at the time of hospital discharge. 2,500,000 people worldwide suffer from MS. MS is an autoimmune disease in which myelin sheaths degenerate, causing an adverse effect on central nervous system (CNS) functionality; particularly by interruption of nerve signals and impulses. If areas of the brain or CNS which control movement are affected, this may result in movement impairment or complete loss of movement. The worldwide estimated stroke prevalence in 2006 was 6,400,000. Depending on the area and extent of brain injury and the type of stroke, motor activity may be affected. Motor neuron damage may be classified into two primary groups, depending on the region of damage. Upper motor neuron (UMN) lesions constitute damage to neurons from the frontal cortex or their tracts. UMN lesions are characterised by spastic paralysis. Lower motor neuron (LMN) lesions constitute damage to neurons or fibres of the ventral horn. This often results in flaccid paralysis in which the affected neurons are unable to relay signals to the muscle fibres to initiate contraction.

Paralysis occurs due to an interruption in the conduction pathways from the brain to the muscle fibres. It is possible for the connection between the brain and motor neurons to be severed whilst still maintaining the functional viability of the motor neurons. In such cases, the motor neurons themselves are undamaged and it is possible to stimulate them electrically to cause muscular contraction. Functional electrical stimulation (FES) has been used as a means of reestablishing basic functionality by stimulating elementary motion, for example in patients suffering from dropped foot due to MS or stroke [Taylor, 2002, Burridge et al., 1997].

FES does not prevent degeneration of nerve tracts and may thus prove ineffective when complete degeneration occurs (which would constitute peripheral nerve damage). Peripheral nerve damage (as may occur in the case of LMN lesions) presents a more complicated case. In this instance, the motor neuron is no longer viable and can thus not be stimulated electrically. It is however possible to elicit contractions by stimulating the denervated muscle directly, although this has proven to be more challenging due to the functional anatomy of muscle fibre innervation. Each motor neuron has many axonal branches, one or more of which innervate a muscle fibre [Feindel et al., 1952, Hunt and Kuffler, 1954]. Stimulation of an undamaged motor neuron to cause the contraction of the associated muscle fibres thus requires 100 to 1000 times less current [Sheffler and Chae, 2007] than that required for direct denervated muscle stimulation [Eken and Gundersen, 1988] due to the volumetric difference in stimulation sites. The higher stimulating current requirement for individual muscle fibre stimulation creates the potential risk of stimulating surrounding pain receptors whose conduction pathways may still be in tact [Merton et al., 1982, Benedetti et al., 1998]. A further

limitation of FES includes the inability to treat multiple muscles simultaneously due to restrictions on the maximum stimulation current [Kern et al., 2002].

Physiologically, undamaged motor neurons communicate with muscle fibres at the neuromuscular junction (NMJ) by means of a neurotransmitter, Acetylcholine (ACh). The post junctional membranes on the surface of the muscle fibres contain a number of specific receptors. Nicotinic acetylcholine receptors (nAChR's) in skeletal muscle fibres bind to release ACh molecules, allowing for sodium/potassium channels to open and for depolarisation, and hence contraction, to occur. An alternative means to electrical stimulation thus exists in the use of ACh as a chemical stimulant. Hypersensitivity to ACh in chronically denervated skeletal muscle fibres has been reported [Axelsson and Thesleff, 1959]. Chronically denervated frog skeletal muscles and cat gastrocnemius were found to be 100 and 1000 times more excitable respectively when compared to their innervated counterparts. Theoretically, it may then be possible to artificially administer ACh to denervated muscle fibre membranes in an effort to stimulate muscular contraction. In order to substantiate the viability of such an application, it is necessary to determine the dynamic response of denervated skeletal muscle fibres to controlled amounts of artificially administered ACh. This could effectively rule out the possibility of pain receptor stimulation and offer an alternative to electrical stimulation in cases of LMN damage. Applications would include incorporation of ACh administration into neural prostheses (for example, stimulation of the blink reflex by micro-fluidic application of ACh in patients with facial paralysis).

1.1 Objectives of Study

To the best of my knowledge, no in-depth investigation has been reported in literature on the effects of denervation periods on the contractile response of mammalian skeletal muscle to ACh. Hence, the objectives of this study are three-fold. The primary objective is to investigate denervated muscle contraction dynamics induced by *in vitro* extracellular ACh administration. This involves determining times to peak force of contraction and maximum force of contraction on denervated skeletal muscles for varying concentrations of ACh. Innervated muscles will be used as a control. A further objective is to determine the effects of varying concentrations of ACh on two different muscle types (fast and slow twitch). The influence of the difference in muscle denervation periods will be investigated by examining three different time periods of denervation (short term, medium term and long term denervation groups). In addition, further signal analysis methods will be applied to the stochastic signals obtained from the raw experimental data.

2 Review of Relevant Literature

A literature search of the biomedical and engineering aspects of muscle denervation and experimentation was conducted and the relevant information is presented in section 2. Section 2.1 provides an overview of the physiology of both innervated and denervated skeletal muscle and section 2.2 comprises the engineering applications to the physiological theory.

2.1 Biomedical aspects

Extensive research has been conducted in the field of muscle contraction and stimulation of denervated muscles mainly due to the simplicity of the denervation model; the need to understand the mechanisms governing muscular disorders and to further rehabilitation schemes for patients suffering from paralysis. Denervation models allow for analysis of the nervous system control of peripheral tissues [Midrio, 2006]. Skeletal muscle morphology is identical in vertebrates, thus allowing for animal models to be used to investigate muscle contraction dynamics and the potential factors which influence them. A thorough understanding of muscle fibre physiology is also necessary, considering their altered state in the face of denervation.

2.1.1 Excitation contraction coupling

The purpose of skeletal muscle is to generate sufficient force to enable controlled movement of associated extremities. In order to do so, the muscle fibres are required to receive signals from the pre-central gyrus and cerebellum via motor neurons directed by the CNS.

Motor units comprise a number of muscle fibres which are innervated by a motor neuron. A cell body (soma), an axon and dendrites constitute a motor neuron. Motor neurons may have many dendrites but only one axon which in turn may branch into many axon terminals. Axon terminals synapse with either the dendrites of an adjacent motor neuron or with the motor end plates of muscle fibres. The process of neural stimulation and consequent muscle contraction is termed excitation contraction (EC) coupling. Each muscle fibre is innervated by its own motor neuron axon. An electrical impulse is conducted from the axon to the neuromuscular junction, of which only one exists on each muscle fibre. The NMJ (whose size has been demonstrated to be directly proportional to muscle diameter [Gauthier and Dunn, 1973]), is the connection zone between the axon terminus (or terminal bouton) and the sarcolemma. These are depicted in Figure 1.

The post-synaptic junction of the membrane is termed the motor endplate. Cell adhesion molecules are proteins found in pre- and post-synaptic plasma membranes. They project from both membranes into the synaptic cleft to bond to one another hence ensuring that the pre- and post-synaptic membranes remain close enough to allow for rapid transmission of neurotransmitters

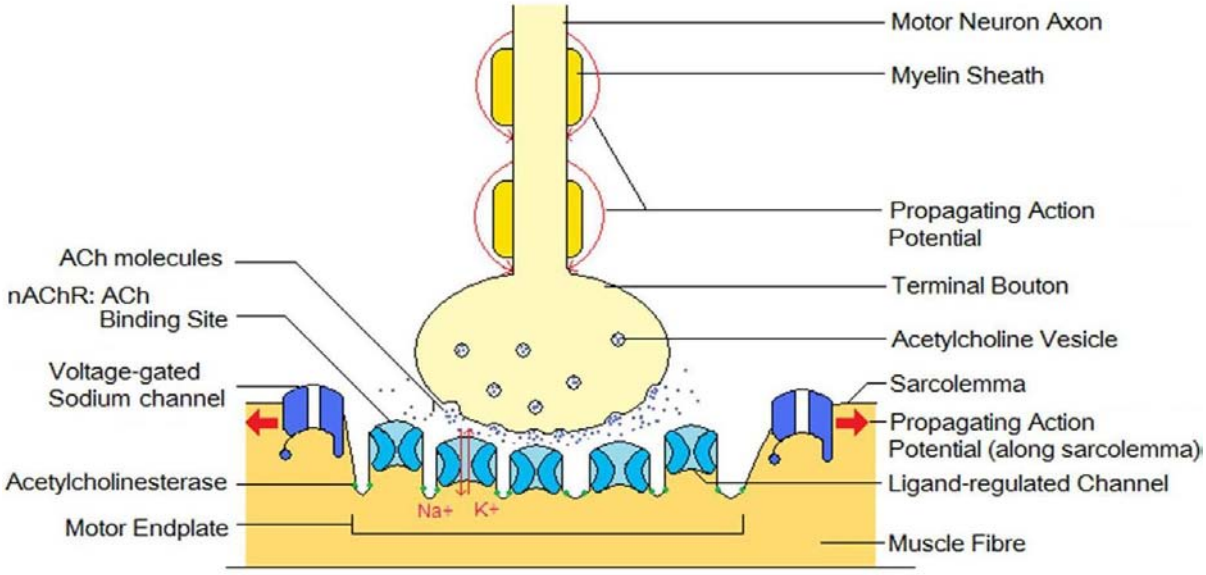

Figure 1: Depiction of neuromuscular junction and propagation of action potential

to occur across the synaptic cleft.

Neurotransmitters are chemicals which initiate action potentials in post-synaptic cells. Loewi [1921] was the first to establish proof of neurotransmitter existence and action [Katz, 1966] in his experiments conducted on cardiac muscle of the frog. In his experiments, the cardiac branch of the vagus nerve was stimulated and a substance, initially termed "Vagustoff" by Loewi, was shown to inhibit the contractile ability of cardiac muscle. This substance was later identified as ACh. Dale et al. [1936] showed that stimulation of motor nerves innervating skeletal muscle in vertebrates results in the release of ACh.

The arrival of an electrical impulse at the terminal bouton stimulates the opening of the calcium channels thus enabling calcium ions in the synaptic cleft to diffuse into the axon terminal. This increase in calcium ions activates regulatory proteins such as calmodulin. These regulatory proteins activate protein kinase (an enzyme) which further phosphorylates other regulatory proteins. Docked vesicles containing ACh are found on the pre-synaptic cleft. The eventual effect of the activation chain of events is to encourage the existing synaptic vesicles in the presynaptic axon terminal to fuse with the plasma membrane of the axon which hence allows for exocytosis to occur by formation of a pore for the release of neurotransmitters such as ACh.

ACh is synthesized by choline acetyltransferase whereupon it is transported into synaptic vesicles by means of vesicular ACh transporter (VAChT) for storage. The membrane of the synaptic vesicle contains an ATP-powered protein pump which acidifies the lumen of the synaptic vesicle causing a

pH gradient to exist between the lumen and the cytoplasm. The VAChT exchanges ACh molecules for protons from the synaptic vesicles. The number of vesicles and frequency of action potentials determine the amount of neurotransmitter which is released into the synaptic cleft. After exocytosis occurs, the vesicles are taken back up into the pre-synaptic axon terminal to be reused for the same purpose. This entire process, from the diffusion of Ca^{2+} into the pre-synaptic cell, to exocytosis, takes less than 100µs.

The released ACh diffuses across the synaptic cleft and binds to the nAChR's on the sarcolemma of the muscle fibre resulting in sodium/potassium channel opening. There are two types of channel regulation, namely chemical or ligand regulated channels and voltage regulated channels. Neurotransmitters are ligands which bind to receptor proteins on the post-synaptic membrane and hence activate ligand regulated channels. Ligand regulated channels are primarily present in post-synaptic membranes, whereas voltage regulated channels may be found in axons. ACh may be used as an excitatory or inhibitory neurotransmitter depending on the type of innervation (somatic or autonomic) and the end stimulus (muscles, organs or glands). Since, this study focuses on the use of ACh at the NMJ, it is important to understand the receptor properties. There are two types of cholinergic receptors (receptors which receive ACh) namely nAChR's and muscarinic ACh receptors. nAChR's are found in the brain and in skeletal muscle fibres whereas muscarinic ACh receptors are found in smooth and cardiac muscles and glands. Only nAChR's are relevant to this study which pertains to paralysed skeletal muscle stimulation.

nAChR's are pentameric molecules and in innervated muscle fibres are found mainly in the vicinity of the NMJ. Two of their extracellular binding sites allow for the attachment of one ACh molecule each. Once two molecules of ACh are bound to the nAChR sites, a channel in the receptor protein is opened thus allowing for Na^+ to flow into the cell and K^+ to flow out of the cell simultaneously and through the same channel. The Na^+ flows into the cell along a steeper electrochemical gradient than the K^+ leaving the cell, causing depolarisation or an excitatory post-synaptic potential (EPSP). The polarity of the membrane remains the same when an EPSP is created , due to the outward flow of potassium (this is not the case with action potentials, which are associated with voltage regulated channels in which the potassium gates only open once the sodium gates have closed). Figure 1 depicts the nAChR's and the ligand regulated channels opened by ACh molecule binding.

This binding process causes the ligand gated ion channels to open and allows Na^+ ions to enter the cell resulting in depolarisation. Upon reaching the threshold value, voltage gated ion channels open and depolarisation occurs whereupon a new action potential impulse is produced to propagate along the sarcolemma. The sarcolemma is then repolarised when the K^+ ion channels open (subsequent to the closing of the Na^+ ions channels) and the K^+ ions leave the cell. Hyperpolarisation occurs when more potassium ions leave the cell than is necessary resulting in a relative refractory period. The resulting ion distribution is eventually restored by means of the Na^+/K^+ pump.

Table 1: Muscle units and their respective sheaths

Muscle Units	Sheaths
Whole muscle	Epimysium
Muscle fascicle	Perimysium
Individual muscle fibre	Endomysium

The impulse encounters invaginations of the sarcolemma known as T-tubules which are located at each Z-disk. This prompts the release of Ca^{2+} ions from the terminal cisterns of the sarcoplasmic reticulum (SR) where it is stored. The Ca^{2+} ions are released into the sarcoplasm surrounding the myofilaments and bind to the Troponin C molecules on the thin myofilaments. This causes a rearrangement of the Troponin (C, I and T) molecules on the thick myofilaments such that the binding site on the actin globule is uncovered to enable cross-bridge attachment.

Energy required for movement of the cross-bridge myosin head is released from the breakdown of adenosine triphosphate (ATP) into adenosine diphosphate (ADP) and a phosphate ion (P).

The movement of the myosin head results in movement of the actin filament since they are attached at the actin globule cross-bridge attachment site. The myosin head then detaches as a new ATP molecule attaches to it. The ATP molecule undergoes hydrolysis again and the myosin head returns to an upright position in anticipation of further stimuli. Once the stimulation halts, Ca^{2+} ions are returned for storage to the SR by means of active transport. The troponin molecules rearrange to their resting position such that Troponin-I covers the cross-bridge attachment site thus preventing myosin head attachment and contraction. Cross-bridge cycling hence translates to muscle force generation. The muscle is relaxed when Acetylcholinesterase (AChE) breaks down the excess ACh at the NMJ to allow for the receptors to respond to another stimulus.

The sequence of events in the EC process is rapid prior to muscle fibre contraction. Contraction lags behind the initial stages of the EC process. Due to this lag, continuous stimulation will result in contraction with increased force by a process of summation. Successive stimuli at high frequencies thus result in stronger contractions since initial stimuli overcome intrinsic resistance from parallel structures (such as tendons) Lieber [1992].

2.1.2 Skeletal muscle morphology and physiology

Skeletal muscle itself is composed of a number of subunits. Each subunit is covered with fascia and sheaths of connective tissue. Table 1 describes the subunits of skeletal muscle composition and their respective sheaths. Figure 2 depicts the units of which skeletal muscles are comprised.

Whole skeletal muscles are composed of muscle fascicles which are in turn composed of muscle fibres. The muscle fibres can be further broken down into myofibrils, sarcomeres and myofilaments

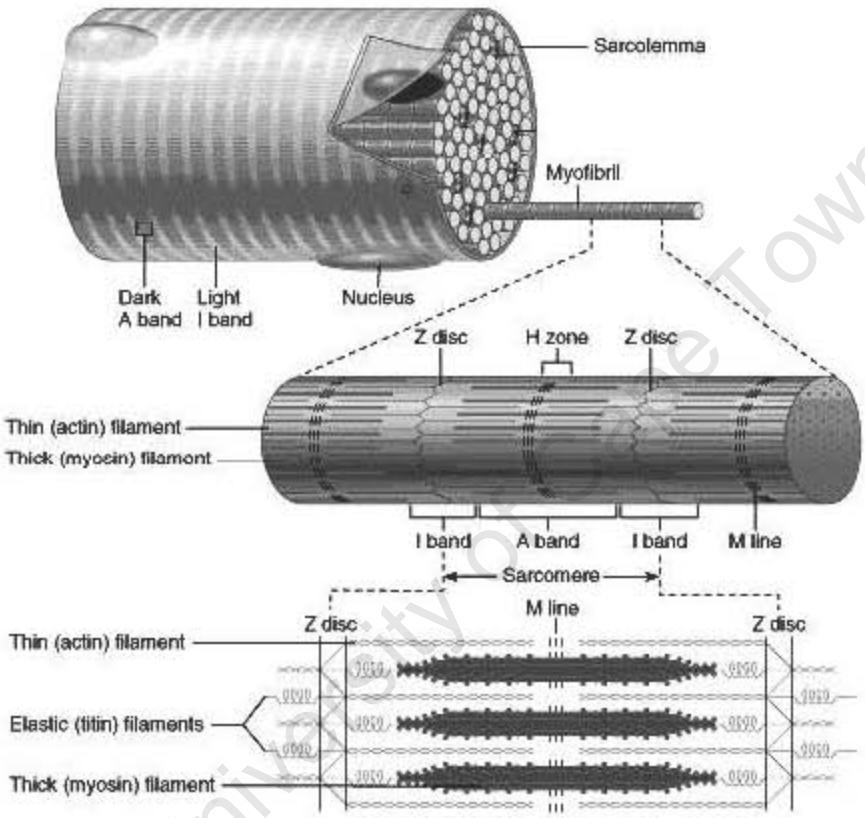

Figure 2: Subunits of skeletal muscle (*Copyright © 2001 Benjamin Cummings, an imprint of Addison Wesley Longman, Inc.*)

(in respective order of decreasing sized subunits). Skeletal muscle is most easily identified microscopically by striations visible due to the arrangement of the myofibrils. The sarcomeres form the basic contractile units of muscles [Fulton and Isaacs, 1991]. Sarcomeres are composed of thin actin and thick myosin protein molecules grouped in bands and framed by Z-lines. Isotropic bands (I-bands) are formed by the actin filaments which are positioned on either side of the Z-lines.

The thick myofilaments are composed of a globular head (composing heavy meromyosin) and a thin tail (composing light meromyosin). The globular heads are found on the ends of the sarcomere. The purpose of the globular head is two fold. Firstly, it acts as a binding site for actin. Secondly, it acts as an enzyme site for catalysis of ATP hydrolysis. This is necessary for the energy release required for muscle contraction. Cross bridges are formed by the globular heads when actin filaments connect to their binding sites and are pulled towards the sarcomere centre. The cross bridges are positioned spirally at 60^{o} from one another, whilst remaining at 14-15nm apart (axial translation) [Shimizu et al., 1985]. Each thick filament has 6 thin surrounding myofilaments. The thin filaments are comprised of actin globules, tropomyosin and troponin. The actin globules are 5nm in diameter and are linked in series. Each thin filament consists of two spiralled actin chains. Tropomyosin, a long protein molecule, is found on the spiral formed grooves of the actin chains. Troponin is found along the actin spirals at 38.5nm apart. There are three types of troponin namely Troponin C, Troponin T and Troponin I. Troponin C acts as a site for Ca^{2+} binding, Troponin T contains tropomyosin and Troponin I inhibits cross-bridge attachment when Ca^{2+} is not present.

Actin and myosin are involved in contraction and are hence termed contractile proteins, whereas tropomyosin and troponin regulate force production by controlling cross-bridge attachment and are hence termed regulatory proteins. Another protein essential to the functioning of skeletal muscle is Titin. Titin is present in myofibrils and is believed to maintain the position of the thick myosin filament in the centre of the sarcomere between the Z-lines. This is necessary during long durations of contraction and unequal force application to the thick filament [Wang et al., 1979, Kellermayer et al., 1997].

Skeletal muscles are comprised of either slow or fast twitch fibres, or a combination of both, which dictates the force velocity relationship of the muscles. Slow twitch fibres (also termed Type I muscle fibres) have an extensive blood supply due to their use of aerobic respiration. These fibres are red in colour and contract with low forces for long durations. Fast twitch fibres (or Type II muscle fibres) on the other hand are considered white fibres and use anaerobic respiration or oxidative metabolism (subtype dependent) to contract with greater forces for shorter periods and are known to fatigue rapidly. The amount of force produced per contraction is the same for both slow and fast twitch fibres. The distinction thus lies in the greater speed with which the fast twitch fibres are able to fire [Fox, 2003]. Figure 9 shows an adenosine triphosphatase (ATPase) stain for innervated fast and slow twitch skeletal muscle fibres.

Skeletal muscle contraction mechanics differ between muscle types. Contraction periods are

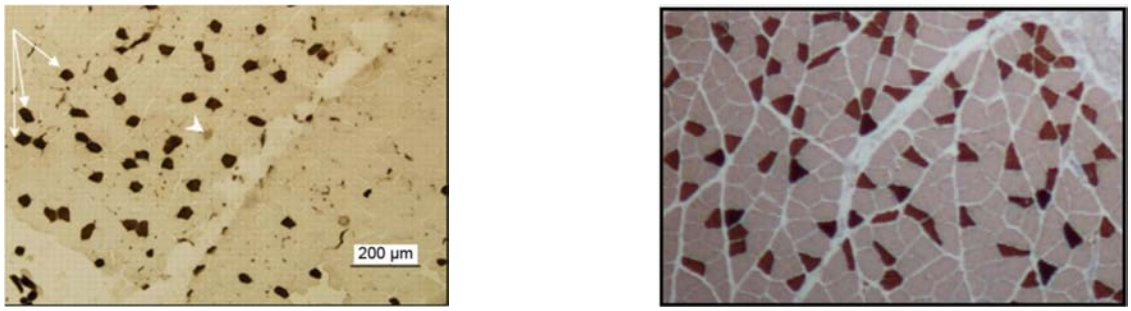

(a) Gastrocnemius (b) Soleus

Figure 3: Histological ATPase stains for (a) fast twitch fibres in rat gastrocnemii (arrowheads Type IIc) [Burnes et al., 2008] and (b) Type II fibres (stained dark) in rat solei [Bye et al., 2008]

specific to muscle functionality, for instance rapid contraction of the gastrocnemius is necessary for fast motion such as running; whereas the primary function of the soleus is to maintain balance against gravitational effects by means of slow contraction [Shier et al., 1996].

Muscle contraction dynamics are dependent upon a number of factors which determine the time constants of the system by means of neurotendinous sensory organ feedback. These factors include fibre composition, length (sensed by type II secondary spindle endings), shortening velocity and tension history (sensed by type Ib golgi tendon organs). Type Ia primary spindle endings sense length and strain rate.

Rats have three major plantar flexors, namely soleus, gastrocnemius and plantaris. The soleus and gastrocnemius will be used in this study. The soleus muscle is a monoarticular ankle extensor mainly comprised (80%) of slow twitch fibres, whereas the gastrocnemius is a biarticular ankle extensor mainly comprised of fast twitch fibres (percentage differs depending on the region of the muscle) [Lieber, 1992]. Albuquerque and Thesleff [1968] conducted a comparative investigation into the membrane properties of fast and slow skeletal muscles of the rat when both innervated and chronically denervated. It was found that in innervated muscle fibres, the electrophysiological properties did not differ significantly. When considering ACh sensitivity however, a difference between the fast and slow twitch muscles (of the extensor and soleus muscles respectively) was apparent. In the innervated extensor site, the ACh sensitivity site was found to be confined to the endplate whereas in the innervated soleus muscle, ACh sensitivity regions were found to exist at the endplate as well as along the muscle fibre in close proximity to the tendon.

Prodanov et al. [2005] mapped the spatial distribution of the motor endplates of the gastrocnemius muscle of the rat. The maps were created from series of cross sections stained for AChE activity. The lateral and medial gastrocnemii were considered as separate entities. The motor endplates of the lateral gastrocnemius (LG) were arranged longitudinally in the middle of the muscle

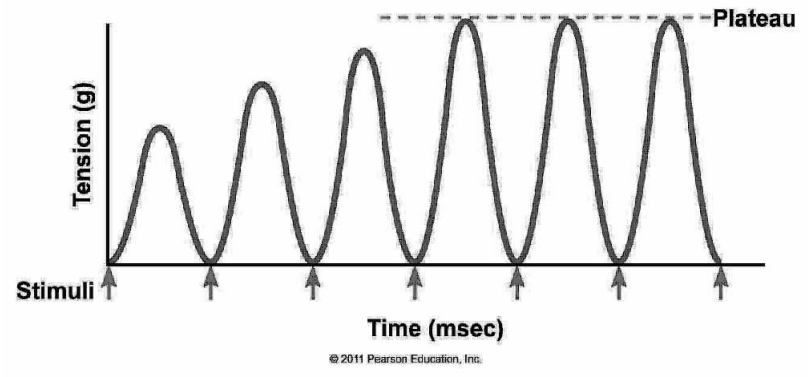

Figure 4: Effect of motor unit summation on degree of contraction. Arrows are indicative of stimuli.

in 3 columnar regions. The motor endplates of the medial gastrocnemius (MG) were found to be distributed in a pattern resembling a leaf, with its main constituents in the distal third of the muscle. Such information is useful in determining the region of injection or application of neurotransmitter substances. Both the MG and the LG are supplied by four different branches (each) of the sciatic nerve, each controlling a section of the muscle independently. Prodanov et al. [2005] further observed that for the LG, only the lateral portion contained motor endplates on the surface of the muscle. They noted that the MG displayed a larger deviation in data. The LG was used in this study.

2.1.3 Characteristic behaviour of skeletal muscle

Motor unit sizes vary depending on the level of control and force. Small motor units are associated with thin (and hence easily excitable) axons, few muscle fibres and fine muscle control whereas larger motor units innervate more muscle fibres and are associated with thick (and hence less excitable) axons and large forces. Stimulation of a motor unit results in the contraction of all the fibres associated with the respective motor unit.

Force summation occurs by means of motor unit summation and wave summation. Motor unit summation involves the recruitment of motor units such that an increase in the number of recruited motor units corresponds to an increase in the degree of contraction. Figure 4 displays this trend.

Wave summation occurs with an increase in stimulation frequency. The motor units are stimulated continuously without being given a chance to completely relax. Some of the Ca^{2+} ions remain in the sarcoplasm, resulting in a larger number of cross bridge formations. Stimulation whilst still in a state of contraction thus results in force summation, marked as section '2' in Figure 5.

In the case where motor units are continuously stimulated at high frequency (with no chance for contractile activity to subside), tetanic contraction occurs in which a constant force is maintained,

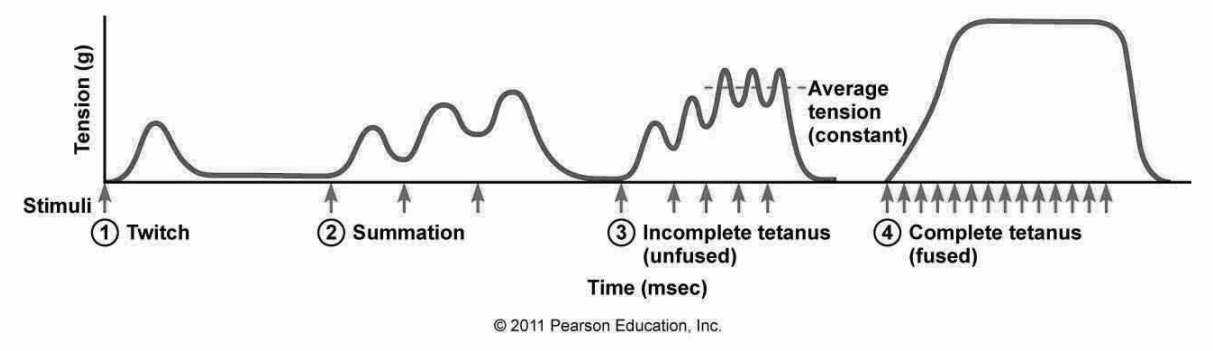

Figure 5: Display of force summation and resulting unfused and fused tetanus.

indicated by the marker '3' in Figure 5. When the release rate ofCa^{2+}ions exceeds the rate of uptake, fused tetanus results, as shown at marker '4' in Figure 5. The smooth constant force is indicative of tetanic contraction. The maximum contractile force eventually begins to decrease over time as the muscle fatigues.

2.1.4 Muscle denervation

Denervated muscles provide good models for investigations of muscle dynamics under varying conditions. They have been used as the focus of studies exploring methods of exercising and or reinnervating denervated fibres [Gutmann and Guttmann, 1944, Gardiner et al., 1984, Kern et al., 1999].

Upon severing of a motor nerve, Wallerian degeneration occurs. This process is characterised by predominantly distal axonal degeneration, although a portion of the proximal end of the axon also degenerates. Additionally, Schwann cells concerned with the distal portion of the axon lose their differentiating properties and rapidly increase, destroying the remaining axon and myelin segments by phagocytosis. Further physiological changes to the cell body also occur (for more detailed descriptions please consult Nicholls [2001]).

Subsequent to severing of a motor nerve, denervated skeletal muscle fibres pass through a number of characteristic physiological changes including the occurrence of fibrillations [Brown, 1937, Langley and Kato, 1915], increased sensitivity to various chemical stimulants and muscle atrophy. Fibrillations occur 2 to 5 days post-denervation in rabbits [Langley and Kato, 1915] and rats (compared to 1 week + in humans) and are marked by allochronic and involuntary contractions which are not due to ACh stimulation but rather caused from direct muscle membrane activity. They do however, initiate from the original endplate region.

Changes in denervated muscle membrane sensitivity can be explained by changes which occur in receptor topography post-denervation. The topography of nAChR's on skeletal muscle fibres differs

in pre- and post-developed muscles and in innervated and denervated muscle fibres [Watson et al., 1976]. Before muscle fibres become innervated, nAChR's may be found spread out along the muscle fibres. A reduction in extrajunctional nAChR's occurs in developed adult skeletal muscle and may be attributed to nAChR gene expression [Chahine and Goldman, 1992]. The nAChR's are found clustered at the NMJ's in fully developed and innervated muscle fibres (15000-20000 nAChR's/μm^2 [Levitt-Gilmour and Salpeter, 1986]) and few extrajunctional nAChR's are present [Miledi, 1960b]. It has been shown that in sites of low sensitivity, the time course of ACh potentials is slower [Katz and Miledi, 1964b]. This was attributed to low nAChR site density in insensitive regions thus involving a larger area of stimulation. Potential change is affected by receptor topography and density. An increase in stimulative means results in the saturation of the closest receptors with later activation of remote receptors due to increased diffusion time.

Receptor gradients from endplate to non endplate regions in adult skeletal muscle occur at a steeper gradient than newly innervated skeletal muscle. In their study on receptor site distribution in innervated muscles (sartorius of the *Rana temporaria* and *Rana esculenta*, rectus abdominus of the *Rana temporaria* and diaphragm and rectus abdominus of the rat), Katz and Miledi [1964b] measured the amplitude of depolarisation as an indicative parameter due to its ease of measurement and the accuracy with which it could be done. They reported low extrajunctional sensitivity of the innervated skeletal muscle fibres and ensured the validity of their results by implementing measures such as muscle cleaning and varying pipette pressure on the muscle. This eliminated any potential barrier effects of connective tissue or tendon layers at the muscle insertion to the tendon.

Subsequent to denervation however, extrajunctional ACh receptors proliferate. The proliferated receptors are not initially evenly distributed along the muscle fibre but rather are spread down a concentration gradient from the junctional folds to the tendons. Levitt-Gilmour and Salpeter [1986] investigated denervation effects on the sternomastoid muscles of the mouse and found the site density 500µm from the endplate to be 4 times higher than non-endplate regions which was defined as 2mm from the endplate. Further, they observed that 4 days post-denervation the density of the receptors in endplate regions were 4 times more than that of non endplate regions and no indication of new receptors possessing a slow degradation rate was found. Such a gradient is not unlike that observed after developing muscles have been innervated. Levitt-Gilmour and Salpeter [1986] suggested the existence of a mechanism which presupposed a maximum number of nAChR's at the NMJ, even whilst in stages of altered synthesis and atrophy.

ACh sensitivity in innervated slow twitch and fast twitch fibres differ in so far as the slow twitch fibres have a low ACh sensitivity along the whole fibre whereas the fast twitch fibres exhibit no extrajunctional ACh sensitivity [Hartzell and Fambrough, 1972]. The sites of ACh sensitivity in denervated muscle fibres however, are similar in both slow and fast twitch fibres and are not regionally specific but rather apply to the entire muscle fibre [Albuquerque and Thesleff, 1968, Axelsson and Thesleff, 1959, Gauthier and Dunn, 1973]. Denervated muscles have been reported

to exhibit an increased sensitivity to ACh [Watson et al., 1976, Katz and Miledi, 1964b]. Increased membrane sensitivity to a number of chemicals signifies lower stimulant concentrations required to initiate contractions. Reduction factors of up to 1000 have been reported [Brown, 1937], as in the case of ACh stimulation, where ACh is administered intra arterially (i.a.) or within the denervated muscle bathing medium. Hartzell and Fambrough [1972] conducted an investigation into the distribution and sensitivity of nAChR's of the rat diaphragm post-denervation[1]. The innervated adult rat diaphragm is comprised of predominantly slow twitch fibres [Kilarski and Sjostrom, 1990]. Extrajunctional nAChR's were seen to increase from 2 to 3 days post-denervation, as too was observed by Levitt-Gilmour and Salpeter [1986]. Levitt-Gilmour and Salpeter [1986] reported that by 8 days post-denervation, extrajunctional receptors proliferated over the entire muscle surface at a site density of between 200-400 binding sites/μm^2; and that the number of receptors at the junctional folds remained constant for a number of weeks before exhibiting a decrease. At 14 days post-denervation Hartzell and Fambrough [1972] stated that the extrajunctional receptors had reached 1695 nAChR's/μm^2 but by 45 days had reduced 3-fold to 529 nAChR's/μm^2 (although still resulting in an overall increase in extrajunctional nAChR's). The decrease in ACh sensitivity between 14 and 45 days is akin to the sensitivity of a 5 day post-denervation fibre. This was hypothesized to be due to a decrease in the number and density of extrajunctional receptors and or a decrease in surface area due to muscle atrophy. Hartzell and Fambrough [1972] established a logarithmic relationship between the density of the nAChR's and ACh sensitivity such that nAChR density was 0.53 times the log of the ACh sensitivity (where the sensitivity was determined by means of iontophoretic application of ACh). The receptors displayed a 19-fold increase after a period of 14 days post-denervation if counted by specific binding methods [Hartzell and Fambrough, 1972]. Three theories exist as to the nature of the increase in extrajunctional receptors post-denervation. These include

1. redistribution of existing receptors
2. latent receptor activation
3. generation of new extrajunctional nAChR's

(1) would result in a marked decrease in the number of junctional receptors. Hartzell and Fambrough [1972] did not observe such a decrease and noted that this was not a general trend in the literature hence concluding that if redistribution were to occur, it would do so in insignificant amounts and would thus not be the sole cause of the increase in extrajunctional receptors. The literature is more supportive of (2) [Katz and Miledi, 1964a] and (3), although a combination of all three possibilities has neither been ruled out nor verified [Hartzell and Fambrough, 1972].

[1] Note that diaphragm muscle is classified as skeletal muscle.

Gauthier and Dunn [1973] investigated the semitendinosis muscle (composed of red, intermediate and white fibres) of the rat at a 14 day denervation period. It was observed that at this period, the fibres were altered to a more homogeneous state resembling that of red or intermediate fibres but that these differed from normal fibres in their ultrastructural properties. The increase in red and intermediate fibres was attributed to a preferential modification of white fibres, confirmed by a myofibrillar ATPase staining technique to distinguish between fibre types before and after denervation. This alteration was considered as either a conversion (from white to red or intermediate) or as a deterioration of fibre type.

The discrimination in fibre type alteration may be due to either inherent muscle fibre properties or their respective motor neurons (with specific motor neurons, differing cytochemically, supplying different muscle types). Type I (red) fibres are considered more independent of the nerve supply, substantiated by muscle proteins which subsist independently of the nerve supply. Gauthier and Dunn [1973] contested such complete independence, alluding to changes in ultrastructural properties. Further observations at this denervation period included an increase in free ribosomes and rough surfaced endoplasmic reticulum. The increase was considered unbiased towards fibre type and attributed to the elimination of the nerve supply as a universal response. The observation was however, more evident in red and intermediate fibres (noted to possess more extensive superficial sarcoplasms). The increase in ACh sensitivity along the muscle fibre was attributed to the observed increase in physiological apparatus of protein synthesis.

Gauthier and Dunn [1973] stated that post-denervation transformations should not be attributed to discontinued use of the muscle, but rather to some trophic control by the respective nerve. It was suggested that the observed increase in the number of ribosomes corresponds to the increased production of a protein receptor. Gauthier and Dunn [1973] further asserted that the change in ACh sensitivity to incorporate the entire fibre post-denervation is curtailed by compounds which inhibit protein synthesis. This increase in sensitivity, apparent after 2-3 days [Levitt-Gilmour and Salpeter, 1986, Lømo and Rosenthal, 1972] is consistent in time with the appearance of additional ribosomes, suggesting that increased ribosome appearance is either adjunct to or precedent to the inception of whole muscle ACh sensitivity. Moreover, Gauthier and Dunn [1973] supported their proposition of increased ribosome-ACh sensitivity correlation, with their further observations of whole skeletal muscle ACh sensitivity at birth (in the rat) corresponding to a wealth of ribosomes in said fibres. They additionally noted that prevention of protein synthesis in undifferentiated fibres (sensitive to ACh in their entirety) *in vitro* inhibits the progression to muscle fibre supersensitivity to ACh. Such findings are consistent with receptor proliferation.

Denervation alters muscle dynamics differently to what immobility or unloading would [Lieber, 1992]. Muscle atrophy (a decrease in total muscle mass) is the first noticeable change subsequent to denervation and occurs in both slow and fast twitch muscle fibres. As a result of this atrophy, a decrease in the muscle fibre diameter and muscle force output is exhibited. Onset of atrophy

occurs practically immediately post-denervation [Shier et al., 1996]. Muscle fibre degeneration ensues approximately 2 months post-denervation. If no reinnervation occurs (for reinnervation, see section 2.1.5), muscle fibres reach the final stage of atrophy which involves replacement of fibres with fibrous, fatty tissue. Remaining fibres comprise a cell membrane and cell nuclei, but a limited ability to contract. This results in almost no capacity for myofibril regeneration.

Post-denervation, muscle fibres transform from slow to fast twitch fibres and thus increase the contractile speed, albeit at a lower force than their innervated counterparts [Lieber, 1992]. Albuquerque and Thesleff [1968] observed a three-fold increase in the electrical time constant in both fast and slow twitch muscle fibres post-denervation in experiments involving rat skeletal muscle. Denervation has been shown to cause an increase in the transverse resistance of the membranes in both slow and fast twitch fibres. Further notable changes post-denervation include an increase in the threshold required to generate an action potential and a reduction in the amplitude and rate of rise of spike, both of which are more pronounced in slow twitch fibres [Albuquerque and Thesleff, 1968].

2.1.5 Denervated muscle fibre functional electrical stimulation and reinnervation

It is possible for denervated muscle fibres to become reinnervated, provided the nerve supply to the muscle fibres redevelops rapidly. Damaged nerves which have not completely degenerated, may regenerate at various rates depending on the nerve. If reinnervation occurs within 3 months, the muscle fibres are likely to reacquire full functionality. As post-denervation time wears on however, regaining of full functionality becomes less probable and after 1 to 2 years, unlikely [Shier et al., 1996]. Eberstein and Eberstein [1996] proclaimed that once a muscle has been denervated for over a period of one year, the muscle could not be restored to its' full contractile functionality. It was accepted that if the damaged nerve regeneration rate was so slow as to exceed this time frame, the respective muscles would not respond to reinnervation. FES has thus been used to maintain denervated muscle viability until reinnervation occurs [Eberstein and Eberstein, 1996]. The one year time period for muscle reinnervation was generally accepted in clinical rehabilitation applications. Kern et al. [2002] however, disproved this by successfully stimulating and training denervated, degenerated muscles 15-20 years post-denervation over a period of 3-4 years, albeit obtaining high variations in contraction forces and fatigue resistance during initial years.

Muscle fibre reinnervation has been shown to result in a decrease in the number of extrajunctional nAChR's. Chahine and Goldman [1992] have ascribed this phenomenon to the suppression of nAChR gene expression. Neural cell adhesion molecules (NCAM's) have also been shown to play a significant role in muscle fibre reinnervation. Denervated muscle fibres make use of NCAM's to instigate the process of reinnervation. It has however been demonstrated [Lieber, 1992] that electrical stimulation of denervated muscle suppresses the expression of NCAM's and hence discourages reinnervation. Reinnervation sites have been shown to favour the original NMJ locations even in

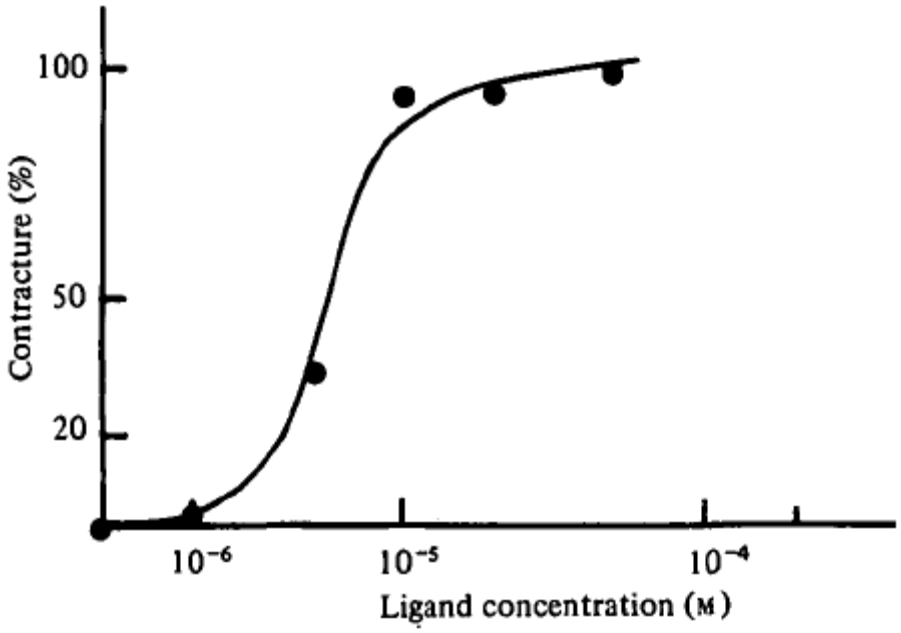

Figure 6: Effect of acetylcholine concentration on contractures developed in crustacean gastric mill muscles [Marder and Paupardin-Tritsch, 1980]

cases of complete destruction of the muscle fibre such that only the basal lamina is left intact, along with damaged muscle fibre constituents. NCAM's thus affect reinnervation but are not the sole cause thereof.

2.1.6 Response of innervated and denervated skeletal muscle to ACh administration

Application of ACh to explanted, innervated, whole skeletal muscles placed in a tissue bath, has been shown to cause the muscle to produce a slow contracture[2]. The muscles' ability to react to this form of stimulation may last for a number of hours [Quilliam, 1955]. Marder and Paupardin-Tritsch [1980] investigated the effect of ACh (amongst other ligands) on contractures developed in (striated) gastric mill muscles of crustaceans. Figure 6 illustrates their findings (adapted from Marder and Paupardin-Tritsch [1980]).

Fast and slow twitch muscles differ in their response to activation. Short bursts of propagated contractile activity are characteristic of fast twitch fibres whereas slow twitch and multiply innervated fibres display a gradual increase in tension, dependent on the degree to which the membrane is depolarised [Sanghvi and Smith, 1969].

[2]Refer to Glossary of Terms on page xix.

Sanghvi and Smith [1969] investigated the effects of a number of cholinomimetics and neuromuscular blocking agents, including ACh and succinylcholine (SCh) respectively, on the extraocular muscles of the cat. ACh was found to induce a contraction which was maintained under both *in vitro* as well as *in vivo* conditions. Small doses resulted in recurring motor unit activation in fast twitch fibres (measured by means of electromyography). Large doses resulted in the cessation of the recurring motor unit activation.

Application of ACh to extraocular muscles has been shown [Sanghvi and Smith, 1969] to result in slow contracture. ACh was also shown to evoke a prolonged contraction of the isolated superior oblique muscles of the cat. Physostigmine (refer to Glossary of Terms on page xx) was used to increase the effect of ACh. Gasser [1930] described a contracture as a reversible and prolonged contraction, not characterised by short bursts of propagated contractile activity along the muscle fibre. Contractures are commonly known to result in shortening and hardening of muscle.

Sanghvi and Smith [1969] presented two reports on the effects of ACh on slow twitch fibres. One reviewed study [Hess and Pilar, 1963] supported that ACh causes only slow contractures in slow twitch fibres whereas another reviewed study [Bach-y Rita and Ito, 1966] added that invocation of contraction by electrical stimulation prior to ACh stimulation resulted in short bursts of propagated contractile activity as well as slow contractures as described by Gasser [1930].

Different doses of SCh were found to result in different stages of contraction. Low doses resulted in a combination of asynchronous tetanus (refer to marker '3' in Figure 5 in section 2.1.3) and slow contracture. Large doses caused slow twitch fibres to produce contractures with some motor activity confined to individual muscle fibres and a reduction in maximal twitch force. Since SCh is a paralytic agent, the twitch depression effect caused by large doses is expected and was further substantiated by a potential inability of the muscle to contract further if already in a contracted state. Sanghvi and Smith [1969] likened the response of extraocular muscles to cholinomimetics and neuromuscular blocking agents to that of amphibian and avian skeletal muscles, all of which exhibit slow contractures upon stimulation with some fast twitch contractions. The type of response elicited was found to be dependent upon the dose (and hence concentration) of the agent.

A difference in cholinomimetic effects under varying conditions was also reported [Sanghvi and Smith, 1969]. Parameters said to affect stimulation included temperature (tests were conducted both *in vivo* – at body temperature and *in vitro* – at room temperature) and exposure time to the stimulating agent (short exposure times occurred with i.a. administration for *in vivo* tests and longer exposure times for *in vitro* exposure times).

Brown [1937] experimented with the stimulation of denervated mammalian (cat) and amphibian (frog *Rana esculenta*) gastrocnemii muscles by means of i.a. injection of ACh. Mammalian muscles were denervated for periods between 4 and 27 days whilst amphibian muscles were denervated for 3 weeks. The development of isometric tension (refer to section 2.2.1) was recorded amongst additional electrical parameters. Attention was drawn to a double peak response consisting of a

quick contraction and a slow contracture, which was a previously noted phenomenon in literature but which had never been thoroughly examined. The double peak phenomenon implied a partial similarity between innervated and denervated muscle contractile response thus warranting further investigation [Brown, 1937]. Mammalian muscles denervated for a period of 1 week were tested with various doses of ACh. Larger ACh doses were administered to innervated muscle. The results were comparable in terms of the quick response and the subsequent relaxation periods, in which the denervated muscle exhibited a longer time period of relaxation after the quick response than that of the innervated muscle. Small doses caused a quick contractile response, quick relaxation, and the recommencement of fibrillations thereafter. The quick contractile response was noted to occur in conjunction with an increase in action potential discharge, where an extended action potential discharge period was evident in denervated mammalian muscle after stimulation by ACh administration, compared to shorter discharge periods in innervated mammalian muscle. An increase in the dose (and hence concentration) of ACh caused the initial quick contraction time to display an increase in tension and the relaxation to be reduced. At such increased doses however, the relaxation phase was inhibited by a gradual increase in isometric tension. Further increases in the administered dose resulted in increased peak tension of the slow contraction phase, whereupon the slow contracture exhibited a greater peak tension than the initial quick response until eventually the quick response was no longer discernable at maximal dose and the increase in action potential discharge shown to accompany the quick response was inhibited. Large contractures further resulted in an increase in the ACh threshold and a reduction in the tension of contractions elicited by maximum dose administration of ACh. Moreover, fibrillations did not recommence quickly after high doses of ACh, taking up to 10 minutes to do so. This effect was found to be in direct proportion to the duration of the period of slow contracture. A third contraction phase was noted in tests conducted with doses of ACh low enough to stimulate a slow contracture with a maximal tension less than or equal to half that of the quick contraction. This third phase of contractile activity was thought to be due to remaining ACh in the interstitial fluid, the effect of which had been temporarily suppressed by the slow contracture phase.

In 3 week denervated frog muscles, no spontaneous fibrillations were noted. In fact, the only significant difference between the innervated and denervated frog muscles worth mentioning here is the lower threshold (dose) required required to stimulate the denervated muscle in comparison to the innervated muscle. The dose of ACh required to elicit a response in denervated muscle equal in tension to that of innervated muscle, is a factor of 10 less than the dose required for the latter. It should be noted here that the discussion of innervated frog skeletal muscle is relevant in that their contractile response to ACh has been shown to be comparable to that of denervated mammalian muscle insofar as the effects on quick response, suppression of fibrillation and suppression of contractile response to direct electrical stimulation [Brown, 1937].

Whilst a similarity does exist in the occurrence of the quick contraction phase in both inner-

vated and denervated mammalian muscle, three important differences have been noted [Brown, 1937]. These include the requirement of a lower dose of ACh to elicit a response in denervated muscle (compared to innervated), the extended period of the mechanical response elicited and the lengthened duration of the action potentials occurring alongside the aforementioned mechanical response. The increased sensitivity of denervated muscles has partly been attributed to the lack of AChE associated with nerve endings. The lengthened periods of activity noted in denervated muscle can thus be explained by a combination of the low threshold dose required and independence from the requirement of rapid application (as needed in innervated muscle to overcome the effects of AChE). The slow contracture phase of the response is not associated with repititive action potentials. In fact, the physiological mechanism involved with the propagation of contractile activity is inhibited by the slow contracture phase. Further, the slow contracture has been reported to involve all the muscle fibres in denervated mammalian and amphibian muscles. Although no rigorous investigation into the contractile response of denervated muscles at varying time periods has been conducted, Brown [1937] hypothesised that an increase in the gradual slow contracture and an increase in membrane sensitivity (characteristic of denervation) occurred simultaneously. This was determined by considering mammalian muscles denervated for periods of 4 and 6 days where at 4 days, $(threshold\,dose)_{4day\,denervation} \geq \frac{1}{2}\,(threshold\,dose)_{0day\,denervation}$, with a barely visible slow contracture; and at 6 days post-denervation, the muscle was considered highly sensitive and the slow contracture was distinct.

The contractile effects on skeletal muscle due to ACh administration can thus be related to the response of the junctional and extrajunctional nAChR's. As discussed in section 2.1.4, the nAChR's of rat skeletal muscle are distributed down a density gradient with the maximum density occurring at the endplate. Sensitivity thus decreases with increasing distance from the reactive area. Frog skeletal muscles differ slightly in that intermittent regions of higher sensitivity exist along the fibre. Miledi [1960a] asserted that regional sensitivity to ACh affects the time course of ACh potentials. Regions of low sensitivity exhibit slow rise time (T^3) due to the delay in the recruitment of surrounding receptors in an attempt to elicit a depolarising response (mV) of the membrane. Feltz et al. [1971] investigated the effect of ACh on junctional and extrajunctional nAChR's in terms of distribution and rise time of synaptic responses (depolarisation) in innervated frog skeletal muscle. The resultant responses differed greatly between junctional and extrajunctional nAChR's. Junctional receptors exhibited highly sensitive behaviour (sensitivity expressed in mV/nC) to ACh administration with rise times below 10ms, independent of ACh dose (Q) increase. Extrajunctional receptors on the other hand exhibited low sensitivity to ACh administration with slow rise times which correlated linearly with a $Q^{\frac{2}{3}}$dose of ACh [Feltz et al., 1971]. The rise time of

[3] Feltz et al. [1971] defined the rise time as $T = \frac{Q^{\frac{2}{3}}}{4\pi D X_0^{\frac{2}{3}}}$, where Q is the dose of ACh administered, D is the constant of diffusion of ACh $10^{-5} cm^2 sec^{-1}$ and X_0 is a function of Q, D, time (t) and position (b), $X_0 = \frac{Q}{8(\pi D t)^{\frac{3}{2}}} exp - \left(\frac{b^2}{4Dt}\right)$

response at the extrajunctional regions increased with an increase in the amplitude of depolarisation. The difference in response between junctional and extrajunctional nAChR's was attributed to the difference in area covered by the receptors. Extrajunctional nAChR's cover a larger area with a more uniform distribution whereas junctional receptors are densely packed into a smaller region which the administered doses cannot saturate hence resulting in rise time independence from Q. The amplitude of depolarisation is dependent upon the concentration of the ACh being administered. Miledi [1960a] and Katz and Thesleff [1957] asserted that the speed of desensitisation (by repetitive application) of a receptor site increases significantly with an increase in concentration of the chemical depolarising stimulant.

In experiments on innervated frog muscle in which ACh was administered i.a., Brown [1937] reported a rapid whole muscle contraction whose tension, at high enough doses, was able to exceed maximal twitch tension.

An important consideration, very pertinent to this study involves the effect of ACh on the contractile response of skeletal muscle to direct electrical stimulation (refer to section 3.3.2). Brown [1937] reported that when doses of ACh were large enough to produce a slow contracture, any subsequent attempt at direct electrical stimulation was futile (no visible contractions occurred). The occurrence of such suppression of a response to direct electrical stimulation was taken as an indication of the presence of a slow contracture. Moreover, additional chemical stimulation was still able to produce a contractile response, despite the muscles' unresponsive result to direct electrical stimulation but this response was merely an extension of the slow contracture. Note that the initial generation of a slow contracture is imperative - if only a quick response is elicited, the response to electrical stimulation is not depressed. The occurrence of a slow contracture thus affects the quick contraction response, fibrillation activity and direct electrical stimulation reactions; but has no influence on slow contracture by further ACh stimulation. These effects may persist long after the tension developed in the muscle during the slow contracture phase has subsided.

2.2 Engineering aspects

A study of muscle contraction dynamics requires a means of analysing the obtained contractile response. In this study, explanted skeletal muscles (solei and gastrocnemii) were stimulated and their contractile responses (i.e. generated force) recorded. The signal analysis applied to the recorded contractile responses included Empirical Mode Decomposition in conjunction with Hilbert spectra. This section describes these principles as well as the application of other engineering and mathematical principles to the experimental design and execution.

2.2.1 Isometric contraction

Explanted muscles stimulated to produce contractile forces may be tested under one of two conditions, isotonic contraction or isometric contraction. Isotonic contraction requires that a constant tension be applied to the muscle and its change in length recorded. Isometric contraction on the other hand requires that the muscle be maintained at constant length whilst the contractile force is recorded upon stimulation. Isometric contraction is applied in this study, as demonstrated in Figure 7 (adapted from Ethier and Simmons [2007]).

2.2.2 Signal characteristics

The output signals obtained in this study were considered to be non-stationary (transient) and non-linear. A stationary signal is one in which the statistical properties (such as the mean or variance) of the signal do not vary over time. Mathematically, a time series $X(t)$ is said to possess weak stationarity if [Huang et al., 1998]

$$\begin{cases} E\left(\mid X\left(t\right)^{2}\mid\right)<\infty \\ E\left(X\left(t\right)\right)=m \\ C\left(X\left(t_{1}\right),X\left(t_{2}\right)\right)=C\left(X\left(t_{1}+\tau\right),X\left(t_{2}+\tau\right)\right)=C\left(t_{1}-t_{2}\right) \end{cases}$$

where
$E\left(.\right)$ is the expected value average, and
$C\left(.\right)$ is the covariance function;
and strict stationarity [Huang et al., 1998] if, for all t and τ,

$$\left[X\left(t_{1}\right),X\left(t_{2}\right),...,X\left(t_{n}\right)\right]$$

and

$$\left[X\left(t_{1}+\tau\right),X\left(t_{2}+\tau\right),...,X\left(t_{n}+\tau\right)\right]$$

are the same.

Systems are considered non-linear when the amplitudes of their variations become finite. Most natural occurring physical systems are intrinsically non-linear. Even the data obtained from linear systems may be deemed as non-linear in their final state due to limitations and imperfections of probes or applied numerical methods [Huang et al., 1998].

There are a select number of methods which allow for the analysis of non-linear and non-stationary data. The most applicable of these methods will be discussed here.

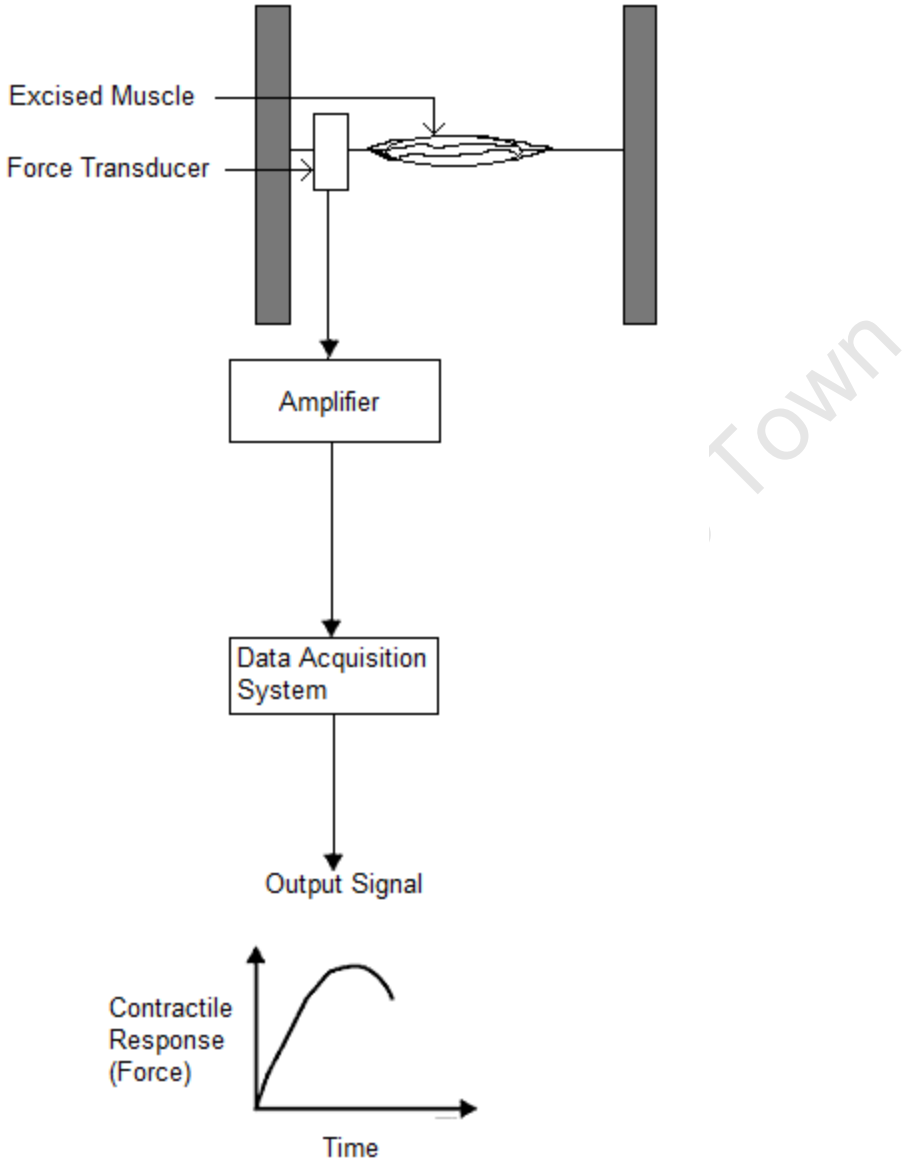

Figure 7: Setup for Isometric Contraction Experiment

2.2.3 Fourier Analysis

Fourier analysis (FA) involves the decomposition of a signal into trigonometric components of different frequencies, essentially transforming the signal from a time-based to a frequency-based domain. As will be demonstrated shortly, this method is not ideal for the analysis of non-linear and non-stationary signals. It does however, form the basis of the underlying principles of other techniques which will be discussed here, hence forming the foundation of a broader explanation to follow.

The downfall of taking the Fourier transform (FT) of a signal is that it only provides the frequency components contained within the signal but provides no indication as to when in the time domain these frequencies occur. FA is thus only useful for stationary signals, or in instances when the user has no interest in the time domain information. The short time Fourier transform (STFT) was thus developed as an attempt at tackling the shortcomings of the FT by using a windowing technique to analyse only select portions of data at a time. STFTs segment a signal and assume stationarity over each segment thus providing a fixed resolution at all times (once a time window is selected, its size is the same for all frequencies). This finite window decreases the frequency resolution and provides limited precision based on the size of the window.

It follows then that a more adaptive approach is necessary if one wants to achieve better precision and accuracy in the time and frequency domains.

2.2.4 Wavelet analysis

Wavelet analysis (WA) provides just such an adaptive approach. WA is in effect a variable window Fourier spectral analysis (FSA) and is defined mathematically as

$$W(a,b;X,\psi) = \mid a \mid^{-1/2} \int_{-\infty}^{\infty} X(t)\, \psi * \left(\frac{t-b}{a}\right) dt \tag{2.1}$$

where

$\psi * \left(\frac{t-b}{a}\right)$ is the basic wavelet function

a is the dilation factor ($\frac{1}{a}$ is indicative of the frequency scale)

b is the translation of the origin (indicative of the time location of an event)

Equation 2.1 represents the energy of X for scale a at $t = b$ [Huang et al., 1998].

The basic wavelet function (as defined above) is selected according to the type of signal being analysed and is applied before the analysis is undertaken. WA is capable of providing time and frequency information of a signal simultaneously and overcomes the resolution problems of the STFT by means of its variability. The technique involves decomposing the signal (to a pre-defined level) into frequency bands by splitting the signal and applying various high pass and low pass filters

to each component. The resulting frequency bands are displayed over time intervals[4]. Variable resolutions may be obtained such that higher frequencies are better resolved in time and lower frequencies are better resolved in frequency (the signal may be analysed at different frequencies with different resolutions). The width of the window is variable and hence changes for every spectral component. Negative frequencies are not computed. WA has been applied to time-frequency distributions of data in time series [Huang et al., 1998, Farge, 1992, Long et al., 1993].

Pitfalls of this method include the time frequency resolution trade off (localised changes require one to analyse the high frequency range thus making it difficult, if not impossible to to determine local changes in the low frequency range), the restriction to the basic wavelet function selected (this presupposes that the user knows the shape of the useful components of the signal) and the assumption of linearity of the signal (since the technique is based on FA as described in section 2.2.3). Despite these shortcomings, WA is still a highly regarded technique in the analysis of non-stationary data.

2.2.5 Empirical mode decomposition and Hilbert spectral analysis

Empirical mode decomposition (EMD) is a digital signal processing technique which allows for the analysis of stochastic signals (generally non-linear and non-stationary) [de Lima et al., 2006] whilst still maintaining information relative to the time domain.

The EMD technique is based on a number of assumptions as defined by Huang et al. [1998], namely

1. a minimum of two extrema (a maximum and a minimum) occur in the signal to be analysed
2. if extrema are non-existent in the data set and only inflection points exist, differentiation will be repeatedly applied to the data until the extrema are identified and the ultimate results achieved by integrating the components
3. the time scale is determined by the time period occurring between said extrema

EMD produces intrinsic mode functions (IMFs) which are complete and locally orthogonal bases of the original signal [Huang et al., 1998] (so-called due to their representation of the oscillatory components fixed in the data). Time varying frequencies within the signal are thus maintained in the IMFs. Huang et al. [1998] defined IMFs as functions which satisfy the following two conditions

1. the number of extrema is equal to the number of zero crossings or differ by a maximum value of one over the whole data set
2. the mean value of the envelope defined by the local maxima, as well as that defined by the local minima, must be zero at any point

[4] Note here the applicability of the Heisenberg Uncertainty Principle which states that the simultaneous momentum and position of a particle cannot be defined, hence the use of frequency *bands* and time *intervals*.

These criteria for defining IMFs allow for both frequency as well as amplitude modulation.

The flowchart in Figure 8 outlines the EMD process and hence the means of obtaining the IMFs of an input signal.

The IMFs may be representative of physical occurrences since they represent different frequency and time scale components of the signal [de Lima et al., 2006, Huang et al., 1998, Mendez et al., 2010, Peng et al., 2005, Sharpley and Vatchev, 2006] and have been used in seismic and biological signal analysis [Battista et al., 2007, de Lima et al., 2006] as well as EMG [Andrade et al., 2006], ECG [Balocchi et al., 2004, Mendez et al., 2010, Salisbury and Sun, 2004] and EEG [ur Rehman and Mandic, 2010, Sweeney-Reed et al., 2004] signal analysis. The raw signal is sifted through the process charted in Figure 8 and the outcome is a set of IMFs with the last output component representing the residual data which were not classified into any of the IMF components. During the spline fitting process errors occur which accrue during sifting and may result in slight inaccuracies of the final amplitude and frequency values. In spite of these small errors, the method is successful in extracting most of the dynamic features from the signals examined [Huang et al., 1998]. The sifting process serves to eradicate the presence of riding waves as well as to improve the symmetry of the wave profiles by smoothing irregularities in the amplitudes [Huang et al., 1998]. The effect of the latter is controlled by applying a limit to the standard deviation (SD) between consecutive siftings in order to avoid the extreme case of obtaining a fixed amplitude signal. The SD is typically fixed between 0.2 and 0.3 and is given by

$$SD = \sum_{t=0}^{T} \left[\frac{| \left(h_{1(k-1)}(t) - h_{1k}(t) \right) |^2}{h^2_{1(k-1)}(t)} \right]$$

The physical significance of each IMF is to be interpreted by the user and thus supposes prior knowledge of the signal, although methods have been developed which aim to select IMFs relevant to the physical significance of the signal. Some such methods are discussed by Peng et al. [2005], Adu-Gyamfi et al. [2010] and Boutana et al. [2010]. IMF selection is essentially equivalent to applying a bandpass filter to the signal, but is superior to bandpass filtering in FA in that signal stationarity is not a limitation [Huang et al., 1998]. It is however, common practice for researchers to make use of all the IMFs [Mendez et al., 2010] (besides the final, representing the signal residuals. The residual may be included if evidence for physical significance exists).

EMD analysis is often used in conjunction with the Hilbert-Huang transform (HHT) and plotted on a Hilbert spectrum (HS) (amplitude squared will represent energy density). The HS allows for the energy contained in the IMFs to be visualised, and events localised (significant for locally inhomogeneous signals), as functions of time and frequency. This method is unique in that it allows for *quantitative* analysis of frequency variation. The IMFs provide a group of local functional components for which the instantaneous frequency is identified everywhere. The combined EMD and HS technique is considered superior to FSA and WA for a number of reasons [Huang et al.,

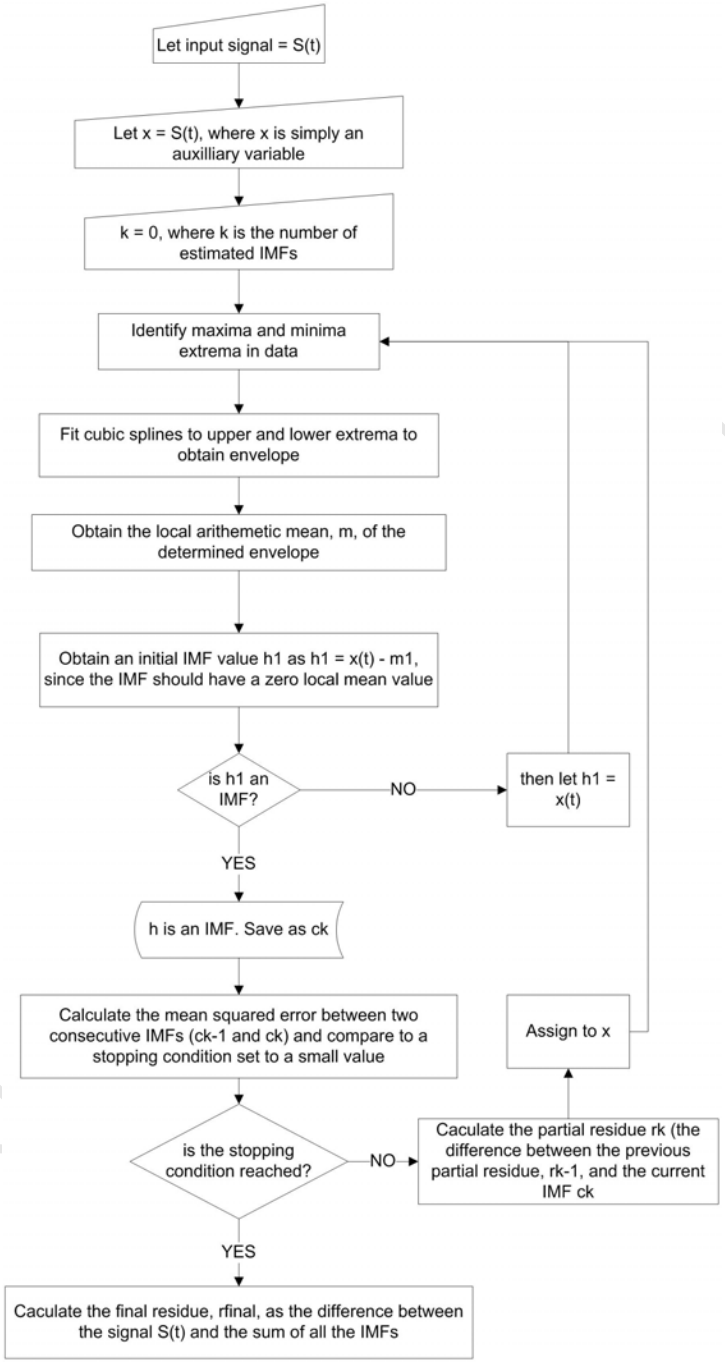

Figure 8: Flowchart outlining EMD process

1998, Peng et al., 2005, de Lima et al., 2006].

FSA is only capable of achieving a global characterisation of uniform harmonic elements in the signal. Since non-stationary data is non-uniform globally, additional harmonic elements are mathematically required to simulate the data. Further, FSA is based on the linear superposition of trigonometric functions. Extra harmonic elements (which credit no physical significance) are thus added to deformed (non-linear, non-stationary) signals when implementing this technique. These features of FSA result in the signals' energy being spread over a broad range of frequencies, which detracts from the grounds of physical interpretation. The HS employs the instantaneous frequency and energy as opposed to those globally defined which does not require the introduction of spurious harmonic components. WA, as mentioned in section 2.2.4, is applicable to non-stationary (but not non-linear) systems; is restricted in time and frequency resolutions depending on the frequency range (high or low) and further constrained by having to select a basic wavelet before analysis can take place. According to Huang et al. [1998], the HS determines the intrawave frequency modulation whereas WA demonstrates an energy spread, lacking in precision, over the primary energy component in the wave. Demonstration of frequency variation within a period of oscillation is unique to the EMD-HS technique. The WA technique often results in energy 'leakage' into adjacent modes. Whilst some frequency variation does occur in the HS due to the Gibbs phenomenon[5] at abrupt frequency changes and due to the end effects introduced by the finite data length, these are insignificant in comparison to the leakage exhibited by WA.

Accuracy in determining the occurrence of events in the time domain is crucial for non-stationary signals. This dictates that the employed method allows for adaptivity and for both frequency and energy (amplitude) to be functions of time [Huang et al., 1998]. Adaptivity allows for the method to detect local variations in the data thus emphasising the physical significance of a signal without merely blindly conforming to mathematical constraints (such conformist activity occurs when FA is applied to non-linear signals, resulting in the generation of spurious harmonics). Such an adaptive basis is achievable through *a posteriori* development. In EMD analysis, the resulting IMFs constitute the adaptive basis as they are derived from the data.

The Hilbert transform (HT) of an arbitrary time series is given by

$$Y(t) = \frac{1}{\pi} P \int_{-\infty}^{\infty} \frac{X(t')}{t-t'} dt'$$

where

P is the Cauchy principle value

$X(t)$ and $Y(t)$ form a complex conjugate pair

An analytic signal $Z(t)$ (which represents an IMF after the application of the HT) can then be represented by

[5] Refer to Glossary of Terms, page xix

$$Z(t) = X(t) + iY(t) = a(t)\, e^{i\theta(t)}$$

where
$a(t) = \left[X^2(t) + Y^2(t)\right]^{1/2}$
$\theta(t) = arctan\left(\frac{Y(t)}{X(t)}\right)$

The instantaneous frequency (ω) definition which best fits these conditions [Huang et al., 1998] is then given by

$$\omega = \frac{d\theta(t)}{dt} \tag{2.2}$$

Based on the stationary phase assumption (see Huang et al. [1998] and Schwartz et al. [1995] for further details), equation 2.2 is applicable locally and hence does not require a full period of oscillation to identify a frequency. The frequency can thus be defined locally at all points. Any changes in frequency may then be considered as frequency modulation, with each frequency being designated to a different IMF component.

For a measure of cumulative amplitude or energy at every frequency component for the complete data set, one may plot the marginal HS, given by

$$h(\omega) = \int_0^T H(\omega, t)\, dt$$

In the context of the complete time span of the data, the energy representation provided by the marginal HS is indicative of the probability of the respective component frequency waves to appear locally.

Additionally, the instantaneous energy density level is given by

$$IE(t) = \int_\omega H^2(\omega, t)\, d\omega$$

which provides an indication of fluctuations of energy within the signal.

3 Experimental Protocol

This study investigates the effects of various concentrations of ACh on denervated skeletal muscle fibres. The number of subjects is limited to 45 Long Evans strain of rats which were divided into 4 test groups with denervation periods of 7, 14, 50-55 and 204-208 days. The experimental protocol will be described in four stages. The first stage involves the denervation procedure, the second stage details the explantation procedure, stage three describes the chemical stimulation protocol of the explanted muscles and the fourth stage details the histological fibre staining process for determination of fast twitch fibres. All procedures adhered to protocols approved by the Animal Ethics Committee (AEC).

3.1 Denervation procedure

The denervation procedure involved severing of the sciatic nerve in the right hind limb of each rat. The procedure was performed on each rat under sterile conditions.

Rats were weighed in order to determine the amount of analgesia, Meloxicam, to be administered. Meloxicam (10mg/kg) was administered 1 hour pre-operatively. An extraction fan was turned on to evacuate the area of halothane vapour. Halothane was added to the halothane vaporiser (Blease) in readiness for administration to the rat. A temperature control heating pad was turned on and used to keep the rat warm. Oxygen, at a flow rate of 5L/min, was mixed with halothane in a chamber. Once the chamber was flooded with the halothane/oxygen mixture, (4%), the rat was placed into the halothane chamber.

Once the rat was unconscious, it was removed from the chamber and a nose-cone, through which halothane and oxygen were administered, was placed over its' face. The halothane flow rate was then readjusted to 2L/min and the vaporiser adjusted to 1.5%. The rat was placed on the heating pad (maintained at 37°C) which was covered with tissue paper to keep the heating pad clean and provide a layer of thermal protection between the heating pad and the rats' body. Care was taken to position the rat and nose-cone such that the rats' airway was not obstructed.

Fur was then removed from the right hind limb using a pair of scissors. The remaining hair was shaved with a blade and cleaned with a betadine and alcohol solution using gauze swabs. The shaved hind limb was positioned such that the posterior aspect was exposed. Betadine and alcohol solution was reapplied to the shaved hind limb once it was securely positioned. The operators' gloved hands were sterilised with alcohol and sterile instruments used henceforth.

An incision was made in the posterior aspect of the right hind limb from the hip to the knee. Two pairs of toothed forceps were utilized to hold the tissue apart whilst a pair of fine scissors was used to cut through the surrounding fascia and fat. The exposed muscle bellies were separated and the sciatic nerve located (this stage of the procedure is illustrated in Figure 9).

The nerve was pinched to check for a knee extension reflex and confirm correct nerve identifi-

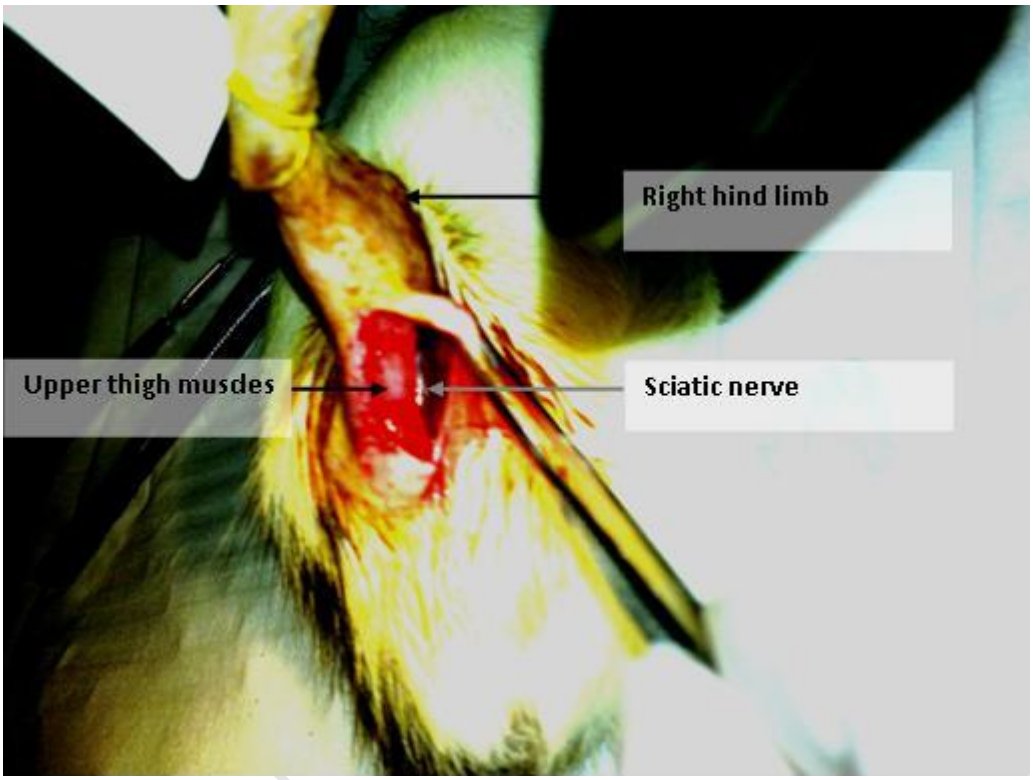

Figure 9: Right hind limb during denervation procedure. Stage of procedure: Location of the sciatic nerve after separation of the muscle bellies.

cation. The sciatic nerve was exposed as far as possible and traced back as proximally as possible using a pair of curved microforceps. A 6-0 silk suture was used to ligate the sciatic nerve in the most proximal position. Ligation prevents regeneration of the sciatic nerve once severed. A section of the nerve was then removed[6] (approximately 1cm). This was done such that the nerve was cut as close to the ligature as possible as well as as distally along the nerve as possible.

Lentrax was injected into the open wound (amounts were not specific as the Lentrax was injected into a cavity and not intramuscularly). The incision was sutured using a 6-0 silk suture. The wound was cleaned again using betadine and alcohol. Lentrax (0.1ml/kg) was then injected intramuscularly into the left hind limb. Ears were clipped as a means of tagging the rat for identification. The clipped ear was cleaned with betadine and alcohol and Lentrax was applied topically. Oxygen was turned off at the mains and the vaporiser was turned off. The nose-cone was removed from the rats face and the rat was kept under observation until it regained consciousness. During this waiting period it remained on the heating pad to maintain regular body temperature. Once the rat regained consciousness and started to move about, it was placed back into the cage and returned to the animal unit.

Rats were monitored daily and Meloxicam (10mg/kg) administered intra-muscularly in the left hind limb every 24 hours for 3 days (starting on the day of the denervation procedure).

3.2 Muscle explantation procedure

Subsequent to the denervation procedure, rats were left for various time periods of denervation before the denervated muscles were removed. Specifically, for four groups of rats, these denervation time periods were 7 days, 14 days, 50-55 days and 204-208 days. At the termination point of these periods, rats were decapitated using a small animal guillotine. The use of decapitation in place of commonly used euthenising agents ensured that no paralytic effect was induced on the muscle fibres.

The muscle explantation procedure for each rat can be described as follows:

Immediately after decapitation the body was placed on an ice pack for the duration of the explantation procedure. The soleus and gastrocnemius muscles from the right (denervated) hind limb were removed first and then the soleus and gastrocnemius muscles from the left (innervated) hind limb were removed to be used as controls for subsequent experimental procedures. In order to remove these muscles, a skin-deep incision was made around the base of the ankle and from the ankle to above the knee. This allowed for the skin to be pulled proximally from the ankle to above the knee hence exposing the underlying muscles. A pair of fine scissors was used to separate the achilles tendon from the bone at the base of the hind limb. The separated part of the achilles tendon was clamped with a pair of forceps and the distal portion of the tendon was then severed

[6] The distal portion of the nerve which remains after severing has been demonstrated to play a pivotal role in the ultrastructural properties of the muscle fibre in early post-denervation periods in the rat [Gauthier and Dunn, 1973].

using a pair of fine scissors. The clamped achilles tendon was lifted away from the bone and a sharp scalpel blade used to further separate the muscles proximal to this region (from the underling bone, surrounding muscles, tissue, fascia and fat).

The denervated soleus (DS) muscle of the right hind limb was identified and removed first, followed by the denervated gastrocnemius (DG). Care was taken to remove muscles whilst still preserving slips of tendon on each end of the muscle (this later allowed for loops to be tied to the tendon slips and attached to the testing rig, as described in Section 3.3). The innervated soleus (IS) and innervated gastrocnemius (IG) were subsequently removed from the left hind limb in much the same way. Innervated soleus and gastrocnemius muscles were used as controls for their specific denervated counterparts of the same rat.

All four excised muscles were placed in a Krebs-Ringer buffer solution and kept on ice. Upon completion of the explantation procedure, the muscles were stored in Kreb's Ringer buffer solution at -15°C until tested.

Muscle fibre samples from the innervated and denervated solei and gastrocnemii were obtained from one rat in each denervation group and frozen using liquid nitrogen, to be used later for histological staining. Frozen samples were stored in a freezer at -80°C.

3.3 Chemical stimulation experimental setup and protocol

Chemical stimulation of the explanted muscles involved the delivery of Acetylcholine chloride (AChCl) to the muscles. AChCl (Sigma-Aldrich) was obtained in powder form and two stock solutions of 1mM and 0.56M were prepared every two weeks due to chemical stability of the solution in this form. Highly hygroscopic properties of the powder form dictated that preparation of the stock solution be performed in a glovebox containing an inert gas (for which nitrogen was used). The stock solution as well as the powder form of AChCl was stored out of sunlight. Additionally, the powder form was stored with nitrogen sealed in the container and the stock solution was stored between 4-8°C between tests.

The concentration of the stock solution of AChCl was dictated by the concentrations required for stimulation. Six concentrations of ACh were used to stimulate muscular contraction. These concentrations and hence the corresponding volumes to be used from the stock solution were calculated by means of the dilution principle, given by

$$(C_{start})\,(V_{start}) = (C_{final})\,(V_{final}) \tag{3.1}$$

where

C_{start} is the AChCl concentration at the start of injection

V_{start} is the volume if the injected quantity

C_{final} is the final AChCl concentration of the solution in the tissue bath

Table 2: Volumes of AChCl stock solution required for corresponding AChCl concentrations

Stock solution	AChCl Concentration [mass/volume]	AChCl stock solution volume [μl]
1mM	4 [$\mu g/ml$]	1.39
	96 [$\mu g/ml$]	33.3
	550 [$\mu g/ml$]	190.6
0.56M	1.6 [g/ml]	100
	3.2 [g/ml]	200
	6.3 [g/ml]	400

V_{final} is the volume of the solution in the tissue bath plus that of the injected quantity

A detailed explanation of the use of equation 3.1 can be found in Appendix C. The results, indicating the doses of stock solution required to obtain the desired concentrations are indicated in Table 2.

Since these experiments were conducted *in vitro*, every attempt was made to simulate *in vivo* skeletal muscle in as near a physiological condition as possible. Table 3 provides a list of the apparatus used during the chemical stimulation procedure and a brief description of the uses of each item. A brief description of the horizontal tissue bath design is provided in section 3.3.1. Detailed design drawings can be found in Appendix B.

The experimental set-up involving the equipment listed in Table 3 is displayed in Figure 10.

3.3.1 Tissue bath design

The horizontal tissue bath was designed to allow for mimicry of the natural physiological muscle environment. The bath was fashioned from a half-pipe of acrylic. The material was practical as it could be easily shaped on a lathe, as opposed to the frequently used glass, and also possesses better insulation properties than glass. Walls of the bath were 8mm thick, allowing for further heat insulation. Heating of the bath solution was achieved by circulation of preheated water through two glass pipes which spanned the length of the bath. The pipes were positioned in parallel to each other in a horizontal plane at 12mm apart. Hot water (the temperature of which was controlled by the heating circulator) circulated through them, which in turn heated the bath solution by convection and ensured that the muscle, which was placed between the heating pipes, was maintained at a constant temperature of 37°C. A 2mm diameter hole was positioned at the base of one wall of the tissue bath and served as an entry point for bubbling of carbogen gas into the bath solution to ensure pH control. O-rings ensured that no leakage between the endcaps and the piped body of the tissue bath occurred. All pipe and tube connectors were made of brass alloys.

Table 3: Description of apparatus used for chemical stimulation procedure

Apparatus symbol	Name of Apparatus	Purpose of apparatus
A	Force transducer	Detection of muscular contractions
B	Amplifier	Amplified signals obtained by force transducer
C	Powerlab (data acquisition recording unit hardware, USB connection, Chart and Scope software)	Collectively enables data acquisition, amplified by B
D	Computer	Allowed for visual display of livetime recording; Stored collected data
E	Horizontal tissue bath	Chamber used to simulate *in vivo* conditions of rat skeletal muscle
F	Heating circulator	Heated and circulated water through water channels built into the tissue bath. Maintained water temperature such that tissue bath temperature remained at 37°C
G	Automated pipette (x3)	Delivered large doses of Acetylcholine chloride to muscle at constant rate
H	Suction pump	Used for flushing bath solution between tests
I	Carbogen tank	Bubbled carbogen into tissue bath to simulate effects of cellular respiration
J	Kreb's Ringer buffer solution (Sigma-Aldrich)	Medium containing salts to simulate *in vivo* physiological conditions of the muscle
K	Fan and temperature probe	Measured temperature in region of bath and maintained at 37°C by means of feedback mechanism and adjustable temperature settings. This assured that the signal did not drift out of range and that any drift introduced was not due to temperature change affecting the sensitive strain gauges.
L	Slide and lock mechanism	Means of pretensioning the muscle in the tissue bath

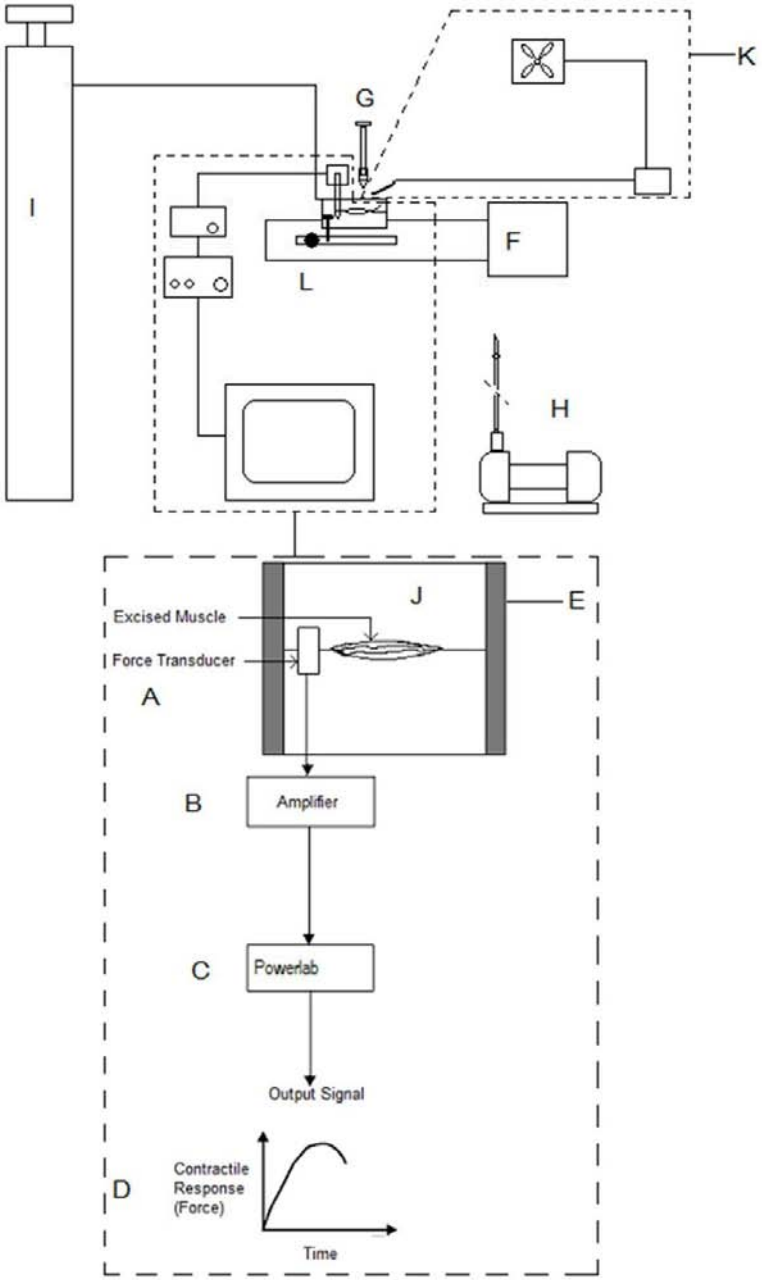

Figure 10: Experimental setup of chemical stimulation procedure

3.3.2 Stimulation procedure

The chemical stimulation procedure performed on each muscle in turn involved the following steps:

The horizontal tissue bath (E) was filled with Kreb's Ringer buffer solution (J). The heating circulator (F) was turned on and allowed to preheat the tissue bath and subsequently maintain a temperature of 37°C (akin to that of a rats' natural body temperature). The temperature probe was placed next to the tissue bath and the temperature controlled fan (K) was turned on. The muscle was removed from the fridge and placed in a dish containing Kreb's Ringer buffer solution at room temperature.

A 6-0 silk suture was used to tie a loop on either end of the muscle. The sutures were attached to the slips of tendon which had been kept intact during the explantation procedure. Carbogen (I) (95% oxygen, 5% carbon dioxide) was bubbled through the tissue bath to aid in preserving muscle viability and maintaining pH of the Kreb's Ringer buffer solution.

The muscle was placed in the horizontal tissue bath (E) by attaching one loop to a hook fixed in the tissue bath and the other loop to the force transducer (A) and allowed to thaw further at 37°C for 10 minutes. The force transducer consisted of strain gauges which allowed for the mechanical force to be expressed in terms of a voltage change. Changes in force were thus pre-calibrated to changes in voltage which allowed for the muscle to be tensioned to a pre-determined force of 1g. The muscle was pretensioned by means of a slide and lock mechanism attached to the base of the force transducer (refer to L in Figure 10).

A low pass filter with a cut off frequency of 25Hz was applied. Once the muscle was pre-tensioned, recording of voltage changes (akin to changes in contraction force) commenced for 3 minutes without any chemical stimulation to serve as a baseline of noise contribution for each test.

AChCl was aspirated into an automated pipette.[7] After 3 minutes, AChCl was delivered to the muscle by means of an automated pipette, set at the maximum delivery rate. Pipette tips were placed directly above the muscle (submerged in Kreb's Ringer bath solution). During initial test stages, a small circulator was used to circulate the Kreb's Ringer buffer solution within the bath. Later, the circulator was removed just before AChCl administration to prevent the AChCl from circulating away from the muscle before reaching the endplates. Each test was allowed to run for 19 minutes (following the 3 minute baseline noise contribution recording). Muscles from the short term groups (7 days and 14 days) were directly stimulated electrically subsequent to AChCl administration. This provided a means of determining (and checking for) slow contracture phases, as described in section 2.1.6 and implemented by Brown [1937]. The chemical-electrical stimulation cycle was repeated if deemed necessary, depending on the results obtained. The horizontal tissue bath (E) was flushed 3 times with double distilled water after each stimulation test to prevent any

[7] The amount of AChCl stock solution aspirated into the automated pipette (and hence the quantity administered to the muscle) was determined by the dilution principle and dependent upon the desired concentration for each test, as given in Table 2.

Table 4: Incubating solution compositions for myofibrillar ATP staining

Veronal Buffer (pH 9.4)	ATP solution (pH 9.4)
0.1M Sodium Barbitone	0.1M Sodium Barbitone
0.18M Calcium Chloride	0.18M Calcium Chloride
Distilled Water	Distilled Water
pH adjusted with 0.1M NaOH	ATP (disodium salt)
pH adjusted with 0.1M HCl	pH adjusted with NaOH

AChCl from remaining in the bath and affecting subsequent tests.

3.4 Histological fibre staining

Muscle samples from each denervation group were frozen in liquid nitrogen and stored at -80°C for later myofibrillar ATPase staining. Only fast twitch fibres were stained for from each denervation group to determine fibre composition during denervation stages and comparisons made by staining of control innervated muscle fibres.

The ATP staining procedure (similar to that used by Gauthier and Dunn [1973]) involved a pre-incubation stage and a substrate (ATP) incubating stage. A Veronal pre-incubation buffer (pH 9.4) was used to accentuate fast twitch (Type II) muscle fibres. Table 4 provides the composition of the pre-incubation buffer as well as that of the substrate incubating solution.

The staining procedure is outlined in the Table 5. .

APTES slides were used for mounting cryosectioned muscle samples which were transverse sectioned to a thickness of 10µm. The inside temperature of the cryostat machine was set to -21°C. Muscle samples were removed from storage at -80°C and positioned on the chuck, stabilised by use of Tissue tech (one muscle sample per chuck). The muscles were placed at the desired orientation to allow for transverse sections to be cut. Muscle samples were left in the cryostat machine with the glass lid closed for a few minutes in order to acclimatise. Samples were then cryosectioned to 10µm thicknesses (the first few samples were discarded to ensure the correct thickness was obtained). Slides contained between 6 and 12 samples each, depending on the cross-sectional diameter of the muscle sample (for instance, denervated muscle samples had atrophied considerably over the various time periods and the smaller the diameter of the muscle sample, the more sections a slide was able to accommodate). Once samples were sectioned, the sections were lifted off the metal bevel (inside the cryostat machine) by means of the APTES slides and immediately labelled according to order and orientation. Care was taken in noting if any of the sections had been transposed during sectioning and any such occurrences were noted lest they should impact the comparison of the final images.

Table 5: Staining procedure for fast twitch muscle fibres

Duration	Staining procedure for fast twitch fibre sections	Notes
	Use 10µm sections of tissue on APTES slides	
15 mins	Place in Veronal Buffer	
4 mins	Place in incubation buffer (pH 9.4)	
10 mins	Place in ATP solution	
Few seconds	Wash in $CaCl_2$	
4 mins	Incubate in $CoCl_2$ (2%)	
As needed	Wash well in 0.01M Sodium Barbitone	
As needed	Rinse in distilled water	
Few seconds	Develop colour in dilute ammonium sulphide (1%)	Use under fume hood
1 min	Rinse in tap water	
As needed	Dehydrate through alcohol solutions	
As needed	Clear in xylol	
As needed	Mount with Entellan	

Slides containing sections were stored at -20°C until the staining procedure was performed[8].

Stained sections were stored in a refrigerator at -4°C until photographed under a light microscope by use of a digital camera. Storage in this manner did not exceed 2 hours.

[8]Slides were stored in this manner for no longer than 48hours before staining.

4 Results and Discussion

This section details the results obtained from stimulation by ACh of the explanted muscles. Further results include explanted muscle dimensions and mass. Results from the histological ATPase staining are also presented. Wherever possible, ANOVA (single factor) was used to attest to statistical viability. However, given the that the sample sizes were limited by ethical constraints, full statistical analysis could not be conducted for data from all groups. This is a noted limitation and potential trends are thus discussed as noted, and verified by literature where possible; hence use of the words 'trend(s)' and 'pattern(s)' do not necessarily imply statistical significance. Later recommendations of larger sample sizes are made in section 7. An in depth discussion of the data is provided as the results are presented.

4.1 Muscle mass and dimensions

Muscle dimensions and mass were recorded in order to normalise the recorded contractile force as described in section 4.2.2. This was necessary as whole muscles were used as opposed to single muscle fibres. Further comparisons were drawn between change in mass and dimension as per length of denervation period.

Table 6 provides the explanted muscle mass for both solei and gastrocnemii at the different denervation periods as well as the percentage mass loss (plotted in Figure 11) and significance thereof, for denervated solei and gastrocnemii at all denervation periods investigated.

Table 6 shows that on average, the muscle masses decreased after denervation (seen when comparing DS to IS and DG to IG at all denervation periods). This is an expected outcome, often noted in literature and is due to muscle atrophy which occurs post-denervation.

Both the DS and DG demonstrate an increase in percentage mass loss with an increase in denervation period. The DS exhibited a higher percentage mass loss over time than the DG. At 7 days post-denervation, the smallest loss occurred in comparison to the difference between muscle types at all later denervation periods. It is noted that at 7 days post-denervation the gastrocnemii displayed a high sensitivity to chemical stimulation. This will be discussed in greater detail with other quantitative data (force response to chemical stimulation, time to peak force, response to electrical stimulation etc. in later section 4.2. Another observation which can be made from the information presented in Figure 11, is the far greater percentage mass loss of the 14 day DS in comparison to the 14 day DG. This time period is considered by literary sources [Axelsson and Thesleff, 1959, Hartzell and Fambrough, 1972, Fambrough, 1974] to be the most sensitive post-denervation period of slow twitch muscles and is supported by the results obtained from this investigation, as will be demonstration later in the discussion. It is thus relevant to note that the graph 'extremes' (or most noticeable differences) appear at the highest periods of sensitivity for DG (6-7 days) and the DS (14 days). An increase in the change in percentage mass loss between

Table 6: Mass of explanted solei and gastrocnemii muscles and percentage mass loss of denervated muscles at various stages of denervation.

	IS	DS			IG	DG		
Denervation period [days]	Ave muscle mass [g]	Ave muscle mass [g]	%mass loss	Significance (ANOVA: Single Factor)	Ave muscle mass [g]	Ave muscle mass [g]	%mass loss	Significance (ANOVA: Single Factor)
7	0.218	0.174	18.85	p=0.024, n=10, df=19	1.805	1.542	14.48	p=0.0078, n=10, df=19
14	0.214	0.101	50.42	p=0.0000368, n=8, df=159	1.683	1.236	22.73	p=0.025, n=8, df=15
50-55	0.337	0.137	59.06	p=0.00002, n=9, df=17	1.555	0.745	45.11	p=0.0089, n=9, df=17
204-208	0.352	0.104	70.72	p=0.00004, n=6, df=11	2.243	0.825	60.06	p=0.00024, n=6, df=11

solei and gastrocnemii from 7 to 14 days denervation was noted, followed by a decrease in the like from 14 days onwards. All percentage mass losses were significant, with all p-values < 0.05.

4.2 Chemical stimulation

The raw data obtained from the experimental muscle contraction recordings was output to LabChart 7 software. The parameters of the output were voltage (mV) and time (sec). Datasets were exported as MATLAB extension files. All data was processed in MATLAB R2010a and Microsoft Office Excel 2007. A database of all tests and pertinent information was generated in Microsoft Office Excel 2007 using Visual Basic (VBA) to code algorithms which standardised dataset names allowing for data filters to be applied according to defined parameters (such as AChCl concentration, denervation period and muscle type) and imported figures generated in MATLAB R2010a. In order to standardise these figures, an algorithm was written in MATLAB R2010a to downsample, shift, convolve, mark and plot all datasets on the same scales for easier comparison. Algorithm details are presented in Appendix D.

Variables investigated included maximum contraction force and time taken to reach maximum contraction.

The parameters defining the basis for comparison between datasets included concentration of AChCl used for stimulation, time periods of denervation and innervated (control) versus denervated

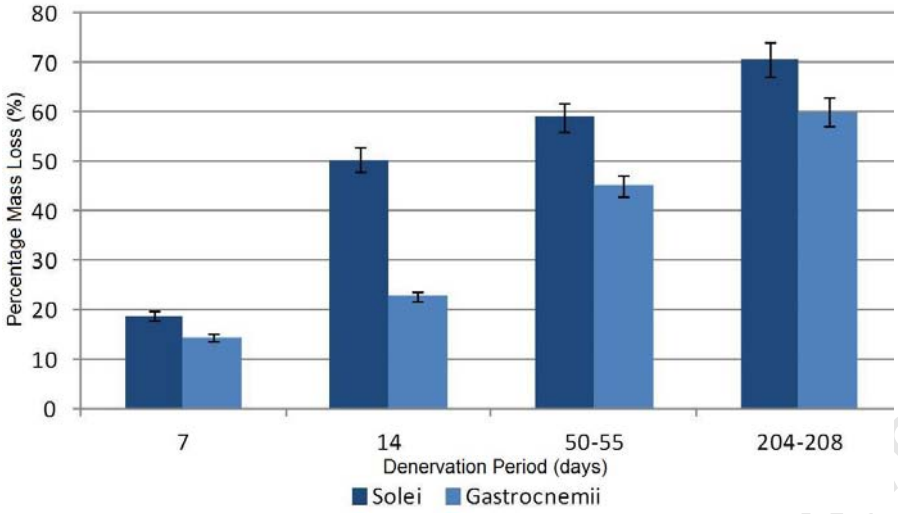

Figure 11: Percentage mass loss of denervated solei and gastrocnemii muscles in comparison to their innervated contralaterals for all investigated periods of denervation (5% error bar).

muscles.

The methods of analysis included direct force readings from the trace after normalisation and further in depth analysis with implementation of EMD, HSA and MHS, the results of which will each be explained in turn in the subsections to follow.

4.2.1 Change in force-time relationship with increasing concentration for denervated and innervated muscles at short and long term denervation periods

This section presents the F-t traces for denervated muscles and their controls for increasing concentrations and for all denervation periods investigated. Only 'pattern' changes will be noted in this section since values are required to be normalised for a direct comparison (as is conducted in section 4.2.2). Any values displayed on the figures are absolute values which have not been normalised. Red lines on the F-t graphs represent the time of injection of ACh.

7 days post-denervation, DG showed gradual increases in force for all concentrations except at the lowest concentration of $4\mu g/ml$ which appears to be too weak a concentration to cause any force variation or slow contracture post ACh administration for DG muscles. The IG however, displayed a small gradual increase in force at this low concentration in comparison to the DG, although not much force variation was noted. The IG displayed a clear increase in force variation with an increase in concentration but only exhibited large visible slow contracture effects at the highest administered concentration of 6.3g/ml, (Figure 14f) which shows a steep gradient of change in force over the full recording time, with no observed modes of tetanus reached. The difference between

the DG and IG responses could be attributed to the fibre type changes which have been reported to occur post-denervation and which have also been observed in this study (see section 4.3), such that DG display an increase in the percentage of slow to fast twitch fibres, hence the observed increase in slow contracture development post-denervation. At 14 days post-denervation, the DG are more sensitive to low concentrations than at 7 days, displaying a gradual increase in force from the lowest administered concentration of $4\mu g/ml$, probably due to further receptor proliferation. Further, an increase in concentration results in the same response from the 14 day DG in comparison to the 7 day DG, but larger concentrations have less of an effect on the slow contracture appearance in the 14 day denervated muscles, as is consistent with literature [David and Pitman, 1982]. David and Pitman [1982] reported rapid desensitisation and depression of muscle response to increased concentrations (doses) of ACh. Larger doses are more likely to saturate all the receptors in the muscle and, in the case of gastrocnemii, result in repetitive fast twitch contraction of fibre bundles (recall that gastrocnemii are predominantly composed of fast twitch fibres) which predominates any slow contracture response from the fewer slow twitch fibres present. The IG muscles from this denervation period reacted in much the same way as those of the 7 day denervation period, although an increase in force variation for all concentrations at 14 days post-denervation was noted. This could be due to an increased sensitivity of IG as a result of increased IG use as a means of physiological compensation after the denervation of the muscles in the contralateral limb. 50-55 day and 204-208 day DG both showed very little force variation post-denervation and no gradual increase in force except for a small rise noted in DG, denervated for 204-208 days and stimulated at $4\mu g/ml$ (Figure 18a). IG for these periods also displayed very little force variation in response to ACh administration, although a higher occurrence of slow contractures was noted. This is expected since the traces were obtained from whole muscles, hence excluding the effects of muscle atrophy from the direct F-t traces (note that these effects are taken into account for all later quantitative analysis presented). These slow contractures were observed at $4\mu g/ml$ for IG from the 50-55 day denervation period and for all concentrations administered to IG from the 204-208 day denervation group. In general, a reduced response, both in force variation as well as slow contracture, were noted for longer term denervation periods (50-55 days and 204-208 days) in comparison to the short term denervation periods of 7 and 14 days.

At 7 days post-denervation, the IS displayed gradual increases in force and small amounts of force variation in comparison to their denervated contralaterals which displayed large force variation and only produced slow contractures at higher concentrations. In fact, the DS response was similar to that of IG from the 7 day denervation period, perhaps further illustrating the shift in fibre type composition. Moreover, the large force variation could be attributed to an increase in the number of fast twitch fibres which appear in solei post-denervation [Bakou et al., 1996]. At 14 days post-denervation, gradual increases in force were noted to occur at lower concentrations than those noted for the 7 day denervation period. This can be attributed to increased sensitivity due to the

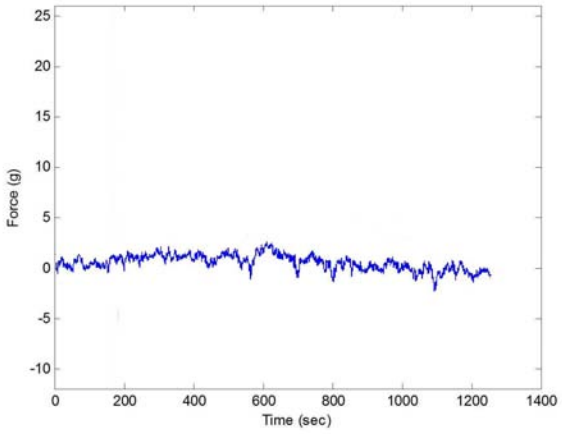

Figure 12: F-t record of IG noise run

proliferation of nAChRs. Whilst larger concentrations at 14 days post-denervation still resulted in slow contracture response, the force increase was more gradual than that noted at 7 days. This may be due to the fibre type changes, namely an increase in the ratio of type II fibres to type I fibres known to occur post-denervation and supported by the histological ATPase staining in section 4.3. IS from the 14 days post-denervation group displayed more gradual increases in force than those from the 7 day post-denervation group. Rosenthal [1977] observed an increase in the number of type II fibres of an IS upon denervation of its ipsilateral limb muscles. This was likely due to a physiological attempt at maintaining mobility and functionality as close to normalcy as possible. It is thus not beyond consideration that such change may occur in the contralateral IS, and would explain the more gradual increase in force for an IS from 14 day denervation period compared to that of a 7 day denervation period, although further investigation would be required to confirm this. No gradual increases in force were noted for solei denervated for periods of 50-55 days and 204-208 days. IS from the 50-55 day denervation period displayed gradual increase in force, as did those from the 204-208 day denervation period (at greater rates than the former), as illustrated in Figures 23 and 24.

In order to determine clear evidence of muscular contraction linked to the delivery of AChCl, longer noise runs were conducted on a muscle from each muscle group for each denervation period. Figure 12 displays one such noise run (in which no chemical or electrical stimulation was applied) involving an IG, the force of which was measured over a period of 1200sec. Whilst some fluctuation is seen to occur, it does so around a mean value. Any fluctuation seen in the 3 minute interval before stimulation is thus considered to behave in much the same manner. Noise runs for other muscles produced much the same results, hence indicating that the recordings of muscles stimulated by ACh represent a response to ACh rather than simply measurement noise.

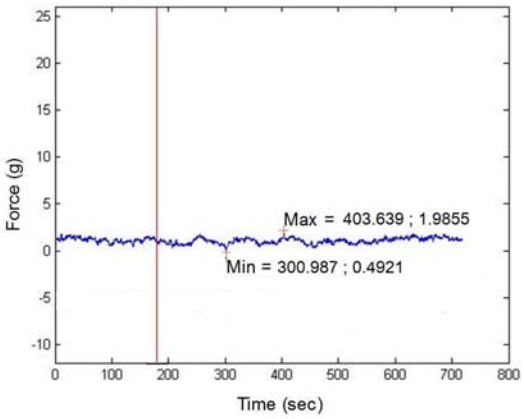

(a) DG 4μg/ml 7 day denervation

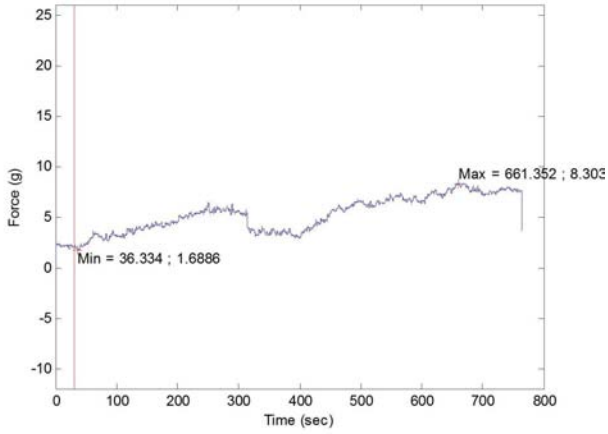

(b) IG 4μg/ml 7 day denervation

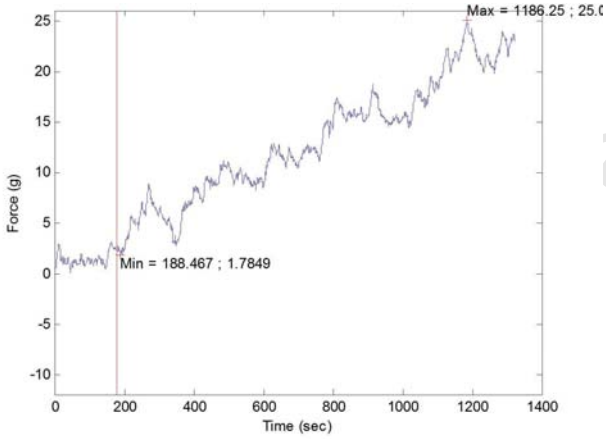

(c) DG 96μg/ml 7 day denervation

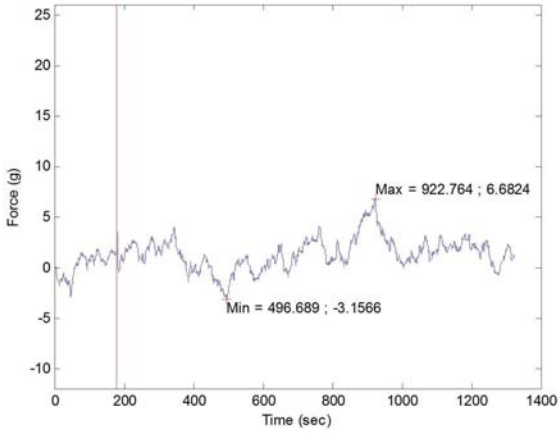

(d) IG 96μg/ml 7 day denervation

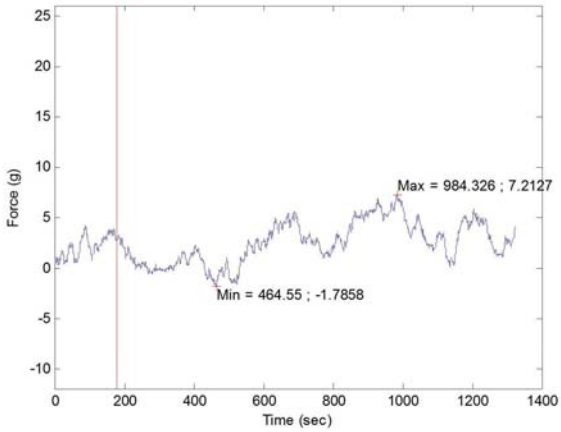

(e) DG 550μg/ml 7 day denervation

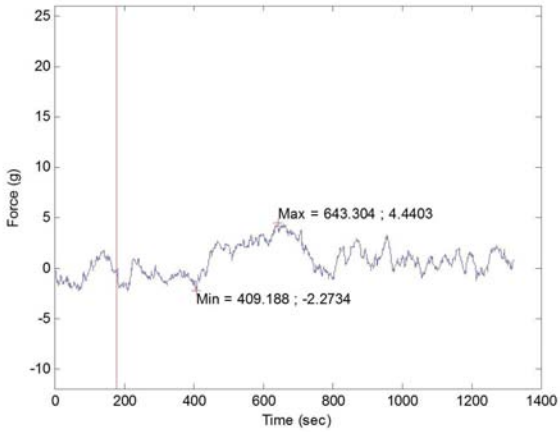

(f) IG 550μg/ml 7 day denervation

Figure 13: Force-time traces of denervated and innervated gastrocnemii at a 7 day denervation period for (13a) DG stimulated with $4\mu g/ml$ of ACh (13b) IG stimulated with $4\mu g/ml$ of ACh (13c) DG stimulated with $96\mu g/ml$ of ACh (13d) IG stimulated with $96\mu g/ml$ (13e) DG stimulated with $550\mu g/ml$ (13f) IG stimulated with $550\mu g/ml$ of ACh.

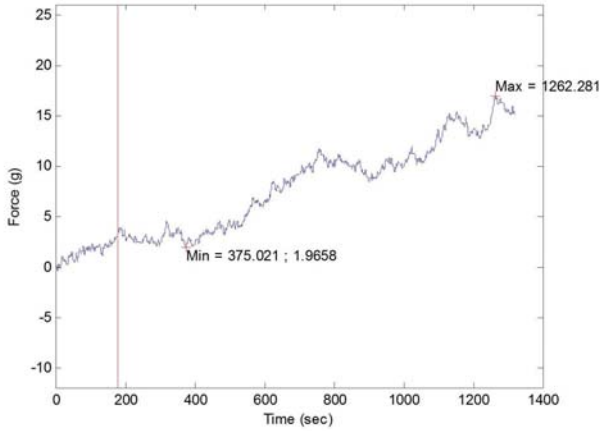

(a) DG 1.6g/ml 7 day denervation

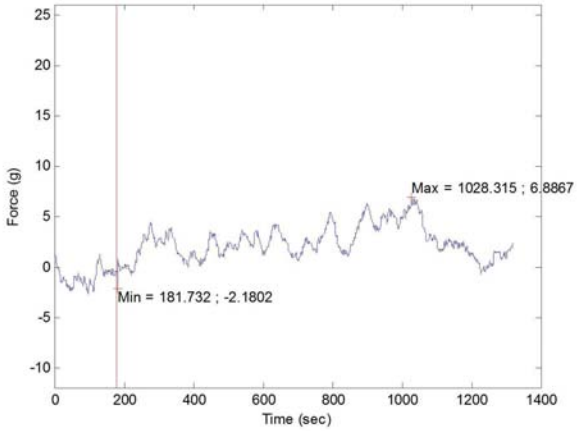

(b) IG 1.6g/ml 7 day denervation

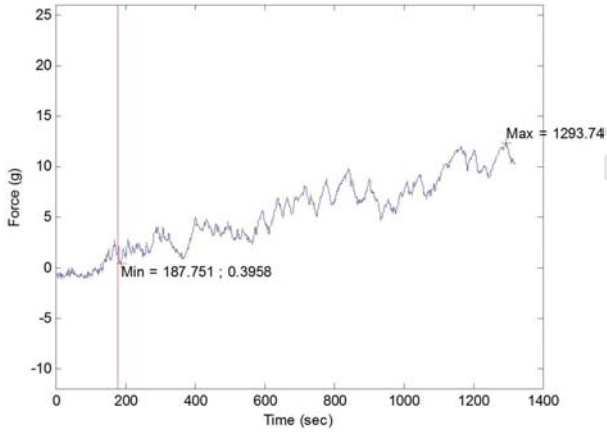

(c) DG 3.2g/ml 7 day denervation

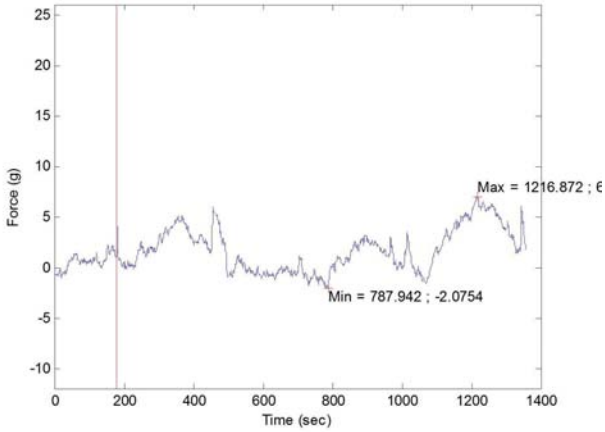

(d) IG 3.2g/ml 7 day denervation

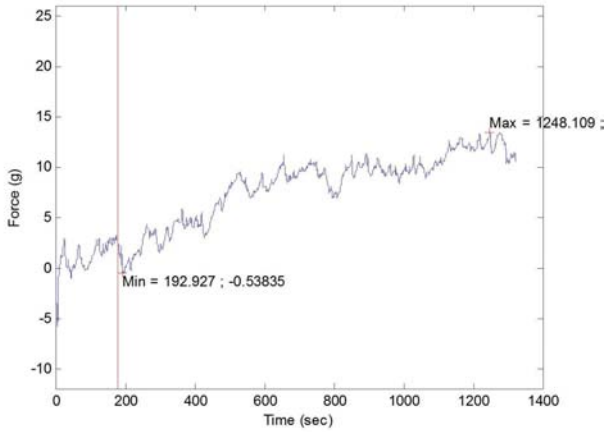

(e) DG 6.3g/ml 7 day denervation

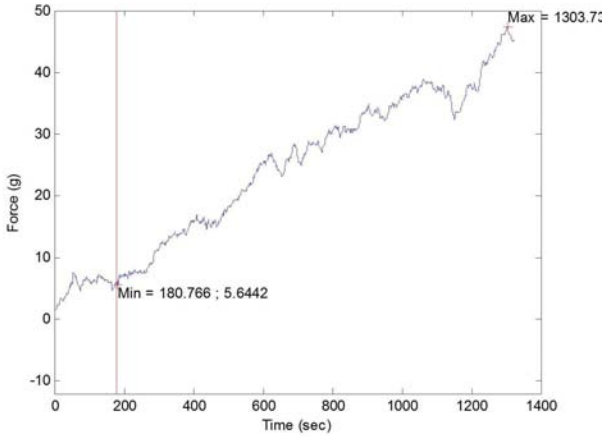

(f) IG 6.3g/ml 7 day denervation

Figure 14: Force-time traces of denervated and innervated gastrocnemii at a 7 day denervation period for (14a) DG stimulated with 1.6g/ml of ACh (14b) IG stimulated with 1.6g/ml of ACh (14c) DG stimulated with 3.2g/ml of ACh (14d) IG stimulated with 3.2g/ml of ACh (14e) DG stimulated with 6.3g/ml of ACh (14f) IG stimulated with 6.3g/ml of ACh.

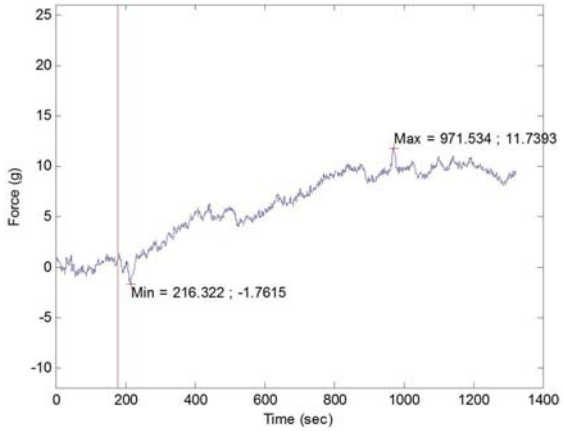

(a) DG 4μg/ml 14 day denervation

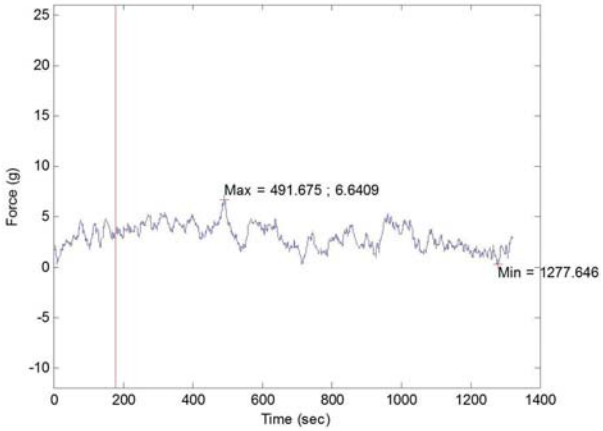

(b) IG 4μg/ml 14 day denervation

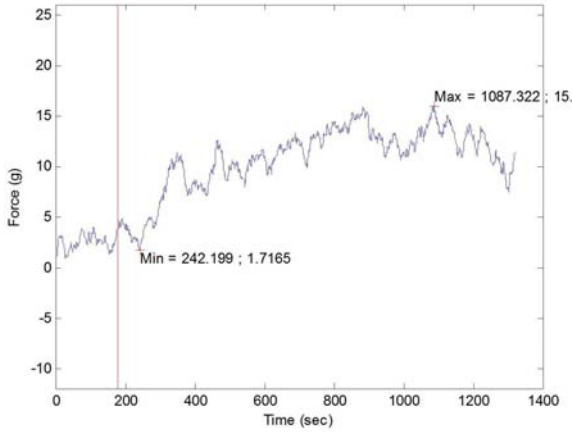

(c) DG 96μg/ml 14 day denervation

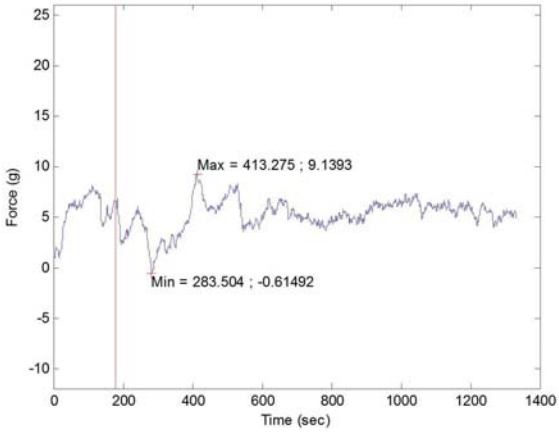

(d) IG 96μg/ml 14 day denervation

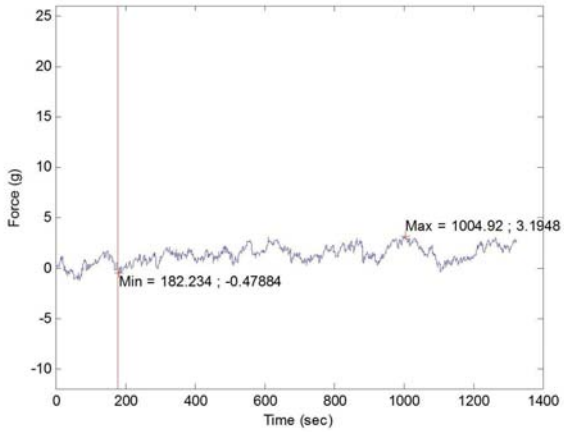

(e) DG 550μg/ml 14 day denervation

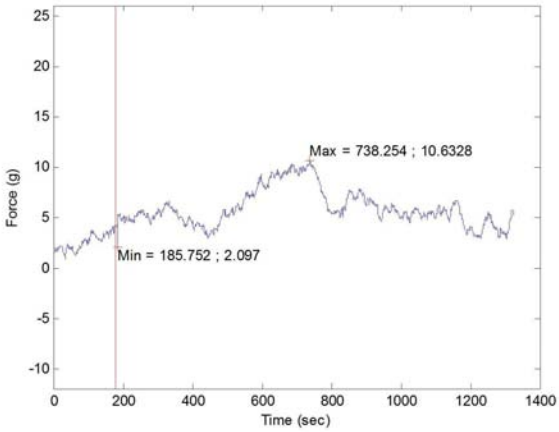

(f) IG 550μg/ml 14 day denervation

Figure 15: Force-time traces of denervated and innervated gastrocnemii at a 14 day denervation period for (15a) DG stimulated with $4\mu g/ml$ of ACh (15b) IG stimulated with $4\mu g/ml$ of ACh (15c) DG stimulated with $96\mu g/ml$ of ACh (15d) IG stimulated with $96\mu g/ml$ (15e) DG stimulated with $550\mu g/ml$ (15f) IG stimulated with $550\mu g/ml$ of ACh.

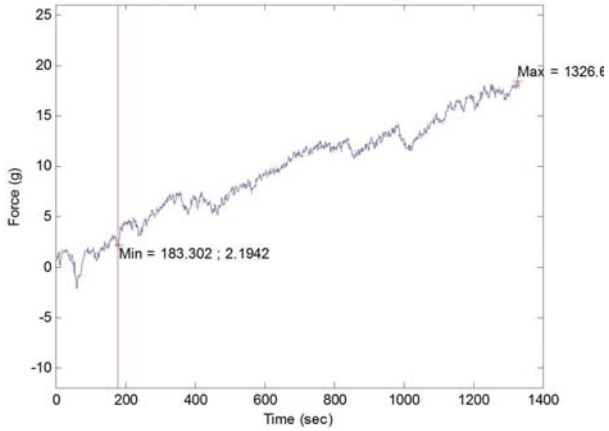

(a) DG 1.6g/ml 14 day denervation

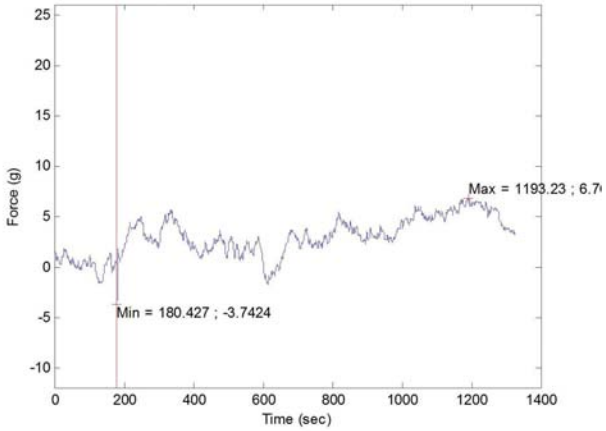

(b) IG 1.6g/ml 14 day denervation

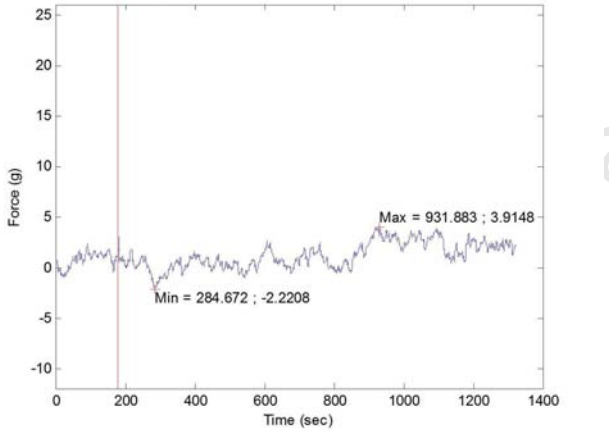

(c) DG 3.2g/ml 14 day denervation

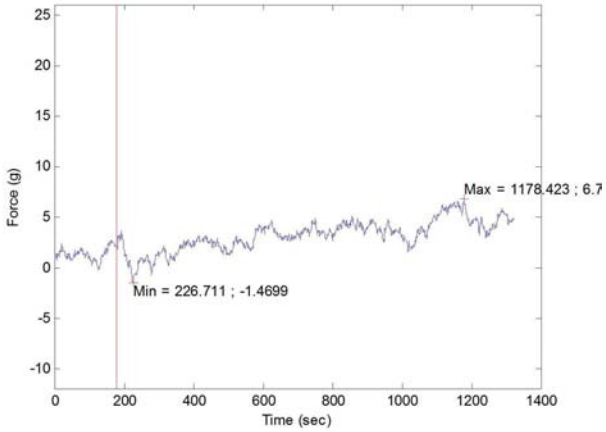

(d) IG 3.2g/ml 14 day denervation

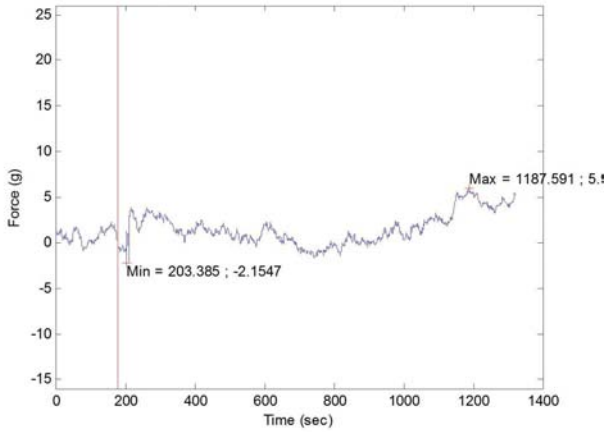

(e) DG 6.3g/ml 14 day denervation

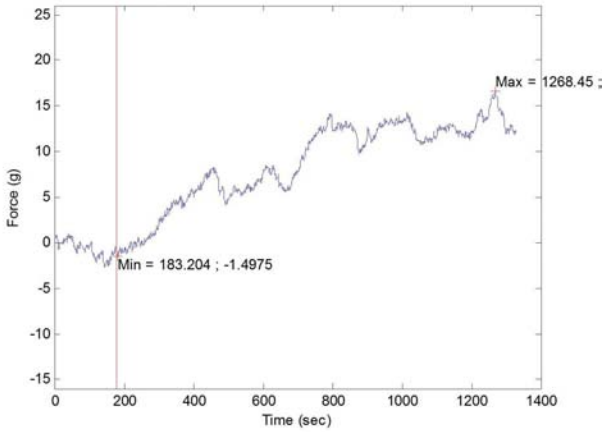

(f) IG 6.3g/ml 14 day denervation

Figure 16: Force-time traces of denervated and innervated gastrocnemii at a 14 day denervation period for (16a) DG stimulated with 1.6g/ml of ACh (16b) IG stimulated with 1.6g/ml of ACh (16c) DG stimulated with 3.2g/ml of ACh (16d) IG stimulated with 3.2g/ml of ACh (16e) DG stimulated with 6.3g/ml of ACh (16f) IG stimulated with 6.3g/ml of ACh.

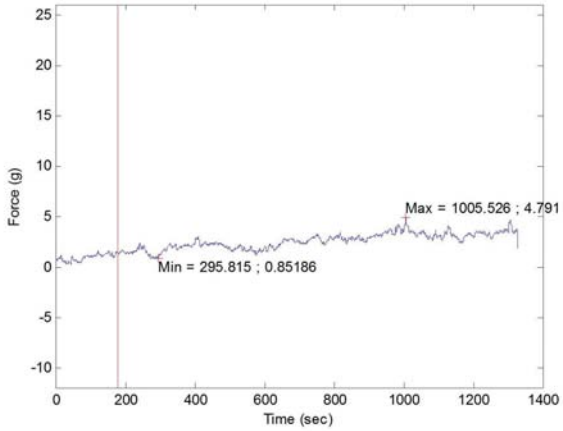

(a) DG 4μg/ml 50-55 day denervation

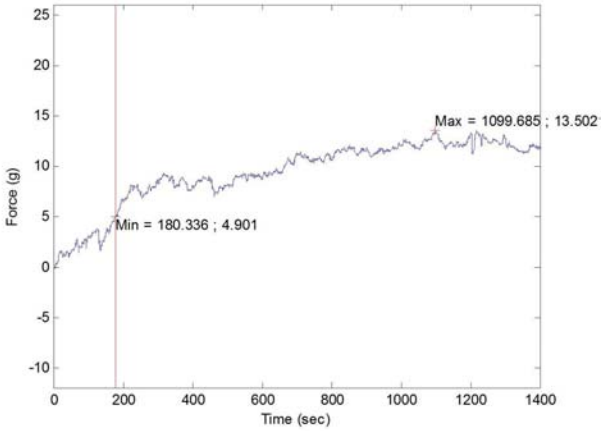

(b) IG 4μg/ml 50-55 day denervation

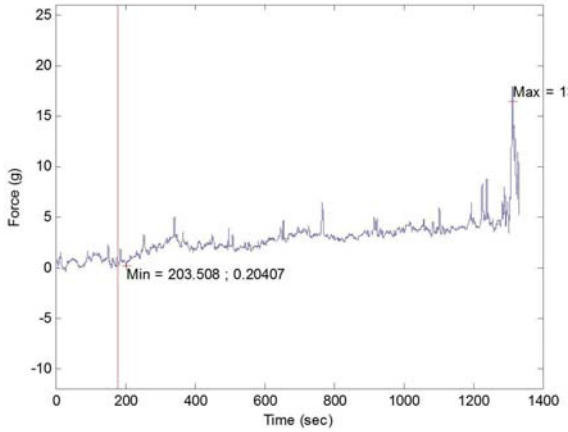

(c) DG 96μg/ml 50-55 day denervation

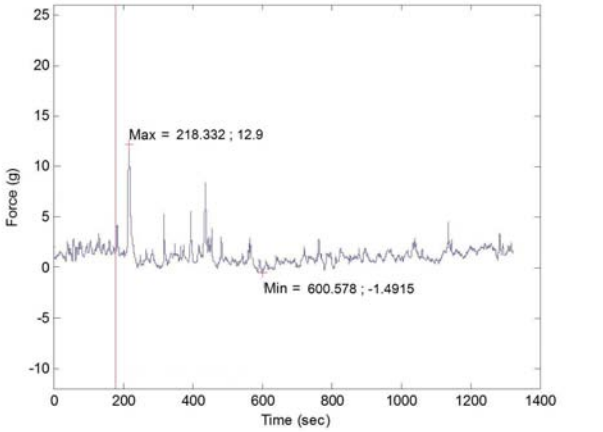

(d) IG 96μg/ml 50-55 day denervation

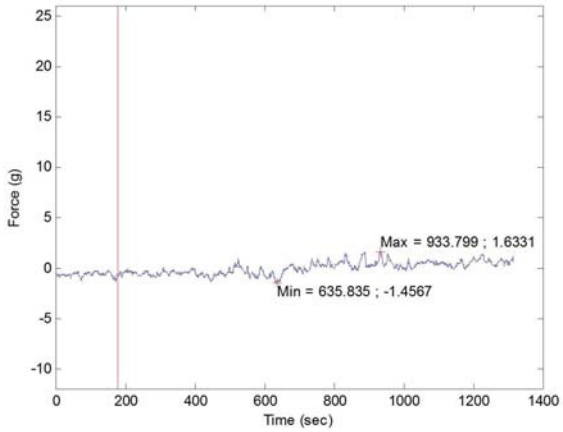

(e) DG 550μg/ml 50-55 day denervation

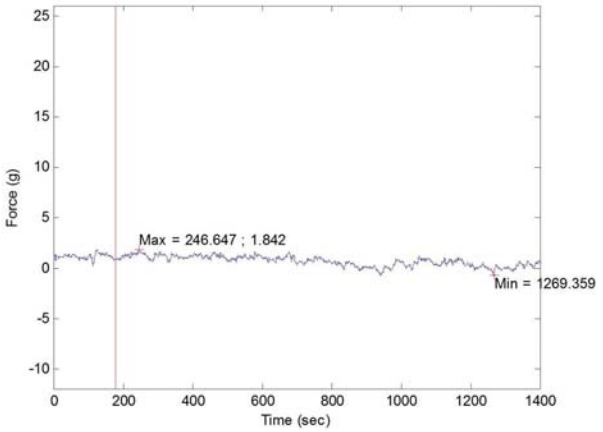

(f) IG 550μg/ml 50-55 day denervation

Figure 17: Force-time traces of denervated and innervated gastrocnemii at a 50-55 day denervation period for (17a) DG stimulated with $4\mu g/ml$ of ACh (17b) IG stimulated with $4\mu g/ml$ of ACh (17c) DG stimulated with $96\mu g/ml$ of ACh (17d) IG stimulated with $96\mu g/ml$ (17e) DG stimulated with $550\mu g/ml$ (17f) IG stimulated with $550\mu g/ml$ of ACh.

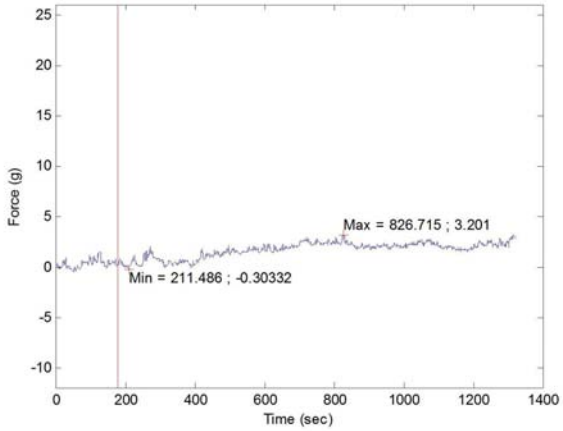

(a) DG 4μg/ml 204-208 day denervation

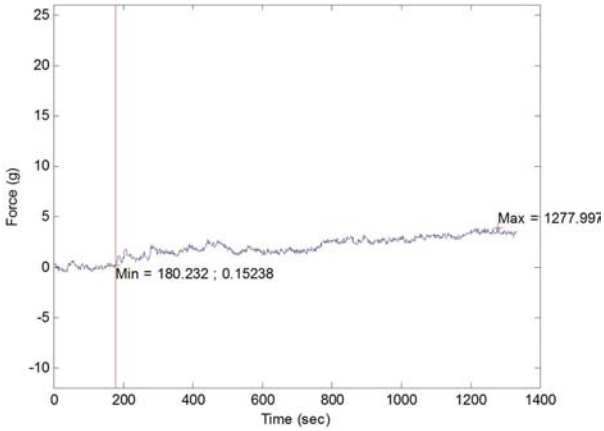

(b) IG 4μg/ml 204-208 day denervation

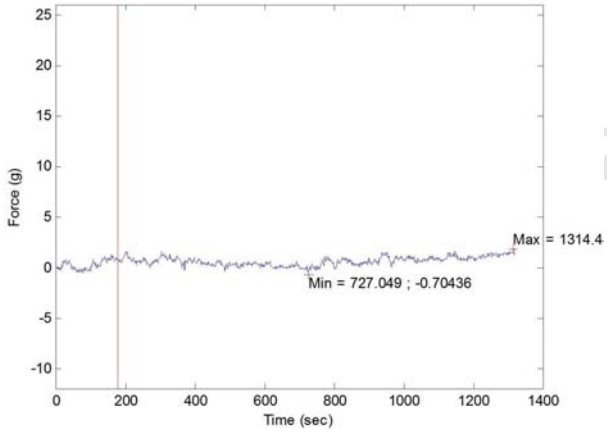

(c) DG 96μg/ml 204-208 day denervation

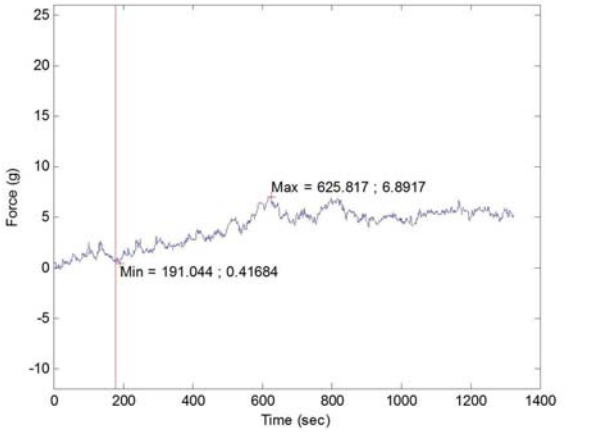

(d) IG 96μg/ml 204-208 day denervation

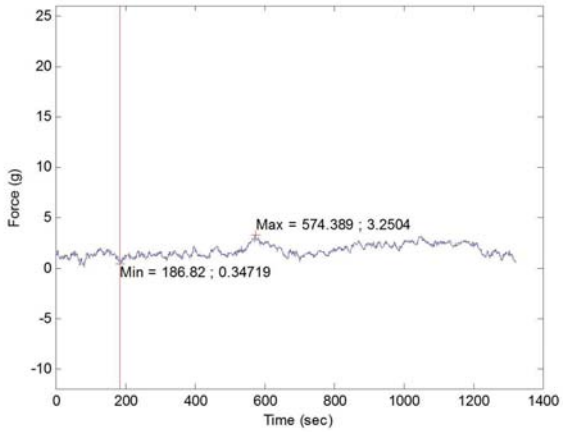

(e) DG 550μg/ml 204-208 day denervation

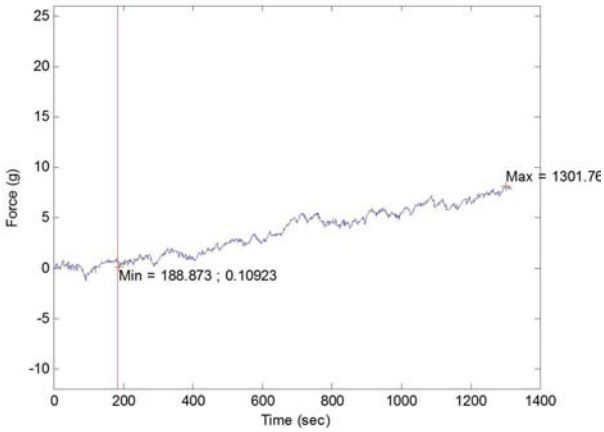

(f) IG 550μg/ml 204-208 day denervation

Figure 18: Force-time traces of denervated and innervated gastrocnemii at a 204-208 day denervation period for (18a) DG stimulated with $4\mu g/ml$ of ACh (18b) IG stimulated with $4\mu g/ml$ of ACh (18c) DG stimulated with $96\mu g/ml$ of ACh (18d) IG stimulated with $96\mu g/ml$ (18e) DG stimulated with $550\mu g/ml$ (18f) IG stimulated with $550\mu g/ml$ of ACh.

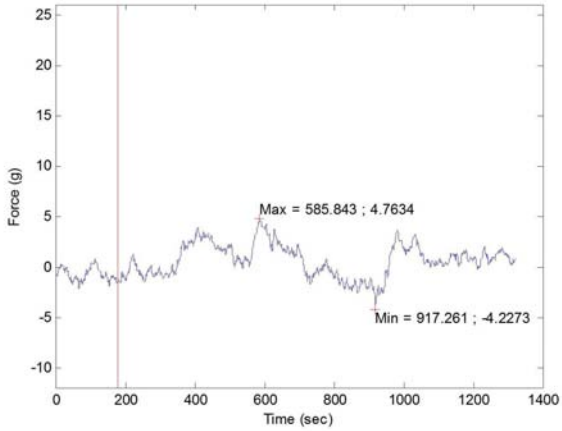

(a) DS 4μg/ml 7 day denervation

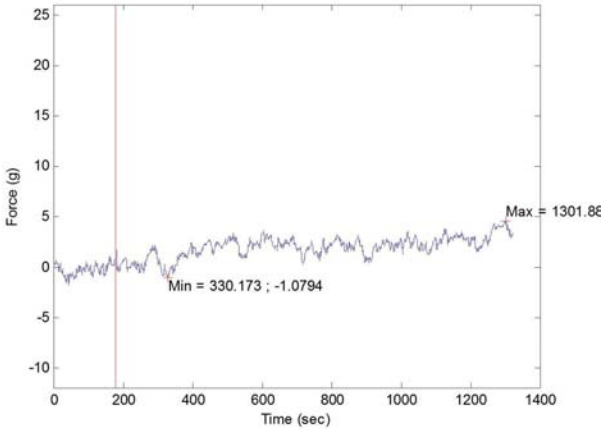

(b) IS 4μg/ml 7 day denervation

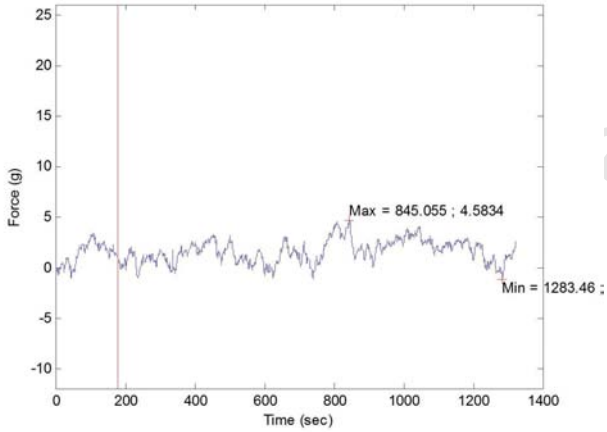

(c) DS 96μg/ml 7 day denervation

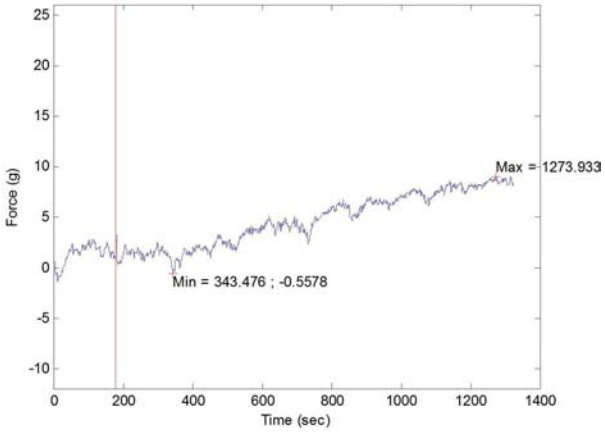

(d) IS 96μg/ml 7 day denervation

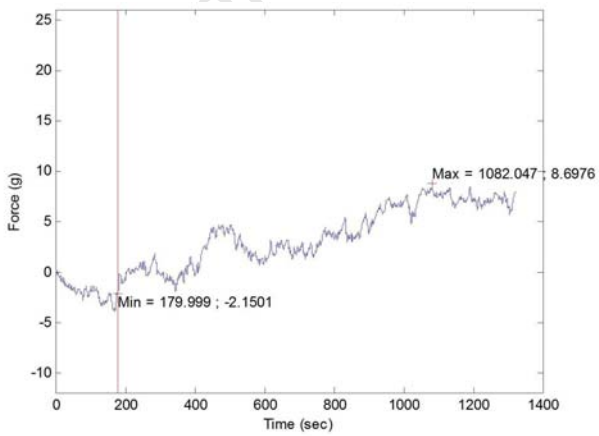

(e) DS 550μg/ml 7 day denervation

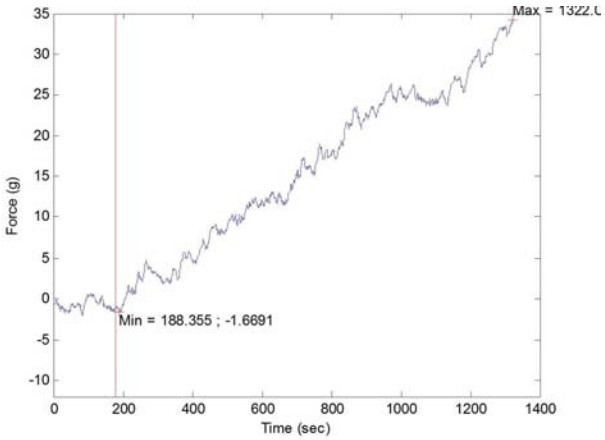

(f) IS 550μg/ml 7 day denervation

Figure 19: Force-time traces of denervated and innervated solei at a 7 day denervation period for (19a) DS stimulated with $4\mu g/ml$ of ACh (19b) IS stimulated with $4\mu g/ml$ of ACh (19c) DS stimulated with $96\mu g/ml$ of ACh (19d) IS stimulated with $96\mu g/ml$ (19e) DS stimulated with $550\mu g/ml$ (19f) IS stimulated with $550\mu g/ml$ of ACh.

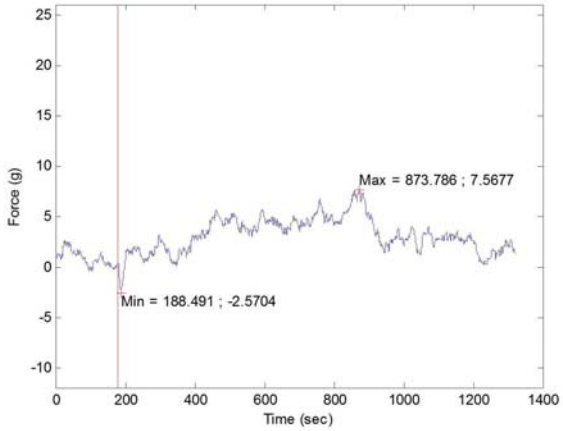

(a) DS 1.6g/ml 7 day denervation

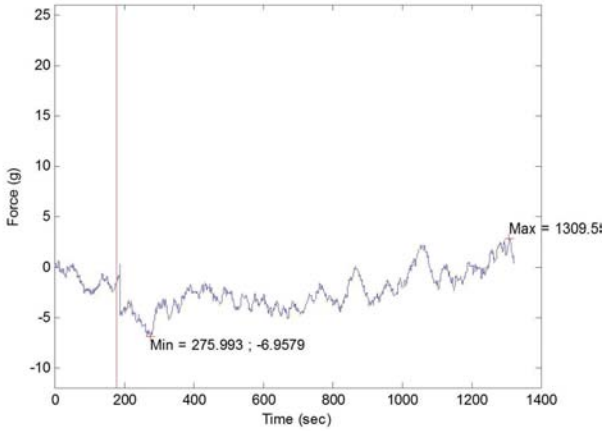

(b) IS 1.6g/ml 7 day denervation

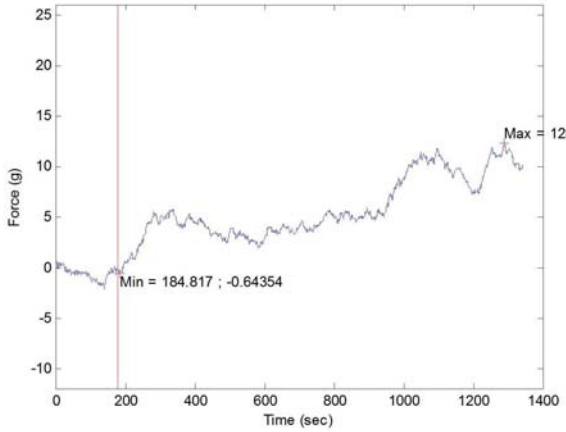

(c) DS 3.2g/ml 7 day denervation

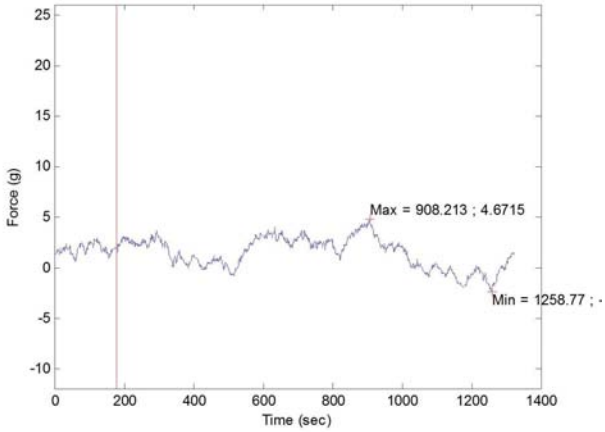

(d) IS 3.2g/ml 7 day denervation

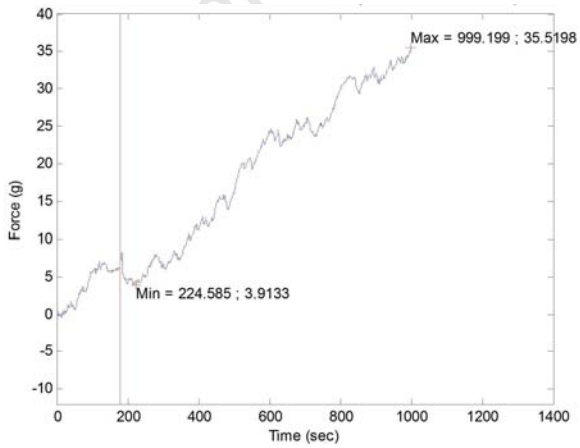

(e) DS 6.3g/ml 7 day denervation

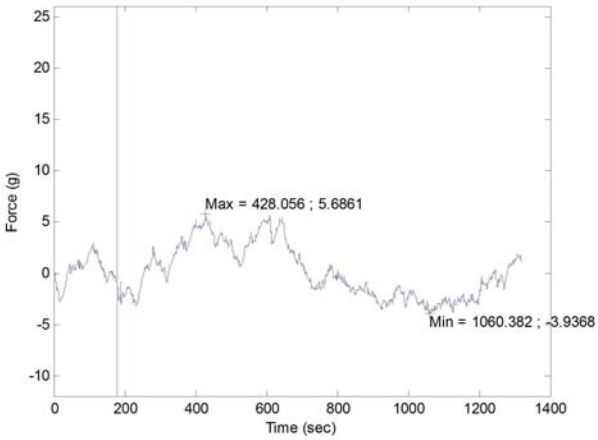

(f) IS 6.3g/ml 7 day denervation

Figure 20: Force-time traces of denervated and innervated solei at a 7 day denervation period for (20a) DS stimulated with 1.6g/ml of ACh (20b) IS stimulated with 1.6g/ml of ACh (20c) DS stimulated with 3.2g/ml of ACh (20d) IS stimulated with 3.2g/ml of ACh (20e) DS stimulated with 6.3g/ml of ACh (20f) IS stimulated with 6.3g/ml of ACh.

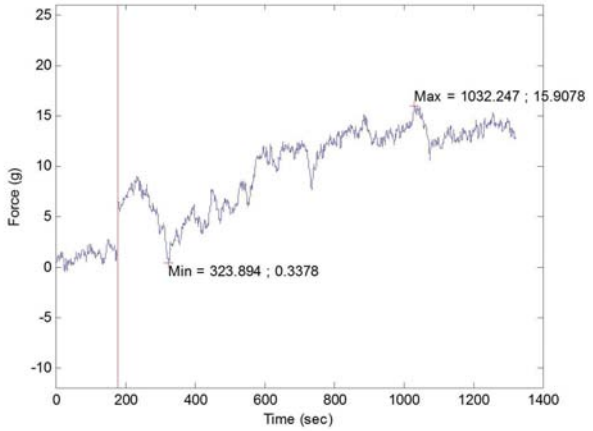

(a) DS 4μg/ml 14 day denervation

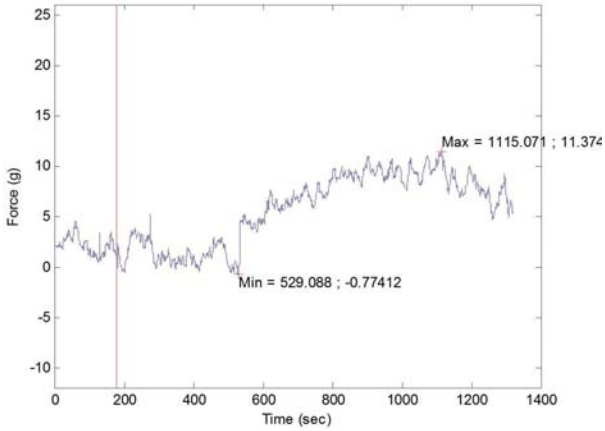

(b) IS 4μg/ml 14 day denervation

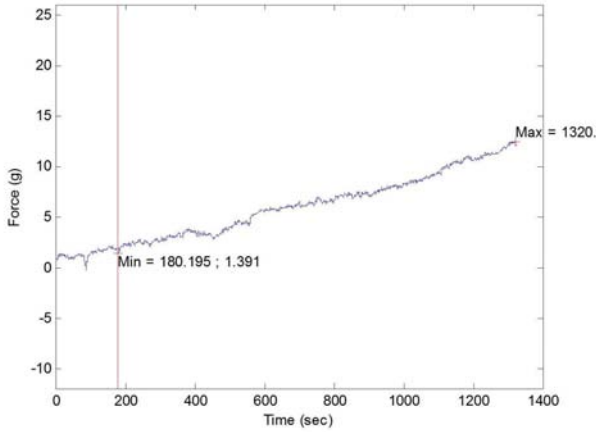

(c) DS 96μg/ml 14 day denervation

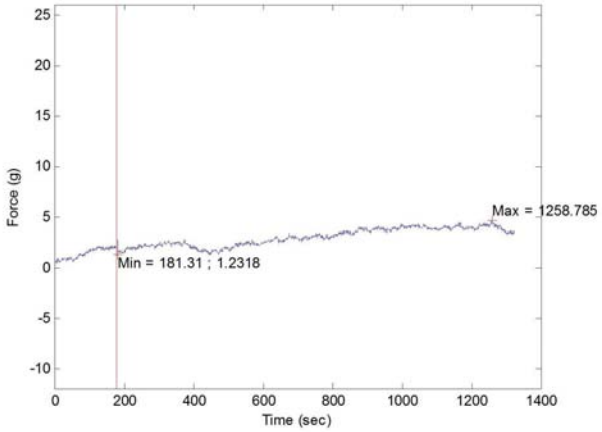

(d) IS 96μg/ml 14 day denervation

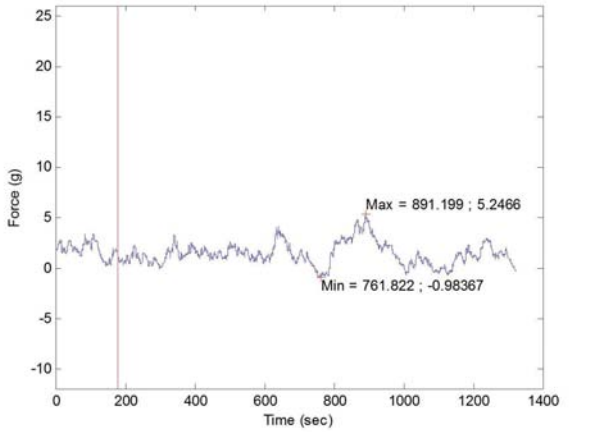

(e) DS 550μg/ml 14 day denervation

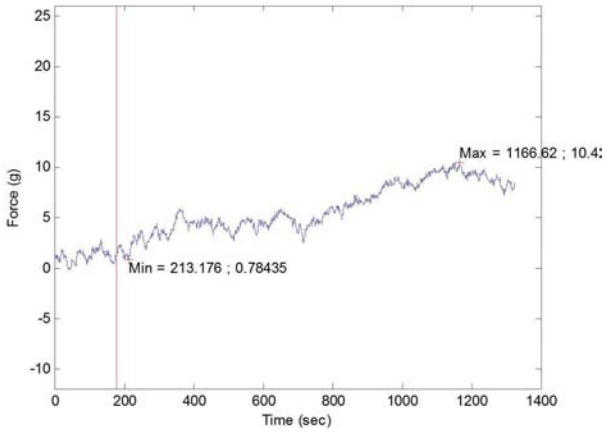

(f) IS 550μg/ml 14 day denervation

Figure 21: Force-time traces of denervated and innervated solei at a 14 day denervation period for (21a) DS stimulated with $4\mu g/ml$ of ACh (21b) IS stimulated with $4\mu g/ml$ of ACh (21c) DS stimulated with $96\mu g/ml$ of ACh (21d) IS stimulated with $96\mu g/ml$ (21e) DS stimulated with $550\mu g/ml$ (21f) IS stimulated with $550\mu g/ml$ of ACh.

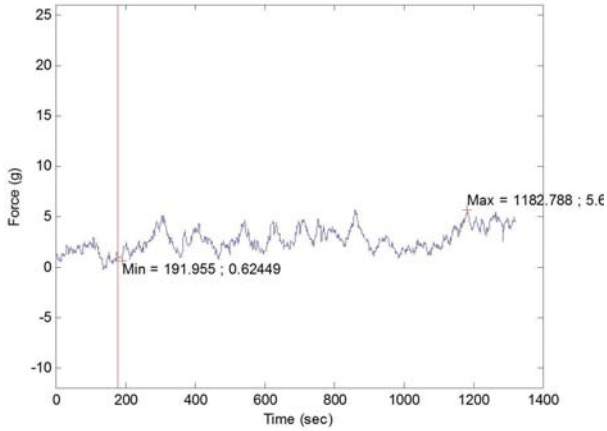

(a) DS 1.6g/ml 14 day denervation

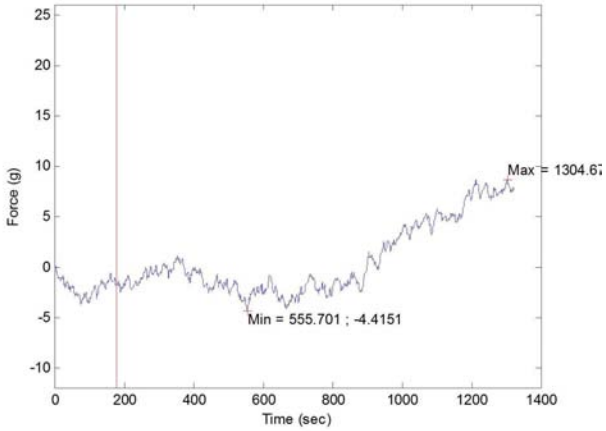

(b) IS 1.6g/ml 14 day denervation

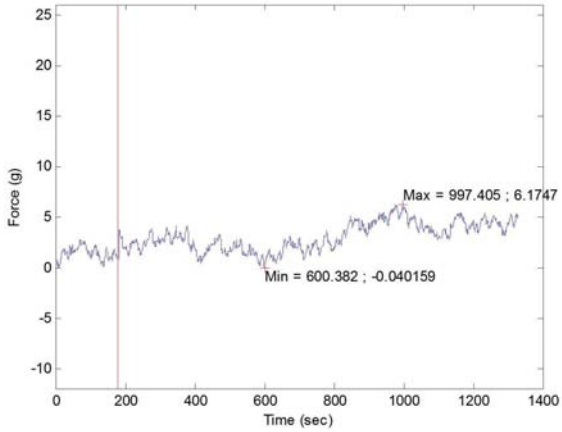

(c) DS 3.2g/ml 14 day denervation

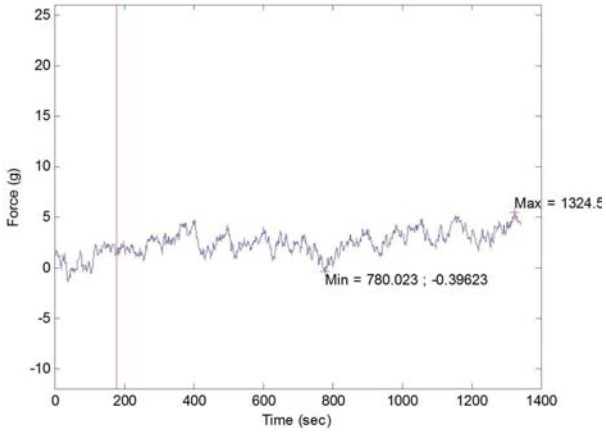

(d) IS 3.2g/ml 14 day denervation

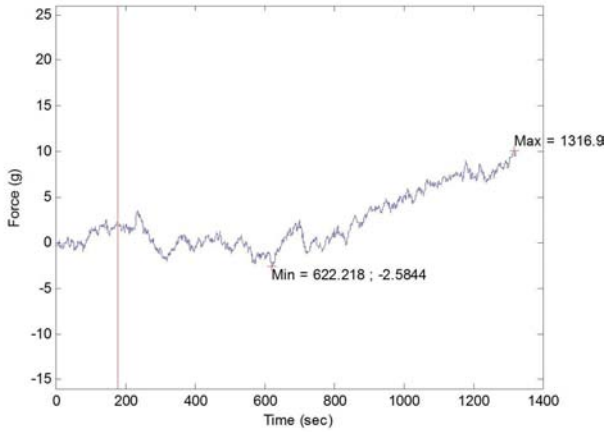

(e) DS 6.3g/ml 14 day denervation

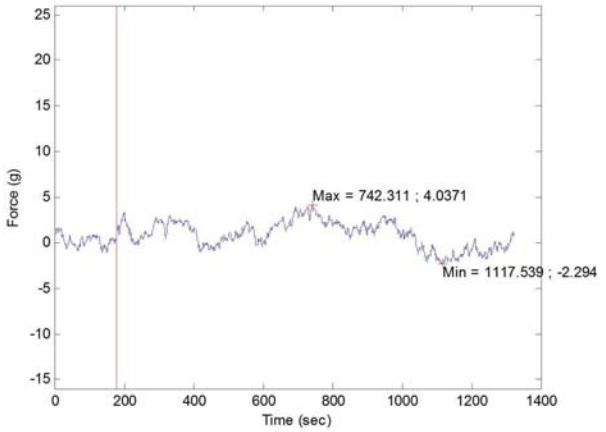

(f) IS 6.3g/ml 14 day denervation

Figure 22: Force-time traces of denervated and innervated solei at a 14 day denervation period for (22a) DS stimulated with 1.6g/ml of ACh (22b) IS stimulated with 1.6g/ml of ACh (22c) DS stimulated with 3.2g/ml of ACh (22d) IS stimulated with 3.2g/ml of ACh (22e) DS stimulated with 6.3g/ml of ACh (22f) IS stimulated with 6.3g/ml of ACh.

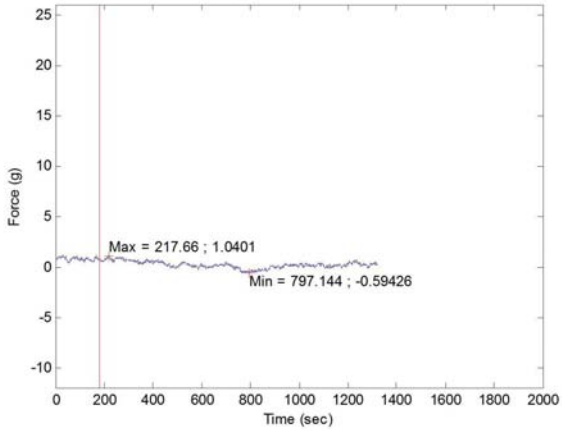

(a) DS 4μg/ml 50-55 day denervation

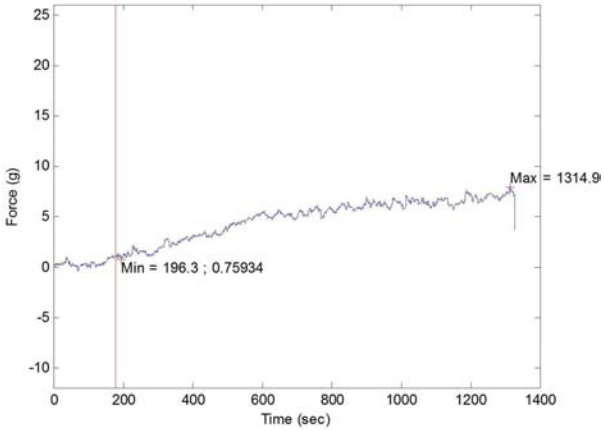

(b) IS 4μg/ml 50-55 day denervation

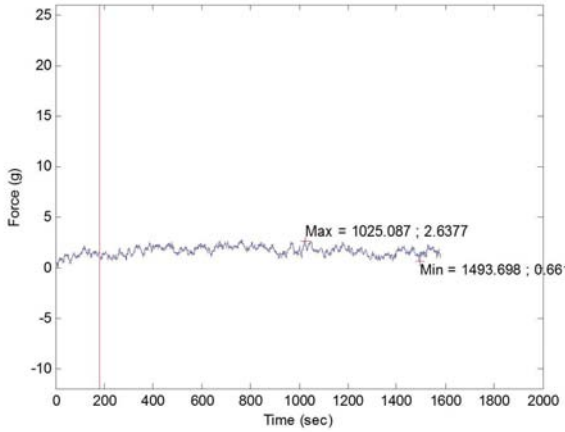

(c) DS 96μg/ml 50-55 day denervation

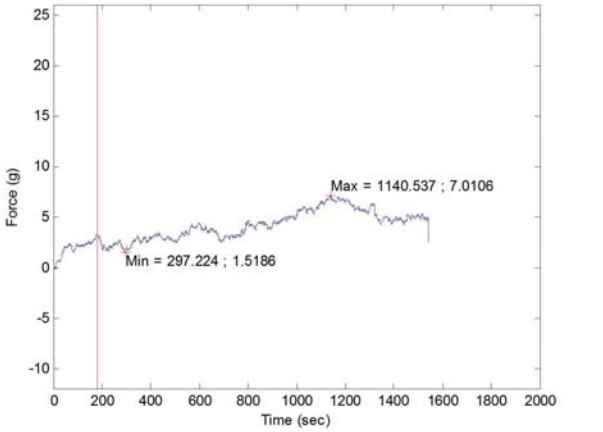

(d) IS 96μg/ml 50-55 day denervation

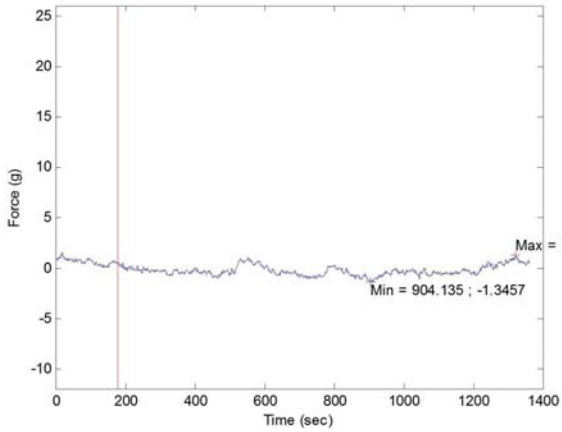

(e) DS 550μg/ml 50-55 day denervation

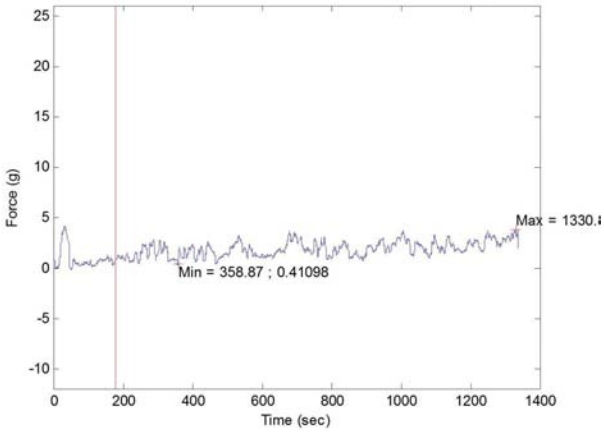

(f) IS 550μg/ml 50-55 day denervation

Figure 23: Force-time traces of denervated and innervated solei at a 50-55 day denervation period for (23a) DS stimulated with $4\mu g/ml$ of ACh (23b) IS stimulated with $4\mu g/ml$ of ACh (23c) DS stimulated with $96\mu g/ml$ of ACh (23d) IS stimulated with $96\mu g/ml$ (23e) DS stimulated with $550\mu g/ml$ (23f) IS stimulated with $550\mu g/ml$ of ACh.

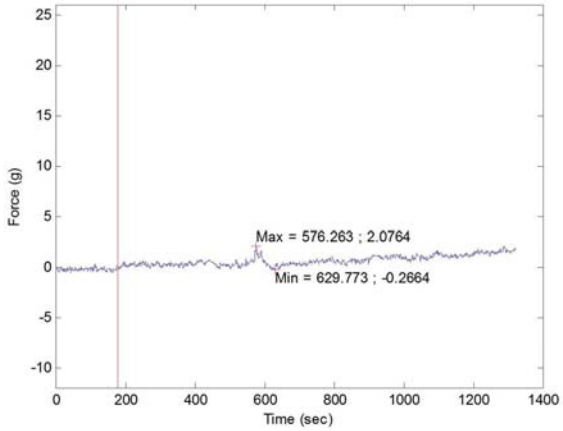

(a) DS 4μg/ml 204-208 day denervation

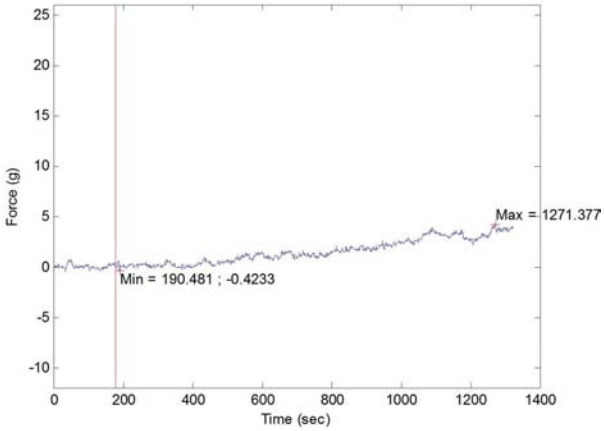

(b) IS 4μg/ml 204-208 day denervation

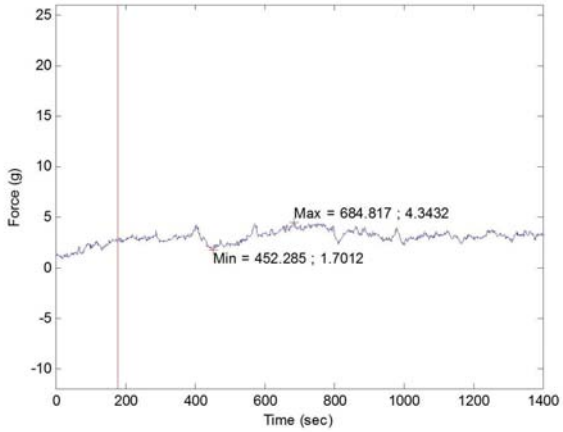

(c) DS 96μg/ml 204-208 day denervation

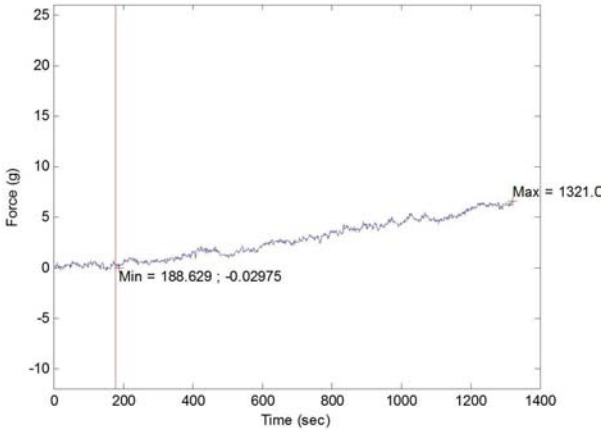

(d) IS 96μg/ml 204-208 day denervation

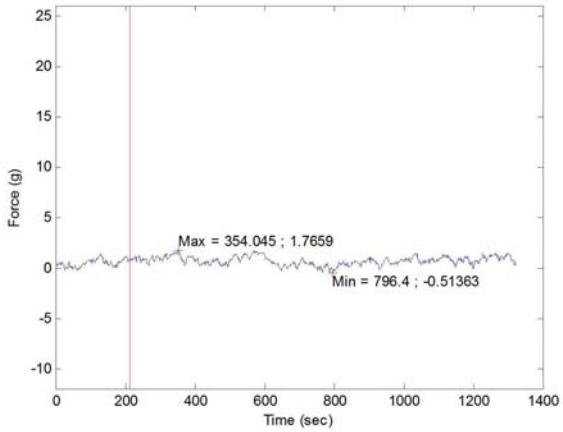

(e) DS 550μg/ml 204-208 day denervation

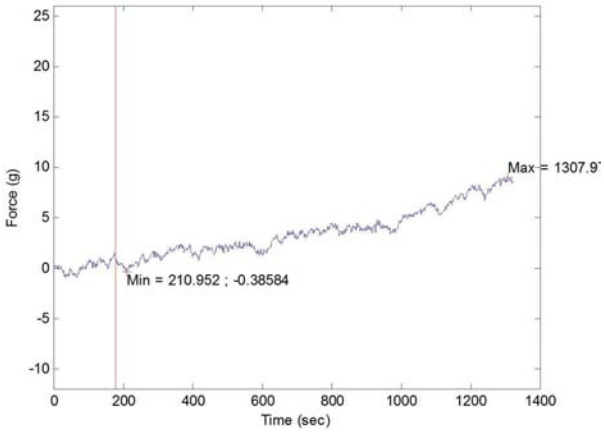

(f) IS 550μg/ml 204-208 day denervation

Figure 24: Force-time traces of denervated and innervated solei at a 204-208 day denervation period for (24a) DS stimulated with $4\mu g/ml$ of ACh (24b) IS stimulated with $4\mu g/ml$ of ACh (24c) DS stimulated with $96\mu g/ml$ of ACh (24d) IS stimulated with $96\mu g/ml$ (24e) DS stimulated with $550\mu g/ml$ (24f) IS stimulated with $550\mu g/ml$ of ACh.

4.2.2 Maximum force of contraction generated by denervated muscles and their contralateral controls

This subsection presents the maximum forces of contraction obtained from the experimental results and discusses them as functions of the four periods of denervation as well as the range of administered ACh concentrations. Maximum forces of contraction as determined directly from the recorded traces, were normalised by cross sectional area (CSA) as described by Brooks and Faulkner [1988]. This was deemed necessary for comparative purposes since experiments were conducted on whole muscles with significant mass and dimension differences. Briefly, the muscle CSA was determined by equation 4.1 as

$$CSA = \frac{m}{L\rho} \tag{4.1}$$

where

m $[g]$ is the whole muscle mass

L $[cm]$ is the length of the muscle

$\rho = 1.06 g/cm^3$ is the density of mammalian skeletal muscle [Mendez and Keys, 1960, Brooks and Faulkner, 1988, Martin et al., 2009]

The recorded muscle force was then divided by the CSA to obtain the normalised force F_{csa}.

The maximum generated F_{csa} will be discussed as functions of each stipulated parameter employed in this study (denervation period and concentration) for each muscle (DS, IS, DG and IG).

Maximum F_{csa} generated by each muscle type as a function of denervation period, presented for each concentration of ACh

Figure 25 displays the results of the maximum F_{csa} for all four muscle types (DS, IS, DG and IG) across all denervation periods and concentrations. Doses falling into the low concentration range ($4\mu g/ml$, $96\mu g/ml$ and $550\mu g/ml$) were administered to muscles from the longer term denervation periods of 50-55 days and 204-208 days and doses from both low as well as high concentration (1.6g/ml, 3.2g/ml and 6.3g/ml) ranges were administered to muscles from the shorter term denervation periods of 7 days and 14 days[9].

From Figure 25, it is evident that the denervated muscles (DS and DG) exhibit a higher sensitivity[10] than their respective innervated contralaterals (IS and IG) for most denervation periods and concentrations. Exceptions occurred only for the gastrocnemii muscles at the extremes of the two highest concentrations of 3.2g/ml and 6.3g/ml, for the two lowest denervation periods, 7 days and 14 days. As previously noted, large doses of ACh have been shown to depress the muscle response.

[9] Only the short term 7 and 14 day denervation period groups were administered high ACh concentration doses. This was due to time and ethics constraints such that a limited number of animals was able to be procured and denervated beyond periods of 14 days.

[10] Refer to Glossary of Terms on page xx.

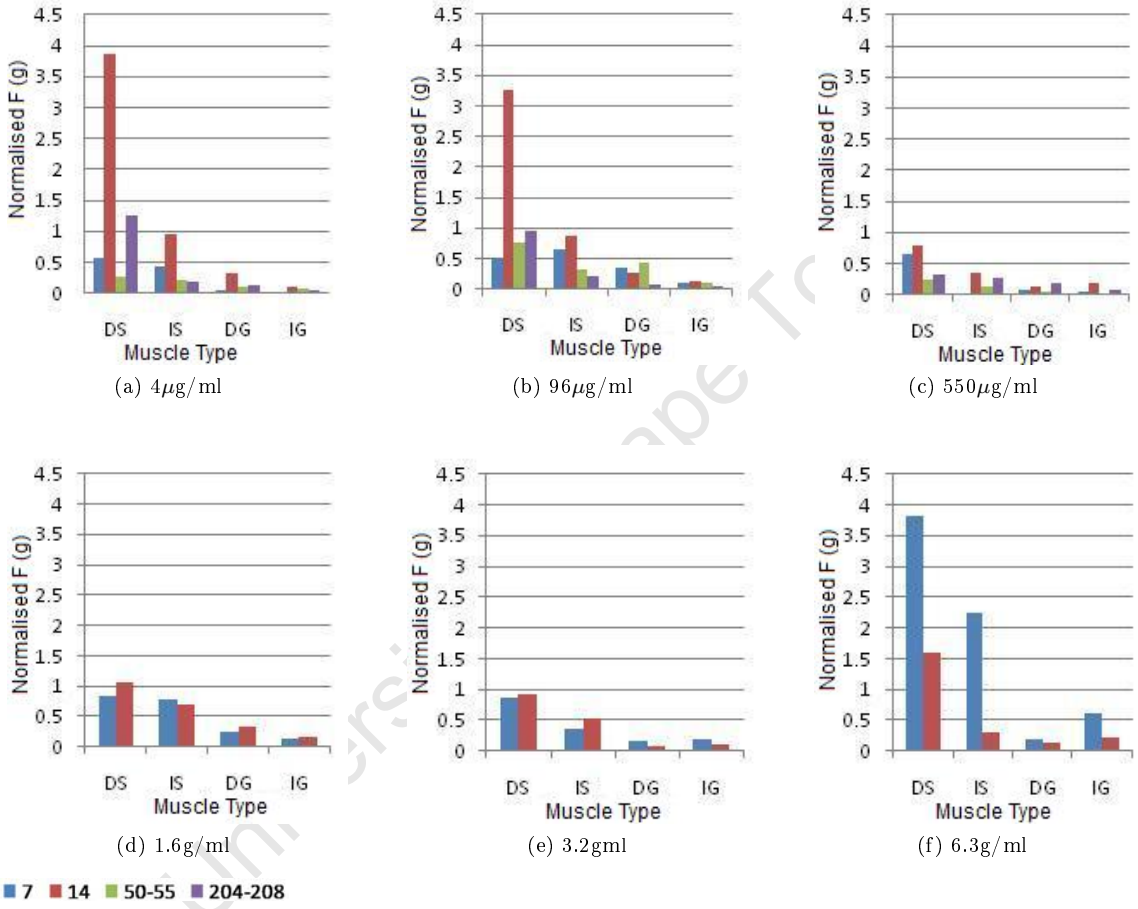

(a) 4μg/ml (b) 96μg/ml (c) 550μg/ml

(d) 1.6g/ml (e) 3.2gml (f) 6.3g/ml

Figure 25: Maximum forces [g] (ordinate) normalised by CSA presented for concentrations of (a) $4\mu g/ml$ (b) $96\mu g/ml$ (c) $550\mu g/ml$ (d) 1.6g/ml (e) 3.2g/ml and (f) 6.3g/ml.

The depressed response noted in this study for muscles at the strongest administered concentrations, is supportive of denervated muscles pre-empting the innervated muscle response. In other words, the depressed response is hypothesized to occur at lower concentrations for denervated than for innervated muscles. Larger denervation periods should be investigated at these concentrations to determine the extent of receptor proliferation and fibre typing. This response was only seen in the DG, indicating that fibre type is an important factor in the underlying physiological rationale responsible for this phenomenon. The difference is more pronounced for the 7 day denervation period than for the 14 day denervation period, complying with literature which cites high sensitivity of gastrocnemii to ACh for this denervation period. In order of decreasing sensitivity, the muscles were ranked as follows: DS, IS, DG, IG. As discussed in section 2.1.4, the IS is known to consist primarily of slow twitch (red, type I) fibres, with the remaining approximate 10-20% being fast twitch (white, type II) fibres and the IG is known to consist mainly of fast twitch fibres. Gauthier and Dunn [1973] reported the preferential alteration of white fibres post-denervation and a resultant increase in the ratio of red and intermediate to white fibres in the mixed semitendinosis muscle of the rat. The slow twitch soleus muscle has been reported to exhibit an increase in the number of fast twitch fibres post-denervation [Bakou et al., 1996]. From this information and a consideration of the results presented here, it can be deduced that the DS still contained the highest ratio of slow to fast twitch fibres, with the ratio decreasing with decreasing sensitivity (or F_{csa}). Since the DS consistently produced the highest forces for all denervation periods, it is hypothesized that a cut off point exists in fibre type changes, such that muscles do not soley consist of one fibre type even after the longest denervation period. This is supported by the histological ATPase fibre type staining results presented in section 4.3. In terms of slow contractures, Hess and Pilar [1963] and Bach-y Rita and Ito [1966] were in agreement that these occurred in slow twitch fibres. Brown [1937] had earlier considered the slow contracture effects to occur in all muscle fibres, but noted a *pari passu* relationship between the increase in membrane sensitivity and that of the slow contracture in denervated muscles. Thus the order of force sensitivity observed in this study indicates that slow twitch fibres produce stronger contractures than fast twitch fibres.

In the low concentration range of 4-550$\mu g/ml$, the 14 day denervation period was consistently the highest period of sensitivity for all solei. This is evident in the red histogram bars in Figures 25(a)-(c). The high sensitivity of the denervated muscles after 14 days of denervation is consistent with literature [Gauthier and Dunn, 1973]. Recall from section 2.1.4 that Hartzell and Fambrough [1972], in their study on the denervated rat diaphragm, observed the occurrence of the highest number of nAChR's at 14 days post-denervation. This supports and explains the increased force output of the denervated muscle as observed in this study at 14 days post-denervation. The number of nAChR's for different denervation periods as reported by Hartzell and Fambrough [1972] is plotted in Figure 26.

No such trend of a high sensitivity denervation period was observed (Figures 25(d)-(f)) in the

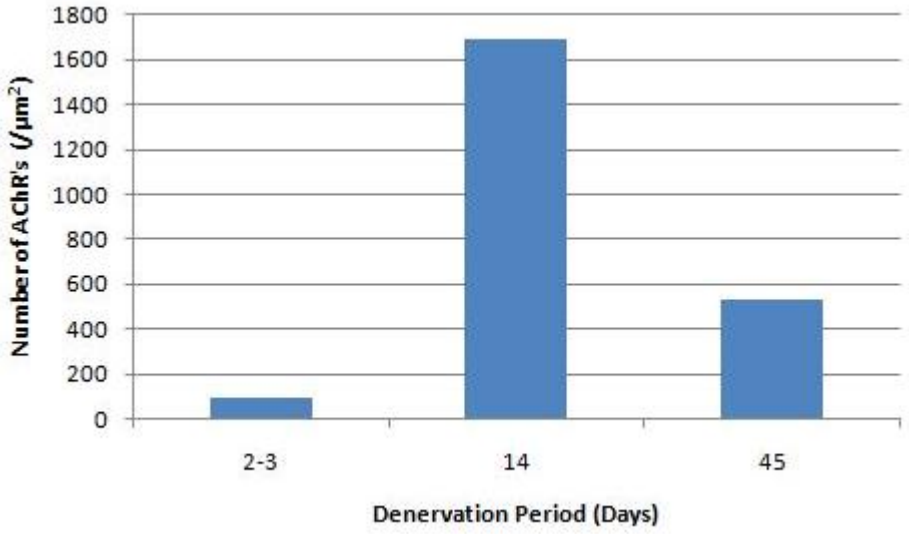

Figure 26: Number of nAChR's/μm^2 in denervated rat diaphragm presented for three denervation periods as reported by Hartzell and Fambrough [1972].

high concentration range of 1.6-6.3g/ml. It was however noted, that the DS and IS from the 7 day denervation period group produced the highest forces at the strongest concentration of 6.3g/ml. The short denervation period suggests predominance in slow twitch fibre types and increased receptor proliferation (not yet peaked, since the largest numbers only occur 14 days post-denervation). Thus a large number of slow twitch fibres with increased ACh sensitivity due to receptor proliferation reacts favourably to large concentrations by producing large forces, supporting the hypothesis that large concentrations under combined conditions of fewer slow twitch fibres and nAChR's result in a depressed response to ACh. A pertinent question is thus presented in which factor (fibre type or receptor number) plays the biggest role in ACh response.

The percentage difference in the maximum F_{csa} between innervated and denervated solei at each denervation period for all concentrations is depicted in Figure 27. The highest percentage difference in force was seen to occur at a 14 day denervation period (indicated by the red series in Figure 27) except at the two highest concentrations of 3.2g/ml and 6.3g/ml. The highest maximum F_{csa} percentage difference at 14 days post-denervation was followed by denervation periods of 204-208 days, 50-55 days and 7 days in order of decreasing percentage difference. This again supports the occurrence of major physiological change at 14 days post-denervation, after which the largest differences were seen to follow a trend of an increase in percentage maximum F_{csa} difference with an increase in denervation periods.

Within the low concentration range, a trend is observed such that an increase in concentra-

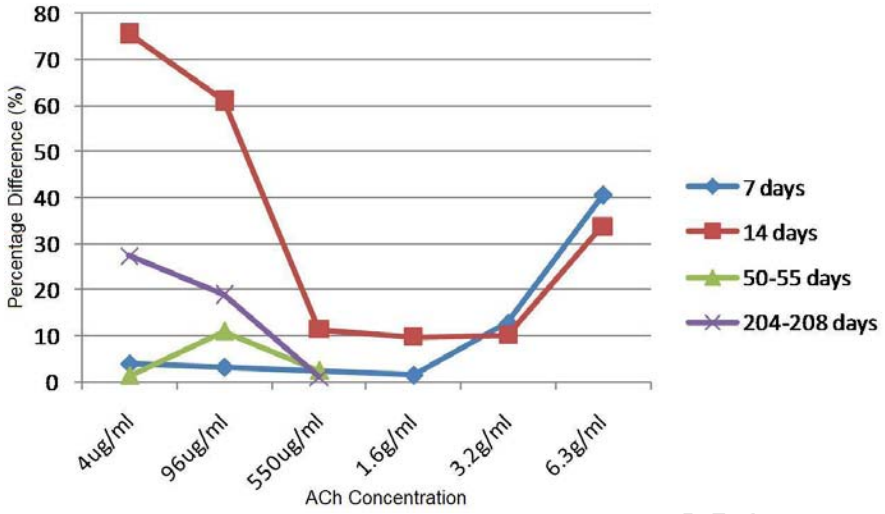

Figure 27: Percentage difference in maximum forces of contraction between innervated and denervated solei over full concentration range and all denervation periods.

tion is accompanied by a decrease in percentage difference. An exception occurs at the 50-55 day denervation period in which a low percentage difference is recorded at a concentration of $4\mu g/ml$, followed by an increase in this difference at the concentration of $96\mu g/ml$. Upon considering the forces generated for this denervation period at all tested concentrations, small forces were observed to accompany small percentage differences in maximum F_{csa} and similarly, large percentage differences in maximum F_{csa} were accompanied by comparatively large generated forces. To illustrate specifically, the maximum F_{csa} generated at $4\mu g/ml$ were 0.26g (DS) and 0.21g (IS). At $96\mu g/ml$, the forces were larger at 0.75g (DS) and 0.32g (IS), as was the percentage difference. At $550\mu g/ml$, the forces decreased (from those at $96\mu g/ml$) to 0.23g (DS) and 0.13g (IS) along with a decrease in percentage difference in F_{csa}. The demonstration of large forces being produced by low concentrations begs the question of comparitive nAChR sensitivity: do either old or new receptors exhibit higher sensitivity than the other, or perhaps even a higher binding affinity to ACh?

Within the high concentration range, an increase in administered ACh concentration was accompanied by an increase in the maximum F_{csa} percentage difference. This is in contrast to the opposite trend observed in the low concentration range (with the exception of the 50-55 day denervation period trend). As mentioned in the discussion on sensitivity, the two highest concentrations administered (3.2g/ml and 6.3g/ml) rendered a higher percentage difference between the 7 day DS and their innervated counterparts than the 14 day DS and their innervated contralaterals. This suggests that a concentration threshold was reached in which all the receptors of the 7 day DS were saturated, thus producing considerably higher forces than those of the 14 day DS.

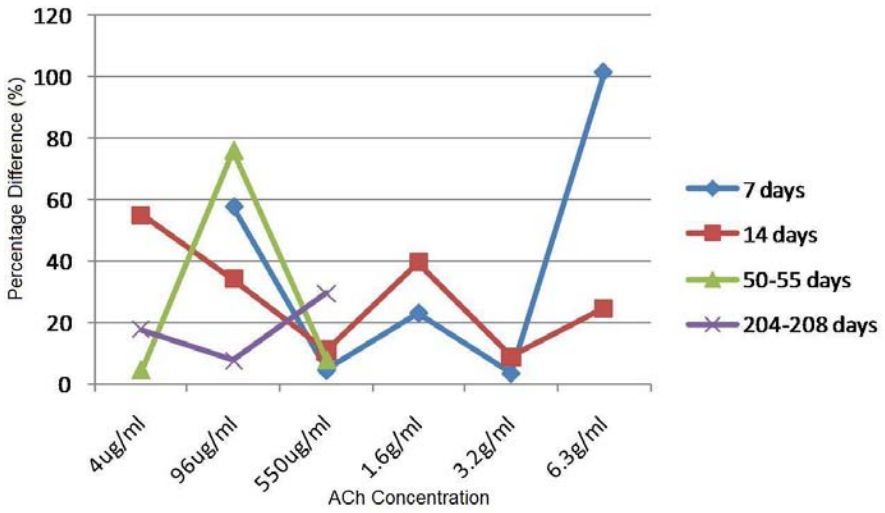

Figure 28: Percentage difference in maximum forces of contraction between innervated and denervated gastrocnemii over full concentration range and all denervation periods.

Thus, in the low concentration range, large percentage differences are accompanied by comparatively large forces and greater numbers of nAChR's/μm^2; and in the high concentration range, large percentage differences are accompanied by large forces, but the high concentrations presumably saturate the receptors and become the maximum F_{csa} deciding factor along with fibre type.

The percentage difference in the maximum F_{csa} between IG and DG at each denervation period for all concentrations is depicted in Figure 28. These plotted series did not display trends as clear as those observed for the slow twitch solei (depicted in Figure 27).

A consideration of the low concentration range exhibits a decrease in the percentage difference with an accompanying increase in concentration for 7 and 14 day DG, with a higher percentage difference between the 7 day DG and their innervated contralaterals than the same 14 day comparison. This may be indicative of the timeline of a number of physiological changes. Either, nAChR proliferation occurs sooner in fast twitch muscles such as the gastrocnemius or the change in ratio of fibre types (type I to type II fibres) plays a significant role in the contractile ability of the muscle, or both. To the best knowledge of the author, no studies between fast and slow twitch muscles which directly compare the times of receptor proliferation and the resulting numbers of nAChR's/μm^2 at different stages of denervation have been conducted. Separate studies however, have considered various muscles (and hence different fibre types) at different stages of denervation [Gauthier and Dunn, 1973, Brown, 1937, Cornachione et al., 2011, Kilarski and Sjostrom, 1990]. Brown [1937] conducted experiments on mammalian gastrocnemii denervated for periods between 4 and 27 days. Specific attention was drawn to the high sensitivity of the mammalian gastrocnemii muscles 6 days

post-denervation which supports the observations made in this study. No mention was made of further increase in sensitivity. Rosenthal [1977] and Gauthier and Dunn [1973] reported a preferential alteration of fast twitch fibres, supporting the author's suggestion of sooner changes in gastrocnemii relating to fibre typing affecting the muscles' contractile response post-denervation.

In tests conducted on DS muscles for periods of 3, 14 and 28 days, muscles were noted to display significant physiological changes 14 and 28 days post-denervation [Hyatt et al., 2006], which again supports the observations made in this study in which 14 day DS have shown superior sensitivity to other denervation periods. The results of the experiments conducted by Hartzell and Fambrough [1972] as depicted in Figure 26, on the mixed fibre type composition of rat diaphragm muscle, enable a comparison based on muscle fibre type composition, fibre type changes and receptor proliferation to be made. The innervated rat diaphragm is composed of 59.8% fast twitch fibres [Jeckel-Neto et al., 1993], the soleus is composed of 10-20% fast twitch fibres [Hyatt et al., 2006] and the gastrocnemius is composed of 80% fast twitch fibres [Cornachione et al., 2011]. High sensitivities at 14 day denervation periods are evident in both solei as well as diaphragmatic muscle, which have a significantly higher slow to fast twitch fibre ratio than the gastrocnemii. 7 days post-denervation, the fast twitch fibres had not yet undergone full physiological changes (hence fast twitch fibres, known to be more dependent on the nerve supply [Bajusz, 1964], are still present at 7 days post-denervation) but by 14 days, Gauthier and Dunn [1973] reported that fast twitch fibres resembled slow twitch (red, type I) fibres, although with significantly less mitochondria. In their experiments on fast twitch fibres of the EDL muscles of Long Evans rats (the same strain used in this study), Ørtenblad and Stephenson [2003] demonstrated that an inhibition of mitochondrial ability to produce ATP resulted in a reduction in the excitability of the fibres. This may provide a further explanation for the lower sensitivity of gastrocnemii muscles at 14 days post-denervation compared to 7 days post-denervation.

Despite these differences in sensitivity between the 7 and 14 day denervation periods of the gastrocnemii, the percentage differences in F_{csa} still remain fairly close in contrasting comparison to the solei under the same conditions in the low concentration range. Here the solei showed a substantial difference between the 7 and 14 day denervation periods, with the 14 day denervation period consistently exhibiting a higher percentage difference than the 7 day denervation period, as well as being higher than the 14 day DG percentage difference.

For the 50-55 day denervation period, the percentage difference in maximum F_{csa} for the gastrocnemii follows the same trend as that of the solei in the low (4-550$\mu g/ml$) concentration range. This is evident in the green traces in Figures 27 and 28. Similar observations to those made with the solei with regard to the size of F_{csa} generated in relation to the percentage difference in maximum F_{csa} can be made with the gastrocnemii. That is, low percentage differences were accompanied by low forces and the high percentage difference at 96$\mu g/ml$ was accompanied by relatively large forces. The 204-208 day denervation period displayed this same trend, although the percentage

difference of maximum F_{csa} as a function of concentration produced a different pattern to that observed for the solei under the same conditions (refer to the purple traces in Figures 27 and 28 for visual clarity).

A consideration of the high concentration range for percentage differences in F_{csa} for gastrocnemii, illustrates a similarity in the 7 and 14 day series as they follow the same trend (refer to the red and blue series in Figure 28). Whilst the solei displayed a clear increase in percentage difference in force as a function of increasing concentration, no such trend was apparent for the gastrocnemii. The biggest discrepancy between the 7 and 14 day denervation periods occurred at the highest concentration of 6.3g/ml, where the 7 day denervation period displayed a higher percentage force difference than that of the 14 day denervation period (not the case with the other two concentrations in the high concentration range). In this concentration range, small percentage differences in force between the DG and IG were again accompanied by small forces (F_{csa}).

Maximum F_{csa} generated by each muscle type as a function of concentration of ACh, presented for each denervation period

Figures 29 and 30 illustrate the effects of an increase in concentration on the maximum F_{csa} produced for each muscle at different stages of denervation.

A consideration of the 7 day denervation period indicates that the DS, IS and IG (Figures 29a and 29b respectively) all exhibited an increase in contractile force with an increase in the full range of (low and high) concentrations ($4\mu g/ml$ - 6.3g/ml) and thus all displayed a peak force at the highest concentration of 6.3g/ml. The graphs display the same trends between the innervated and denervated muscles as well as between solei and gastrocnemii with change in concentration for this denervation period.

For a denervation period of 14 days, the DS peak force occurred at the lowest concentration of $4\mu g/ml$ (see Figure 29c). Within the low concentration range the DS displayed a decrease in peak force with an increase in concentration. Within the high concentration range (1.6-6.3g/ml) however, the forces generated by the DS increased with an increase in concentration, but the maximum force in this range was noted to be less than half that of the maximum generated in the low concentration range. The stable trend of the forces generated by the IS in the low concentration range demonstrated a very slight decrease with an increase in concentration in comparison to the dramatic decrease displayed by the DS in this concentration range. In the high concentration range, the IS exhibited a steeper decreasing trend with an increase in concentration, in contrast to the DS increase in force with an increase in concentration.

For a denervation period of 50-55 days, the peak force which the DS generated across the low concentration range occurred at $96\mu g/ml$. The IS followed the same force trend as the DS (see Figure 30a) over this concentration range, but the forces generated were lower than those of the DS, as was the case for all denervation periods explored. The IS force generated at $4\mu g/ml$ was

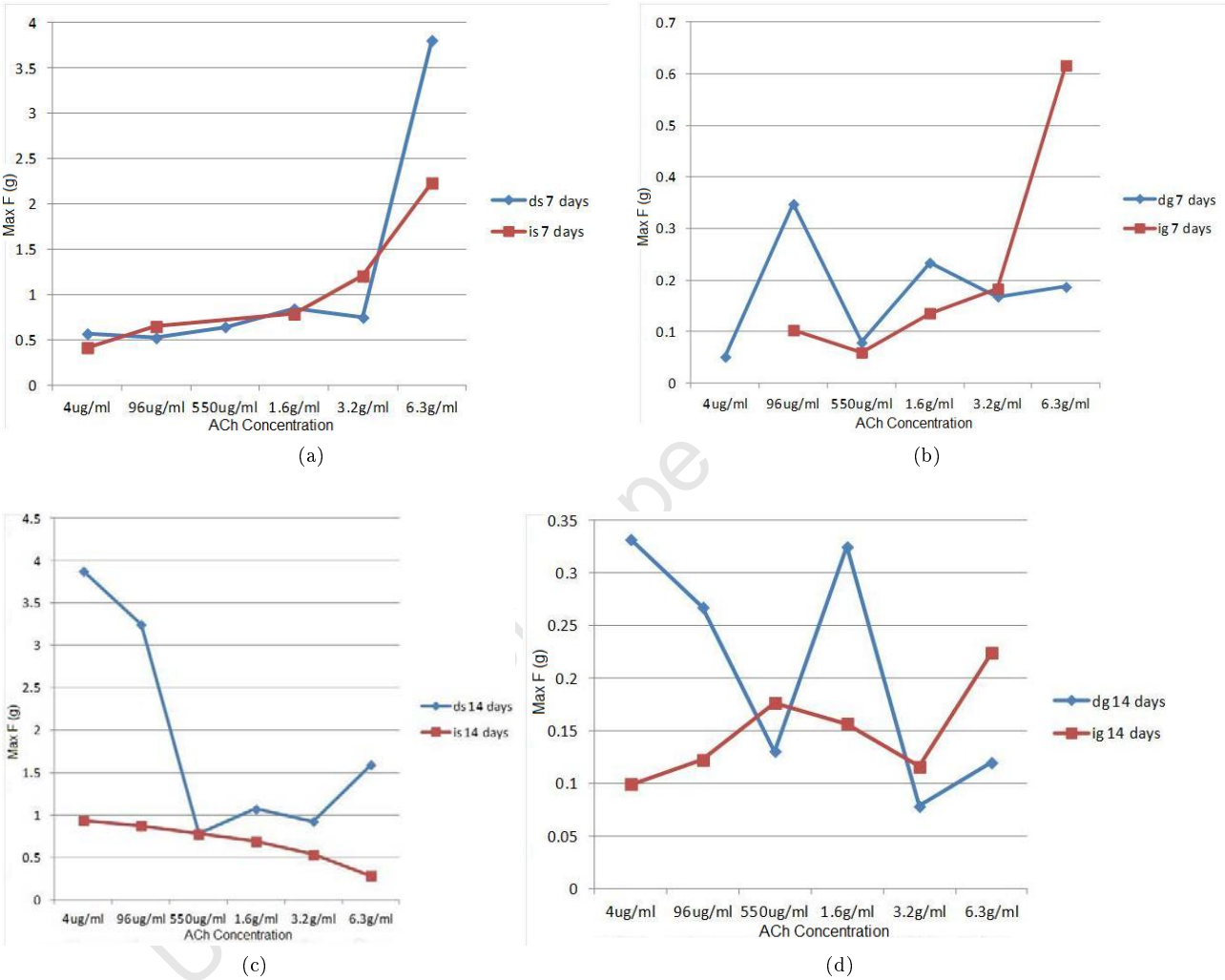

Figure 29: Maximum forces [g] of contraction (ordinate) for denervated and innervated solei and gastrocnemii as a function of concentration for short term denervation periods. (29a) IS, DS at 7 day denervation (29b) IG, DG at 7 day denervation (29c) IS, DS at 14 day denervation (29d) IG, DG at 14 day denervation

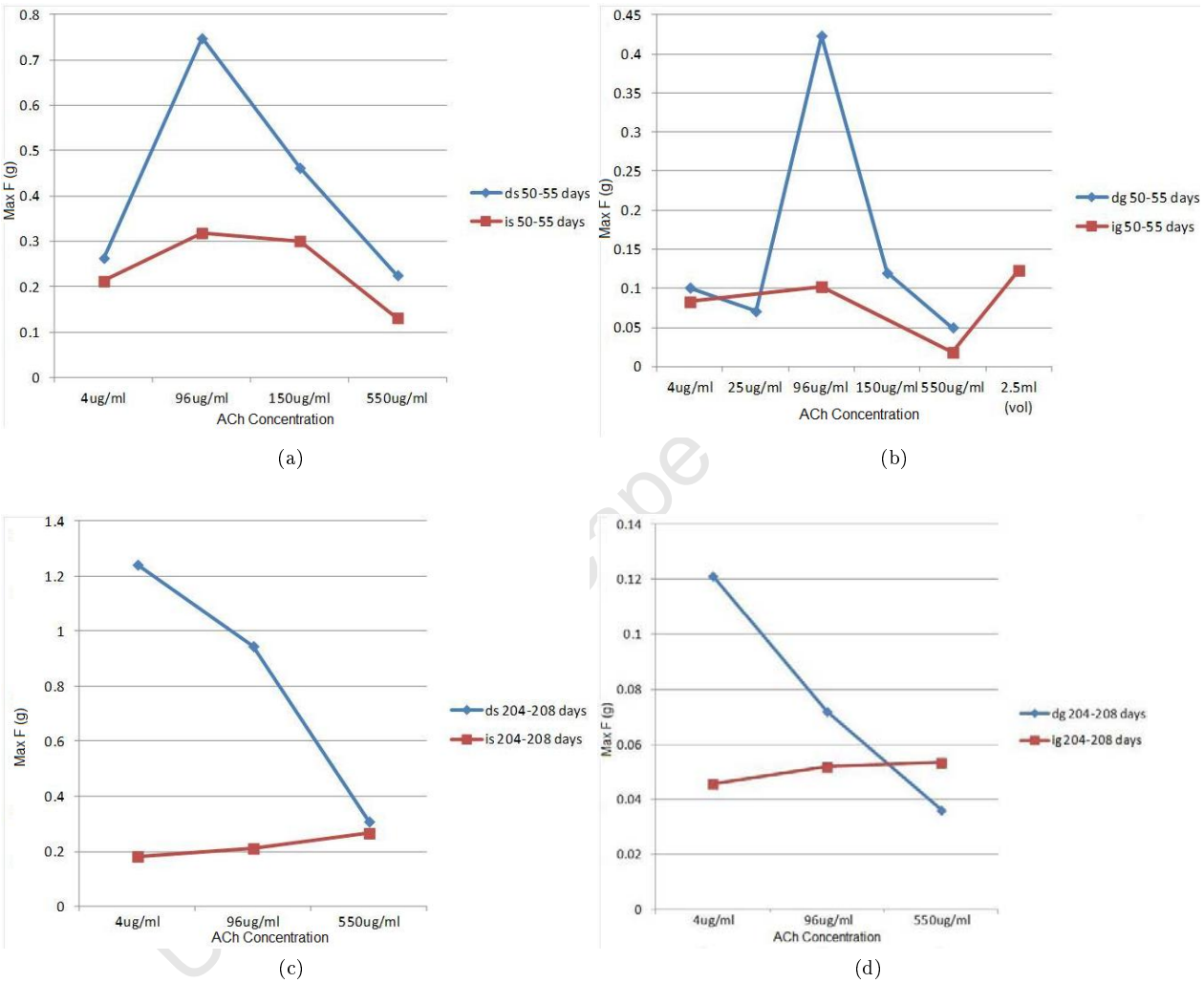

Figure 30: Maximum forces [g] of contraction (ordinate) for denervated and innervated solei and gastrocnemii as a function of concentration for long term denervation periods. (30a) IS, DS at 50-55 days denervation (30b) IG, DG at 50-55 day denervation (30c) IS, DS at 204-208 day denervation (30d) IG, DG at 204-208 day denervation.

low, peaked at $96\mu g/ml$ and was followed by a steady decrease with an increase in concentration thereafter. The same holds true for the DS, but the gradient of decrease in force with increase in concentration was steeper than that of the IS. The peaks at lower concentrations suggest that different ideal concentrations for different periods of denervation may exist which will generate maximum forces.

For a denervation period of 204-208 days, the DS peak force occurred at the lowest concentration of $4\mu g/ml$. The forces generated under these conditions were shown to decrease with an increase in concentration, as was the case with the 14 day denervation period (see the blue series in Figures 30c and 29c respectively). However, the forces generated at 204-208 days were smaller than those generated at 14 days and exhibited smaller decreases with increasing concentrations. The forces generated by the IS 204-208 days post-denervation in the low concentration range displayed an increase in force with a corresponding increase in concentration, as was observed with the 7 day denervation period.

For a denervation period of 7 days the IG followed the same force generation trend as the IS at this period of denervation (see Figures 29a and 29b), both of which displayed an increase in concentration across all ranges. The forces generated by the IG were however, lower than those generated by the IS. The IG peak force occurred at the highest concentration of 6.3g/ml. The DG did not follow the same force generation trend as either the DS or the IG at this denervation period. Instead, the DG peaked at $96\mu g/ml$, its low concentration range trend following the same pattern of force generation as the DS denervated for a 50-55 day period (refer to Figure 30a). The DG produced a second (lower) force peak at the lowest concentration of 1.6g/ml in the high concentration range (Figure 29b).

For a denervation period of 14 days, the DG generated a peak force at $4\mu g/ml$ within the 4-$550\mu g/ml$ concentration range, similar to the case of the DS under the same conditions. This is evident in the blue series in Figures 29c and 29d. Furthermore, it can be seen from these figures that the DG decreased in much the same manner as the DS denervated for this period and within the low concentration range. Still within the 14 day denervation period, an increase in the force generated with an increase in the concentration (within the 4-$550\mu g/ml$ range) was observed with the IG. This trend is comparable to that of the IS at a denervation period of 204-208 days, illustrated in Figure 30c. The IG was further noted to generate a higher force than the DG at $550\mu g/ml$ at 14 days post-denervation. The DG generated a second peak in the high concentration range at the lowest concentration of 1.6g/ml. This 'two peak' observation was similarly made for the DG at a denervation period of 7 days (Figure 29b), although the second peak in this 14 day instance was considerably higher and similar to the first peak, whereas the second force peak noted at 7 days was significantly lower than the first. The first 7 day denervation peak and both peaks noted in the 14 day denervation period were all within the same range (just below 0.35g). The IG and DG followed the same force trend in the high concentration range 14 days post-denervation but the IG

generated larger forces than those generated by the DG.

For a denervation period of 50-55 days, the DG peak force was generated at $96\mu g/ml$. The DG followed the same trend as the DS under the same conditions (compare the blue series in Figures 30a and 30b). Both force trends peaked at a concentration of $96\mu g/ml$. The IG and DG followed the same force generation trend for this denervation period, with the IG generating lower forces than the DG, as was the case with the DS and IS at this denervation period.

For a denervation period of 204-208 days, the DG followed the same trend as the DS under the same conditions (refer to Figures 30c and 30d). Both the DG and DS in this case peaked at lowest concentrations of $4\mu g/ml$. Similarly, the IG under these conditions followed the same force generation trend as the IS (compare the red series in Figures 30c and 30d), although the force generated by the IG when $550\mu g/ml$ was administered, was higher than that generated by the DG for the same concentration. This same occurrence was observed between the IG and DG for the same concentration at 14 days post-denervation (refer to Figure 29d). Upon consideration of the high concentration range, it may be noted that the IG, unlike the IS (in comparison to its denervated contralateral) generated higher maximum F_{csa} than than the DG (204-208 day denervation period). This was also true for $550\mu g/ml$ (the highest concentration in the low concentration range) for denervation periods of 14 and 204-208 days.

Brown [1950] reported that large concentrations of ACh at the NMJ were demonstrated to cause a neuromuscular block such that local continuous depolarisations were able to cause local contractions, but blocked the conduction along the muscle fibres. This effect appears to be more apparent in solei denervated for periods beyond 7 days and for all periods of denervation for the gastrocnemii (further supporting that changes occur more quickly in fast twitch muscle and that denervation has more of an effect on fast twitch fibres than slow twitch fibres) within the low concentration range. DS display an increase in force output with an increase in concentration in the high concentration range, again pointing to the suggestion that a threshold concentration exists such that the conduction blocking effect of large doses of ACh may be overcome, thus enabling the development of slow contracture. This is evident in short term denervation periods of 7 and 14 days, but would benefit from trend confirmation by further testing with longer denervation periods. Denervated gastrocnemii do not display any trends with increase in concentration for the 7 day denervation period, but appeared to follow the effects reported by Brown [1950] in the low concentration range for all other periods of denervation (as with the DS).

4.2.3 Relationship between concentration, denervation period and time to maximum force of contraction

It is necessary to note at this point that time courses of contraction in this study were observed to be longer than those reported in literature. This may be due to a difference in a number of experimental features between the experimental set-up employed in this study and those reported

in literature. For example, whilst Hess and Pilar [1963] conducted *ex vivo* experiments on skeletal muscles suspended in an oxygenated Krebs solution contained within a tissue bath, their experiments also differed from the present study in a number of ways. The animals which were used (cats) were anaesthetised with sodium pentobarbital (proven to have an acute and direct effect on skeletal muscle contractility [Taylor et al., 1984]), where the effect is more pronounced in slow twitch fibre reactions (slow twitch fibres were tested by Hess and Pilar [1963]). Additionally, a larger tissue bath was used in the present study. Whilst care was taken to ensure that ACh was always administered at the same distance away from the muscle of each test for consistency, use of a larger tissue bath may have resulted in a longer diffusing time for ACh to reach the nAChR's. It is postulated that one or more of these differences may have impacted the time course of contraction.

As expected, the solei and gastrocnemii produced their maximum forces at different times post ACh administration. The (predominantly fast twitch) innervated gastrocnemii reached maximum contractile forces faster than the (predominantly slow twitch) solei. Figure 31 depicts the differences between time to maximum force of contraction for denervated muscles and their innervated contralaterals for all concentrations used (plotted on a log scale on the horizontal axis) as well as for the various denervation periods.

Figure 31a illustrates that gastrocnemii from every denervation period implemented in this study (dotted series) took longer to reach maximum forces of contraction than their innervated contralaterals. Further, gastrocnemii from the 7 and 14 day denervation periods followed the same trends with increasing concentrations, which both follow the same trend as the IG from the 7 day denervation period group, albeit at slower times. The IG from the 14 day denervation period group differs from this same trend only slightly (in its response to the low concentration of $96\mu g/ml$). The IG from the 50-55 day and 204-208 day denervation period groups follow the same trend of decreasing time to maximum output force with increasing concentration. Their denervated counterparts too, together are similar in their response, but differ from the innervated muscles of these periods, as shown in Figure 31a. Inflection points are observed at $96\mu g/ml$ for both these muscles, as seen for the IG from the 7 day denervation period. Thus, all the denervated muscle responses appear to be mimicking the response trend of the IG from the 7 day denervation period group, although at a lag.

In terms of maximum contraction force, the response of DS in comparison to IS followed the opposite trend to that of the gastrocnemii. That is, the DS muscles from every denervation period produced their maximum contractile output faster than all their innervated contralaterals. Similarities in grouping were also noted. This involved the 7 and 14 day DS muscles following the same trend (similar to that of the IS). Recall the same grouping from the gastrocnemii observations, although displaying different trends to the solei. Moreover, the long term denervation periods (50-55 days and 204-208 days), again followed the same patterns of time to maximum contraction with respect to increase in concentration, and were again similar to that produced by the IS of the 7 day

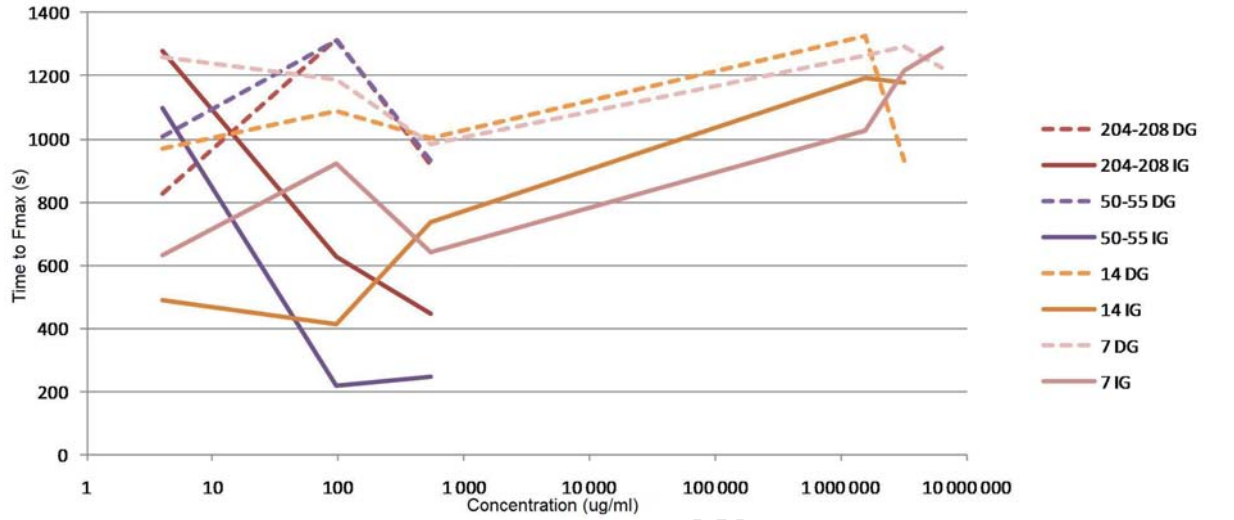

(a) Gastrocnemii

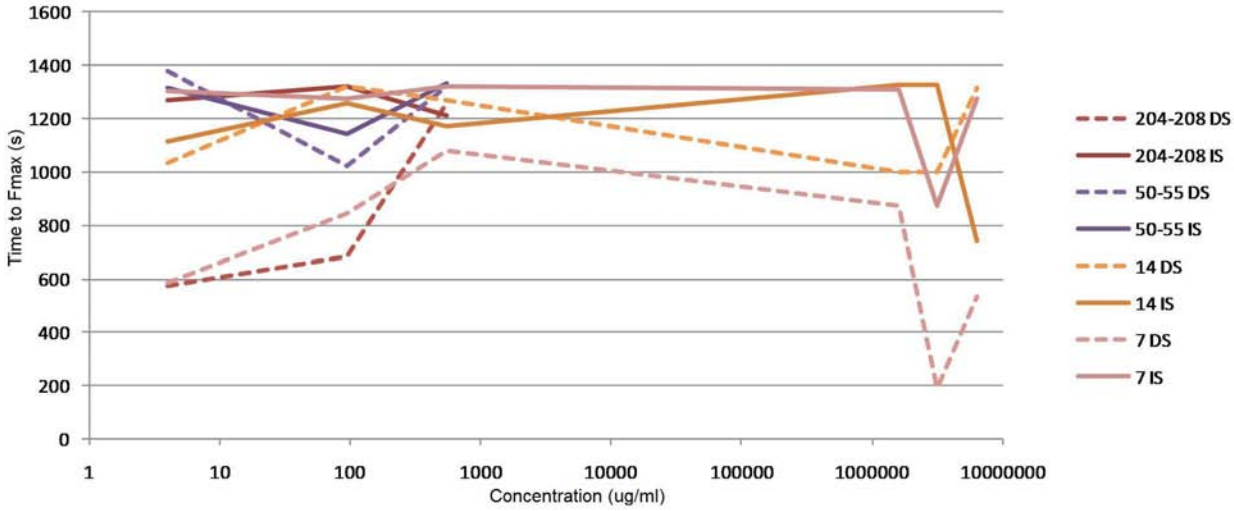

(b) Solei

Figure 31: Time to maximum contraction force (ordinate [s]) versus concentration (abscissa $[\mu g/ml]$) for (31a) DG and IG and (31b) DS and IS, for all denervation periods.

denervation group (with similar response grouping noted from gastrocnemii muscles). Inflection points were again noted at a concentration of $96\mu g/ml$. In general, the muscle and trend producing the fastest time to contraction was the DS, at a 7 day denervation period. The slowest was the 204-208 day IS.

Figures 31a and 31b illustrate that the responses of the slow twitch solei and that of the fast twitch gastrocnemii and their denervated counterparts, at varying stages of denervation, appear to produce "mirror image" reactions of one another.

Figures 32 and 33 provide a direct visual correlation of time to maximum contraction with maximum forces of contraction for various time periods. Each image is presented for denervated muscles and their innervated contralaterals for a different concentration.

Figure 32a illustrates the maximum force-time-denervation period relation for a concentration of $4\mu g/ml$. As previously demonstrated, the DS produced higher forces than the IS. Additional information from this figure shows that denervation periods of 7, 14 and 204-208 days exhibit shorter times to contraction than the IS. At 50-55 days the time to maximum contraction of the DS showed no significant difference to that of the IS. The largest generated force at this concentration for these muscles was produced by the DS at 14 days of denervation, which also displayed the longest time to maximum contraction. An increase in concentration to $96\mu g/ml$ further demonstrated this effect. Moreover, the maximum contraction time of the DS at 14 days of denervation was even closer to that of its respective IS, but again the former produced a higher force. The times to maximum contraction of the remaining denervation periods (7, 50-55 and 204-208 days) for the DS were less than the IS for this increased concentration. For stimulation by $550\mu g/ml$, the times to peak force for the DS showed no significant difference to that of the IS, despite contracting at larger forces. The times were slightly greater at 14 days post-denervation for the DS than the IS (1272s and 1172s respectively) and slightly less at 7 days post-denervation for the DS compared to the IS (1082s and 1322s respectively).

Figure 33 illustrates the time to peak force for increasing concentration within the high concentration range (1.6g/ml-6.3g/ml). The DS times to contraction were consistently shorter than those of the IS except at the highest concentration of 6.3g/ml at 14 days of denervation (the highest sensitivity period of the DS) where the DS took a longer time to reach its' peak force than the IS. The DS forces were again consistently higher than the forces produced by the IS muscles (as was observed in the low concentration range). Increasing time to peak force occurred simultaneously with decreasing peak force of contraction for the DS.

Thus in general, an increase in concentration within the low concentration range resulted in the DS contracting at times closer to those of the IS. The denervation periods themselves however, showed no clear correlation with time. Only the 7 day and 204-208 day DS displayed an increase in time to contraction with an increase in concentration (see Figure 31b, series *7 DS* and *204-208 DS*). The 14 day and 50-55 day denervation periods do not follow this trend.

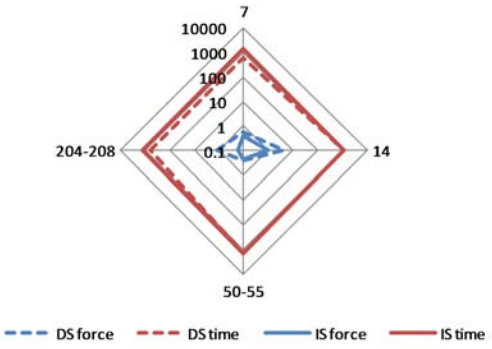

(a)

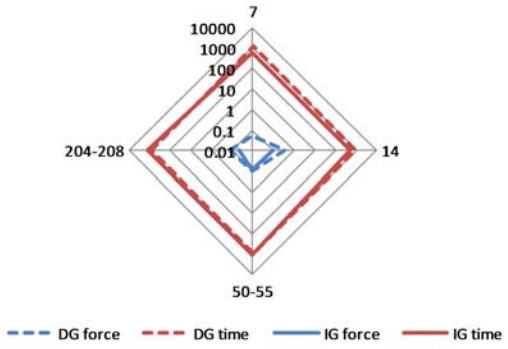

(b)

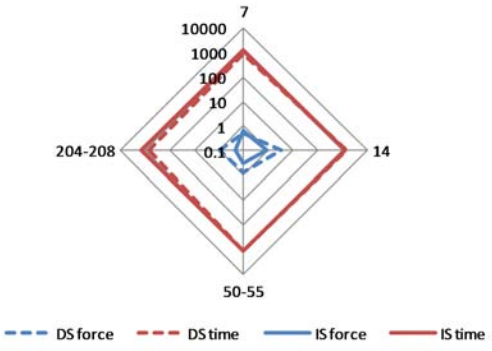

(c)

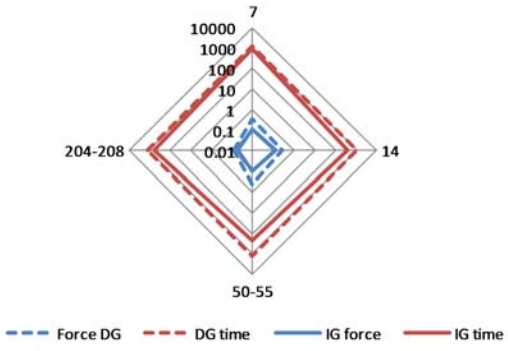

(d)

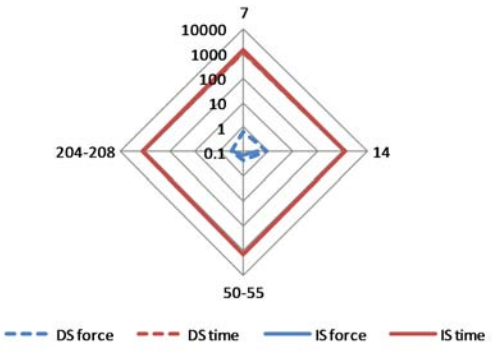

(e)

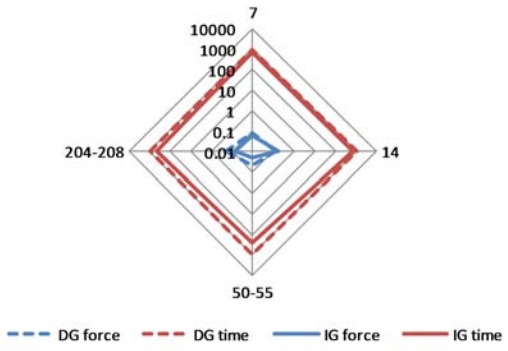

(f)

Figure 32: Correlation between time to contraction, maximum force of contraction and denervation periods for (32a) DS and IS at a concentration of $4\mu g/ml$ (32b) IG and DG at a concentration of $4\mu g/ml$ (32c) DS and IS at a concentration of $96\mu g/ml$ (32d) DG and IG at a concentration of $96\mu g/ml$ (32e) DS and IS at a concentration of $550\mu g/ml$ and (32f) DG and IG at a concentration of $550\mu g/ml$.

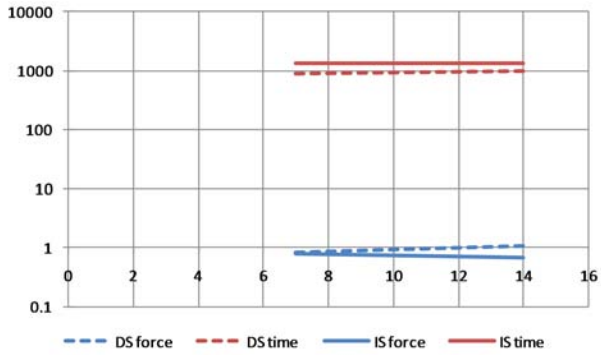

(a) Solei, 1.6g/ml

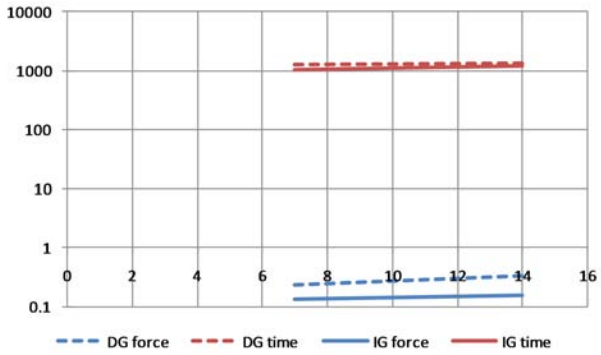

(b) Gastrocnemii, 1.6g/ml

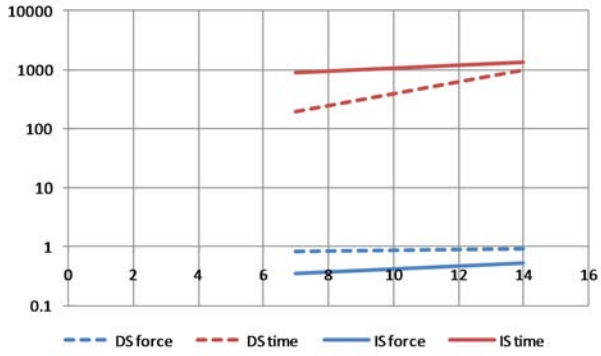

(c) Solei, 3.2g/ml

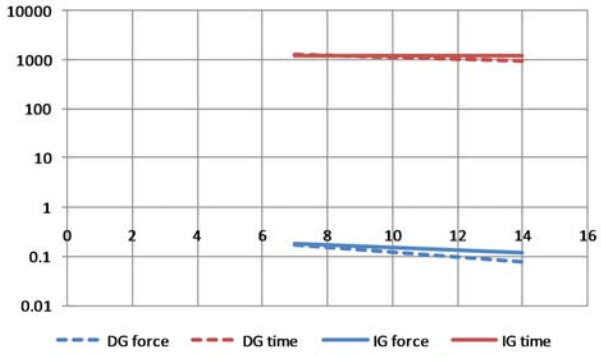

(d) Gastrocnemii, 3.2g/ml

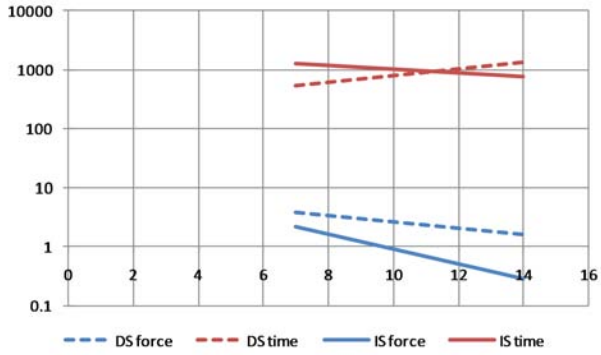

(e) Solei, 6.3g/ml

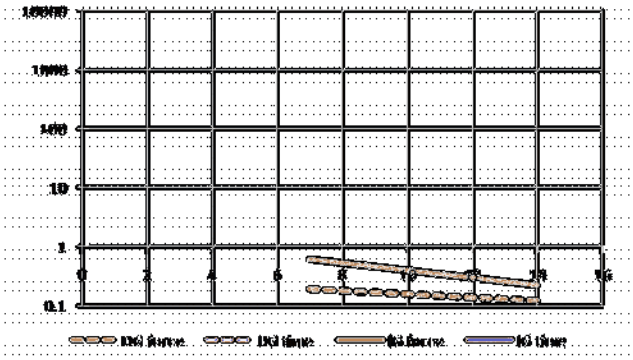

(f) Gastrocnemii, 6.3g/ml

Figure 33: Correlation between time to contraction, maximum force of contraction and denervation periods for (33a) DS and IS at a concentration of 1.6g/ml (33b) IG and DG at a concentration of 1.6g/ml (33c) DS and IS at a concentration of 3.2g/ml (33d) DG and IG at a concentration of 3.2g/ml (33e) DS and IS at a concentration of 6.3g/ml and (33f) DG and IG at a concentration of 6.3g/ml.

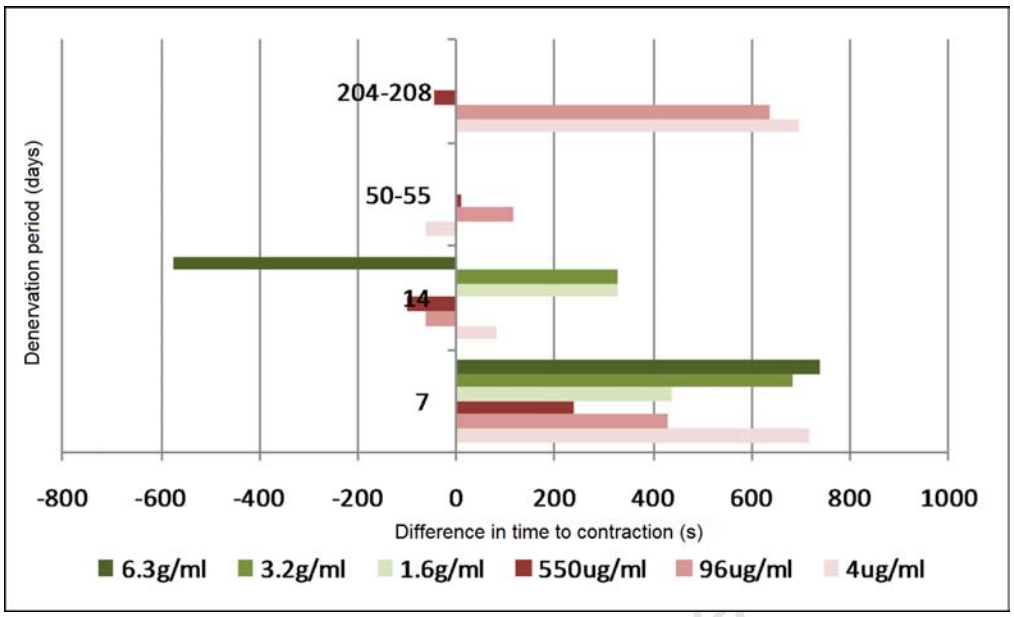

(a) Solei

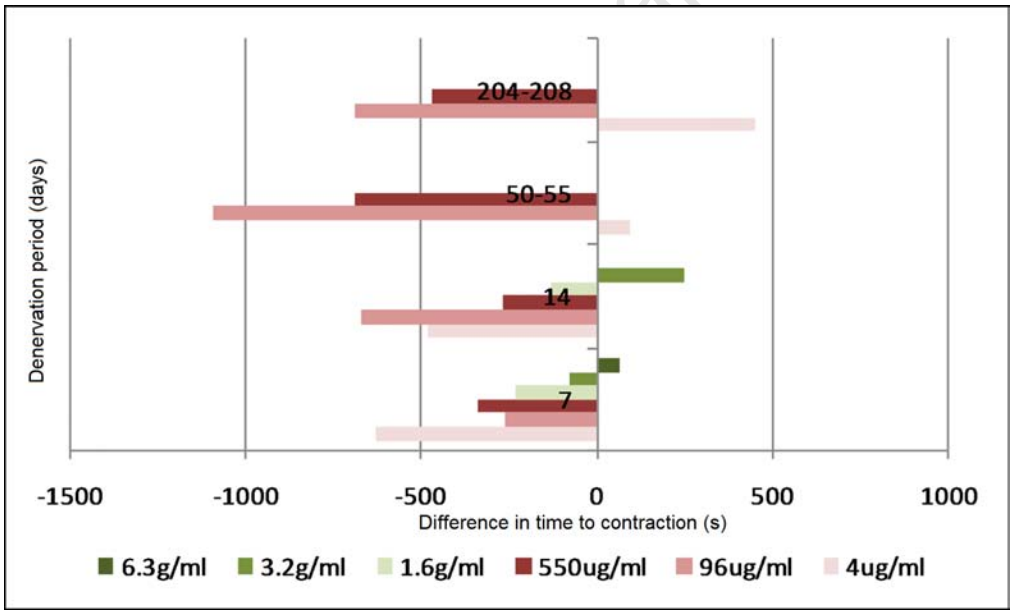

(b) Gastrocnemii

Figure 34: Difference in time to contraction (s) between (34a) DS and IS and (34b) DG and IG at increasing concentrations for all denervation periods.

Figure 34 provides the difference in time to peak force between denervated and innervated muscles for all concentrations and all denervation periods. The positive region of the graph indicates that the time to peak force of the innervated muscles was greater than those of the denervated muscles and the negative region of the graph indicates that the time to peak force of the denervated muscles was greater than that of the innervated muscles. For solei at 7 days post-denervation the difference in time to peak force decreases with increasing concentration within the low concentration range and the IS demonstrated longer times to contraction. Within the high concentration range the opposite is true (green series Figure 34a), i.e. an increase in difference in times to contraction between DS and IS occurred with an increase in concentration, although the IS still exhibited longer times than the DS. At 14 days post-denervation, the lowest concentration of $4\mu g/ml$ produces longer times to the peak force for the IS than the DS, but an increase in concentration within the low range resulted in the DS taking longer times to reach peak forces than their innervated contralaterals, additionally displaying an increase in the time difference between them. Within the high concentration range, still considering the 14 day post-denervation period, the differences in times to peak tension between DS and IS muscles were noted to be higher than for the low concentration range. Longer times were noted for IS for the higher 1.6g/ml and 3.2g/ml whereas the highest concentration of 6.3g/ml results in a shorter time to contraction for the IS (indicated by the negative range). The low concentration of $4\mu g/ml$ in the 50-55 day denervation period displayed a shorter time to contraction for the IS than the DS. Larger concentrations of $96\mu g/ml$ and $550\mu g/ml$ resulted in shorter times to peak tension in the DS compared to the IS. The difference decreased with an increase in concentration from $96\mu g/ml$ to $550\mu g/ml$. The longest denervation period of 204-208 days displayed an increase in difference in time to peak tension between DS and IS muscles with an increase in concentration. Administration of the low concentrations of $4\mu g/ml$ and $96\mu g/ml$ resulted in longer times to contraction for the IS than the DS. The highest concentration of $550\mu g/ml$ resulted in a significantly smaller difference in times to peak tension, as well as causing a shorter time to peak tension for the IS than the DS. These results all indicate that different concentration thresholds exist at which the DS will be more likely to respond faster than the IS for different time periods of denervation. The DS reached peak tension faster for all concentrations in the 7 day denervation period. The 14 day denervation period showed higher dependency on concentration in terms of contraction times, size and DS-IS bias. The 50-55 day denervation periods demonstrated the smallest dependency on concentration increase, with little difference between times to contraction for DS and IS muscles and the lowest concentration causing the fastest DS reaction time. The 204-208 days denervation period produced a shorter contraction time for the DS at the highest concentration (used for this denervation period) of $550\mu g/ml$.

Figure 32b illustrates the time to peak tension of DG and IG muscles at a concentration of $4\mu g/ml$. Whilst the DG consistently displayed higher forces than the IG for all denervation periods at this concentration, the DG exhibited shorter times to contraction for the long term denervation

periods of 50-55 days and 204-208 days. An increase in concentration to $96\mu g/ml$ resulted in the DG taking longer times to reach peak tension for all denervation periods. In order of increasing difference between DG and IG, the denervation periods rank as 7 days, 204-208 days, 14 days and 50-55 days. Further increase in concentration still resulted in the DG taking longer to reach peak tension than the IG, but a reduction in the time difference (between DG and IG) was noted. Administration of higher concentrations continued to result in longer times to peak tension for the DG in comparison to the IG. The times eventually reach a point of coincidence at the second highest concentration used (3.2g/ml) (Figure 33d). At the lower concentration of 1.6g/ml, the times to peak tension and peak forces increased with time periods of denervation (Figure 33b) whereas at the higher concentrations (3.2g/ml and 6.3g/ml) the opposite was true as these parameters displayed a decrease with an increase in denervation period (Figure 33d and 33f). These two higher concentrations also displayed higher forces for the IG than for the DG.

By way of reference to Figure 34, a number of differences can be clearly noted between the DS and DG responses. The DG were much less responsive to the administration of high concentrations of ACh than the DS, both in the relative difference in time to peak tension between innervated and denervated muscles, as well as in the magnitude of these differences. Further, the DG mostly displayed longer times to contraction than their innervated counterparts (note the negative region of Figure 34b), which is in contrast to the DS and IS observation. The 7 day denervation period displayed the biggest difference in time to peak tension with the lowest administered concentration of ACh, $4\mu g/ml$. All the times to peak tension were shorter for the IG than the DG for this denervation period, except at the highest concentration of 6.3g/ml. The high concentration range displayed a decrease in difference in times to peak tension between DG and IG for this period of denervation. The same observation in pattern can be made for these muscles at 14 days post-denervation, except that the largest difference in time to peak tension occurred at a higher concentration of $96\mu g/ml$ (compared to $4\mu g/ml$ from the 7 day denervation period group) and longer times to peak tension occurred for the IG than the DG at 3.2g/ml. The long term denervation groups (50-55 days and 204-208 days) displayed similar trends to each other. That is, the lowest concentration of $4\mu g/ml$ resulted in longer times to contraction for the the IG and the larger concentrations of $96\mu g/ml$ and $550\mu g/ml$ resulted in longer times to contraction for the DG muscles. The largest differences in time to peak tension between DG and IG occurred at the concentration of $96\mu g/ml$ for both denervation periods, which was also noted for the 14 day denervation period.

4.2.4 Effect of ACh administration, as determined by electrical stimulation checks

Electrical stimulation was used after chemical (ACh) stimulation in order to determine the effects of various concentrations of ACh on the contractile properties of the various muscles (and hence fibre types). The procedure involved an initial chemical stimulation by ACh (recorded for 19 minutes), followed by electrical stimulation of five successive 10ms pulses (resultant 20Hz) by two

steel electrodes. If large contractions were observed as a result of electrical stimulation, a large dose of ACh was administered to the muscle and its' response recorded. A repeat electrical test was then conducted. The frequency of response of the muscles to ACh occurred in a low frequency range; hence for comparative purposes only the low frequency components of the electrical signal are investigated here (note however that higher frequency components may exist in the muscles' response to electrical stimulation, but are beyond the scope of this thesis). The results of the combined chemical and electrical stimulation protocol are presented in this section for denervation periods of 7 and 14 days in terms of varying concentrations of ACh applied to muscles and their effects as illustrated by F-t traces, HS, WA and MHS. The reader is referred to sections 2.2.4 and 2.2.5 for the underlying theory of these data analysis methods.

Spectral plots of ACh-stimulated muscles are plotted for the first half of the full test run as the length of that portion of the signal was sufficient for visualisation of spectral components. Muscles stimulated by ACh were noted to produce slow contractures, which occur gradually over time as fibres are recruited. For this reason, longer time periods than spectra of electrical plots are necessary (electrical stimulation causes rapid whole muscle contractions). Longer time periods used for the spectral plots may result in some loss of resolution; therefore figure 35 has been included as an example demonstrating the immediate effects of ACh stimulation at various time periods.

The HS of a noise run, that is, an isometric recording of the Force-time (F-t) output of a muscle (in this case a 14 day DS) which has been neither chemically nor electrically stimulated, is presented in Figure 36. From this figure it is evident that two frequencies exist within the signal at 4Hz and 4.5Hz (potentially due to fibrillation of various fibres comprising the muscle), as well as some low frequency components which are inherent in the signal. Denervated rat solei are known to fibrillate post denervation for up to 3 weeks [Robinson et al., 1991]. Once stimulated by ACh, the fibres will react by contracting in bundles at different frequencies, thus in a sense 'overriding' the fibrillation effects depending on the degree of reaction to stimulation. Only the noise run thus contains these components.

Alternate chemical and electrical stimulation of muscles denervated for a 7 day period

This section primarily presents and discusses muscles denervated for a 7 day period, first comparing denervated muscle responses to their innervated contralaterals, followed by the effect of increasing concentration on muscle response.

Refer to Figure 37. Stimulation of the DG with $4\mu g/ml$ ACh, displayed an increase in force variation (peak-to-peak fluctuation) with time post ACh administration (the point of administration is indicated by a red line at 180s in the F-t trace Figure 37a). The MHS (Figure 37e) illustrates that the signals' largest energy contribution lies within the 0.31-0.44Hz frequency range (peak at +-0.37Hz). Electrical stimulation post-denervation (Figure 37b) resulted in a small contractile response from the muscle (top figure in (b)), not large enough to produce a highly localised region

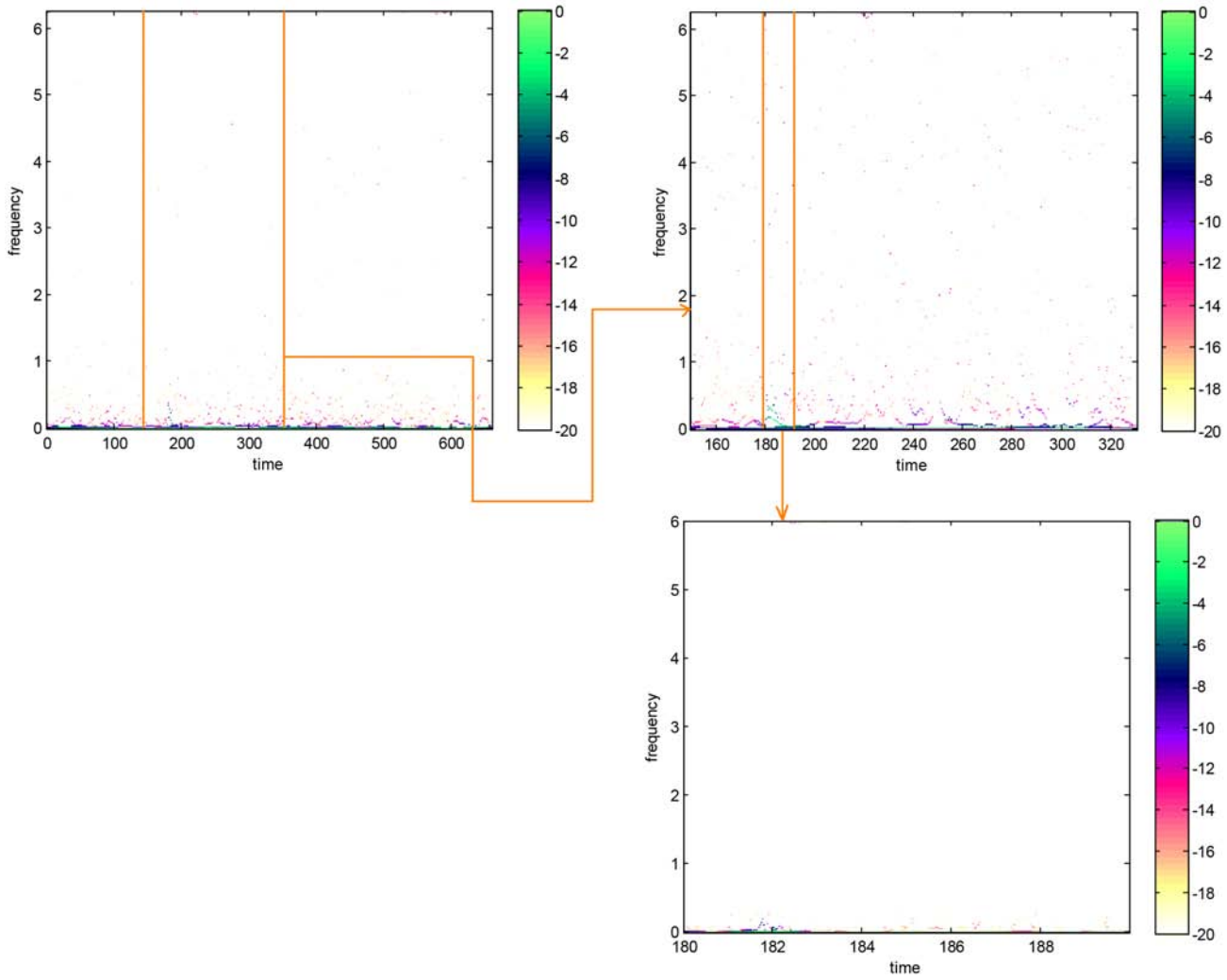

Figure 35: Hilbert spectra of a 7 day IG stimulated at 96ug/ml. Top left: 700sec interval; Top right: 3 minute interval (120sec-300sec); Bottom right: 10sec interval (180-190sec).

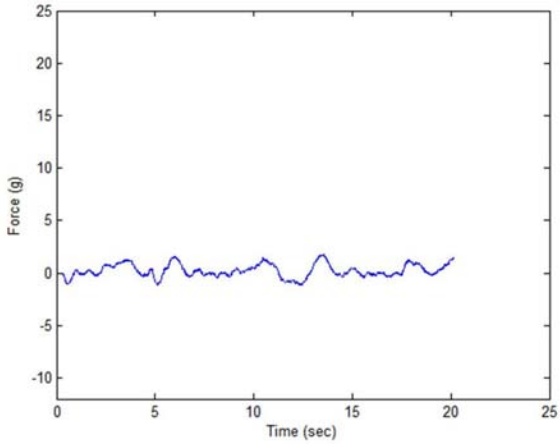

(a)

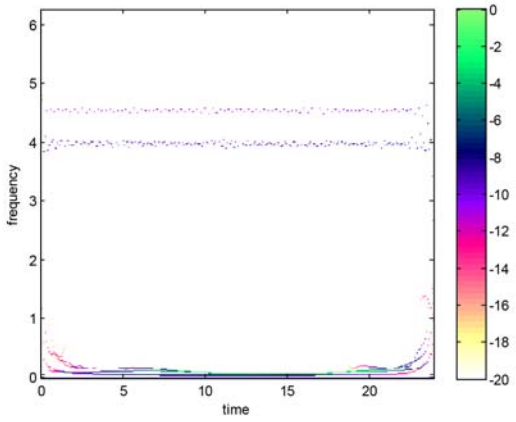

(b)

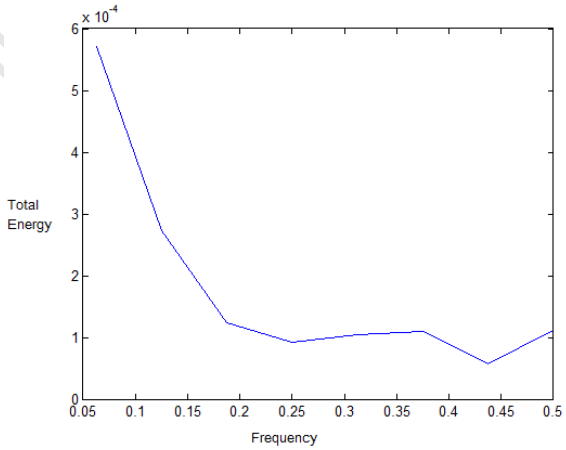

(c)

Figure 36: (36a) F-t record of DS noise run(36b) HS and (36c) MHS of a noise run conducted on a DS from a 14 day denervation period group.

in frequency, energy and time in the HS (Figure 37d). The lower figure in (b) is indicative of the onset of 5 successive electrical stimuli and the top figure in (b) demonstrates the muscle reaction to the electrical stimuli. The MHS of the electrical stimulation check illustrated a significant energy component in the 0.44-0.5Hz range (Figure 37f), as well as the low frequency ranges (0.13-0.18Hz and 0.18-0.25Hz), possibly indicating slow fibre recruitment (at the low end of frequency spectrum) and fast contraction (at the high end of frequency spectrum).

Refer to Figure 38. Post injection the DS displayed the same increase in force variation with time as the DG stimulated at $4\mu g/ml$ (compare Figures 37a and 38a), but a greater variation in force than that of DG was observed. High energy contributions of both signals exist between 0.31-0.44Hz (peak at +-0.37Hz), but the DG exhibited slightly more energy than the DS (illustrated in Figures 37e and 38e). Electrical stimulation post ACh administration showed high frequency-time-energy locality within the spectrum, correspondimg to the MHS (Figure 38f) which indicated a large energy contribution from 0.44-0.5Hz range. This appears to be indicative of a contractile reaction of the muscle to electrical stimulation, as demonstrated by the wavelet cluster analysis in Figure 37b.

Refer to Figure 39 in which the results of an IS, stimulated with $4\mu g/ml$ of ACh, is depicted. The F-t record (Figure 39a) displays an increase in force variation (peak-to-peak fluctuation) as well as a small gradual or slow rise in force over time. The MHS (Figure 39e) of this chemical stimulation, indicates a large amount of energy within 0.37-0.5Hz range (peak at 0.44Hz). Clear locality was visible in the HS of the electrical stimulation test post ACh administration. The MHS of the muscles' electrical response illustrates a large energy, low frequency contribution as well as notable contribution of energy in the frequency range of 0.37-0.44Hz (Note that there is no energy contribution from the 0.44-0.5Hz frequency range).

The DS displayed a higher degree of force variation than the IS when both stimulated at $4\mu g/ml$. The DS produced contractions of smaller force upon chemical stimulation in comparison to the IS (compare Figures 38a and 39a). This is indicative of a larger response of the DS to ACh. The HS corresponding to the DS showed a more localised response to electrical stimulation than that of the IS. A comparison of the MHS of the chemical stimulation tests (Figures 38e and 39e), indicates that the DS exerted more energy in a lower and wider frequency range in relation to the IS, but the absolute energy of the IS was slightly larger. This is likely due to the larger number of fibres within the IS. Both muscles displayed large energy low frequency contributions, but the DS exhibited more energy in the higher frequency range of 0.44-0.5Hz in its respective electrical stimulation MHS.

Figure 40 displays the response of a DG to $96\mu g/ml$ of ACh. Post injection, an increase in peak-to-peak force variation as well as gradual increase in force over time (indicative of a slow contracture) was noted. The MHS of the muscles' response to chemical stimulation (Figure 40e) indicates a large energy contribution between 0.25-0.37Hz (peak at 0.31Hz). Electrical stimulation post ACh administration showed clear indications of locality in the HS (Figure 40d), and a very small energy

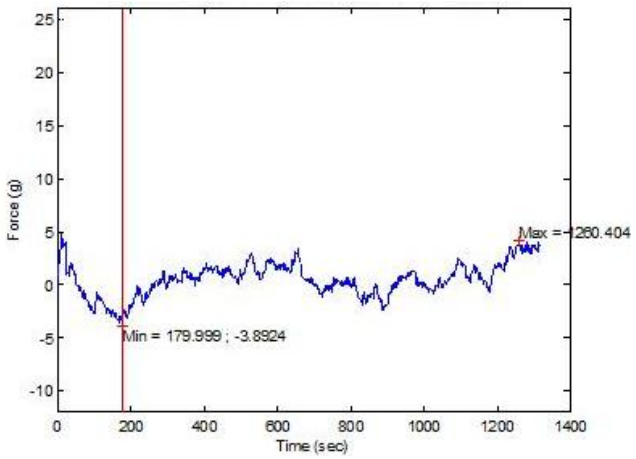

(a)

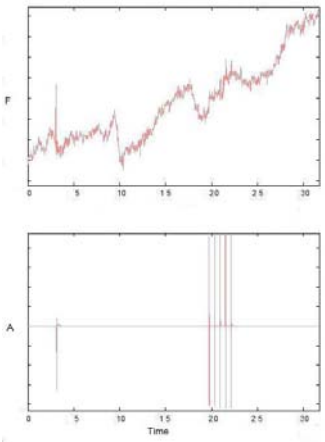

(b)

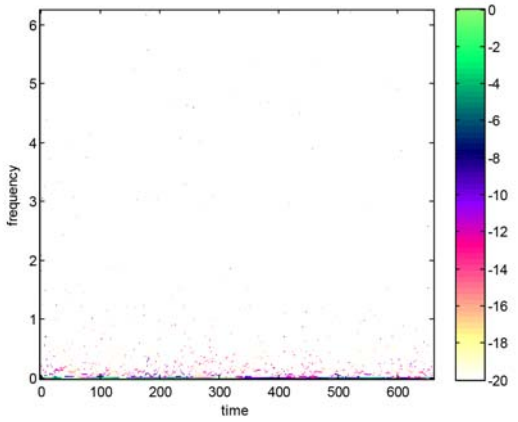

(c) injection at 180 sec

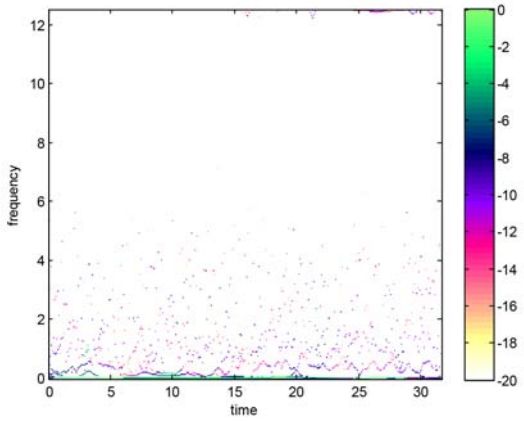

(d) stimulation as in (b)

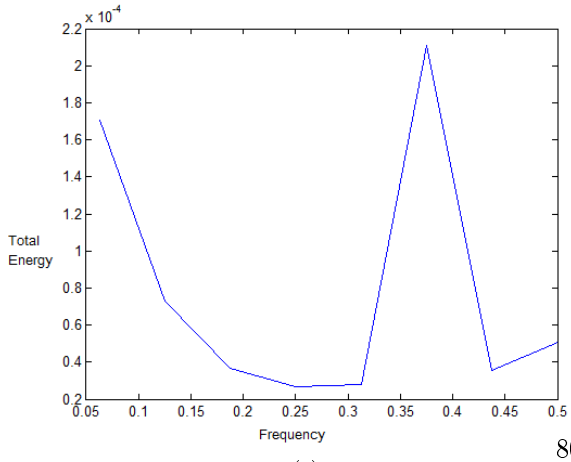

(e)

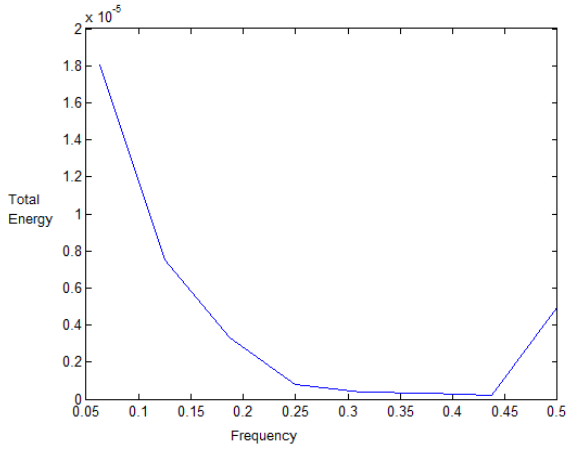

(f)

Figure 37: Results of 7 day DG stimulated at $4\mu g/ml$. (37a) F-t record of $4\mu g/ml$ ACh stimulation (37b) F-t record (top) and amplitude (A)-t indication of stimulation (bottom) for electrical stimulation post ACh administration (37c) HS of $4\mu g/ml$ ACh stimulation (37d) HS of electrical stimulation post ACh administration (37e) MHS of $4\mu g/ml$ ACh stimulation (37f) MHS of electrical stimulation post ACh administration.

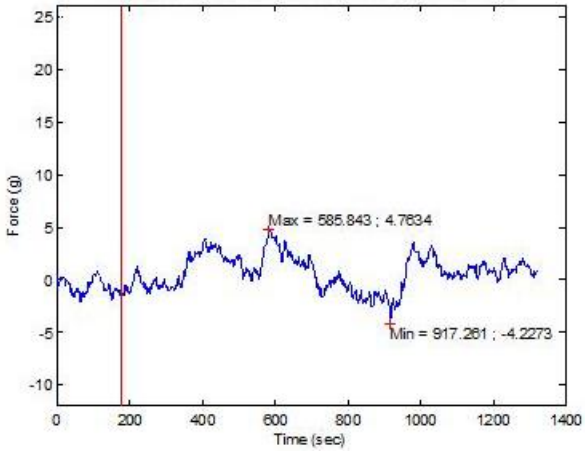

(a)

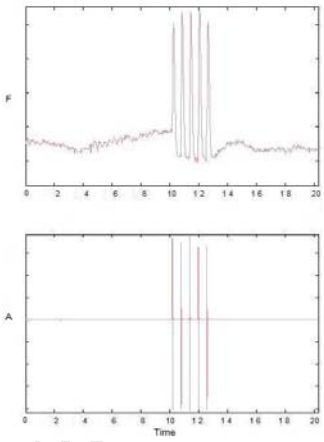

(b)

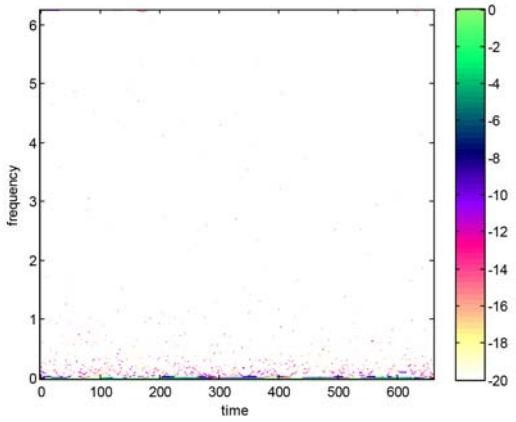

(c) injection at 180 sec

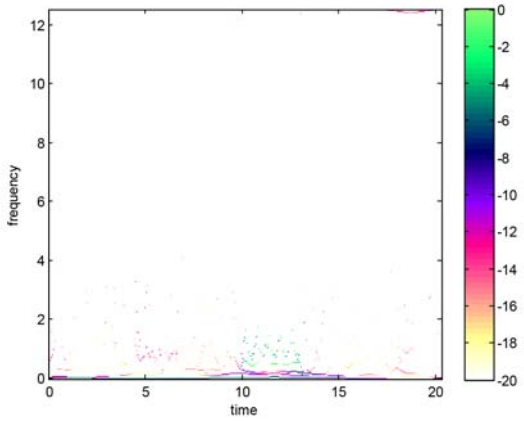

(d) stimulation as in (b)

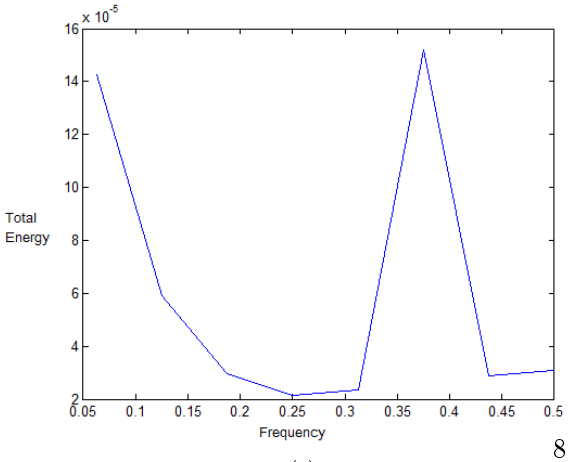

(e)

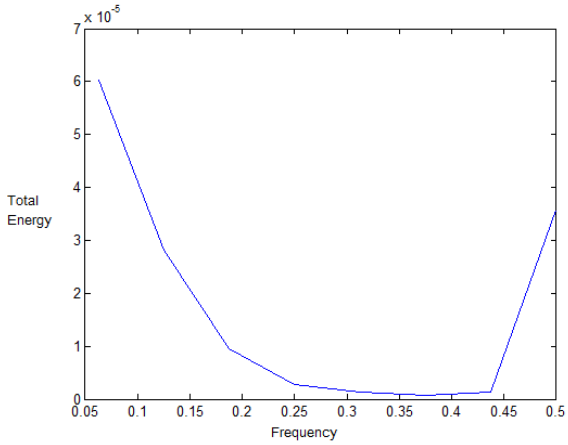

(f)

Figure 38: Results of 7 day DS stimulated at $4\mu g/ml$. (38a) F-t record of $4\mu g/ml$ ACh stimulation (38b) F-t record (top) and amplitude (A)-t indication of stimulation (bottom) for electrical stimulation post ACh administration (38c) HS of $4\mu g/ml$ ACh stimulation (38d) HS of electrical stimulation post ACh administration (38e) MHS of $4\mu g/ml$ ACh stimulation (38f) MHS of electrical stimulation post ACh administration.

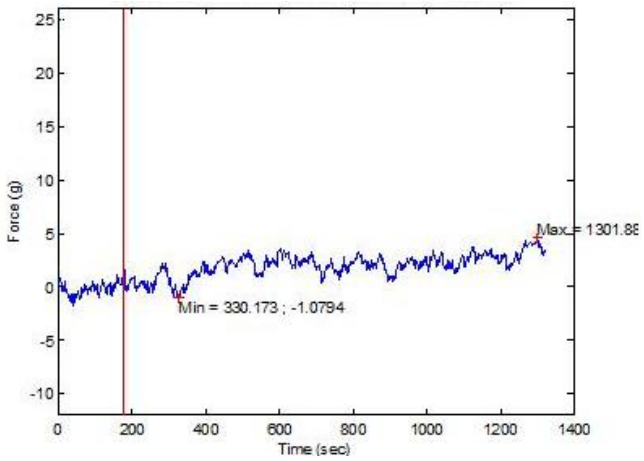

(a)

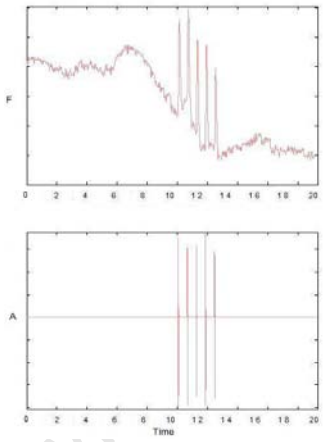

(b)

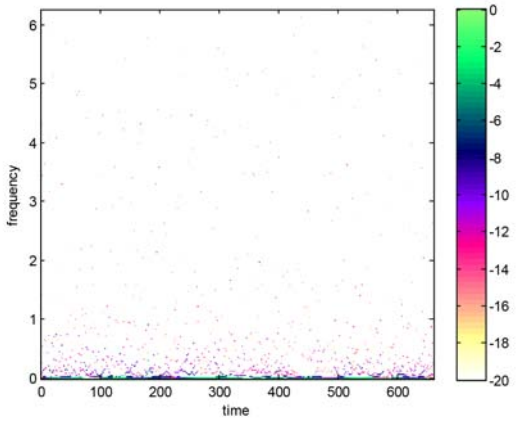

(c) injection at 180 sec

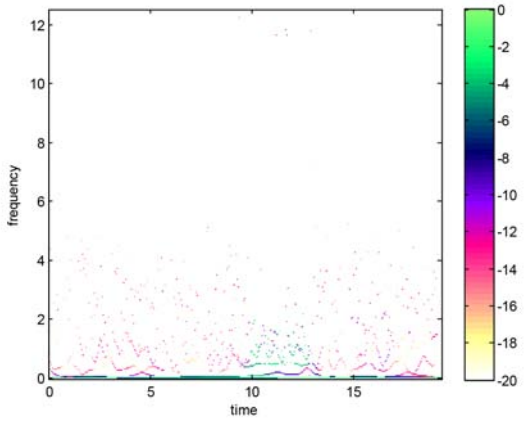

(d) stimulation as in (b)

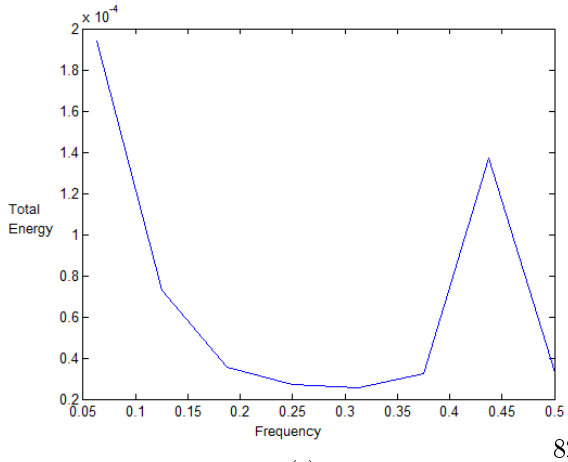

(e)

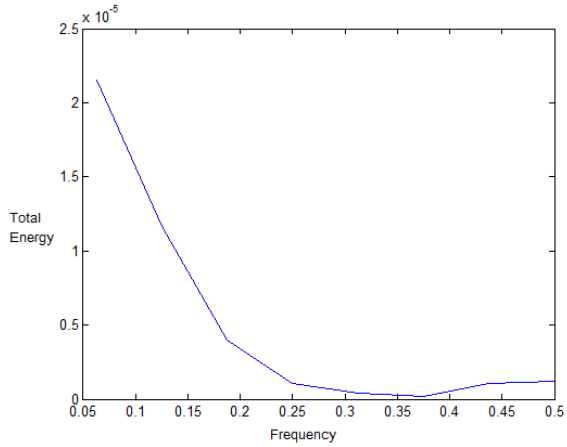

(f)

Figure 39: Results of IS from 7 day denervation group, stimulated at $4\mu g/ml$. (39a) F-t record of $4\mu g/ml$ ACh stimulation (39b) F-t record (top) and amplitude (A)-t indication of stimulation (bottom) for electrical stimulation post ACh administration (39c) HS of $4\mu g/ml$ ACh stimulation (39d) HS of electrical stimulation post ACh administration (39e) MHS of $4\mu g/ml$ ACh stimulation (39f) MHS of electrical stimulation post ACh administration.

contribution within 0.44-0.5Hz range (shown in the MHS, Figure 40f). Clear contractions occurred upon electrical stimulation, as may be seen in Figure 40b.

The response of a DS to $96\mu g/ml$ of ACh is depicted in Figure 41. The DS again displayed an increase in peak-to-peak force variation post injection. No gradual increase in force was evident (indicative of little or no slow contracture). The MHS displays the largest energy contribution in the 0.18-0.31Hz range (peak at 0.25Hz). Clear locality was seen in the HS of the post-ACh electrical stimulation. A large energy contribution in the frequency range between 0.37-0.44Hz was noted from the MHS of the muscles' response to electrical stimulation (Figure 41f). This was noted to be similar to that observed for the IS at a low concentration stimulation of $4\mu g/ml$ for the same denervation period).

The reaction of an IS to $96\mu g/ml$ was such that a small amount of force variation occurred post ACh administration in comparison to the pre injection range. A later, gradual increase in force from about 400s on the F-t graph (Figure 42a) (220s post injection) was observed. The MHS (Figure 42e) shows an energy contribution within a 0.25-0.37Hz frequency range. This contribution was small in comparison to the low frequency contribution already present within the signal. Electrical stimulation displayed no locality in the HS, supported by the weak signal illustrated by the F-t trace in Figure 42b, whilst the MHS illustrates an increased energy contribution between 0.44-0.5Hz.

The DS displayed a higher force variation post injection than the IS (see the F-t traces, Figures 41a and 42a). More energy was 'scattered' throughout the frequency range over time in the IS than in the DS (see HS in Figures 41c and 42c). This seems to be the trend in tests which exhibited slow contractures (increased force over time) and small frequency variations in comparison to the pre injection range. The energy observed from the IS was concentrated within a higher frequency range than that of DS at the same concentration of $96\mu g/ml$ (compare the MHS in Figures 41e and 42e). The DS energy contribution in the lower frequency range was more comparable to that of the IS stimulated at a low concentration of $4\mu g/ml$). Again, greater locality was demonstrated in the HS of the DS than that of the IS.

A DG stimulated at $550\mu g/ml$ displayed an increase in force variation post injection (see Figure 43a). The MHS shows very large and significant energy contribution from 0.31-0.44Hz (peak at 0.37Hz). (This was noted for the DG and DS muscles stimulated at a concentration of $4\mu g/ml$ as well). The HS of the muscles' reaction to electrical stimulation showed some locality in its energy-frequency-time distribution corresponding to the stimulation time. The MHS displayed a small energy contribution from 0.44-0.5Hz, with most of the energy contribution being from the low frequency range.

The response of the IG to ACh at a concentration of $550\mu g/ml$ was similar to that of the DG for the same concentration, that is an increased force variation post injection. No gradual rise in force was noted. A relatively large energy contribution was noted between 0.13-0.25Hz (peak at 0.18Hz, a smaller range than that of the DG) (see MHS Figure 44e). The highest energy peak

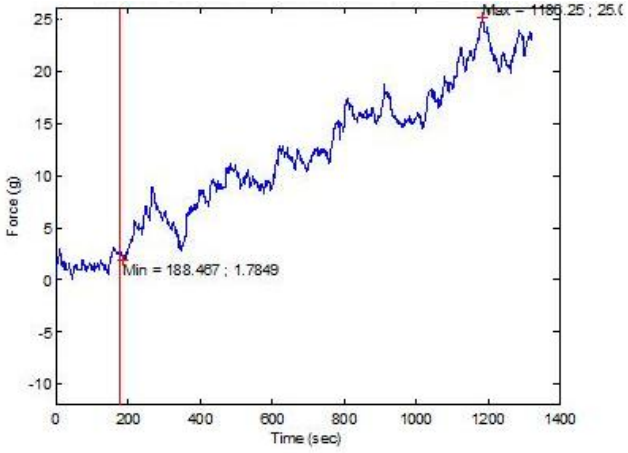

(a)

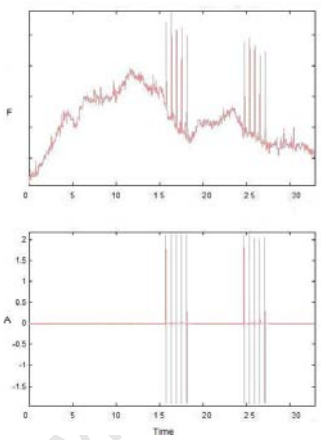

(b)

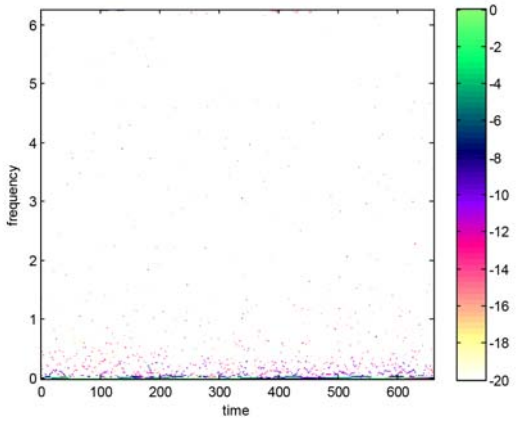

(c) injection at 180 sec

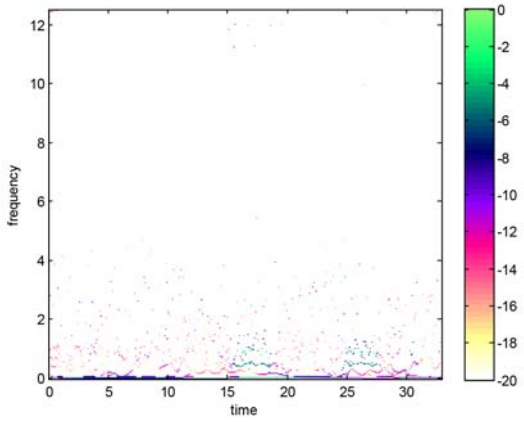

(d) stimulation as in (b)

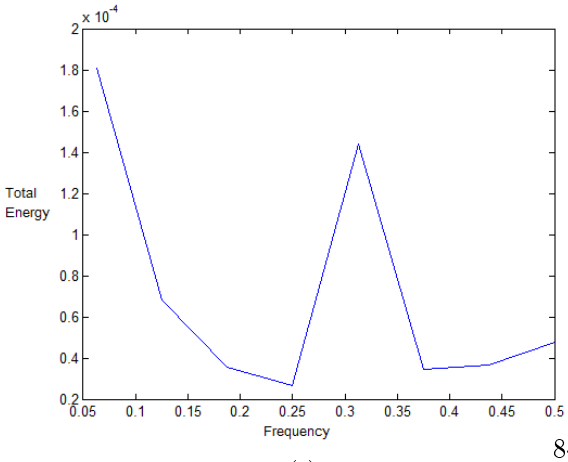

(e)

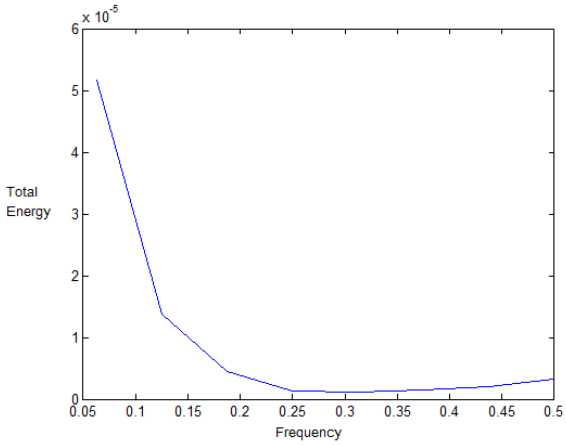

(f)

Figure 40: Results of 7 day DG stimulated at $96\mu g/ml$. (40a) F-t record of $96\mu g/ml$ ACh stimulation (40b) F-t record (top) and amplitude (A)-t indication of stimulation (bottom) for electrical stimulation post ACh administration (40c) HS of $96\mu g/ml$ ACh stimulation (40d) HS of electrical stimulation post ACh administration (40e) MHS of $96\mu g/ml$ ACh stimulation (40f) MHS of electrical stimulation post ACh administration.

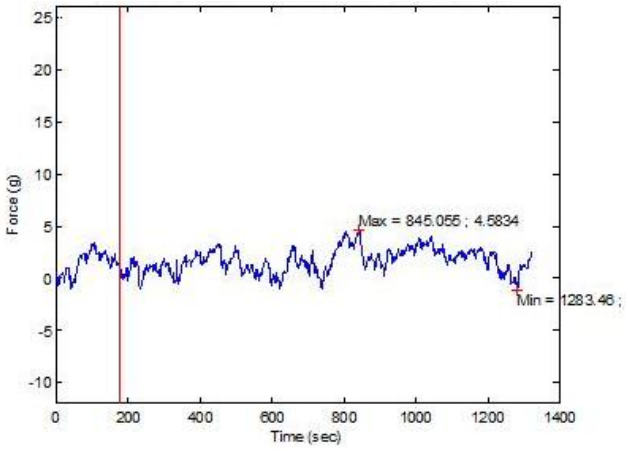

(a)

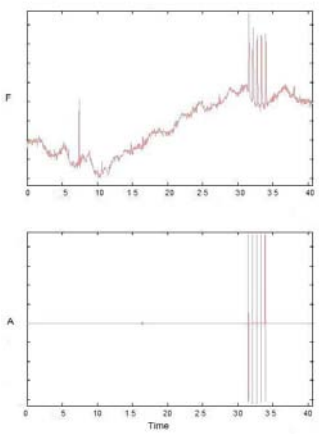

(b)

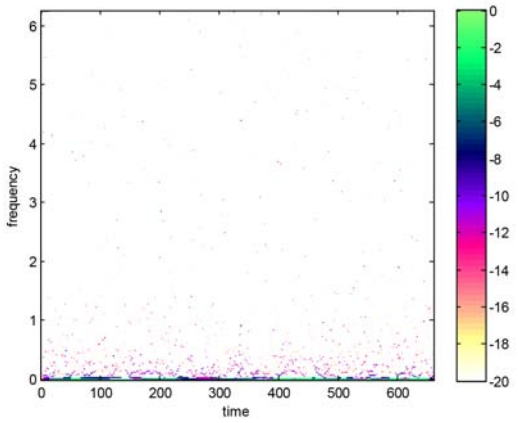

(c) injection at 180 sec

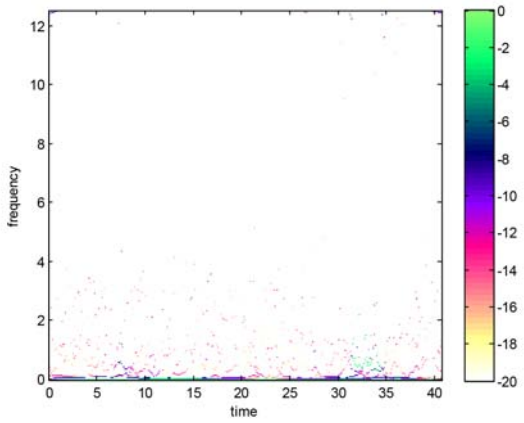

(d) stimulation as in (b)

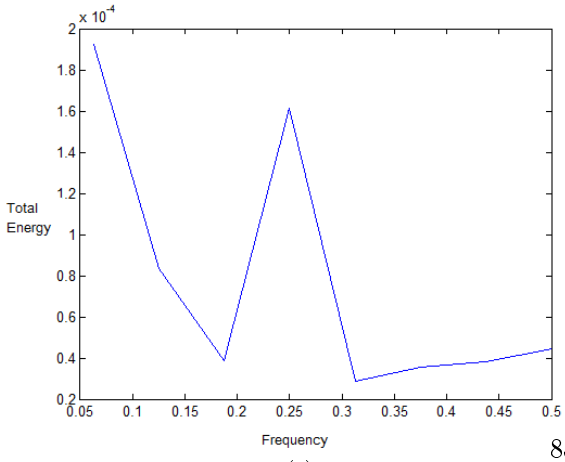

(e)

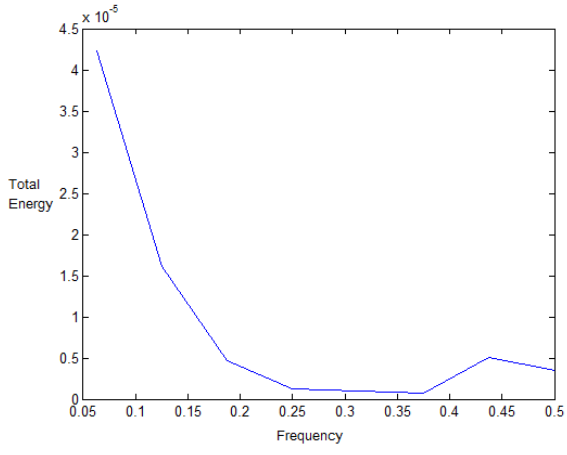

(f)

Figure 41: Results of 7 day DS stimulated at $96\mu g/ml$. (41a) F-t record of $96\mu g/ml$ ACh stimulation (41b) F-t record (top) and amplitude (A)-t indication of stimulation (bottom) for electrical stimulation post ACh administration (41c) HS of $96\mu g/ml$ ACh stimulation (41d) HS of electrical stimulation post ACh administration (41e) MHS of $96\mu g/ml$ ACh stimulation (41f) MHS of electrical stimulation post ACh administration.

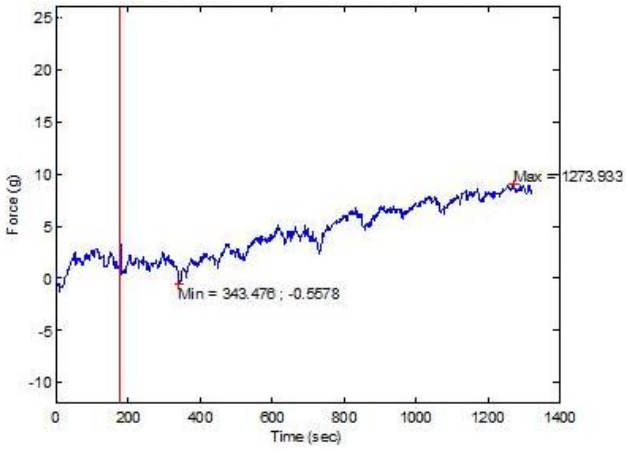

(a)

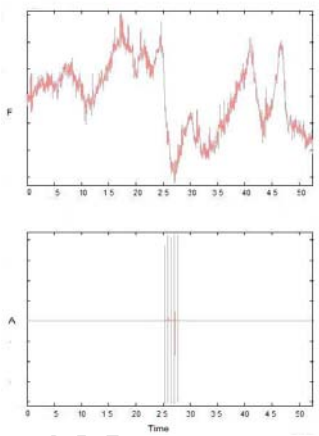

(b)

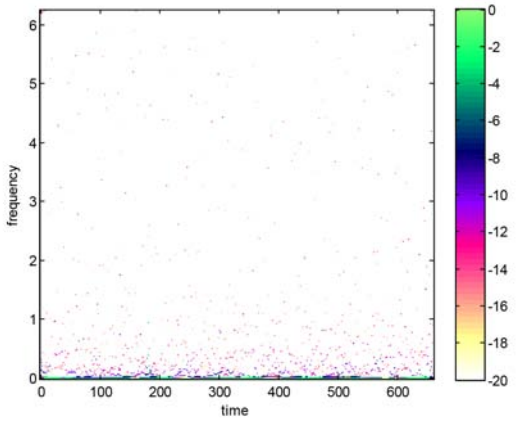

(c) injection at 180 sec

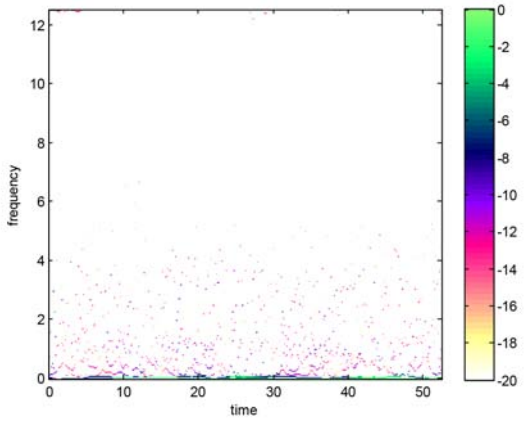

(d) stimulation as in (b)

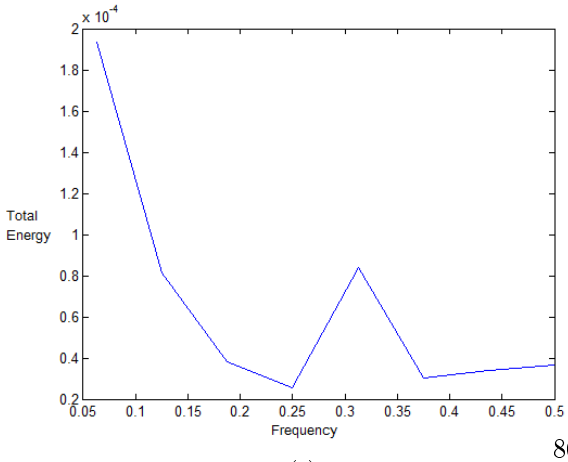

(e)

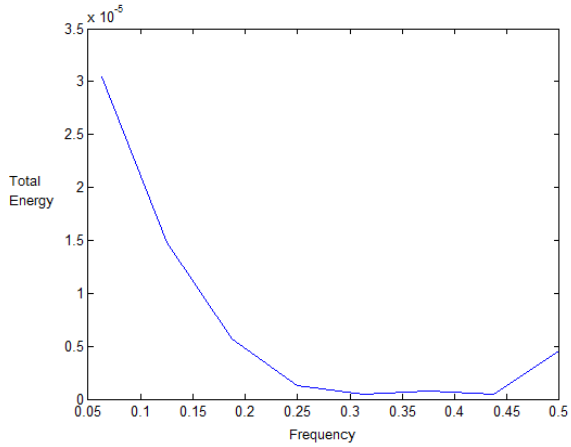

(f)

Figure 42: Results of IS from 7 day denervation group, stimulated at $96\mu g/ml$. (42b) F-t record of $96\mu g/ml$ ACh stimulation (42b) F-t record (top) and amplitude (A)-t indication of stimulation (bottom) for electrical stimulation post ACh administration (42c) HS of $96\mu g/ml$ ACh stimulation (42d) HS of electrical stimulation post ACh administration (42e) MHS of $96\mu g/ml$ ACh stimulation (42f) MHS of electrical stimulation post ACh administration.

from this range was greater than that of the low frequency energy contribution. The electrical stimulation reaction showed no locality in the signal (similar to that of the DG). The MHS of the electrical response illustrated a large, low frequency energy contribution and a slight contribution from 0.44-0.5Hz, similar to the DG. The overall absolute energy was small, in the range of 10^{-5}.

A DS stimulated at $550\mu g/ml$ exhibited increased force variation as well as gradual increase in force over time (see F-t graph in Figure 45a) post injection. High energy contributions were all within the low frequency range, with no additional frequency range contribution. Note however, that the low frequency energy contribution to the signal was comparatively large, in the range of 10^{-3}, suggesting the additional energy contribution due to ACh administration occurred within the same low frequency range already inherent in the signal. Some locality was visible in the HS of the muscles' response to electrical stimulation. A slight increase in energy distribution was observed in the 0.37-0.44Hz range (see MHS in Figure 45f).

The IS reaction to $550\mu g/ml$ ACh was a gradual increase in force post injection, as well as increased force fluctuation. This is similar to the trend observed in the F-t trace of the DS, but the IS force increases at a steeper gradient (i.e. the force developed more quickly and reaches higher values) than the DS. Very large forces were reached by the IS but no tetanus of any mode was evident in the F-t signal. All the significant energy contribution occurred in the 0.06-0.13Hz range, again, noting a substantial absolute energy in the range of 10^{-3}, thus additional energy due to ACh administration fell in the same range as the inherent system energy (within the low frequency range). This is again the same as that observed in the DS. The HS of the muscles' response to electrical stimulation also demonstrated high locality in energy, frequency and time (see Figure 46d), as in the DS. The spectrum is indicative of potential slow fibre recruitment (in the low frequency range), with the highest energy component occurring between 12-15sec, coinciding with stimulation time. The MHS of the muscles' response to electrical stimulation (Figure 46f), shows a very large energy contribution in the 0.37-0.5Hz range (the large energy contribution is expected; special note is taken of the increased range from 0.37Hz rather than the more often observed 0.44Hz).

An IS stimulated by 1.6g/ml of ACh displayed an increased force variation post injection. A slight gradual increase in force was only observed after 700s (visible on the F-t recording, Figure 47a). The MHS illustrates a large energy contribution occurring in a 0.37-0.5Hz range (peak at 0.44Hz). This energy contribution is much higher than low the frequency energy contribution (see Figure 47e). Electrical stimulation of the muscle showed a small amount of visible locality in the HS. The MHS shows a slight increase in energy contribution in the 0.44-0.5Hz range.

An IS stimulated at a high concentration of 3.2g/ml demonstrated an increase in force variation, as well as a gradual increase in force until unfused tetanus was reached at a low force, fluctuating around 5g. The MHS displayed an energy contribution of 0.25-0.37Hz which was lower than the low frequency contribution, but still considered substantial (in the range of 10^{-4}). The HS of the electrical stimulation reaction demonstrated increased energy in the low frequency component,

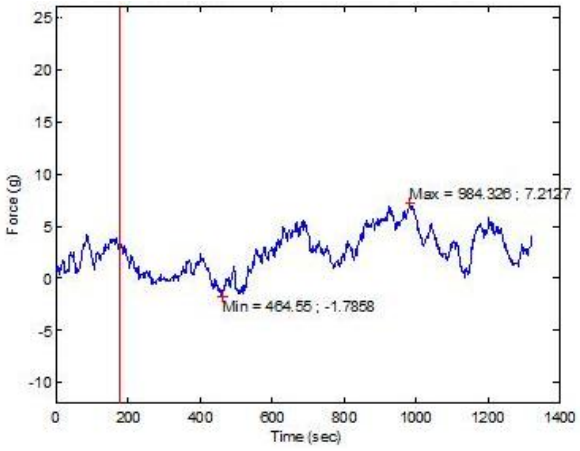

(a)

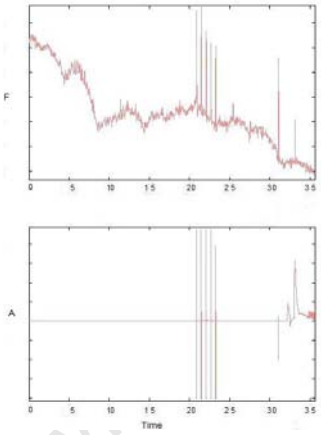

(b)

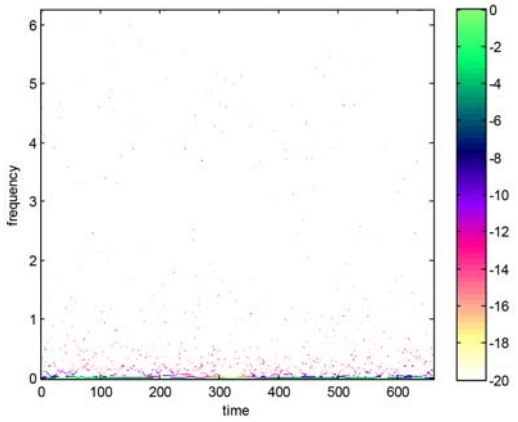

(c) injection at 180 sec

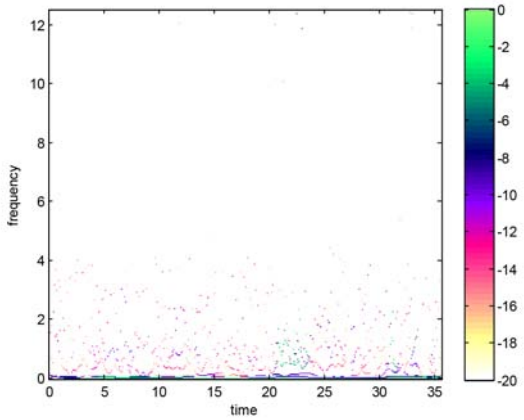

(d) stimulation as in (b)

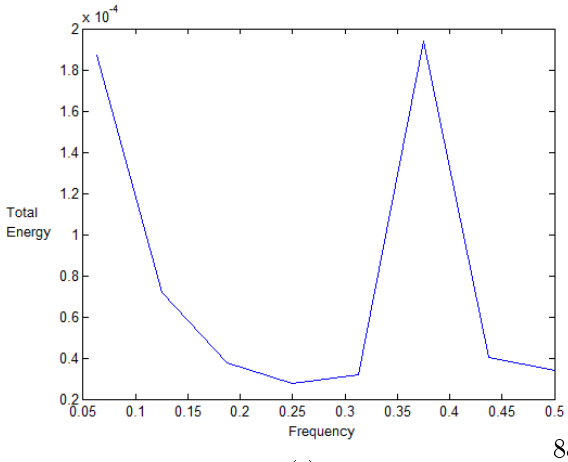

(e)

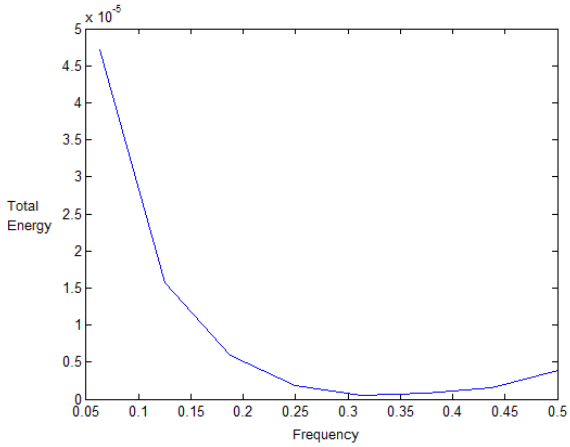

(f)

Figure 43: Results of 7 day DG stimulated at $550\mu g/ml$. (43a) F-t record of $550\mu g/ml$ ACh stimulation (43b) F-t record (top) and amplitude (A)-t indication of stimulation (bottom) for electrical stimulation post ACh administration (43c) HS of $550\mu g/ml$ ACh stimulation (43d) HS of electrical stimulation post ACh administration (43e) MHS of $550\mu g/ml$ ACh stimulation (43f) MHS of electrical stimulation post ACh administration.

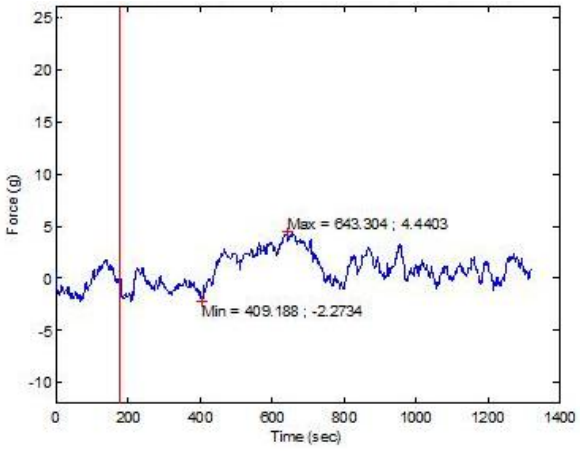

(a)

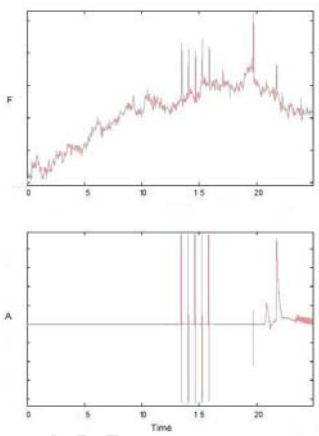

(b)

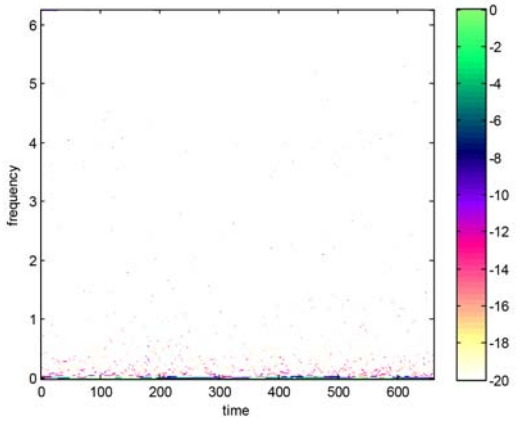

(c) injection at 180 sec

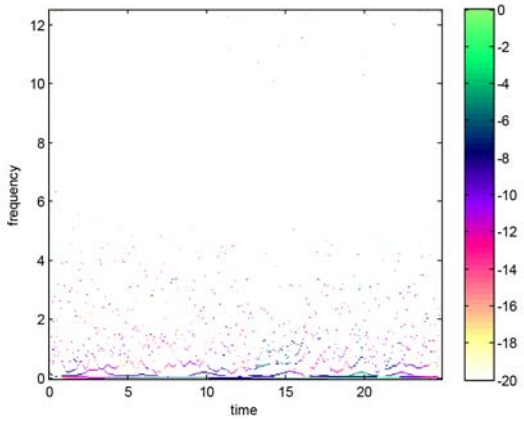

(d) stimulation as in (b)

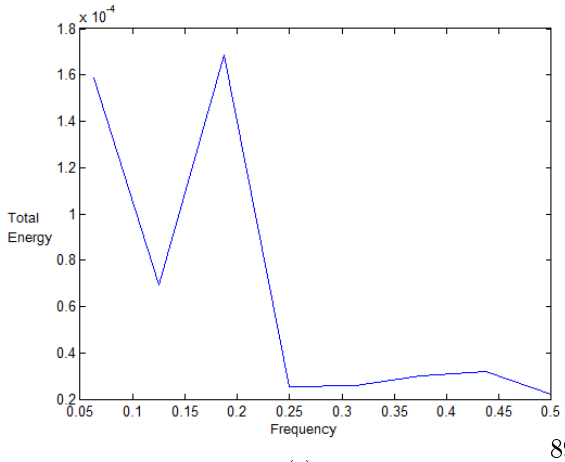

(e)

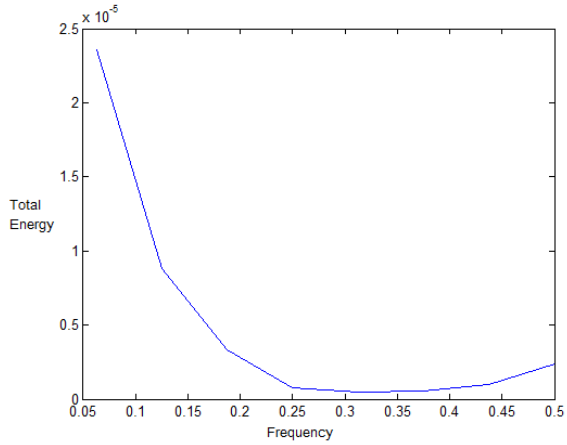

(f)

Figure 44: Results of IG from 7 day denervation group, stimulated at $550\mu g/ml$. (44a) F-t record of $550\mu g/ml$ ACh stimulation (44b) F-t record (top) and amplitude (A)-t indication of stimulation (bottom) for electrical stimulation post ACh administration (44c) HS of $550\mu g/ml$ ACh stimulation (44d) HS of electrical stimulation post ACh administration (44e) MHS of $550\mu g/ml$ ACh stimulation (44f) MHS of electrical stimulation post ACh administration.

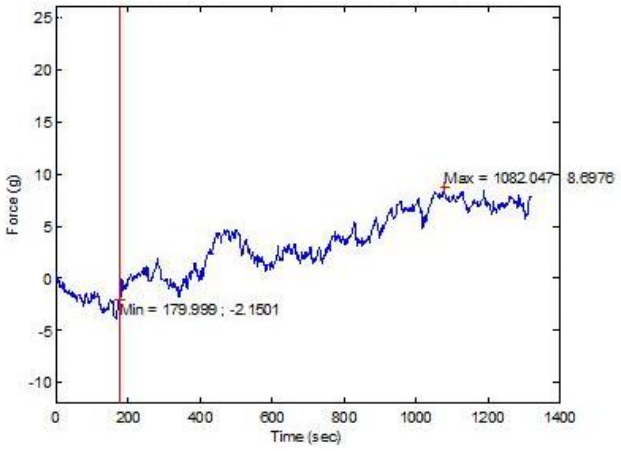

(a)

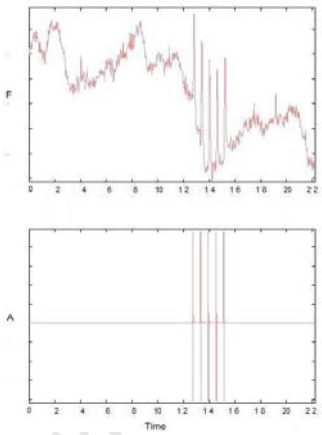

(b)

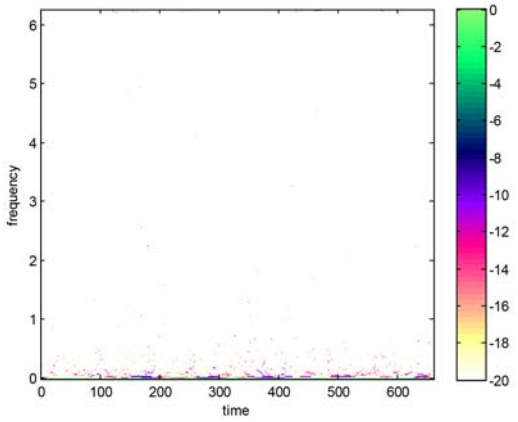

(c) injection at 180 sec

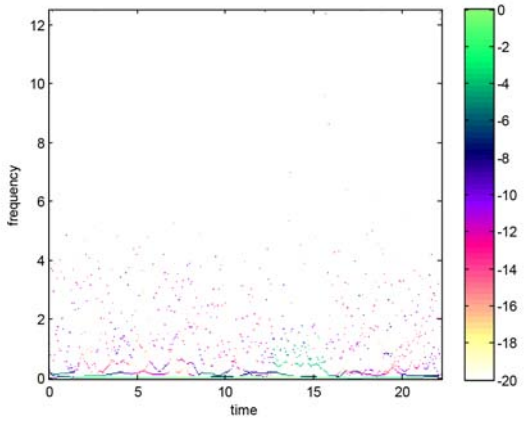

(d) stimulation as in (b)

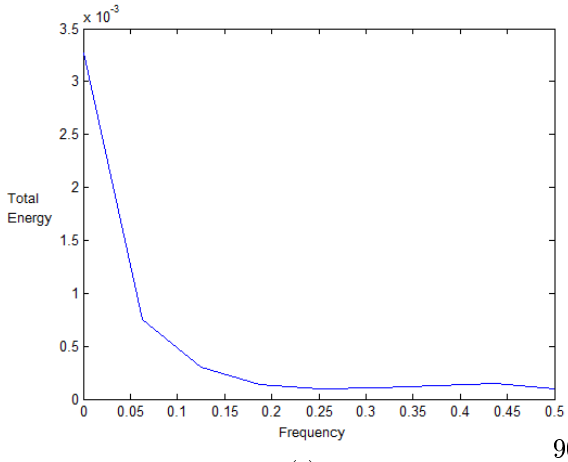

(e)

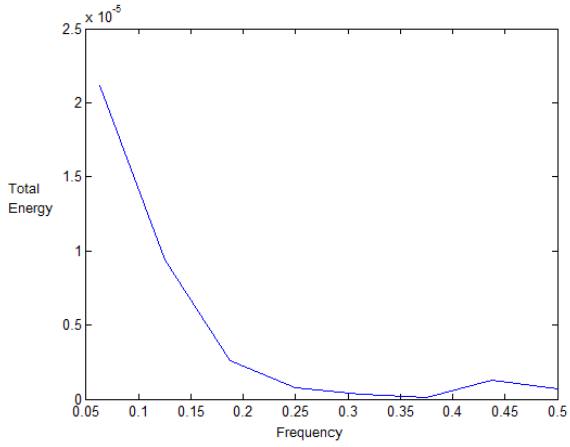

(f)

Figure 45: Results of 7 day DS stimulated at $550\mu g/ml$. (45a) F-t record of $550\mu g/ml$ ACh stimulation (45b) F-t record (top) and amplitude (A)-t indication of stimulation (bottom) for electrical stimulation post ACh administration (45c) HS of $550\mu g/ml$ ACh stimulation (45d) HS of electrical stimulation post ACh administration (45e) MHS of $550\mu g/ml$ ACh stimulation (45f) MHS of electrical stimulation post ACh administration.

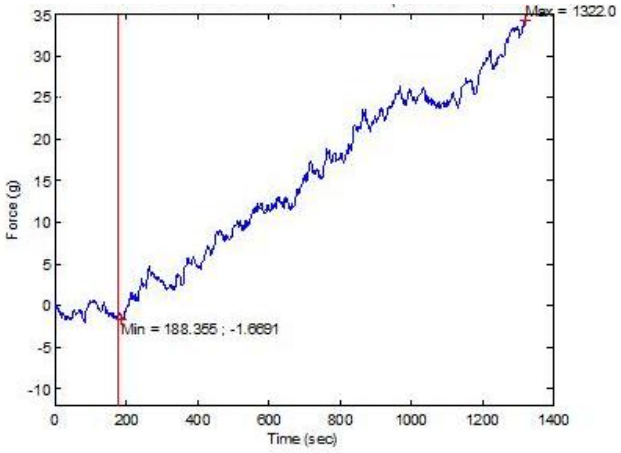

(a)

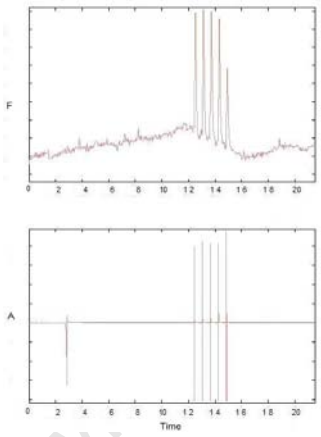

(b)

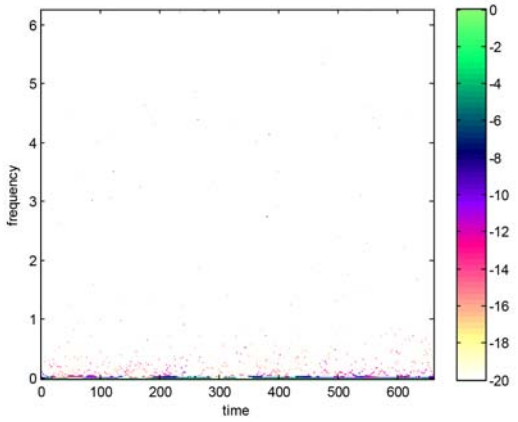

(c) injection at 180 sec

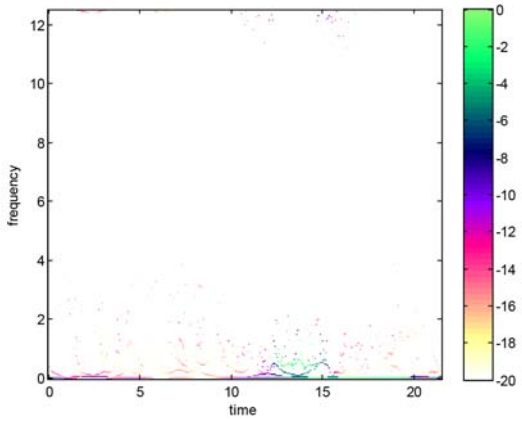

(d) stimulation as in (b)

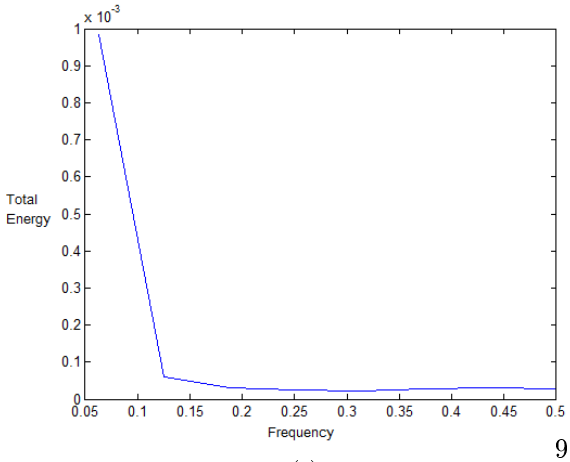

(e)

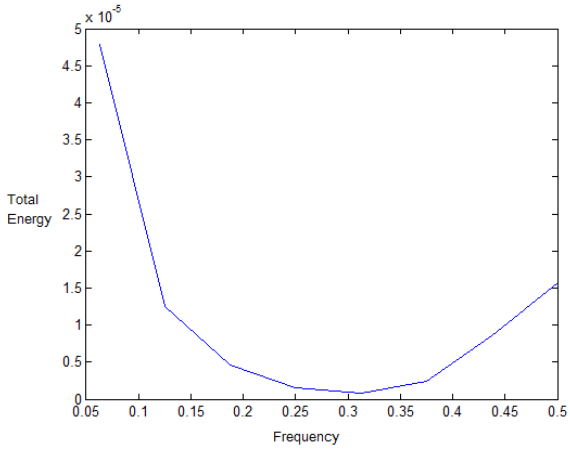

(f)

Figure 46: Results of IS from 7 day denervation group, stimulated at $550\mu g/ml$. (46a) F-t record of $550\mu g/ml$ ACh stimulation (46b) F-t record (top) and amplitude (A)-t indication of stimulation (bottom) for electrical stimulation post ACh administration (46c) HS of $550\mu g/ml$ ACh stimulation (46d) HS of electrical stimulation post ACh administration (46e) MHS of $550\mu g/ml$ ACh stimulation (46f) MHS of electrical stimulation post ACh administration.

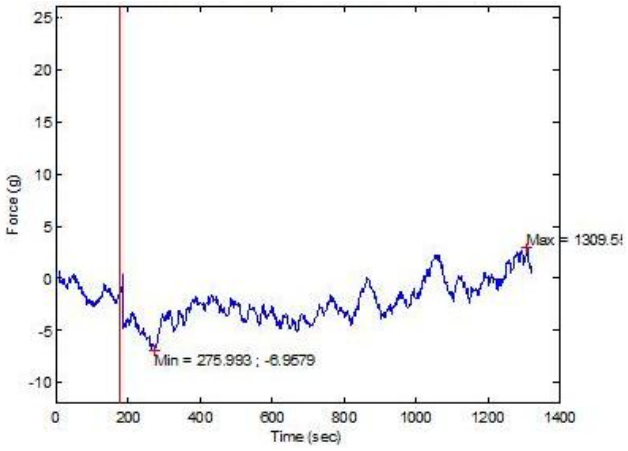

(a)

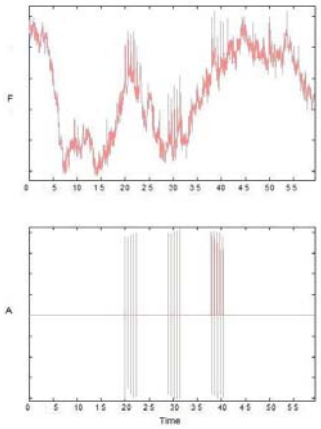

(b)

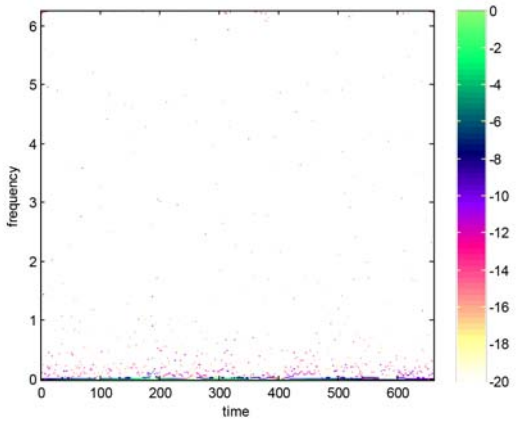

(c) injection at 180 sec

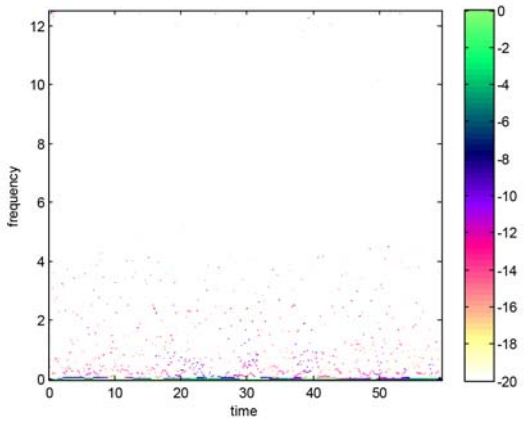

(d) stimulation as in (b)

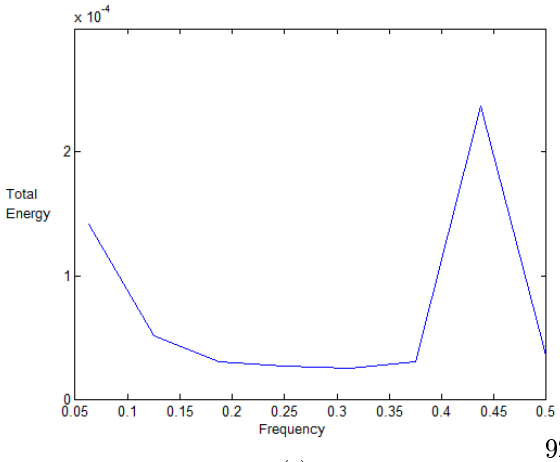

(e)

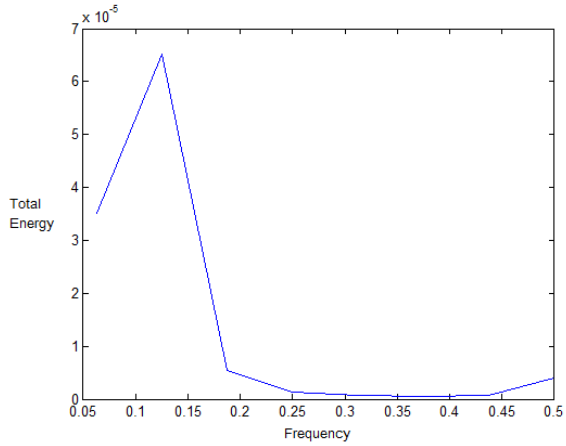

(f)

Figure 47: Results of IS from 7 day denervation group, stimulated at 1.6g/ml. (47a) F-t record of 1.6g/ml ACh stimulation (47b) F-t record (top) and amplitude (A)-t indication of stimulation (bottom) for electrical stimulation post ACh administration (47c) HS of 1.6g/ml ACh stimulation (47d) HS of electrical stimulation post ACh administration (47e) MHS of 1.6g/ml ACh stimulation (47f) MHS of electrical stimulation post ACh administration.

and in the high frequency component between 7-12sec. The MHS supports this with high energy low frequency component contribution. An increased energy contribution is further noted to span 0.31-0.44Hz (see Figure 48e).

A DS stimulated with the same concentration of 3.2g/ml displayed an increased force variation but differed from the IS in that no notable gradual F-t increase was observed, nor was any tetanus observed. The MHS depicted a large energy contribution between 0.31-0.44Hz (but not as large as the low frequency energy contribution), which is a higher frequency range than the IS high energy contribution. The HS generated from the electrical stimulation test demonstrated some locality and a slight energy contribution was noted in the 0.44-0.5Hz range. The results of the stimulation of the DS muscle are depicted in Figure 49.

Figure 50 illustrates the response of an IG to 3.2g/ml of ACh. An eventual gradual increase in force from about 700s onwards in F-t trace was observed (see Figure 50a). The force was seen to drop off after a peak was reached. The MHS displays the large energy contribution in a 0.31-0.44Hz frequency range (with a peak at 0.37Hz). This energy contribution was larger than that of the lower frequency range. Electrical stimulation resulted in a display of high locality in the HS, showing two stimulation regions in Figure 50d (corresponding to time locations of stimulation). The MHS of the muscles' response to electrical reaction illustrates a very large low frequency energy contribution (relative to itself; since the absolute energy is small, in the range of 10^{-5}). An increased energy contribution was noted in the 0.44-0.5Hz range.

A DG stimulated with the highest ACh concentration of 6.3g/ml (see Figure 51), displayed a gradual increase in force over time and appeared to reach unfused tetanus, fluctuating around 10g. The MHS displayed the majority of energy contribution as being from within the low frequency range of 0.06-0.13Hz but the absolute energy was observed to be high (10^{-3} range). Electrical stimulation showed no clear locality, although clear components were noted throughout the signal, presumably a continuation of the effects of previous ACh administration. The MHS showed a large, low frequency, energy contribution (relatively, but the absolute energy was only in the 10^{-5} range). No energy contributions from higher frequency ranges were observed, although small contractions in the electrical F-t trace were visible.

A DS, tested at the highest used concentration of 6.3g/ml ACh showed a gradual increase in force with time. A large amount of scatter visible in the HS plot, indicated that the energy was not confined to small frequency bands. The MHS showed a large energy contribution from the low frequency range. A further increased contribution was observed between 0.25-0.37Hz. The MHS from the electrical stimulation test showed a very small energy contribution (relative to the low frequency contribution) from a higher 0.37-0.5Hz frequency range. The results are illustrated in Figure 52.

An IS stimulated at 6.3g/ml (Figure 53) demonstrated an initial increase in force variation, followed by a drop in force just after 700s on the F-t trace. The MHS showed a large low frequency

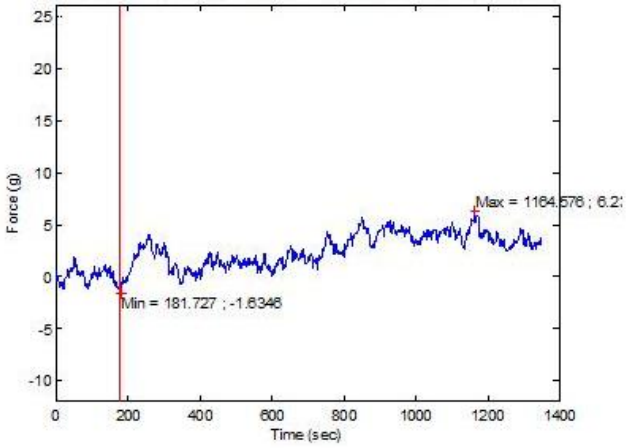

(a)

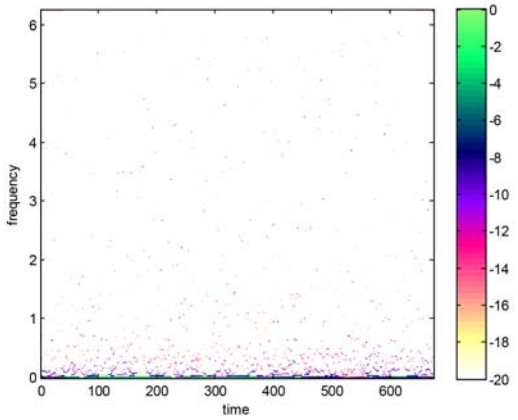

(b) injection at 180 sec

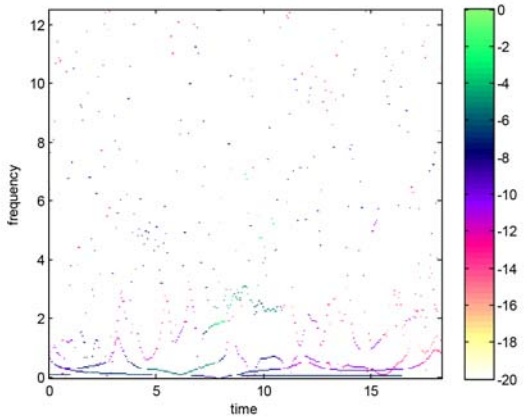

(c)

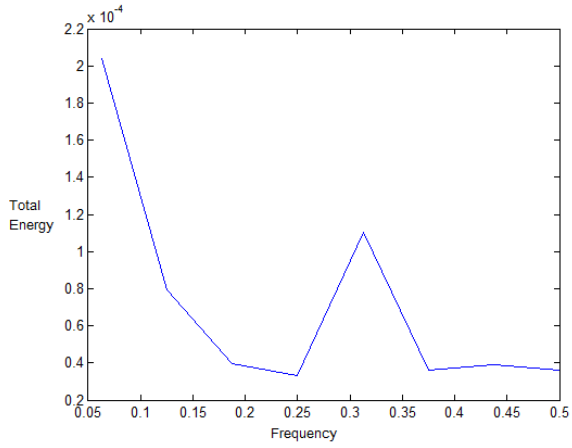

(d)

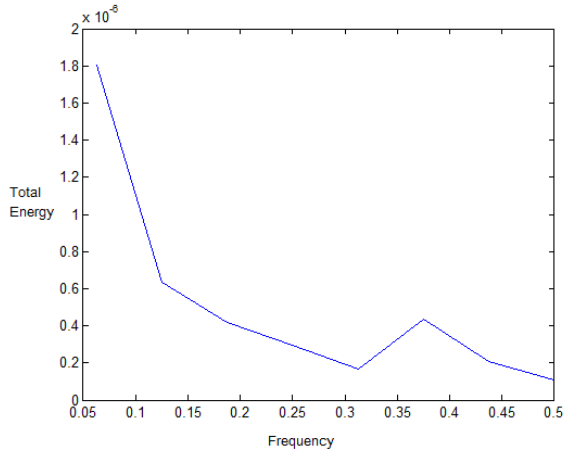

(e)

Figure 48: Results of IS from 7 day denervation group, stimulated at 3.2g/ml. (48a) F-t record of 3.2g/ml ACh stimulation (48b) HS of 3.2g/ml ACh stimulation (48c) HS of electrical stimulation post ACh administration (48d) MHS of 3.2g/ml ACh stimulation (48e) MHS of electrical stimulation post ACh administration.

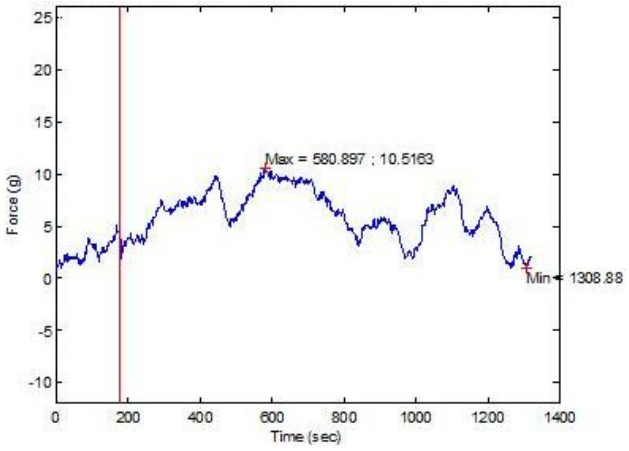

(a)

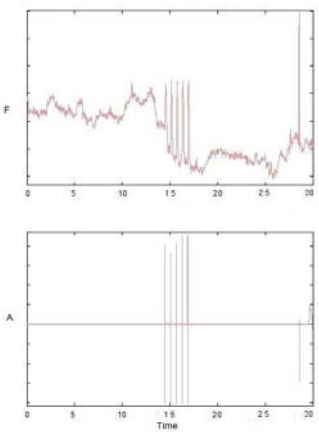

(b)

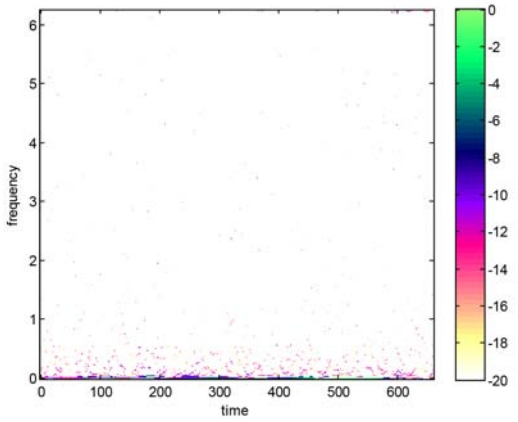

(c) injection at 180 sec

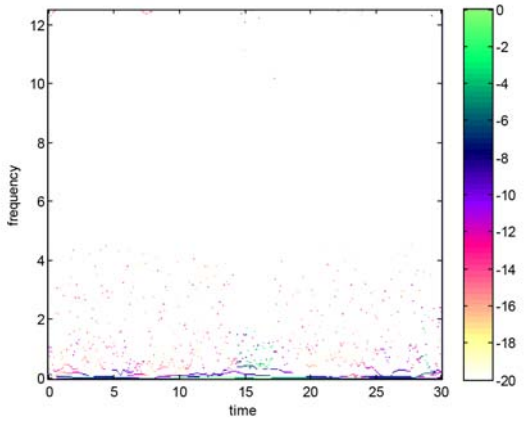

(d) stimulation as in (b)

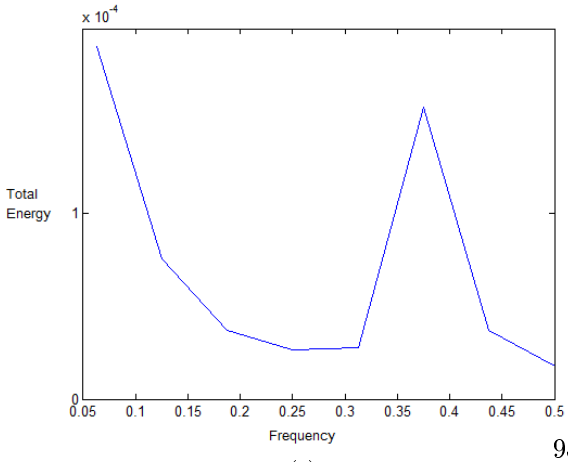

(e)

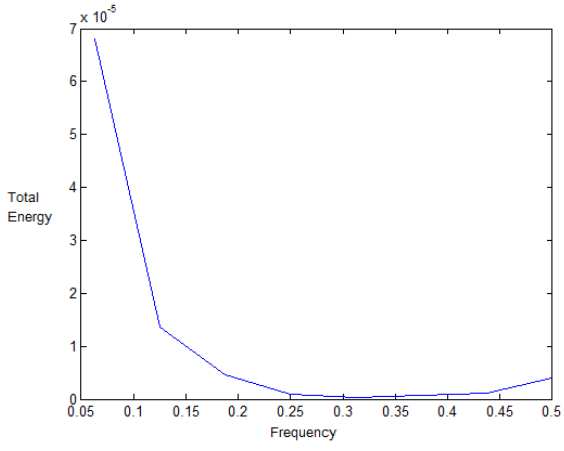

(f)

Figure 49: Results of 7 day DS stimulated at 3.2g/ml. (49a) F-t record of 3.2g/ml ACh stimulation (49b) F-t record (top) and amplitude (A)-t indication of stimulation (bottom) for electrical stimulation post ACh administration (49c) HS of 3.2g/ml ACh stimulation (49d) HS of electrical stimulation post ACh administration (49e) MHS of 3.2g/ml ACh stimulation (49f) MHS of electrical stimulation post ACh administration.

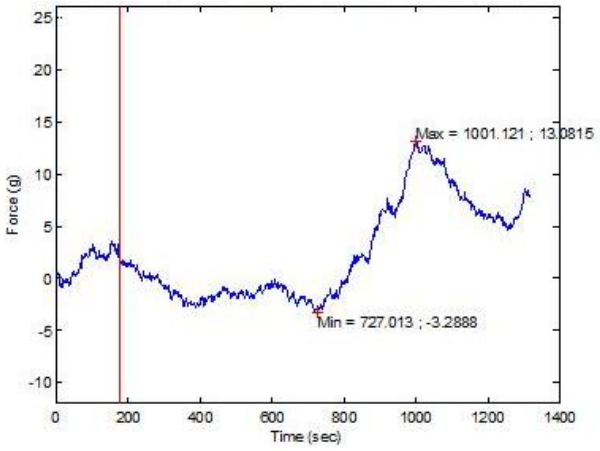

(a)

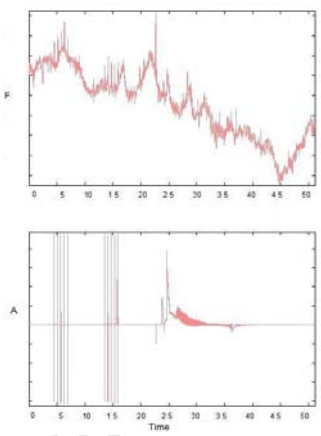

(b)

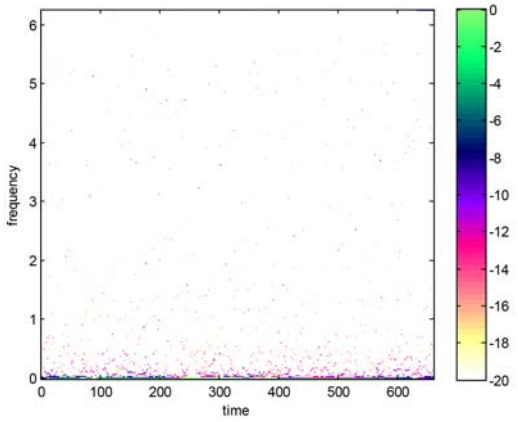

(c) injection at 180 sec

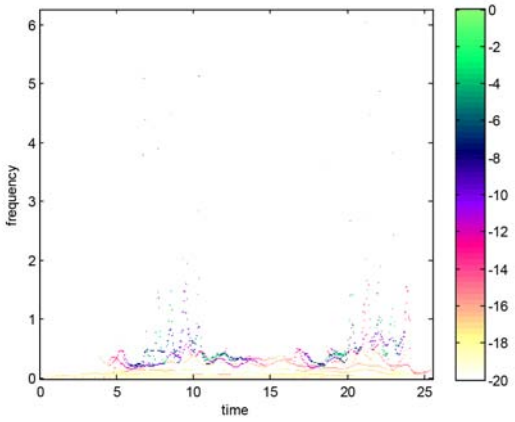

(d) stimulation as in (b)

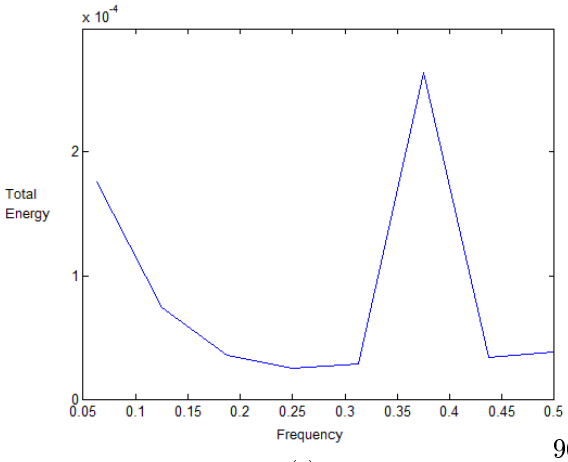

(e)

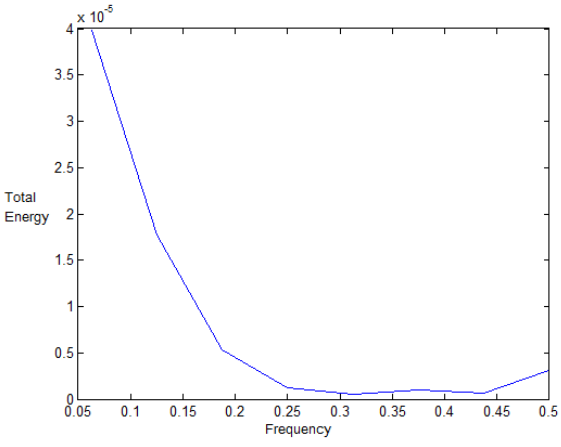

(f)

Figure 50: Results of IG from 7 day denervation group, stimulated at 3.2g/ml. (50a) F-t record of 3.2g/ml ACh stimulation (50b) F-t record (top) and amplitude (A)-t indication of stimulation (bottom) for electrical stimulation post ACh administration (50c) HS of 3.2g/ml ACh stimulation (50d) HS of electrical stimulation post ACh administration (50e) MHS of 3.2g/ml ACh stimulation (50f) MHS of electrical stimulation post ACh administration.

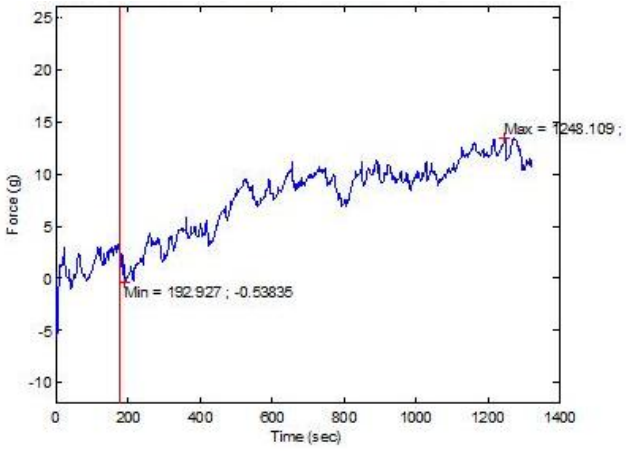

(a)

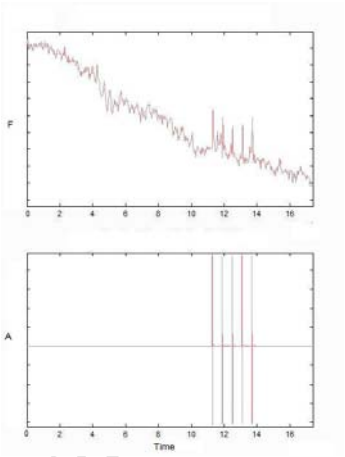

(b)

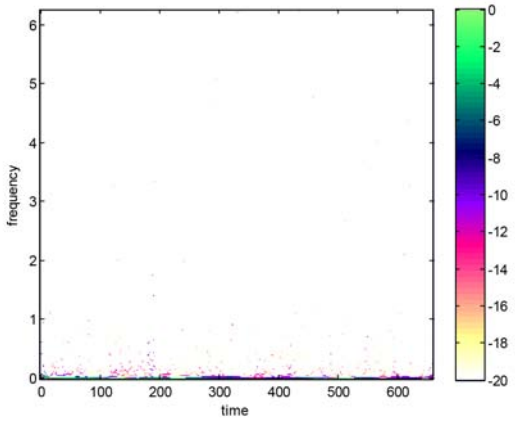

(c) injection at 180 sec

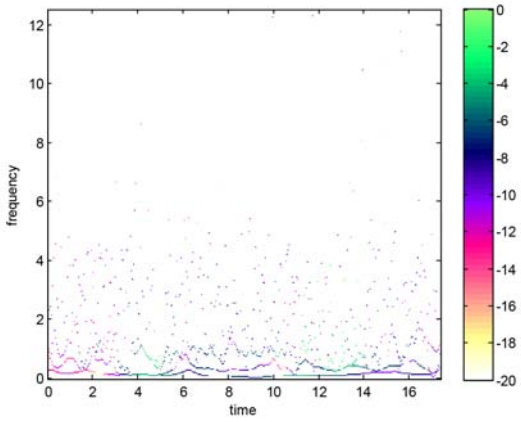

(d) stimulation as in (b)

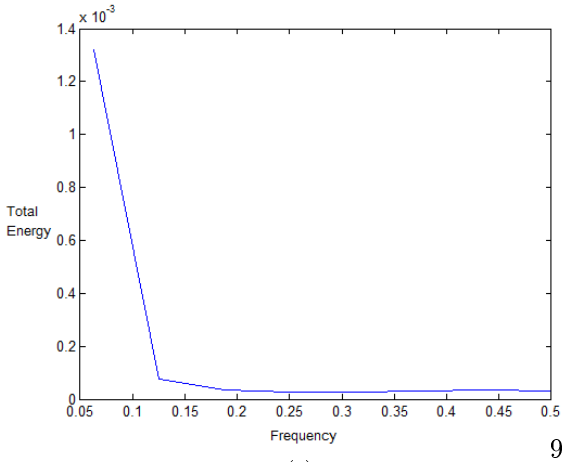

(e)

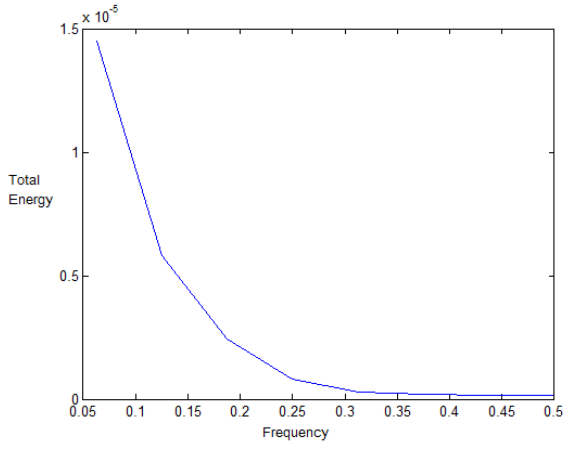

(f)

Figure 51: Results of 7 day DG stimulated at 6.3g/ml. (51a) F-t record of 6.3g/ml ACh stimulation (51b) F-t record (top) and amplitude (A)-t indication of stimulation (bottom) for electrical stimulation post ACh administration (51c) HS of 6.3g/ml ACh stimulation (51d) HS of electrical stimulation post ACh administration (51e) MHS of 6.3g/ml ACh stimulation (51f) MHS of electrical stimulation post ACh administration.

energy contribution in a 0.13-0.25Hz frequency range (in addition to the low frequency contribution between 0.06-0.13Hz). The HS supports this, demonstrating well confined energy (very little frequency 'scatter' occurred). Electrical stimulation produced small contractions post ACh administration. The HS of the electrical test demonstrates no clear locality, although clear components are visible throughout the signal, again presumably a continuation of the effects of previous ACh administration.

Alternate chemical and electrical stimulation of muscles denervated for a 14 day period

The F-t trace of the initial chemical stimulation of a 14 day DG by $4\mu g/ml$ (see Figure 54a) displayed a steady increase in force post injection, which stabilised at around 750s on the graph (corresponding to 9m30s after injection), fluctuating about a 10g force. This steady fluctuation around a force value was considered unfused tetanus, as described in section 2.1.3 and illustrated in Figure 5. (The HS of the chemical stimulation test displays a small increase in energy in the low frequency range post injection, with frequency 'scatter' occurring in a 0-1Hz range). The MHS pertaining to this chemical stimulation test displayed a large energy component within a 0.37-0.5Hz frequency range (peaking at 0.44Hz). Electrical stimulation after the application of $4\mu g/ml$ of ACh, resulted in a very weak response from the muscle, barely discernable from the high frequency fluctuations present in the signal. These could be due to continued action of the ACh on the muscle. The MHS of the electrical stimulation test demonstrated that energy was only present in low frequency components. This is consistent with literature reporting that the muscle can not be further electrically stimulated by a significant amount if it has already been exposed to a high concentration (or dose) of ACh [Brown, 1937].

Stimulation of a 14 day DS by $4\mu g/ml$ of ACh, resulted in a steady increase in force with time, which reached unfused tetanus by 800s, fluctuating around 14g. The HS displays an increase in energy post injection, concentrated in the low frequency range. The MHS displayed a larger than usual amount of energy in the full frequency range, with increases occurring at the extremes of very low frequencies and a high frequency range of 0.44-0.5Hz, the latter contributing the most energy. Further electrical stimulation resulted in a clearer response than that of the DG under the same conditions. This is further depicted more clearly in the F-t trace of Figure 55b. The HS depicting the energy-frequency-time distribution of the electrical stimulation is displayed in Figure 55d, with clear locality and some intrawave frequency modulation occurring in regions corresponding to stimulation (compare to F-t trace of electrical test, Figure 55b). Further chemical stimulation was applied, the HS of which is illustrated in Figure 56d. The low frequency components show a substantial increase in energy after injection (at 30s). The signal was comprised of more localised energy components (i.e., displaying less scatter) The MHS illustrates an increased energy contribution in the 0.18-0.31Hz range and a higher than usual energy contribution between 0.31-0.44Hz. Further electrical stimulation resulted in a (still clear) contractile response, indicative of a high muscle sensitivity.

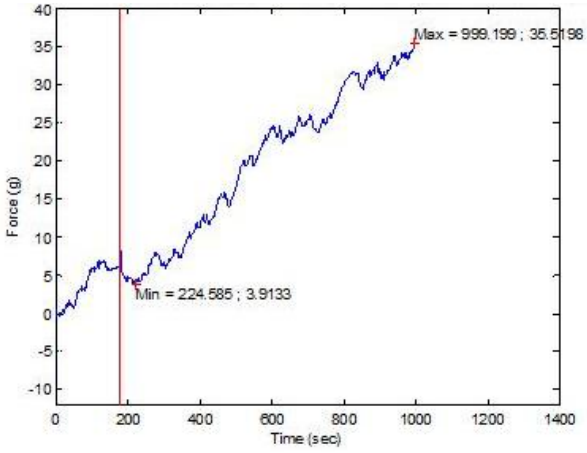

(a)

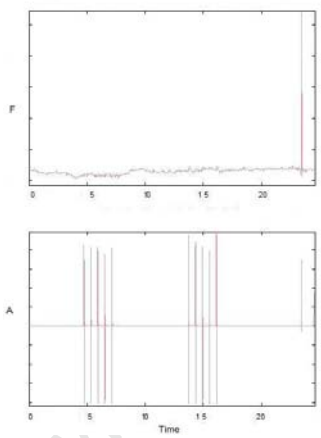

(b)

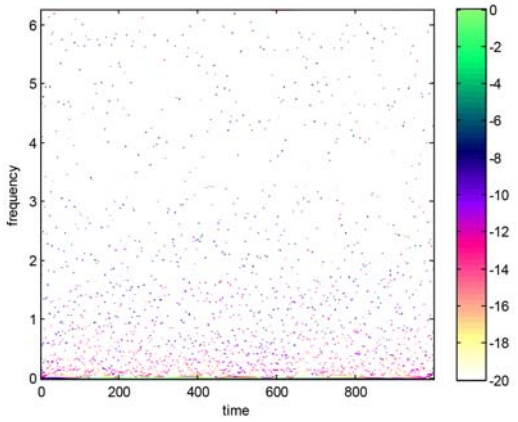

(c) injection at 180 sec

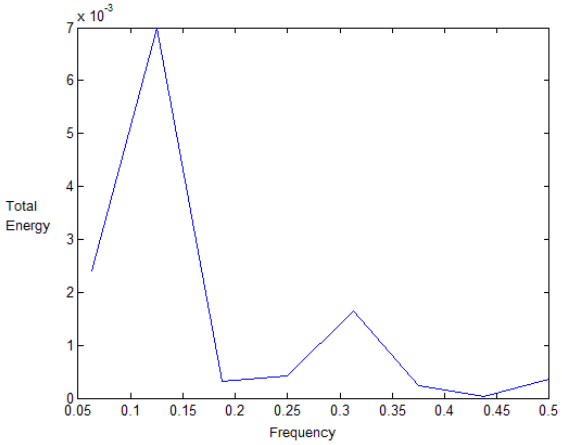

(d)

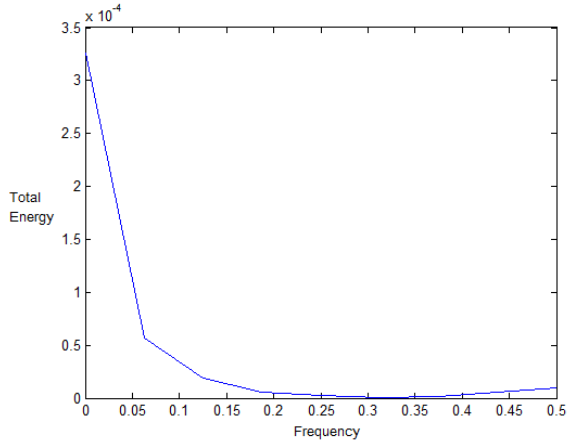

(e)

Figure 52: Results of 7 day DS stimulated at 6.3g/ml. (52a) F-t record of 6.3g/ml ACh stimulation (52b) F-t record (top) and amplitude (A)-t indication of stimulation (bottom) for electrical stimulation post ACh administration (52c) HS of 6.3g/ml ACh stimulation (52d) MHS of 6.3g/ml ACh stimulation (52e) MHS of electrical stimulation post ACh administration.

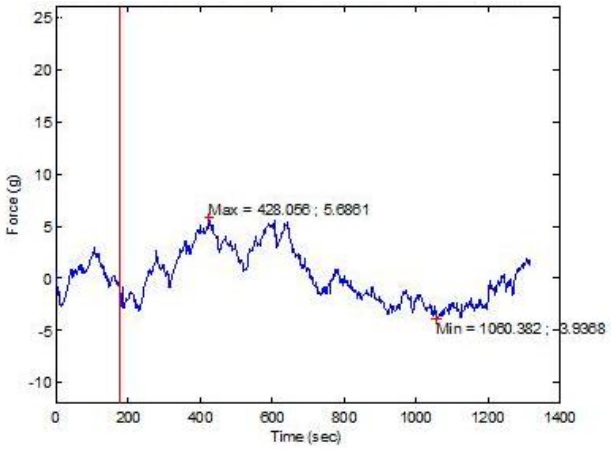

(a)

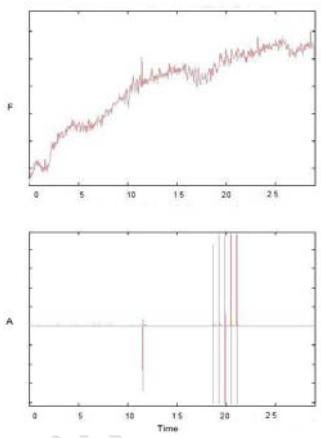

(b)

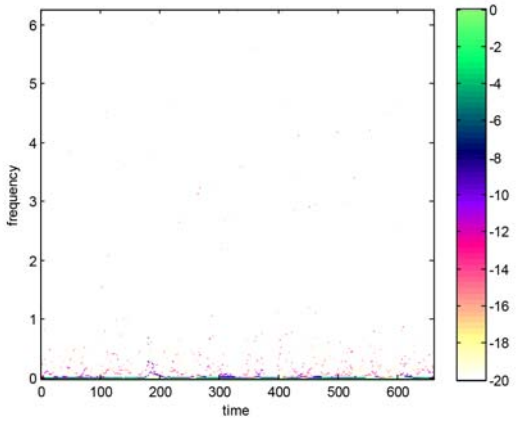

(c) injection at 180 sec

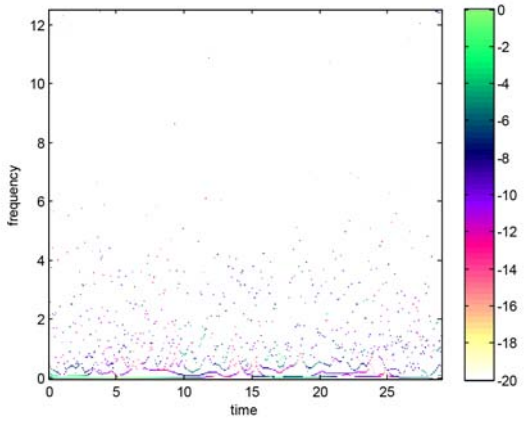

(d) stimulation as in (b)

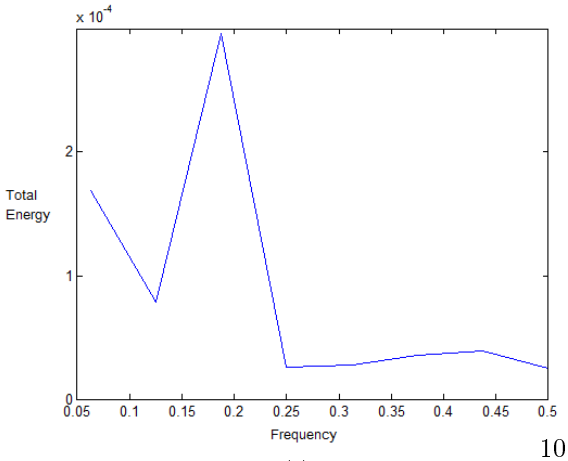

(e)

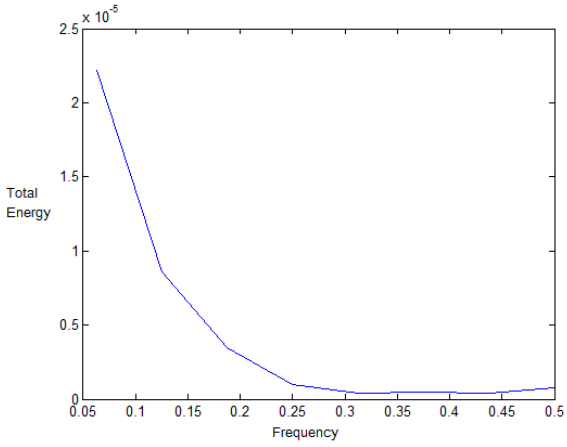

(f)

Figure 53: Results of IS from 7 day denervation group, stimulated at 6.3g/ml. (53a) F-t record of 6.3g/ml ACh stimulation (53b) F-t record (top) and amplitude (A)-t indication of stimulation (bottom) for electrical stimulation post ACh administration (53c) HS of 6.3g/ml ACh stimulation (53d) HS of electrical stimulation post ACh administration (53e) MHS of 6.3g/ml ACh stimulation (53f) MHS of electrical stimulation post ACh administration.

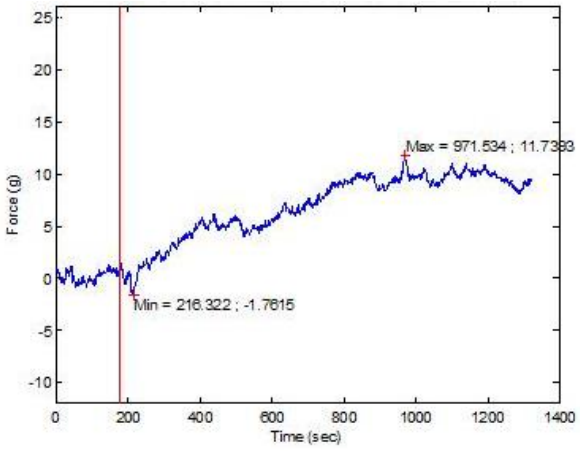

(a)

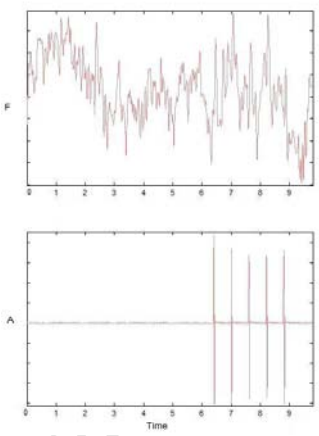

(b)

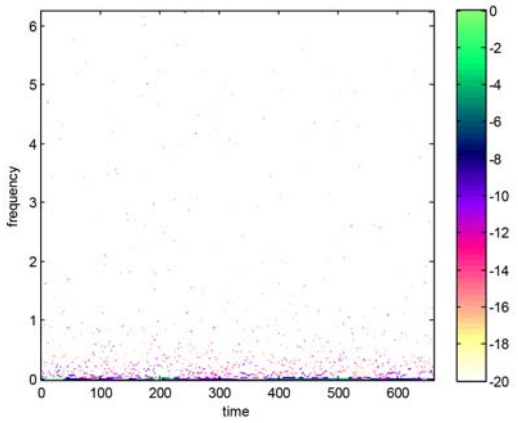

(c) injection at 180 sec

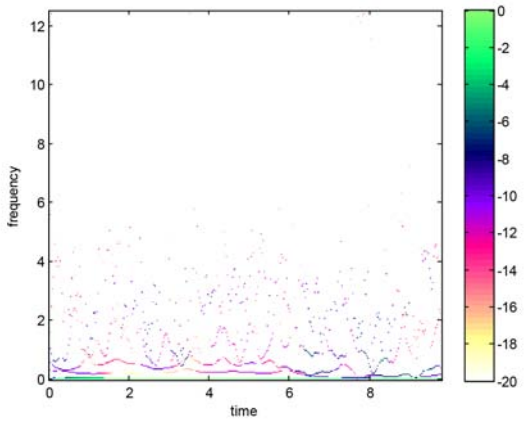

(d) stimulation as in (b)

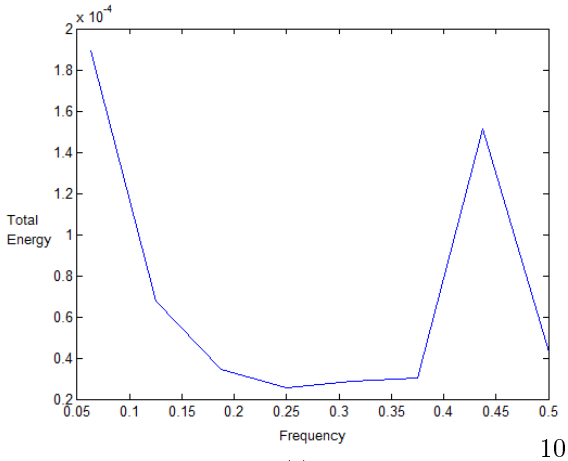

(e)

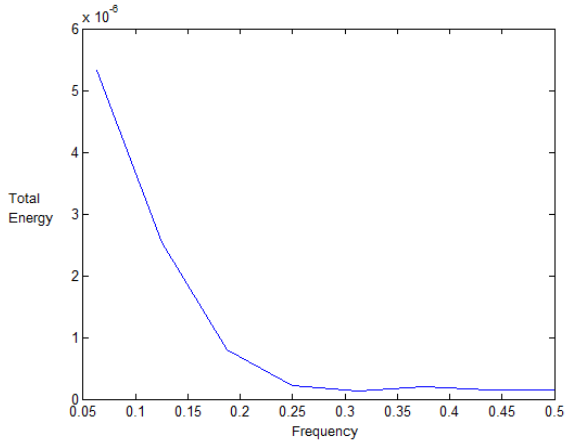

(f)

Figure 54: Results of 14 day DG stimulated at $4\mu g/ml$. (54a) F-t record of $4\mu g/ml$ ACh stimulation (54b) F-t record (top) and amplitude (A)-t indication of stimulation (bottom) for electrical stimulation post ACh administration (54c) HS of $4\mu g/ml$ ACh stimulation (54d) HS of electrical stimulation post ACh administration (54e) MHS of $4\mu g/ml$ ACh stimulation (54f) MHS of electrical stimulation post ACh administration.

An IS (control) from a 14 day denervated rat, stimulated with $4\mu g/ml$ of ACh, only displayed a significant increase in force 320s post injection (post 500s on the F-t graph in Figure 57a). Unfused tetanus was reached by 800s but the muscle displayed signs of fatigue after 1100s. Localised energy was observed and confined to low frequency components, as illustrated in its HS (Figure 57c). The MHS demonstrated high energy contributions in a 0.18-0.31Hz frequency range. Post injection activity was observed in the HS to occur in a slightly higher frequency range than pre injection activity, this is supported by the observations made from the MHS. Electrical stimulation displayed no clearly discernable contractions, despite some larger than usual energy contributions from the low frequency range (presumably due to continued ACh effects) and a slight increase in energy in the 0.44-0.5Hz range.

The DS and IS stimulated at the same concentration differed in a number of observations. The IS exhibited a delay in rate of rise of force not observed in the DS. Both reached a state of unfused tetanus, but the IS displayed later signs of fatigue, indicated by a decrease in force. Electrical stimulation failed to produce contractile activity in the IS, whereas a clear response was visible in the DS, even after additional ACh stimulation. This further attested to increased sensitivity of denervated muscles in comparison to their innervated contralaterals. The frequency ranges of energy contribution differed between muscles, the DS displaying full frequency range sensitivity and low and high frequency extreme energy contribution, and the IS maintaining a localised contribution between 0.18-0.31Hz.

Administration of $96\mu g/ml$ of ACh to a 14 day DG resulted in large force variation (peak-to-peak fluctuation), a gradual increase in force over time, unfused tetanus and eventual muscle fatigue (see Figure 58a). The HS shows activity very localised in frequency, with more 'scatter' across a larger frequency range post ACh administration. The MHS illustrates a considerably high energy contribution in the 0.25-0.37Hz range (note the large frequency range in comparison to ranges of other tests) with a peak at 0.31Hz. This energy contribution is higher than that of the low frequency energy contribution. Electrical stimulation resulted in small, but discernable twitches, a clearer response than that achieved by electrical stimulation after chemical stimulation by $4\mu g/ml$ of ACh. No clear localised activity is visible in the HS corresponding to the electrical test, but continued effects of previous ACh administration are evident throughout the signal.

Figure 59 and 60 illustrate the response of an IG to multiple stimulation. The F-t trace in Figure 60a does not display much change in force post injection of $96\mu g/ml$. Large force fluctuation was observed up until 600s, after which the force variations were smaller. Moreover, no gradual increase was visible. The HS of this test is illustrated in Figure 59c, which demonstrates very little frequency scatter, the energy being confined to low frequency components. This is confirmed by the MHS which indicates high concentrations of energy in frequency ranges of 0.06-0.18Hz and 0.25-0.37Hz. Electrical stimulation produced a weak contractile response, weaker than that observed for the DG under the same conditions, with the MHS showing all the energy confined to the low

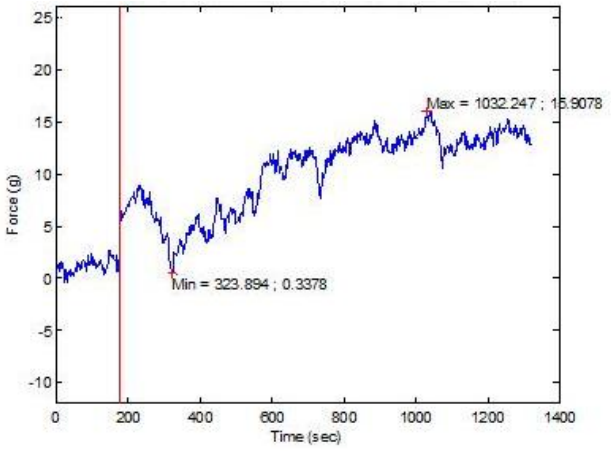

(a)

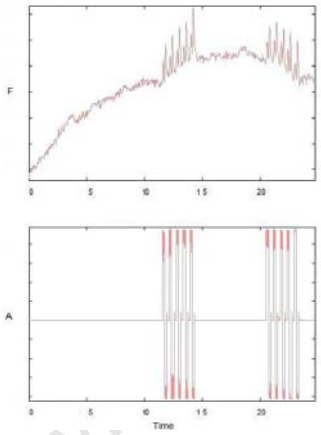

(b)

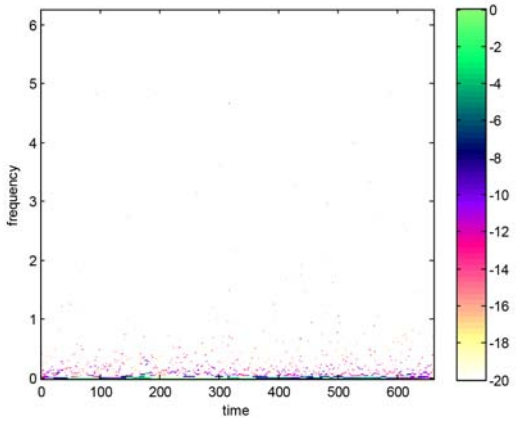

(c) injection at 180 sec

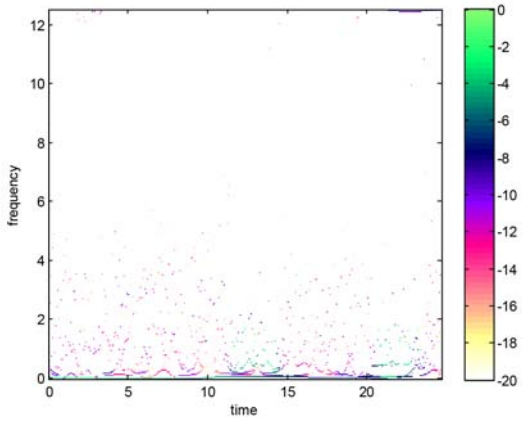

(d) stimulation as in (b)

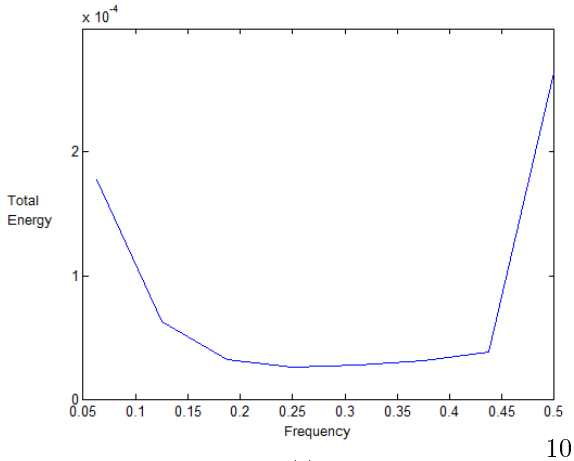

(e)

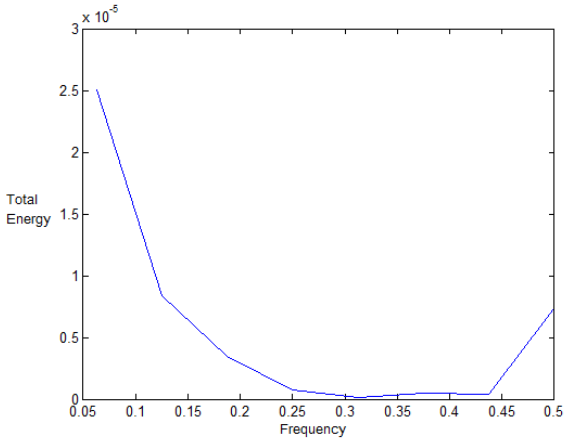

(f)

Figure 55: Results of 14 day DS stimulated at $4\mu g/ml$. (55a) F-t record of $4\mu g/ml$ ACh stimulation (55b) F-t record (top) and amplitude (A)-t indication of stimulation (bottom) for electrical stimulation post ACh administration (55c) HS of $4\mu g/ml$ ACh stimulation (55f) HS of electrical stimulation post ACh administration (55e) MHS of $4\mu g/ml$ ACh stimulation (55f) MHS of electrical stimulation post ACh administration.

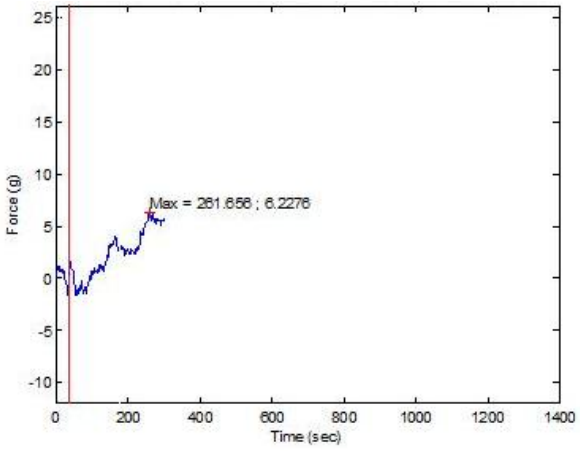

(a)

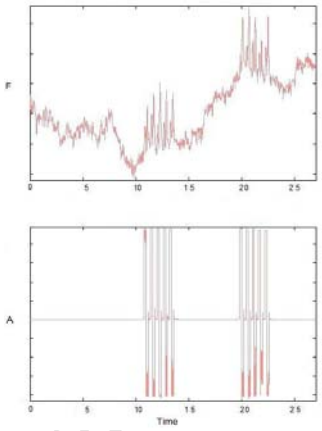

(b)

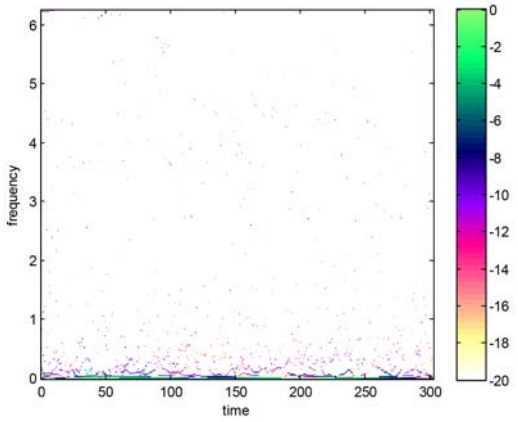

(c) injection at 180 sec

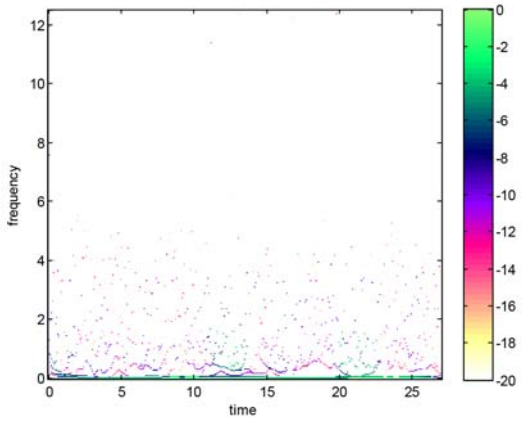

(d) stimulation as in (b)

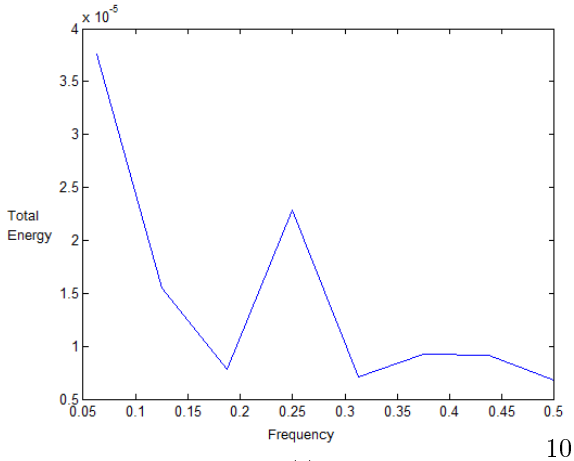

(e)

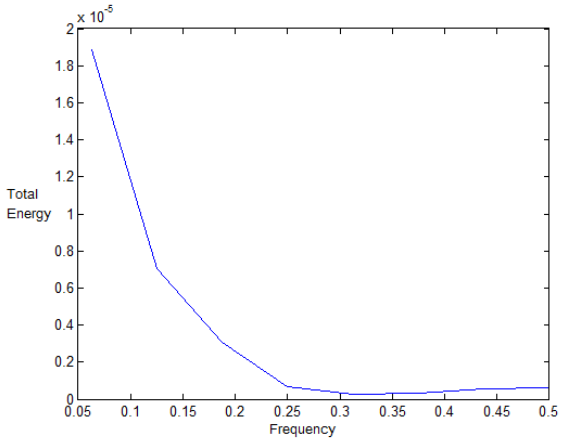

(f)

Figure 56: Results of further chemical and electrical stimulation of 14 day DS, initially stimulated at $4\mu g/ml$ (see Figure 55). (56a) F-t record of stimulation by large dose of ACh (56d) F-t record (top) and amplitude (A)-t indication of stimulation (bottom) for electrical stimulation post ACh administration (56c) HS of large dose ACh stimulation (56d) HS of electrical stimulation post ACh administration (56e) MHS of large dose ACh stimulation (56f) MHS of electrical stimulation post ACh administration.

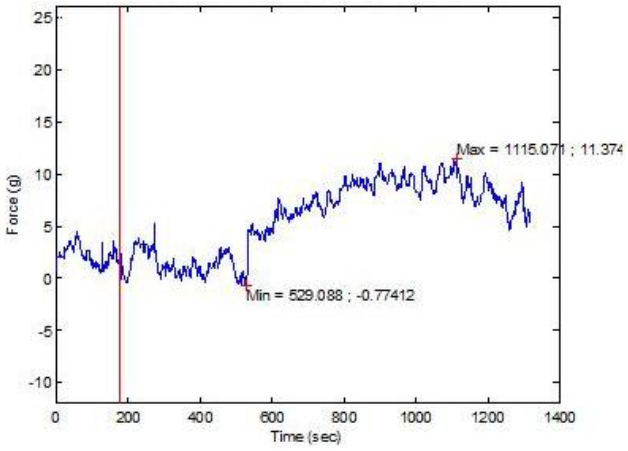

(a)

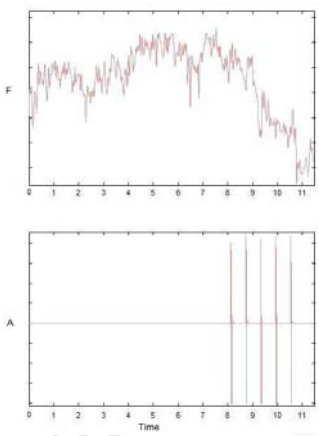

(b)

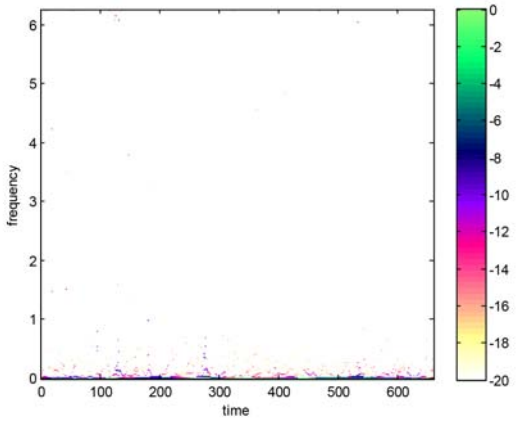

(c) injection at 180 sec

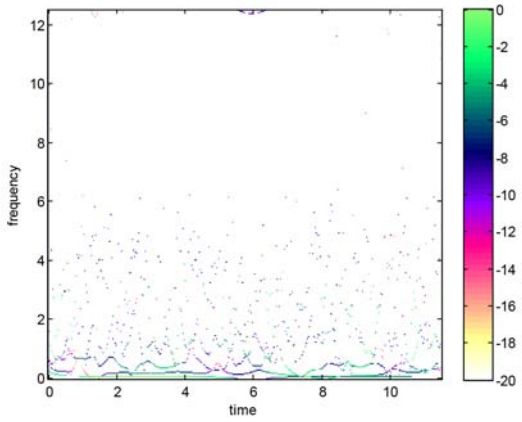

(d) stimulation as in (b)

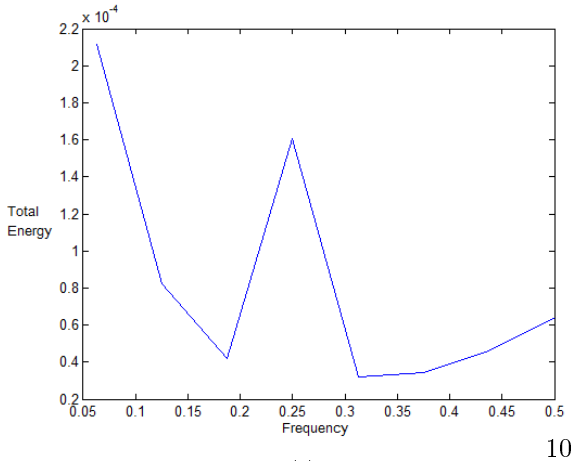

(e)

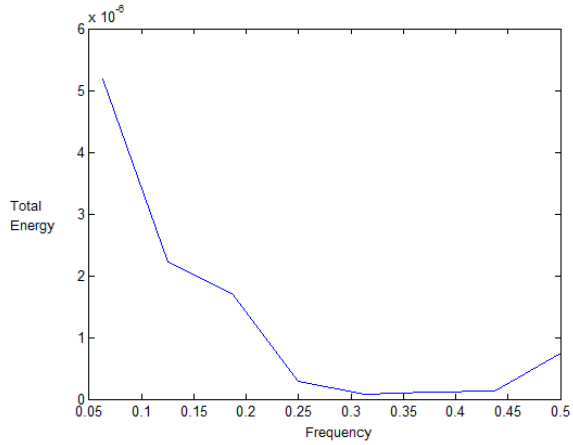

(f)

Figure 57: Results of IS from 14 day denervation group, stimulated at $4\mu g/ml$. (57a) F-t record of $4\mu g/ml$ ACh stimulation (57b) F-t record (top) and amplitude (A)-t indication of stimulation (bottom) for electrical stimulation post ACh administration (57c) HS of $4\mu g/ml$ ACh stimulation (57d) HS of electrical stimulation post ACh administration (57e) MHS of $4\mu g/ml$ ACh stimulation (57f) MHS of electrical stimulation post ACh administration.

frequency range. Further chemical stimulation produced an increase in the low energy components of the signal post injection in the HS, although no change was observed in the F-t trace (shown in Figure 60a). The MHS displays energy mostly concentrated in the low frequency range, with small contributions from the 0.25-0.37Hz range. Further electrical stimulation resulted in small contractions of low energy (hence no localisation on the HS) and no notable energy contributions observed from the MHS outside of the usual low frequency energy contribution.

The DG and IG were similar in their response in that they both exhibited large force fluctuations post ACh administration (although this lasted only a short time in the IG). The DG displayed more energy scatter across frequencies than the IG which displayed a more localised energy distribution in frequencies. As mentioned, the electrical response evoked in the IG was smaller than that of the DG.

A 14 day DS tested at $96\mu g/ml$ (Figure 61) displayed a steady yet gradual increase in force which does not appear to reach a tetanic state of any mode. No large fluctuations in force were observed. The HS demonstrates a large amount of energy 'scatter' throughout a large frequency range over time. The MHS is supportive of this observation, showing energy contributions in the signal to exist over all frequencies, the majority of the energy being in the low frequency range. Electrical stimulation resulted in visible contractile activity, with higher energy components visible in the HS at the corresponding stimulation time. The MHS shows the main energy contribution of the signal to be from the 0.06-0.25Hz frequency range.

An IS stimulated with $96\mu g/ml$ of ACh resulted in a very small and gradual rise in force over time (see Figure 62a). This increase is a lot more gradual than that observed in the DS and reaches a state of unfused tetanus, at less than 5g. No large force fluctuations occurred, as in the case of the DS. A slight increase in energy occurred at the injection point, as illustrated in the HS in Figure 62c. The energy was a lot more scattered in frequency in the HS of the DS (stimulated at the same concentration) than that of the HS for the IS, whose energy was more localised in frequency. Electrical stimulation of this muscle after the initial chemical stimulation resulted in a localised region of energy-frequency-time, as illustrated in Figure 62d,similar to that of the DS. Further chemical stimulation resulted in a scattered energy-frequency-time plot (Figure 63b), whose MHS indicates an increased energy contribution in the 0.25-0.37Hz frequency range. Further electrical stimulation no longer showed a region of high locality, maintaining the "scattered" HS plot, with the MHS supporting this observation by indicating that most of the signals' energy occurred in the low 0.06-0.25Hz range.

Refer to Figure 64. Stimulation of a DS with $550\mu g/ml$ of ACh resulted in a gradual increase in force, but only low forces were obtained (less than 5g) upon reaching unfused tetanus. The HS shows an increase in energy after injection (visible from 180-300s) at the lowest frequency. The HS displays a large amount of energy scatter across the frequencies present in the signal throughout the time period of the test. The MHS shows the frequency components contributing the most

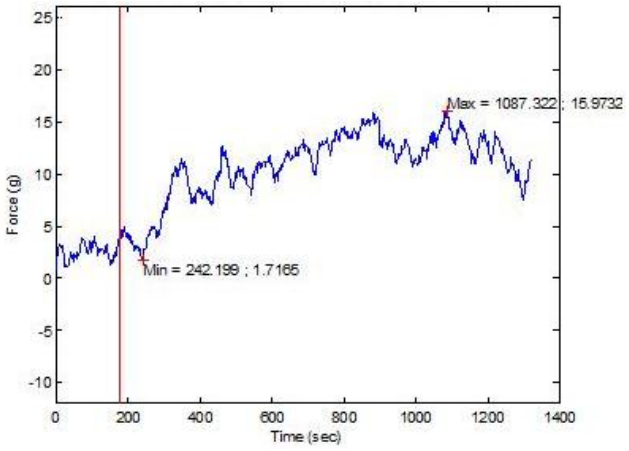

(a)

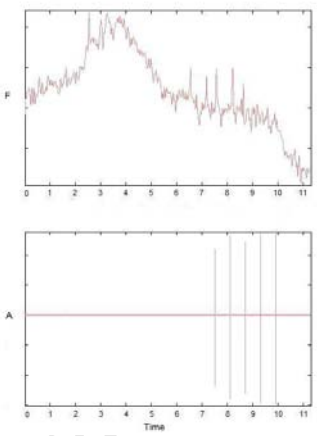

(b)

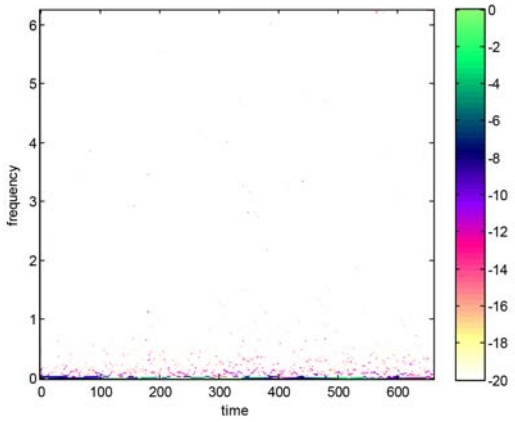

(c) injection at 180 sec

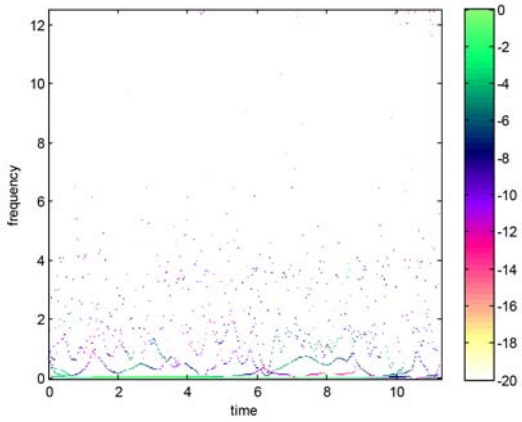

(d) stimulation as in (b)

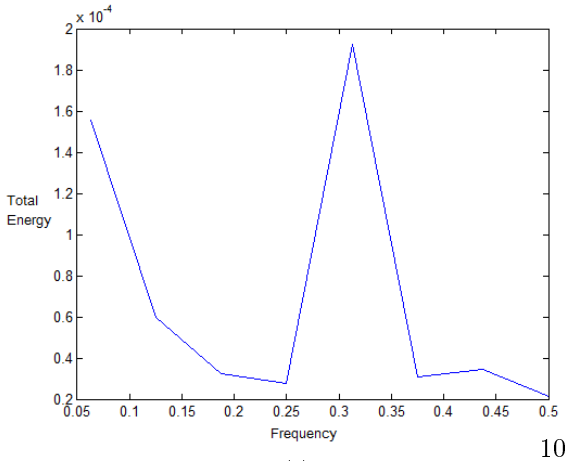

(e)

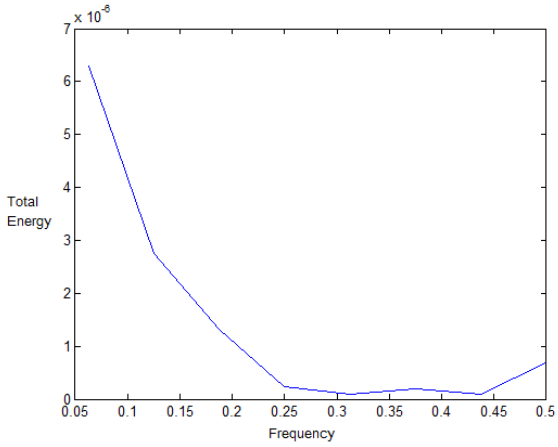

(f)

Figure 58: Results of 14 day DG stimulated at $96\mu g/ml$. (58a) F-t record of $96\mu g/ml$ ACh stimulation (58b) F-t record (top) and amplitude (A)-t indication of stimulation (bottom) for electrical stimulation post ACh administration (58c) HS of $96\mu g/ml$ ACh stimulation (58d) HS of electrical stimulation post ACh administration (58e) MHS of $96\mu g/ml$ ACh stimulation (58f) MHS of electrical stimulation post ACh administration.

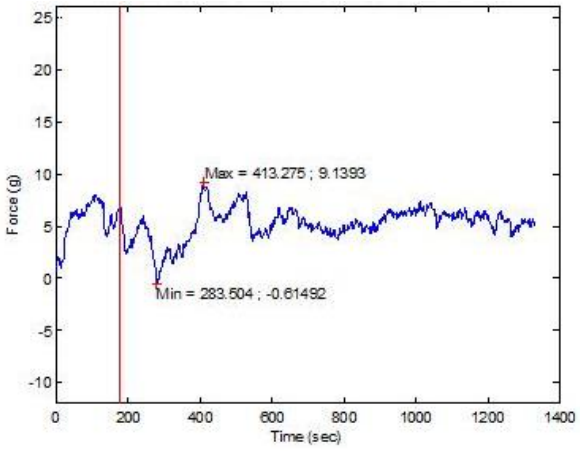

(a)

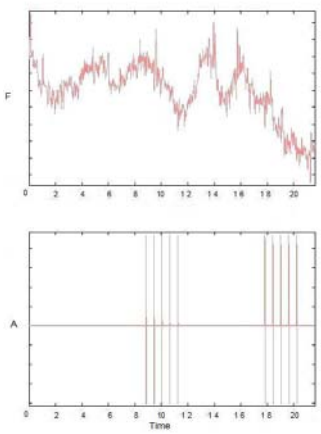

(b)

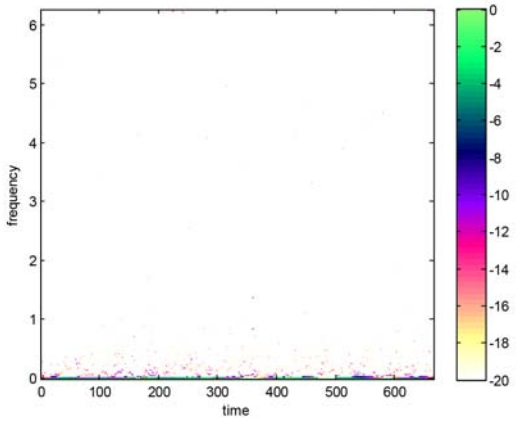

(c) injection at 180 sec

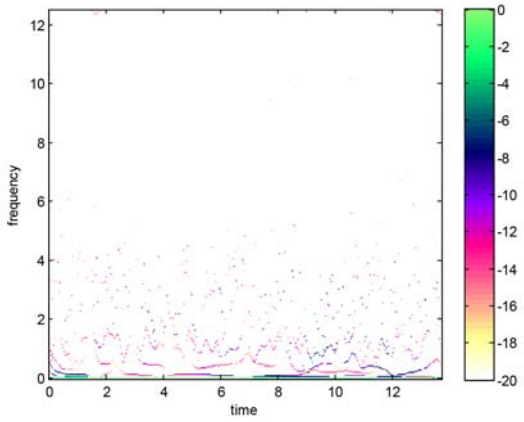

(d) stimulation as in (b)

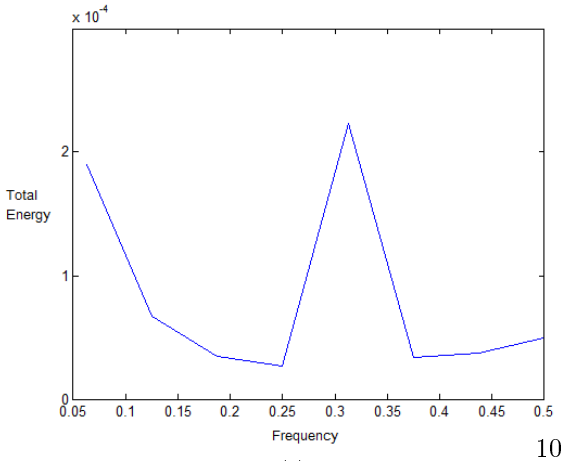

(e)

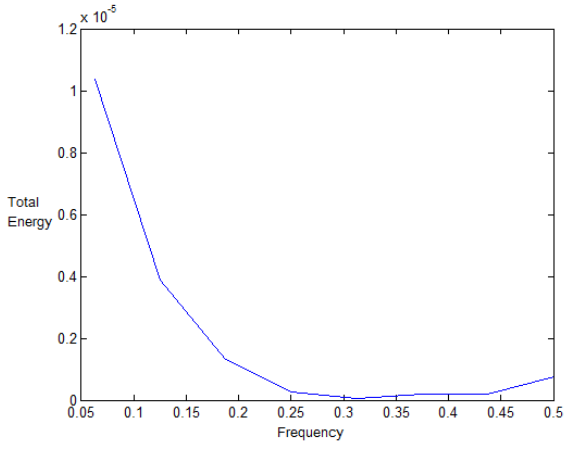

(f)

Figure 59: Results of IG from 14 day denervation group, stimulated at $96\mu g/ml$. (59a) F-t record of $96\mu g/ml$ ACh stimulation (59b) F-t record (top) and amplitude (A)-t indication of stimulation (bottom) for electrical stimulation post ACh administration (59c) HS of $96\mu g/ml$ ACh stimulation (59d) HS of electrical stimulation post ACh administration (59e) MHS of $96\mu g/ml$ ACh stimulation (59f) MHS of electrical stimulation post ACh administration.

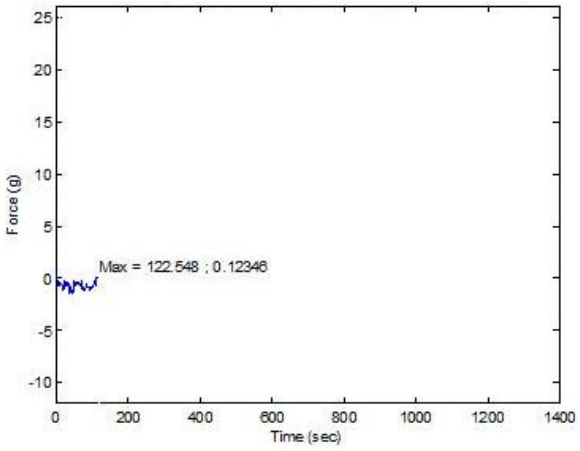

(a)

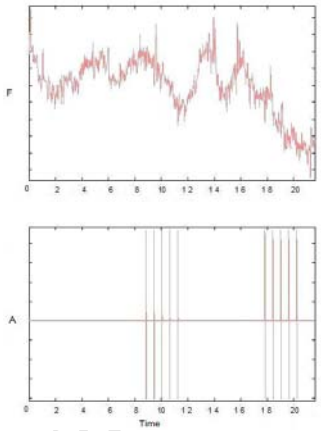

(b)

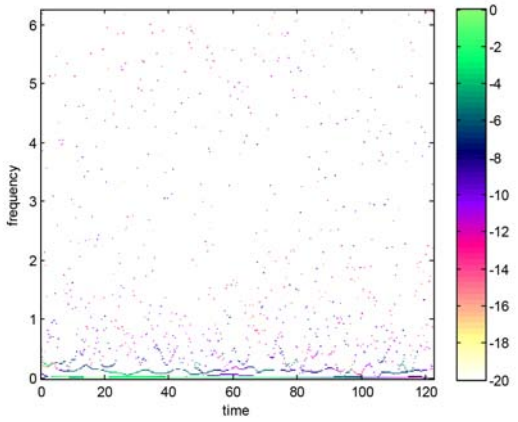

(c) injection at 180 sec

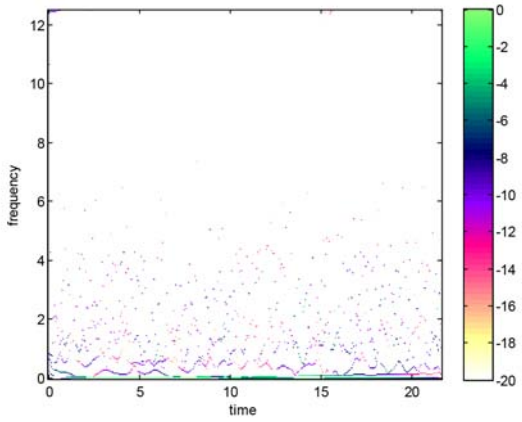

(d) stimulation as in (b)

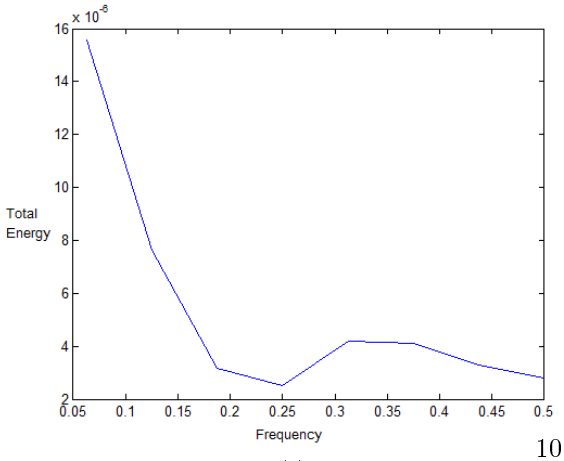

(e)

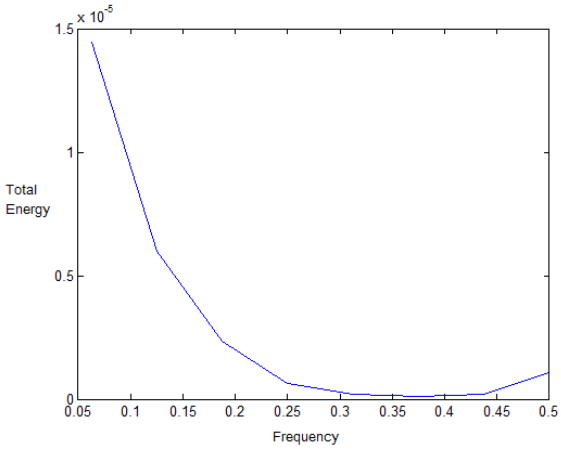

(f)

Figure 60: Results of further chemical and electrical stimulation of IG from 14 day denervation period group, initially stimulated at $96\mu g/ml$ (see Figure 59). (60a) F-t record of stimulation by large dose of ACh (60b) F-t record (top) and amplitude (A)-t indication of stimulation (bottom) for electrical stimulation post ACh administration (60c) HS of large dose ACh stimulation (60d) HS of electrical stimulation post ACh administration (60e) MHS of large dose ACh stimulation (60f) MHS of electrical stimulation post ACh administration.

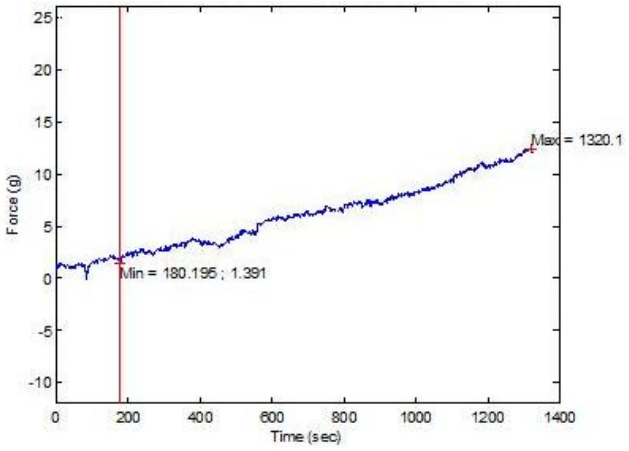

(a)

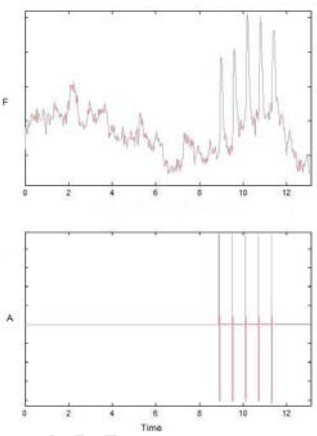

(b)

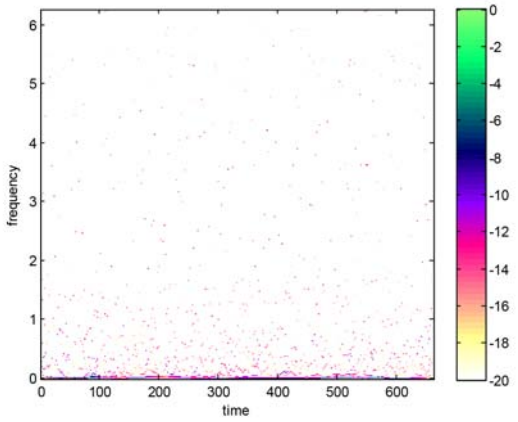

(c) injection at 180 sec

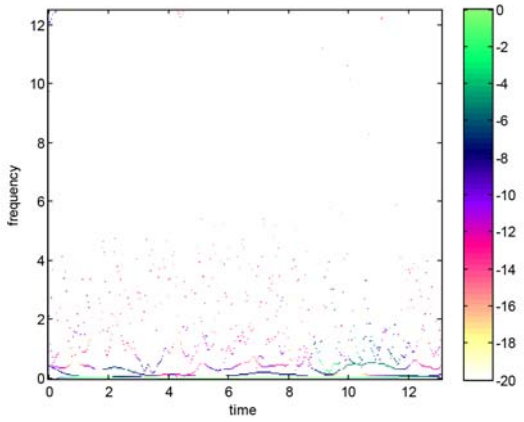

(d) stimulation as in (b)

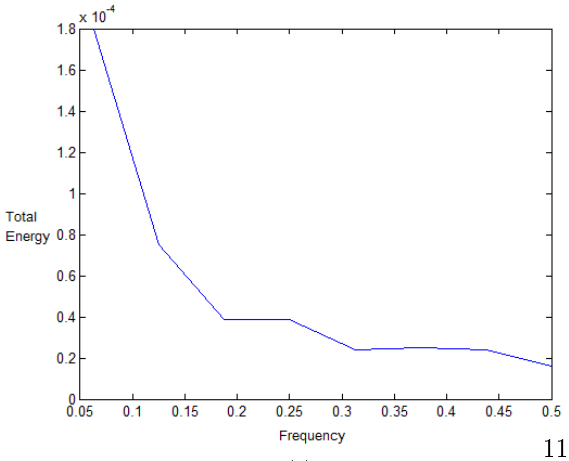

(e)

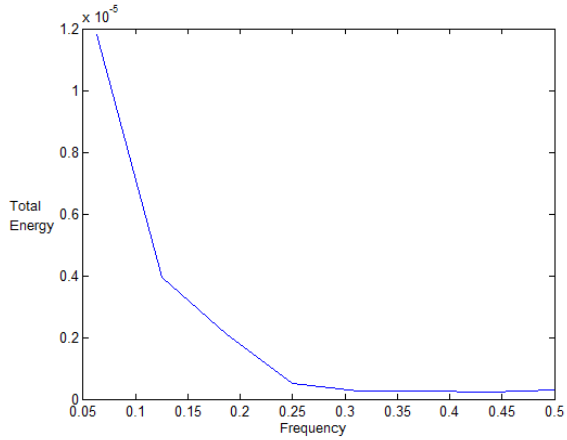

(f)

Figure 61: Results of 14 day DS stimulated at $96\mu g/ml$. (61a) F-t record of $96\mu g/ml$ ACh stimulation (61b) F-t record (top) and amplitude (A)-t indication of stimulation (bottom) for electrical stimulation post ACh administration (61c) HS of $96\mu g/ml$ ACh stimulation (61d) HS of electrical stimulation post ACh administration (61e) MHS of $96\mu g/ml$ ACh stimulation (61f) MHS of electrical stimulation post ACh administration.

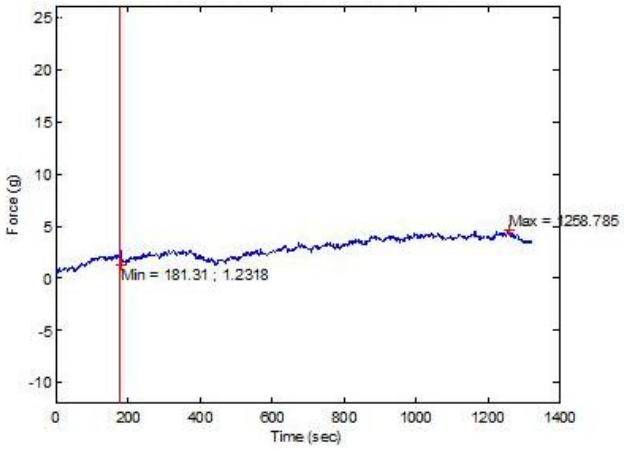

(a)

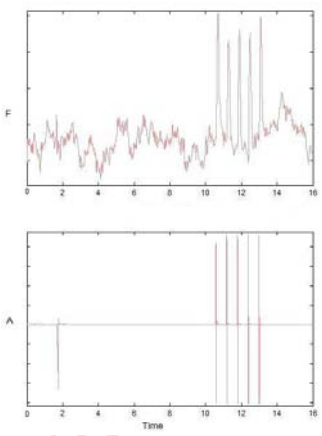

(b)

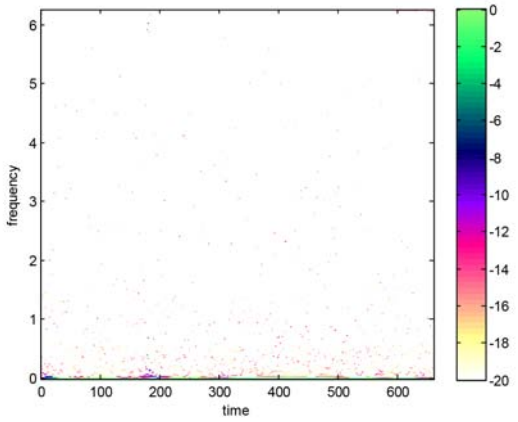

(c) injection at 180 sec

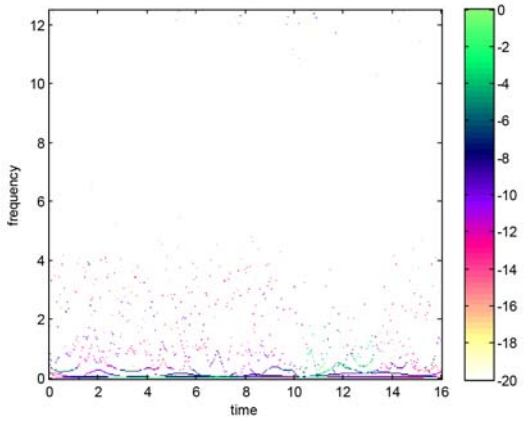

(d) stimulation as in (b)

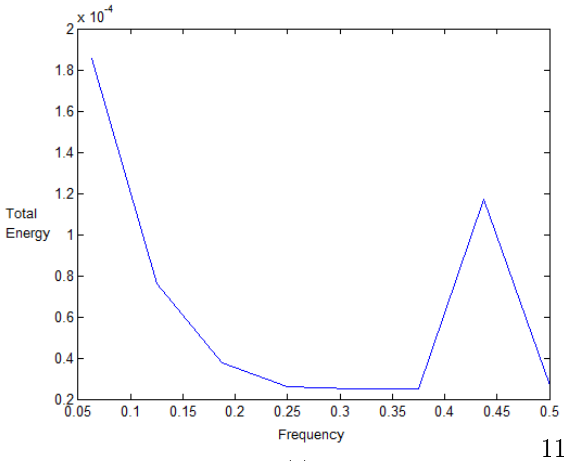

(e)

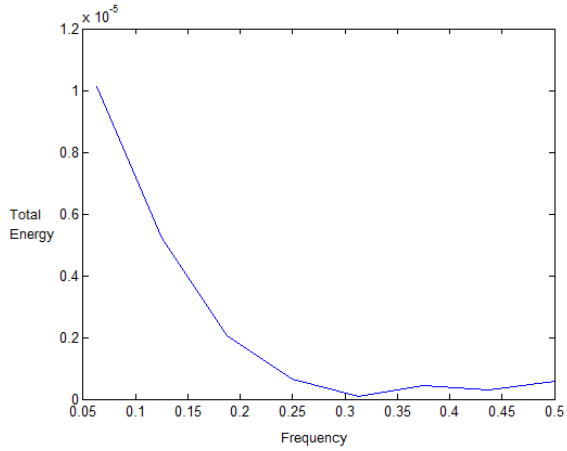

(f)

Figure 62: Results of IS from 14 day denervation group, stimulated at $96\mu g/ml$. (62a) F-t record of $96\mu g/ml$ ACh stimulation (62b) F-t record (top) and amplitude (A)-t indication of stimulation (bottom) for electrical stimulation post ACh administration (62c) HS of $96\mu g/ml$ ACh stimulation (62d) HS of electrical stimulation post ACh administration (62e) MHS of $96\mu g/ml$ ACh stimulation (62f) MHS of electrical stimulation post ACh administration.

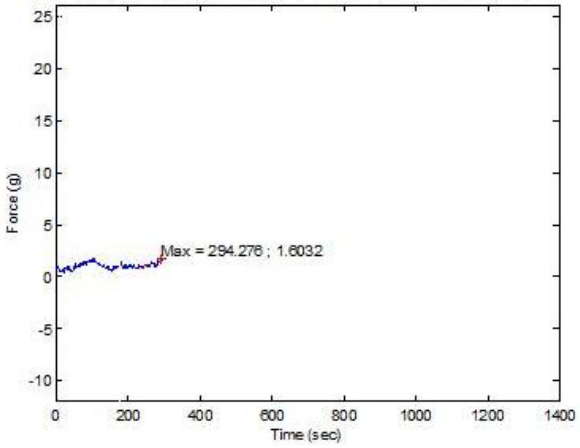

(a)

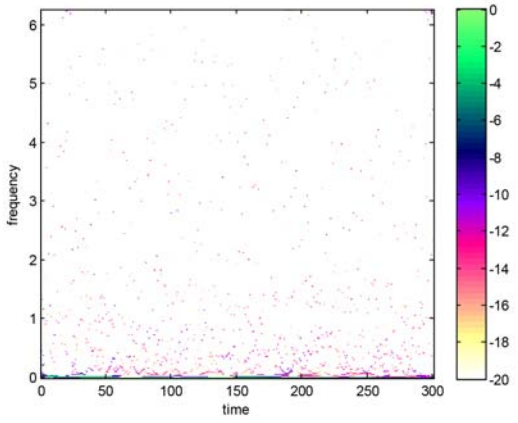

(b) injection at 180 sec

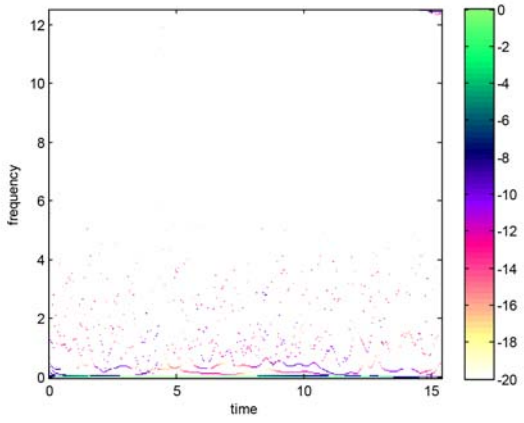

(c)

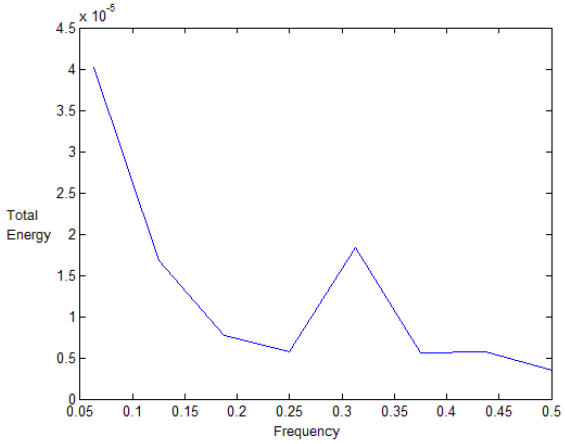

(d)

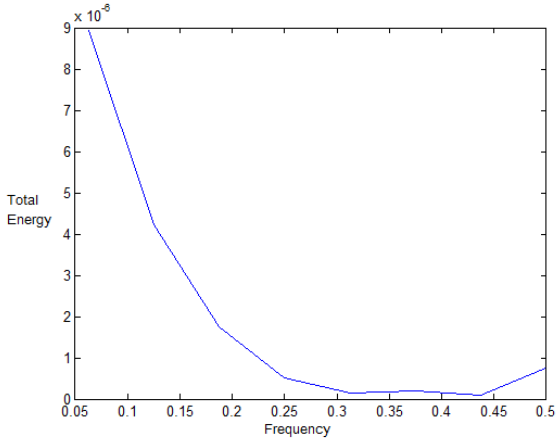

(e)

Figure 63: Results of further chemical and electrical stimulation of 14 day IS, initially stimulated at $96\mu g/ml$ (see Figure 62). (63a) F-t record of stimulation by large dose of ACh (63b) HS of large dose ACh stimulation (63c) HS of electrical stimulation post ACh administration (63d) MHS of large dose ACh stimulation (63e) MHS of electrical stimulation post ACh administration.

energy in the signal. Low energy was contributed from all frequencies, higher energy components occurred between 0.06-0.18Hz and 0.31-0.44Hz. Electrical stimulation post contraction resulted in large contractions, visible in the HS as a localised, high energy signal (the energy was localised in frequency and in time).

The F-t trace of an IS stimulated by $550\mu g/ml$ exhibited a steady increase post injection, with unfused tetanus reached after 720s of exposure to ACh, fluctuating around 10g. The trend is thus similar to that of the DS. The muscle appears to exhibit signs of fatigue towards the end of the test whereas no signs of fatigue were noted in the DS. The MHS indicates that the main energy components of the signal occurred within the low frequency range as well as between 0.13-0.25Hz. The DS frequency range of energy contribution was higher at 0.31-0.44Hz. The electrical stimulation post ACh administration displayed high energy components and reduced 'scatter' in the HS during the period of stimulation. The MHS of the electrical signal shows only a significant contribution of energy from the low frequency range, with a small energy increase in the 0.37-0.44Hz. In addition, another, low energy component, exists within the signal (seen in the HS), its activity fluctuating within a 0.5-2.2Hz range. The lowest energy components contain the highest energy in the signal.

An IG from a 14 day post-denervation group did not reach tetanus when stimulated with $550\mu g/ml$ of ACh. An increase in force occurred after about 300s post injection, followed by a decrease which reestablished stability around 5g from around 800s. The HS of this test indicates that activity fell within a 0-0.5Hz range with a small energy increase "spike" upon injection at 180s. The MHS of the chemical test shows the main energy component was contributed from the 0.06-0.18Hz frequency range, with a peak at 0.13Hz. The HS of an electrical test conducted after the chemical stimulation is displayed in Figure 66d. No clear localisation corresponding to the period of stimulation was observed. Clear low energy components may be indicative of muscle fibre recruitment. The MHS indicates that the highest contribution of energy occurs between 0.06-0.25Hz. Further chemical stimulation caused an increase in the activity frequency band (mostly between 0-2Hz) with the most energy wielding components being the lowest frequency components. An energy increase was visible post ACh administration, although a large amount of energy scatter across frequency bands is visible. The MHS displays high energy contributions from a 0.13-0.25Hz range. The HS of a second electrical test is void of locality with activity ranging in a frequency band of 0-3Hz. The MHS shows high energy contributions from 0.06-0.25Hz.

The F-t trace of a 14 day DG stimulated by $550\mu g/ml$ of ACh, displayed a gradual increase in force over time, with no notable fluctuations within the signal and stabilised (reached unfused tetanus) at 1200s on the F-t graph (Figure 68a). The gradual increase in force was similar to that of the IG, although no drop in force occurred as with the IG. The highest energy (seen in the HS) lies between 400-500s, which can be seen from the F-t trace to represent a stepped up increase in force (less gradual than the overall force increase). The main energy contributing frequencies in the signal were 0.06-0.18Hz and 0.18-0.25Hz. The HS of a subsequent electrical

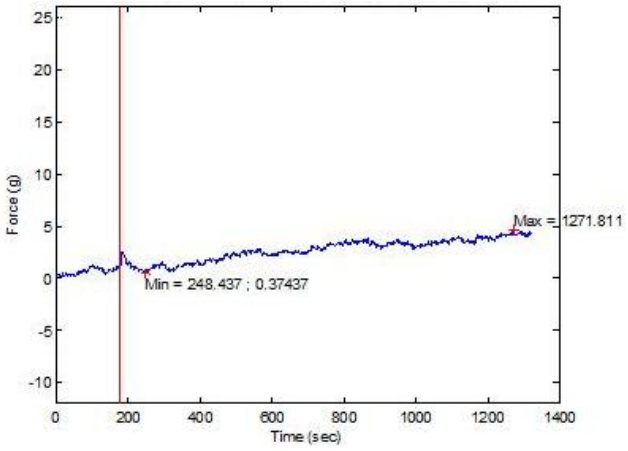

(a)

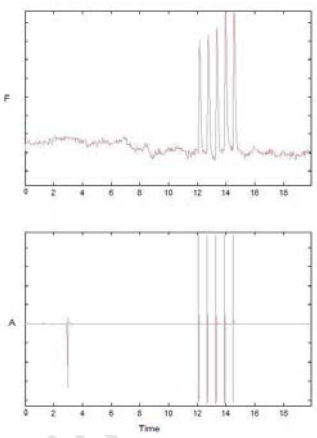

(b)

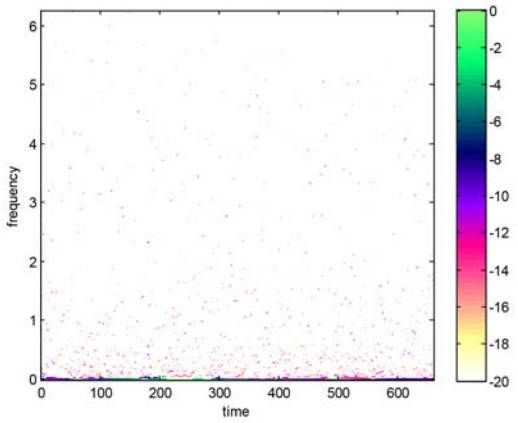

(c) injection at 180 sec

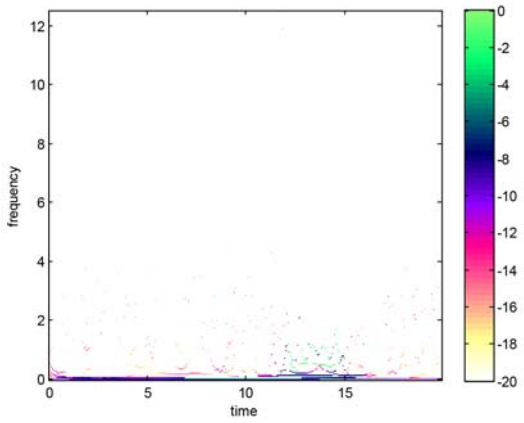

(d) stimulation as in (b)

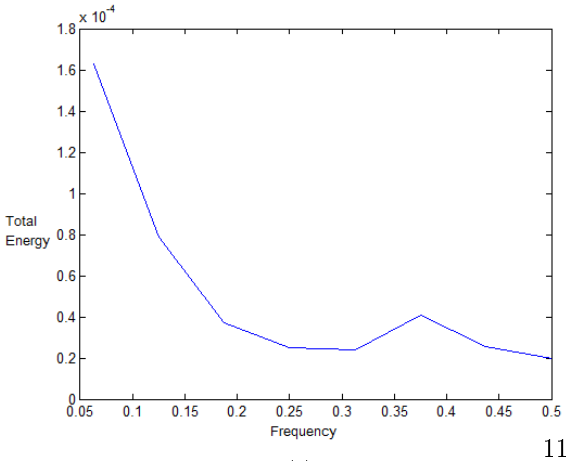

(e)

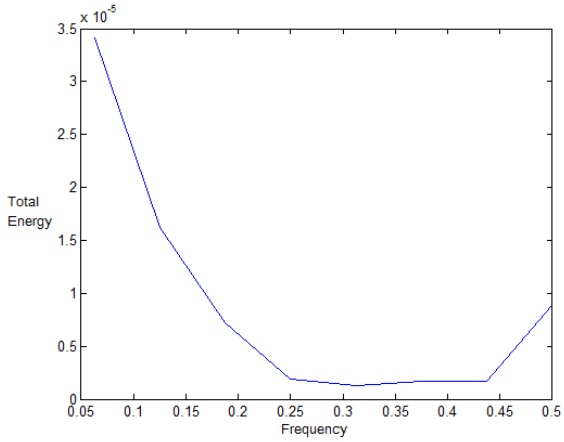

(f)

Figure 64: Results of 14 day DS stimulated at $550\mu g/ml$. (64a) F-t record of $550\mu g/ml$ ACh stimulation (64b) F-t record (top) and amplitude (A)-t indication of stimulation (bottom) for electrical stimulation post ACh administration (64c) HS of $550\mu g/ml$ ACh stimulation (64d) HS of electrical stimulation post ACh administration (64e) MHS of $550\mu g/ml$ ACh stimulation (64f) MHS of electrical stimulation post ACh administration.

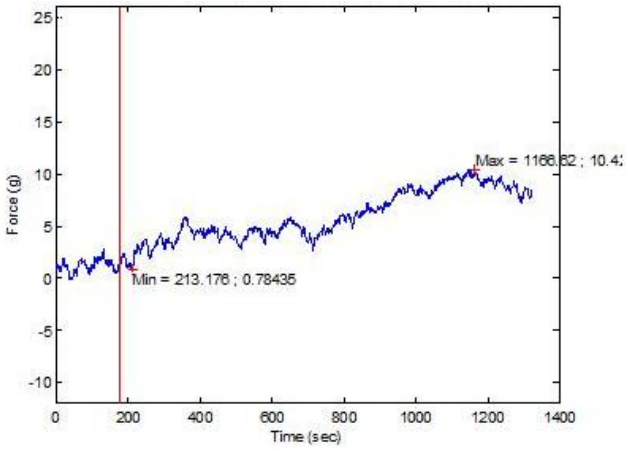

(a)

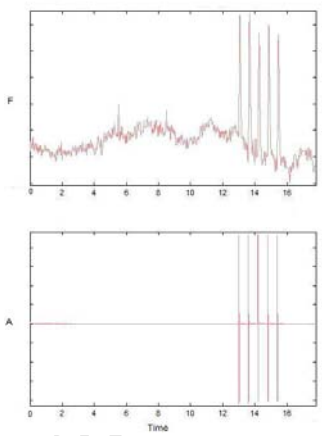

(b)

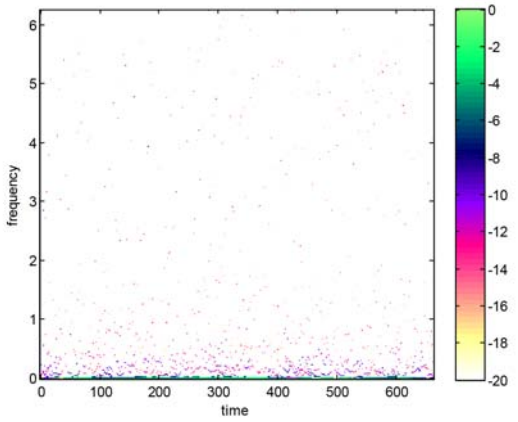

(c) injection at 180 sec

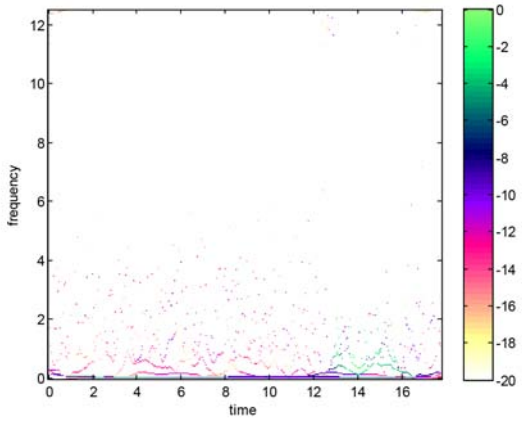

(d) stimulation as in (b)

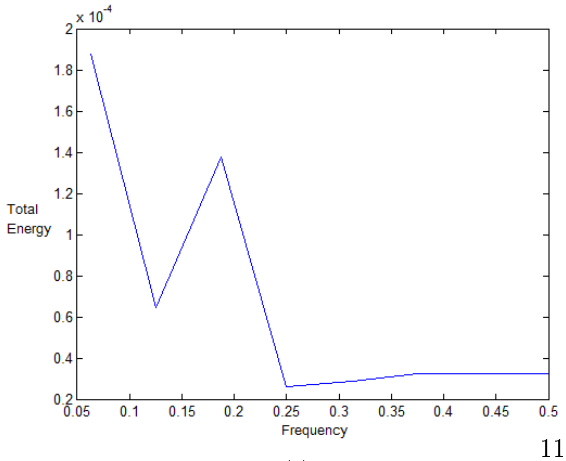

(e)

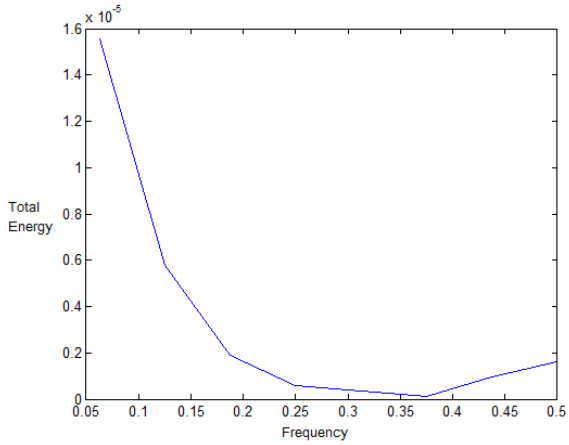

(f)

Figure 65: Results of IS from 14 day denervation group, stimulated at $550\mu g/ml$. (65a) F-t record of $550\mu g/ml$ ACh stimulation (65b) F-t record (top) and amplitude (A)-t indication of stimulation (bottom) for electrical stimulation post ACh administration (65c) HS of $550\mu g/ml$ ACh stimulation (65d) HS of electrical stimulation post ACh administration (65e) MHS of $550\mu g/ml$ ACh stimulation (65f) MHS of electrical stimulation post ACh administration.

test showed clear frequency components within the signal which additionally displayed intrawave frequency modulation. No locality for contractile activity was evident. The MHS displayed low frequency energy contributions (0.06-0.25Hz). Further administration of ACh, this time of a large concentration, displayed an increase in energy for some 50s post injection in the low frequency range (refer to HS Figure 69c) and then decreased in energy again thereafter. The MHS indicated most of the signal energy occurred in a 0.31-0.44Hz range. High energy and less frequency 'scatter' were evident upon further electrical stimulation. Clear components visible in the HS displayed increases in energy over time.

Stimulation of a 14 day DG with 1.6g/ml of ACh (Figure 70) resulted in an increase in force over time, with no clear display of unfused tetanus. The HS indicated that the signals energy was slightly scattered within a frequency range of 0-1Hz, with the MHS indicating a large energy component within the 0.13-0.25Hz range (peaking at 0.18Hz). The HS of the electrical check displayed no high energy components at the time of stimulation, although clear intrawave frequency modulation and low energy components are evident during this period. This was supported by the MHS of the electrical stimulation test which indicated that most of the signals energy was contributed by a 0.06-0.25Hz (i.e. low) frequency range.

Stimulation of an IG with 1.6g/ml of ACh (Figure 71) caused the F-t signal to display larger fluctuations in force (albeit at low forces). No slow increase in force over time was observed as in the case of the DG. The HS displayed little spread in spectral energy (more energy is confined to fewer frequency bands) compared to the more scattered energy representation of the DG. The MHS supported this, displaying a large amount of cumulative energy in the 0.25-0.37Hz frequency range. The HS of the electrical stimulation test did not provide any clear indication of contraction (although an increase in energy in the low frequency band is noted during the stimulation period), neither were any indications visible in the force trace of the electrical stimulation signal. The MHS displayed a large high energy low frequency component, corresponding to the observation made from the HS.

The F-t trace of a DS stimulated at 1.6g/ml displayed multiple fluctuating peaks within the signal post injection, not seen in other, lower concentration tests. An increase in energy was observed in the HS post injection in the low frequency range. A pertinent observation was made from the MHS, in which a large energy component existed within the 0.25-0.37Hz frequency range, higher than the previously noted frequency ranges of cumulative energy contribution in lower concentration tests for the same denervation period. This indicates the presence of higher frequencies of contraction upon the administration of higher concentrations of ACh. This energy contribution frequency range was noted for gastrocnemii and for IS at high ACh concentrations following previous electrical stimulation. Administration of high concentrations of ACh thus indicates greater activity or contribution of fast twitch fibres. The HS of the muscles' response to electrical stimulation post ACh simulation is given in Figure 72d and illustrates low energy, low frequency, intrawave

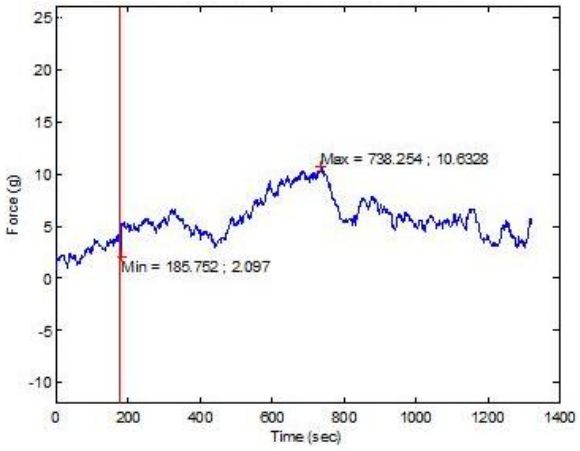

(a)

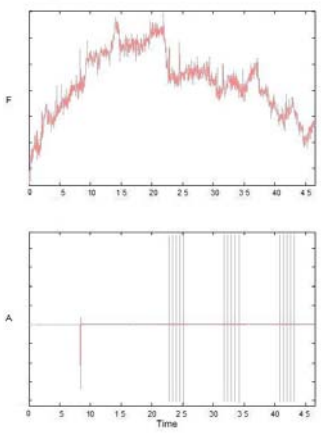

(b)

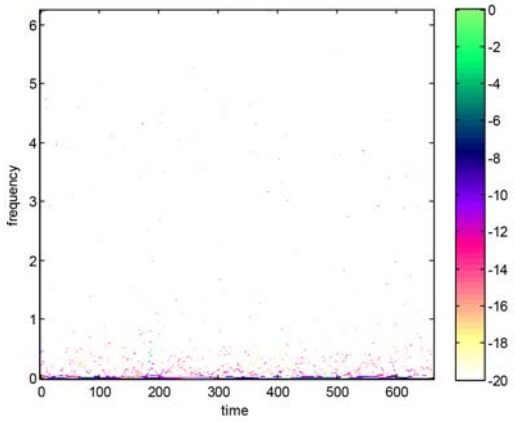

(c) injection at 180 sec

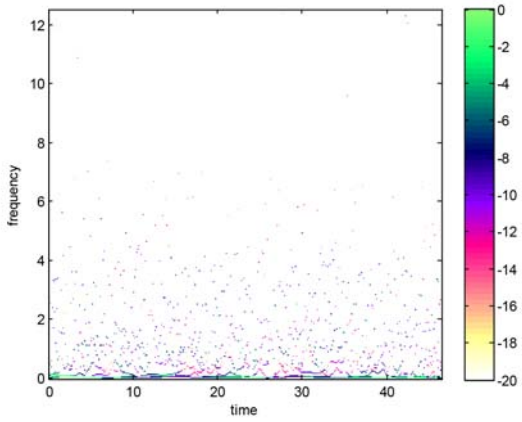

(d) stimulation as in (b)

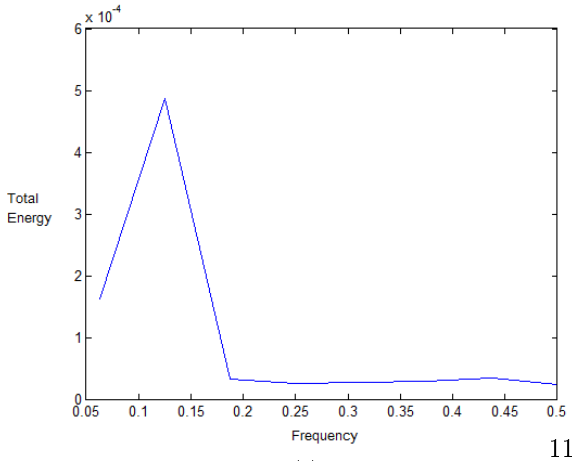

(e)

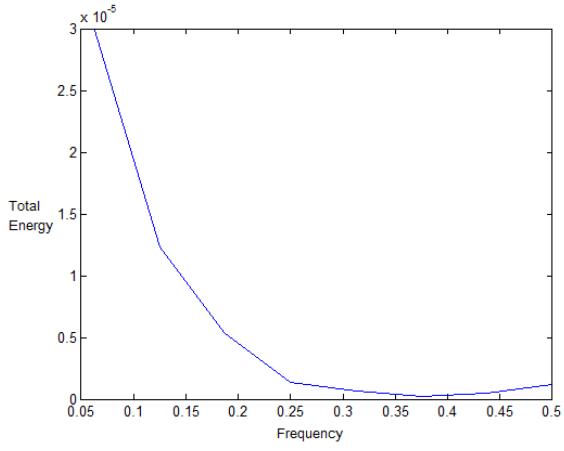

(f)

Figure 66: Results of IG from 14 day denervation group, stimulated at $550\mu g/ml$. (67a) F-t record of $550\mu g/ml$ ACh stimulation (66b) F-t record (top) and amplitude (A)-t indication of stimulation (bottom) for electrical stimulation post ACh administration (66c) HS of $550\mu g/ml$ ACh stimulation (66d) HS of electrical stimulation post ACh administration (66e) MHS of $550\mu g/ml$ ACh stimulation (66f) MHS of electrical stimulation post ACh administration.

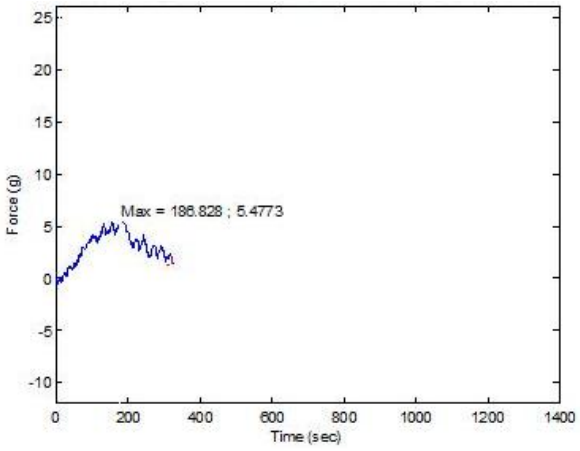

(a)

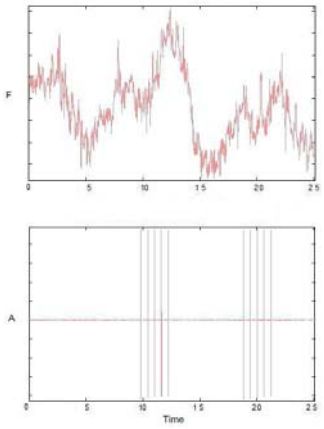

(b)

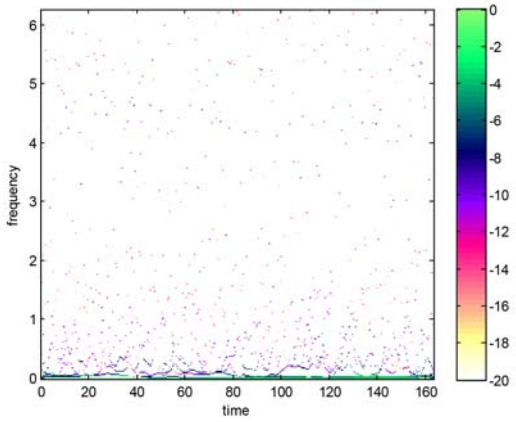

(c) injection at 180 sec

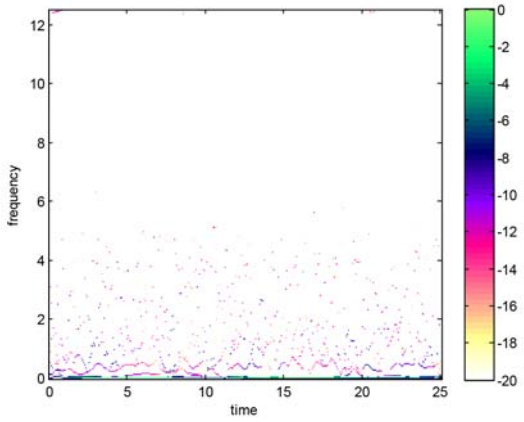

(d) stimulation as in (b)

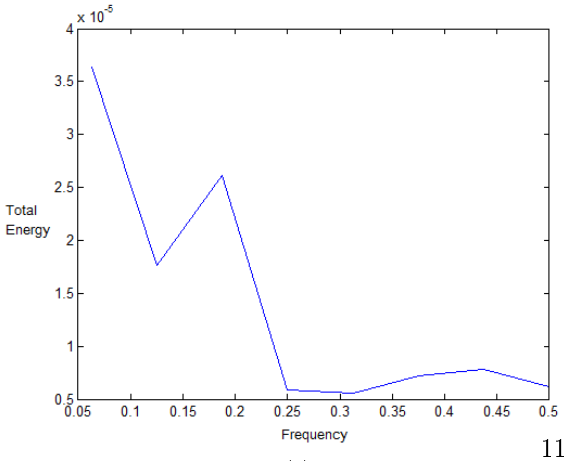

(e)

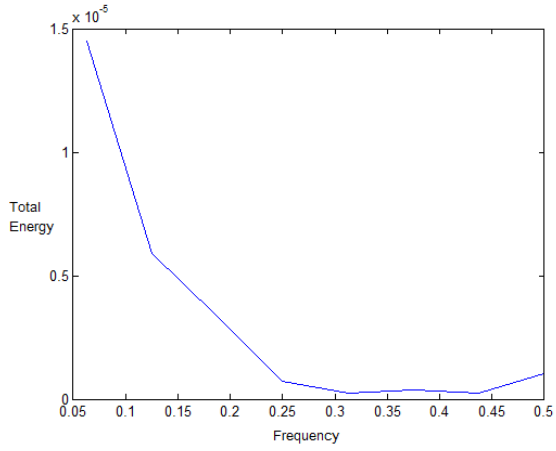

(f)

Figure 67: Results of further chemical and electrical stimulation of an IG from a 14 day denervation group, initially stimulated at $550\mu g/ml$ (see Figure 66). (67a) F-t record of stimulation by large dose of ACh (67b) F-t record (top) and amplitude (A)-t indication of stimulation (bottom) for electrical stimulation post ACh administration (67c) HS of large dose ACh stimulation (67d) HS of electrical stimulation post ACh administration (67e) MHS of large dose ACh stimulation (67f) MHS of electrical stimulation post ACh administration.

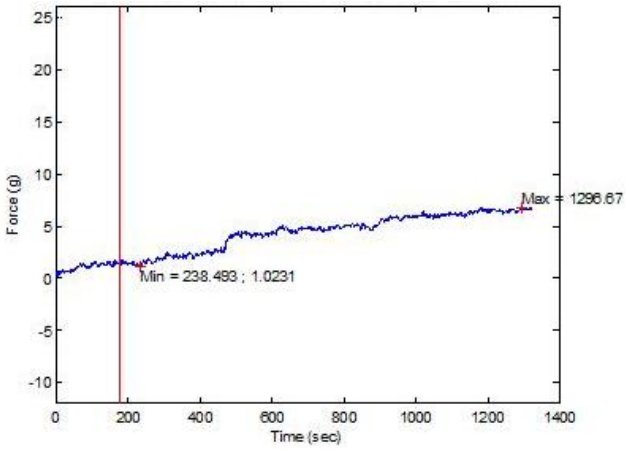

(a)

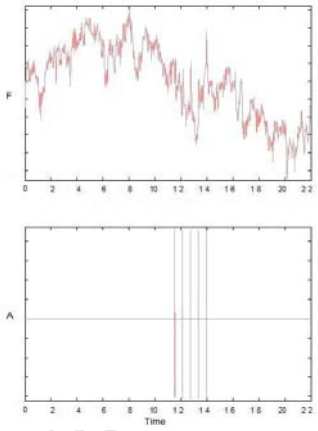

(b)

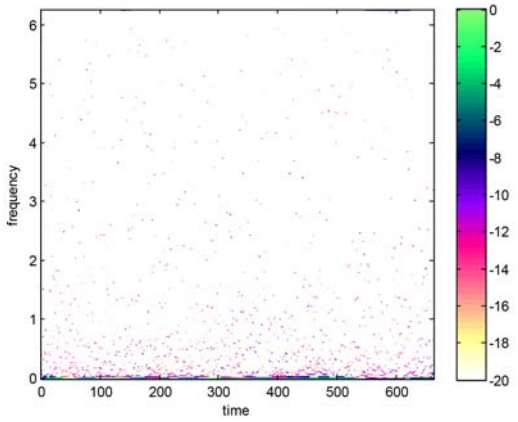

(c) injection at 180 sec

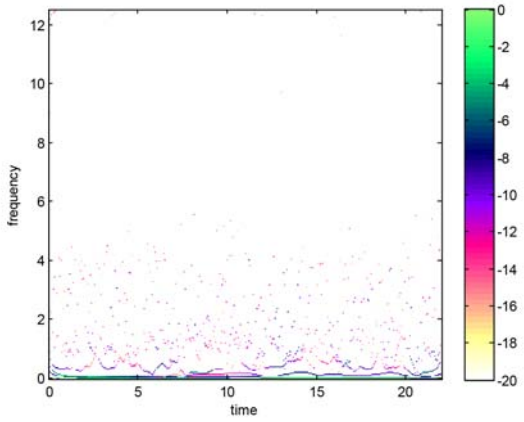

(d) stimulation as in (b)

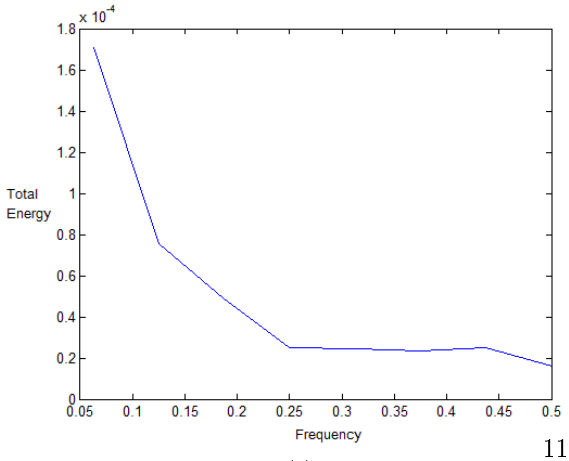

(e)

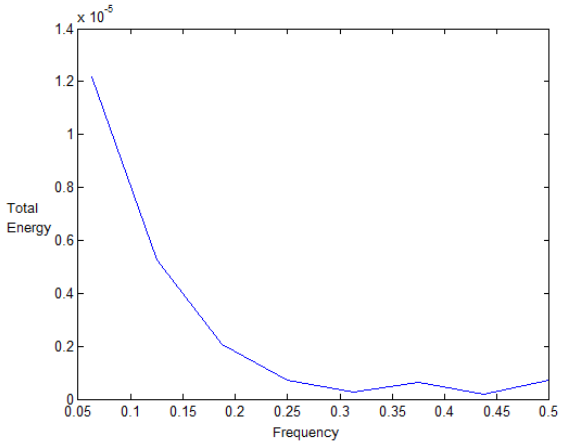

(f)

Figure 68: Results of 14 day DG stimulated at $550\mu g/ml$. (68a) F-t record of $550\mu g/ml$ ACh stimulation (68b) F-t record (top) and amplitude (A)-t indication of stimulation (bottom) for electrical stimulation post ACh administration (68c) HS of $550\mu g/ml$ ACh stimulation (68d) HS of electrical stimulation post ACh administration (68e) MHS of $550\mu g/ml$ ACh stimulation (68f) MHS of electrical stimulation post ACh administration.

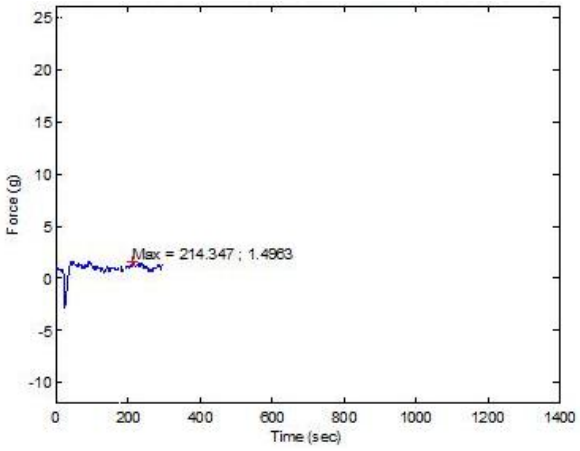

(a)

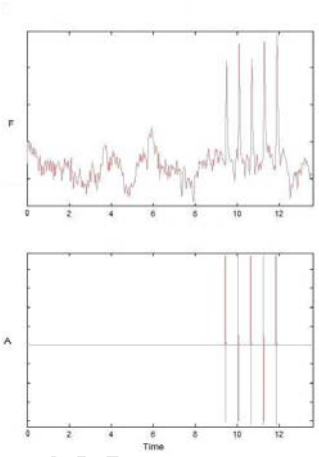

(b)

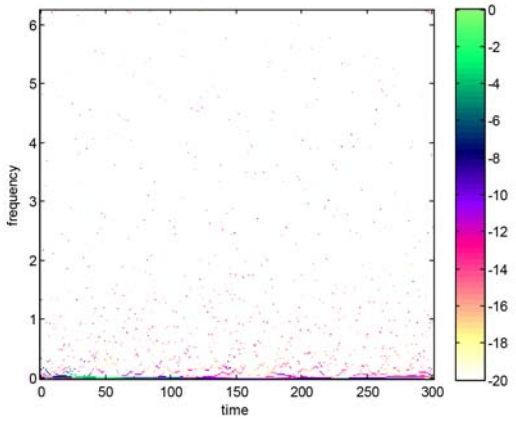

(c) injection at 180 sec

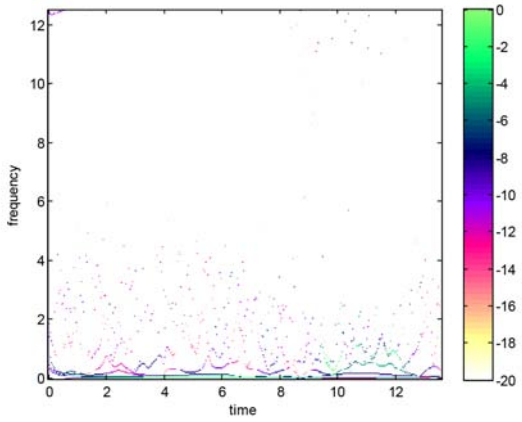

(d) stimulation as in (b)

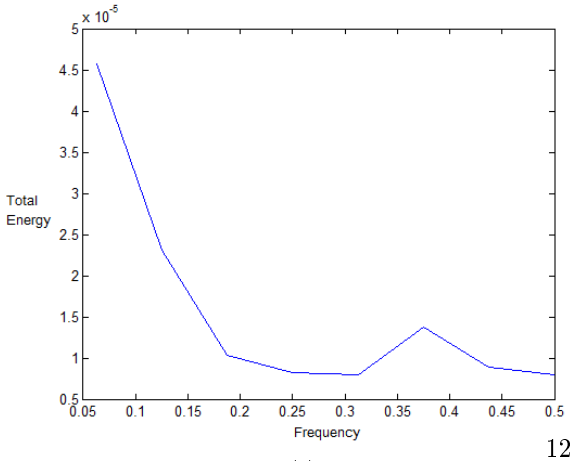

(e)

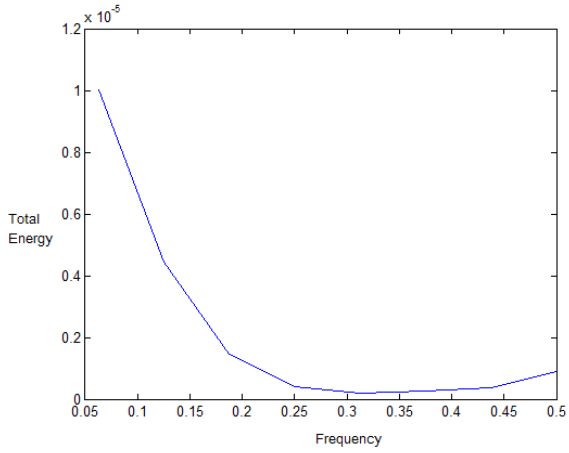

(f)

Figure 69: Results of further chemical and electrical stimulation of 14 day DG, initially stimulated at $550\mu g/ml$ (see Figure 68). (69a) F-t record of stimulation by large dose of ACh (69b) F-t record (top) and amplitude (A)-t indication of stimulation (bottom) for electrical stimulation post ACh administration (69c) HS of large dose ACh stimulation (69d) HS of electrical stimulation post ACh administration (69e) MHS of large dose ACh stimulation (69f) MHS of electrical stimulation post ACh administration.

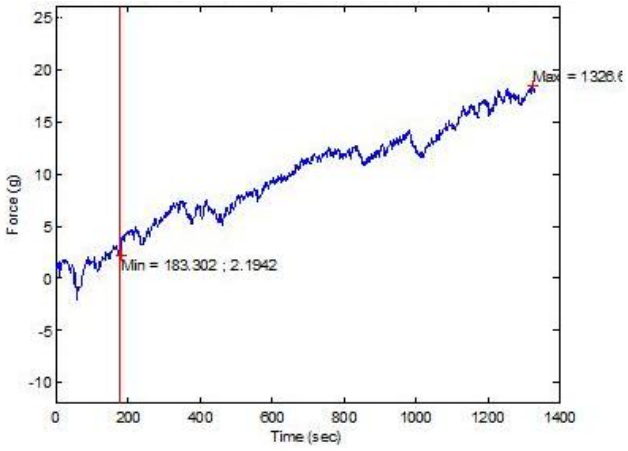

(a)

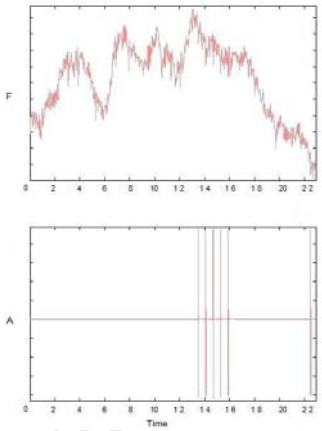

(b)

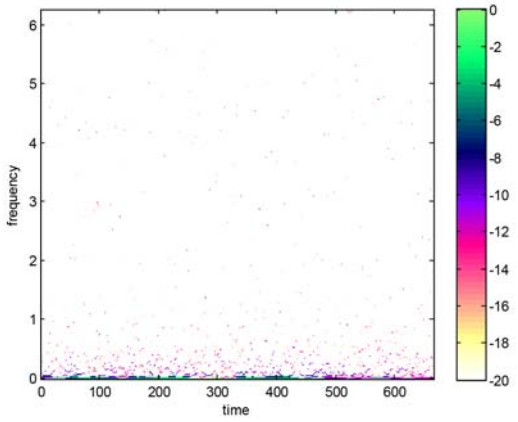

(c) injection at 180 sec

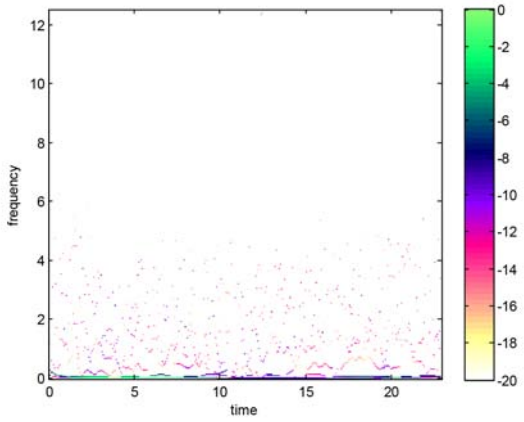

(d) stimulation as in (b)

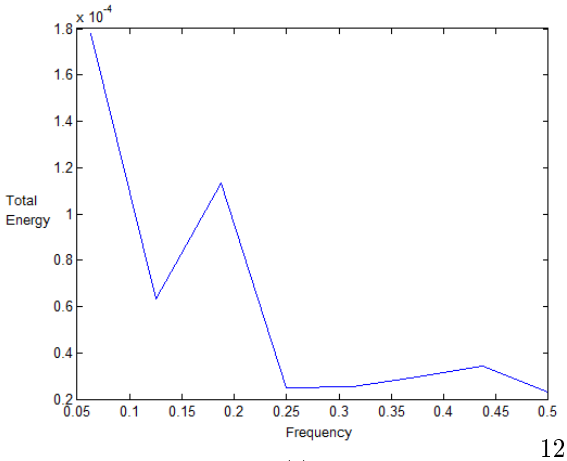

(e)

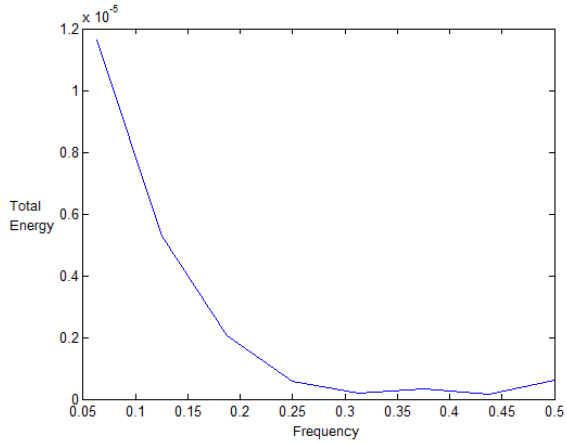

(f)

Figure 70: Results of 14 day DG stimulated at 1.6g/ml. (70a) F-t record of 1.6g/ml ACh stimulation (70b) F-t record (top) and amplitude (A)-t indication of stimulation (bottom) for electrical stimulation post ACh administration (70c) HS of 1.6g/ml ACh stimulation (70d) HS of electrical stimulation post ACh administration (70e) MHS of 1.6g/ml ACh stimulation (70f) MHS of electrical stimulation post ACh administration.

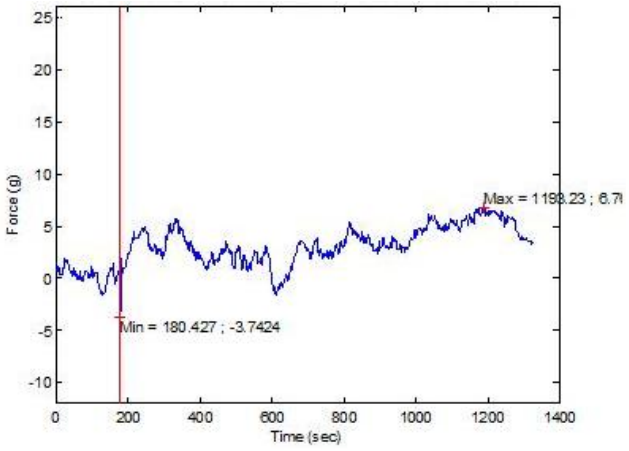

(a)

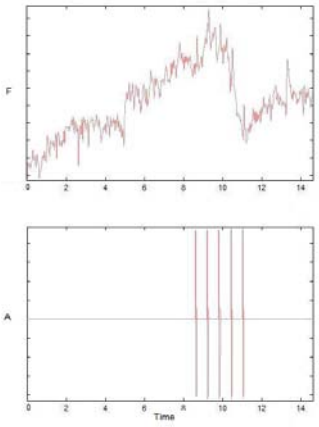

(b)

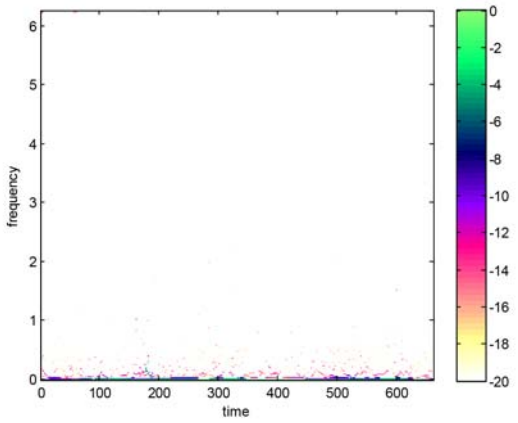

(c) injection at 180 sec

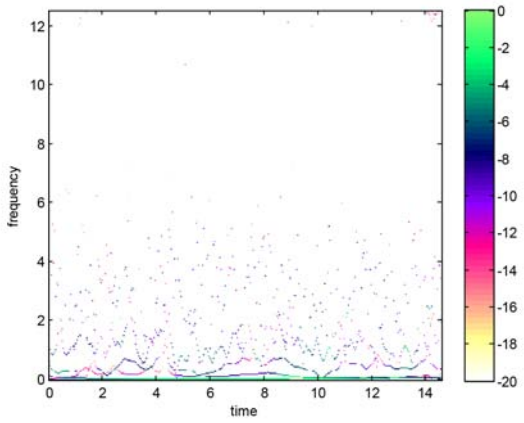

(d) stimulation as in (b)

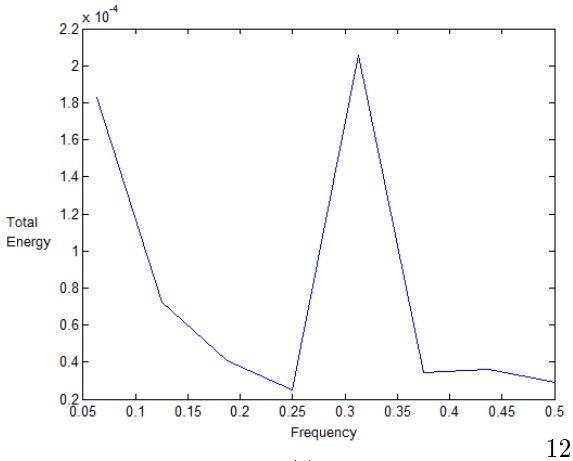

(e)

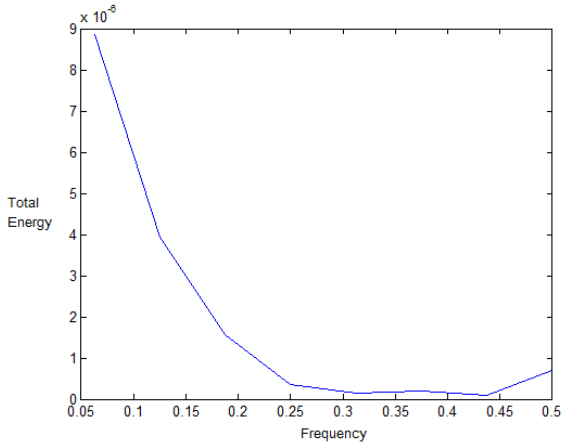

(f)

Figure 71: Results of IG from 14 day denervation group, stimulated at 1.6g/ml. (71a) F-t record of 1.6g/ml ACh stimulation (71b) F-t record (top) and amplitude (A)-t indication of stimulation (bottom) for electrical stimulation post ACh administration (71c) HS of 1.6g/ml ACh stimulation (71d) HS of electrical stimulation post ACh administration (71e) MHS of 1.6g/ml ACh stimulation (71f) MHS of electrical stimulation post ACh administration.

frequency modulation between 8-11sec (corresponding to the stimulation period). This shows a clear muscular response which is not immediately evident in the corresponding F-t trace.

An IS, stimulated at 1.6g/ml (Figure 73), demonstrated greater fluctuation of force per unit time post ACh administration, which is indicative of a higher frequency existing within the signal. This was supported by the MHS of this test which displayed high energy components within a frequency range of 0.31-0.44Hz, higher than the frequency range of the IG and DS under the same conditions. The electrical stimulation check indicated higher energy components (as with the locality in the DS) between 10-13 seconds, although it still displayed energy "spread" in all frequency ranges over time.

A DS stimulated at 3.2g/ml (Figure 74) displayed an increase in frequency which was apparent after injection, and supported by the MHS which indicated the largest amount of cumulative energy was within a 0.37-0.5Hz range. The HS of the muscles' response to electrical stimulation indicated a clear region of increased energy corresponding to the period of electrical stimulation. Further chemical stimulation indicated that the main energy components of the signal existed within a 0.31-0.44Hz range (Figure 75e). The electrical stimulation appeared to have reduced the signal energy (and hence muscle energy) as well as causing a reduction in the frequency band in which the energy components were present. This resulted in the muscle contracting at lower frequency and outputting less energy. Further electrical stimulation indicated no changes in energy or frequency with time in the HS plot. The cumulative energy within a 0.44-0.5Hz range in the MHS is indicative of a response of the muscle to electrical stimulation, although large amounts of 'scatter' in the HS and low energy contribution point to a small response of the muscle to the further electrical stimulation.

The IS stimulated at 3.2g/ml (Figure 76a) displayed a higher frequency of force fluctuation (as with the DS) but little increase in force. The signals' energy components were mainly present in a 0.37-0.5Hz range (also the same as that of the DS), higher than the range of the IS stimulated at a lower concentration of 1.6g/ml. The HS of the electrical stimulation check illustrates high energy components during the stimulation period, as well as a reduction in frequency 'scatter'. The MHS displayed a concentration of energy in the 0.44-0.5Hz range, supporting the observation of contractile activity in response to electrical stimulation (which was clearly visible in the force trace; clearer than that of the DS). The range of frequency in which energy is mainly distributed may be indicative of a gradual recruitment of fibres (corresponding to the low end of the frequency range) with a peak occurring at the maximum force of contraction (corresponding to the high end of the frequency range).

A DG stimulated at 6.3g/ml was seen to follow the same trend as other high concentration range tests on the DG, that is, a notable increase in force variation post stimulation, fluctuating around a low force. The MHS showed a cumulative energy contribution in the 0.37-0.5Hz range (peak at +-0.44Hz). The HS showed hardly any scatter (hence little energy spread across frequencies, but more than in some other tests). The HS of the electrical stimulation result displayed a higher

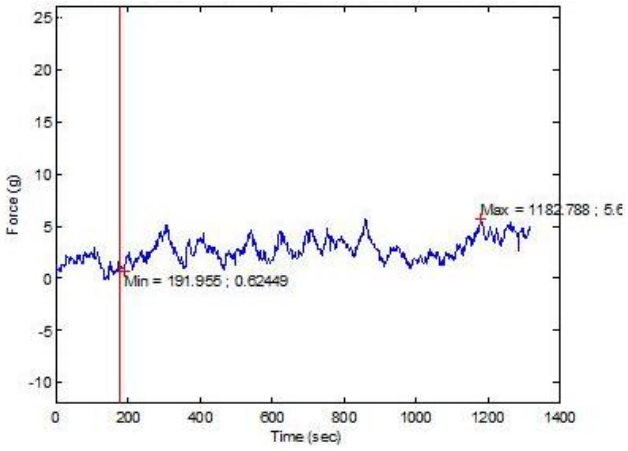

(a)

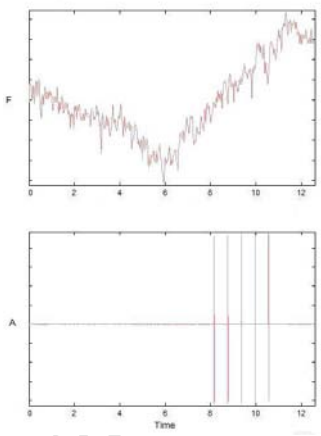

(b)

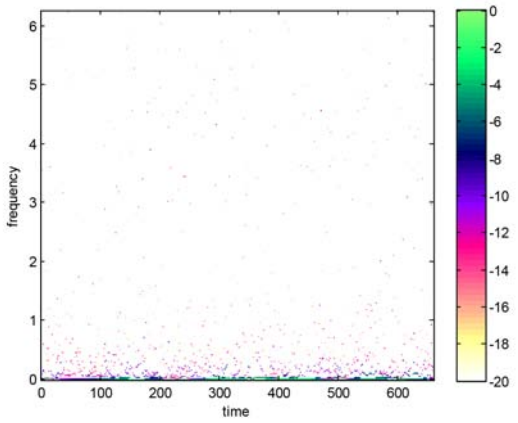

(c) injection at 180 sec

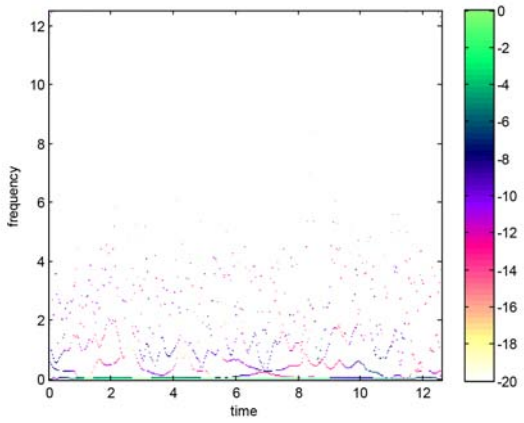

(d) stimulation as in (b)

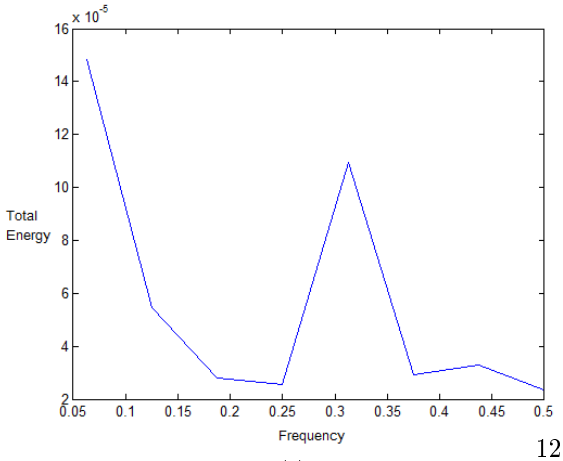

(e)

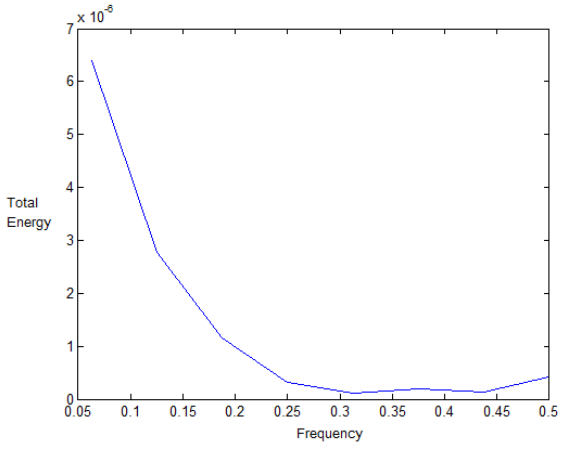

(f)

Figure 72: Results of 14 day DS stimulated at 1.6g/ml. (72a) F-t record of 1.6g/ml ACh stimulation (72b) F-t record (top) and amplitude (A)-t indication of stimulation (bottom) for electrical stimulation post ACh administration (72c) HS of 1.6g/ml ACh stimulation (72d) HS of electrical stimulation post ACh administration (72e) MHS of 1.6g/ml ACh stimulation (72f) MHS of electrical stimulation post ACh administration.

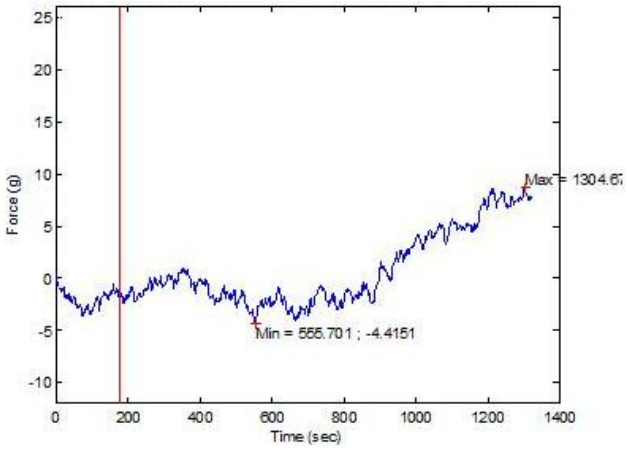

(a)

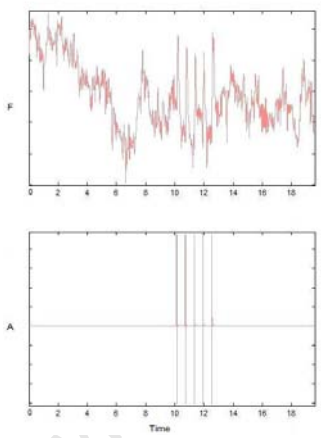

(b)

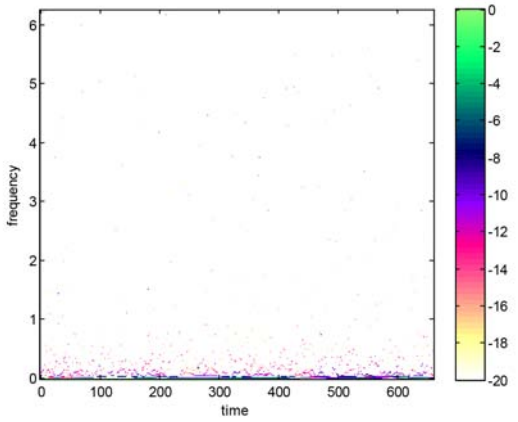

(c) injection at 180 sec

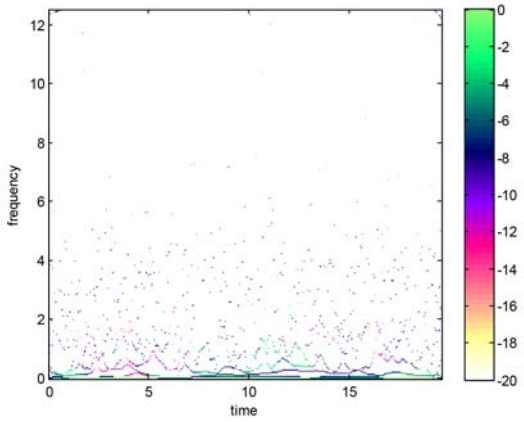

(d) stimulation as in (b)

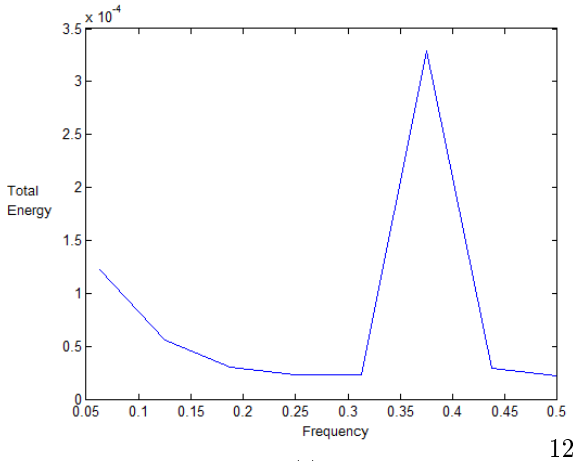

(e)

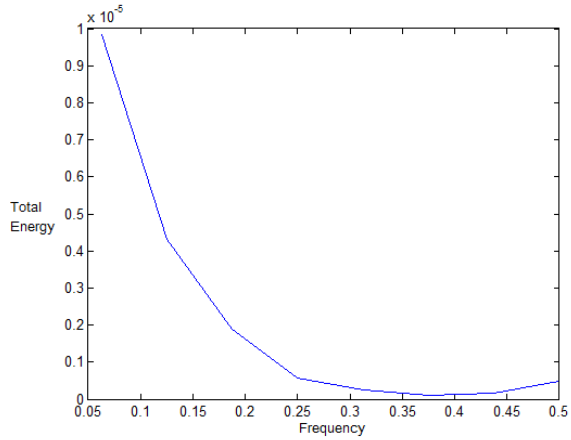

(f)

Figure 73: Results of IS from 14 day denervation group, stimulated at 1.6g/ml. (73a) F-t record of 1.6g/ml ACh stimulation (73b) F-t record (top) and amplitude (A)-t indication of stimulation (bottom) for electrical stimulation post ACh administration (73c) HS of 1.6g/ml ACh stimulation (73d) HS of electrical stimulation post ACh administration (73e) MHS of 1.6g/ml ACh stimulation (73f) MHS of electrical stimulation post ACh administration.

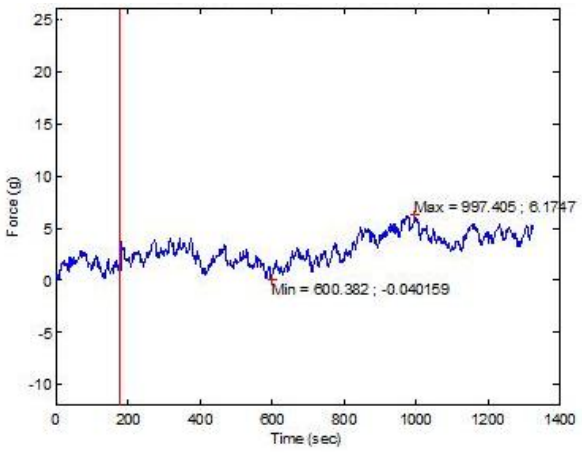

(a)

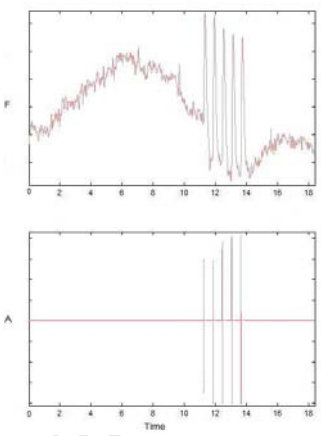

(b)

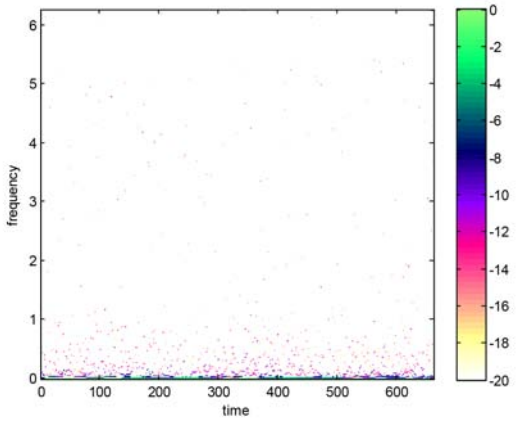

(c) injection at 180 sec

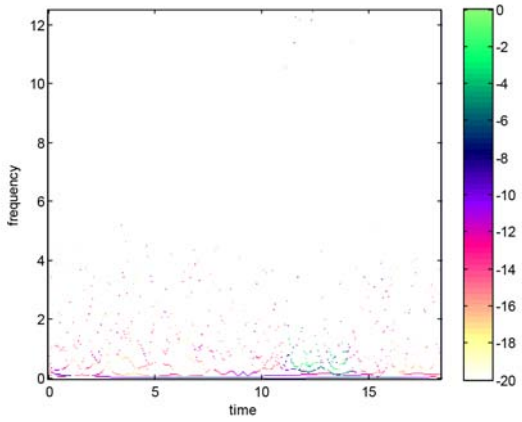

(d) stimulation as in (b)

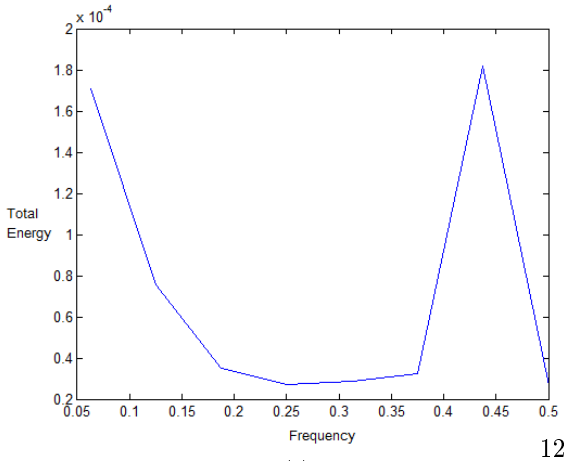

(e)

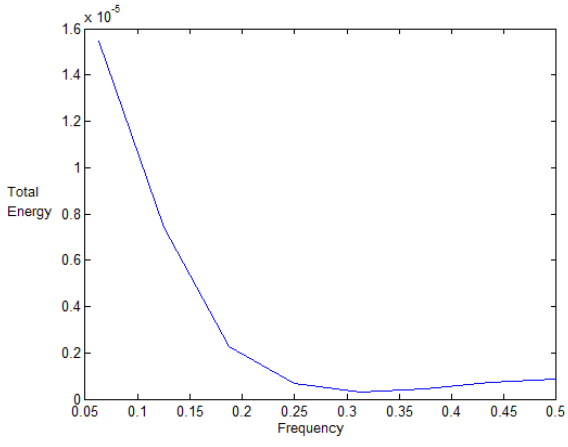

(f)

Figure 74: Results of 14 day DS stimulated at 3.2g/ml. (74a) F-t record of 3.2g/ml ACh stimulation (74b) F-t record (top) and amplitude (A)-t indication of stimulation (bottom) for electrical stimulation post ACh administration (74c) HS of 3.2g/ml ACh stimulation (74d) HS of electrical stimulation post ACh administration (74e) MHS of 3.2g/ml ACh stimulation (74f) MHS of electrical stimulation post ACh administration.

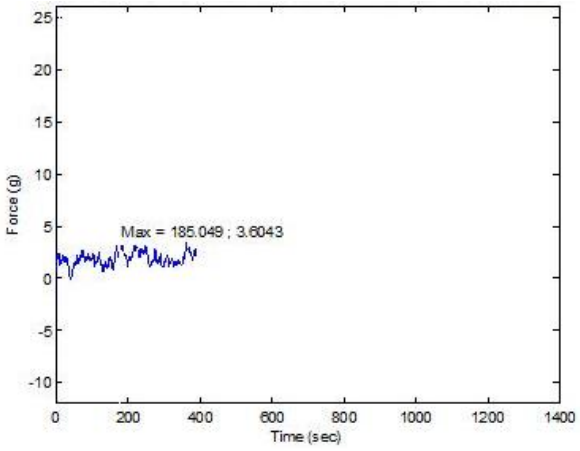

(a)

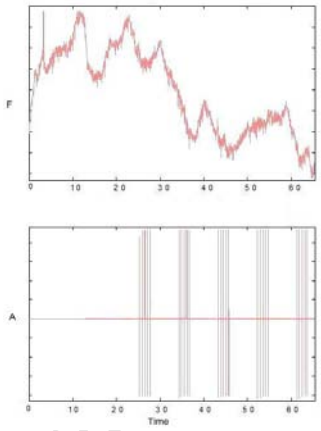

(b)

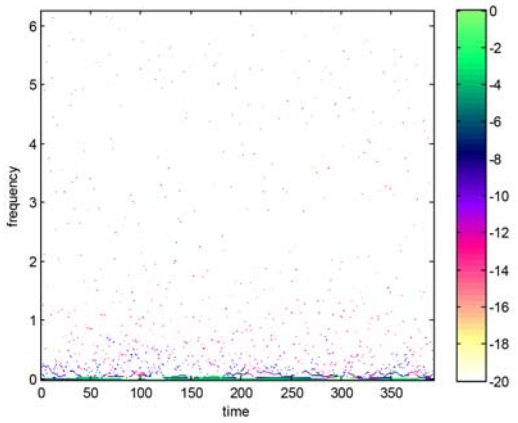

(c) injection at 180 sec

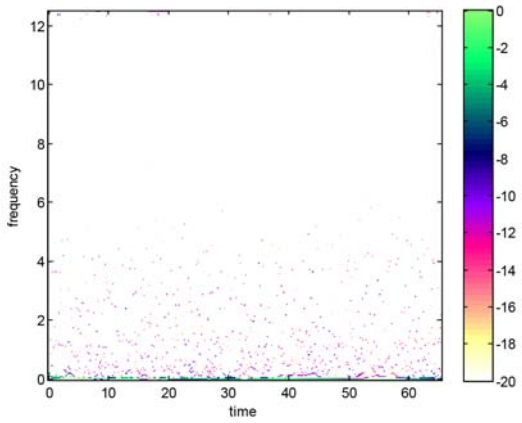

(d) stimulation as in (b)

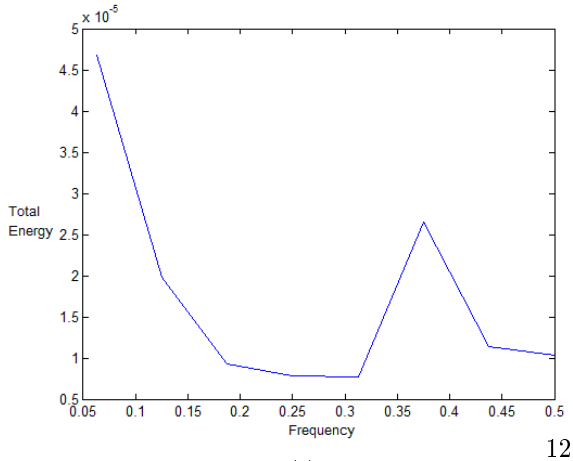

(e)

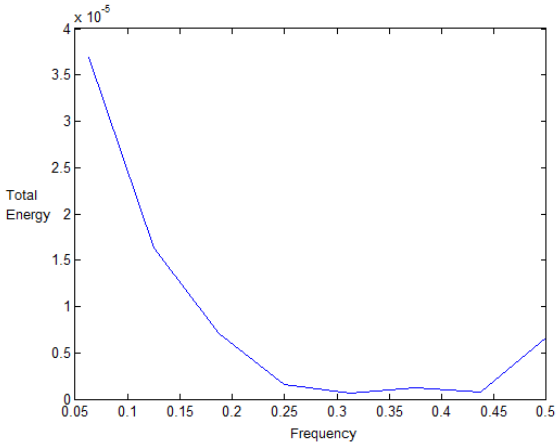

(f)

Figure 75: Results of further chemical and electrical stimulation of 14 day DS, initially stimulated at 3.2g/ml (see Figure 74). (75a) F-t record of stimulation by large dose of ACh (75b) F-t record (top) and amplitude (A)-t indication of stimulation (bottom) for electrical stimulation post ACh administration (75c) HS of large dose ACh stimulation (75d) HS of electrical stimulation post ACh administration (75e) MHS of large dose ACh stimulation (75f) MHS of electrical stimulation post ACh administration.

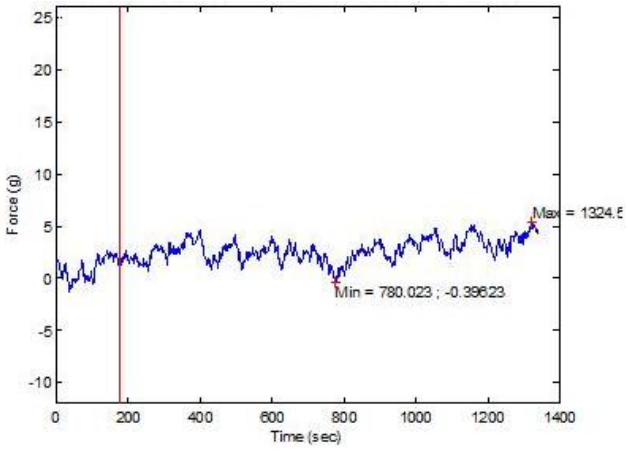

(a)

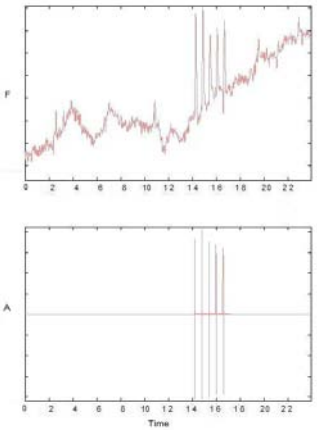

(b)

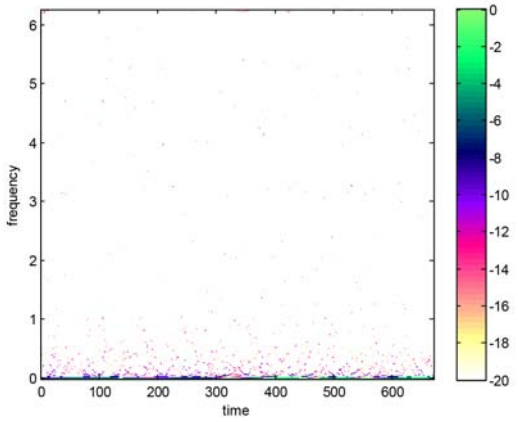

(c) injection at 180 sec

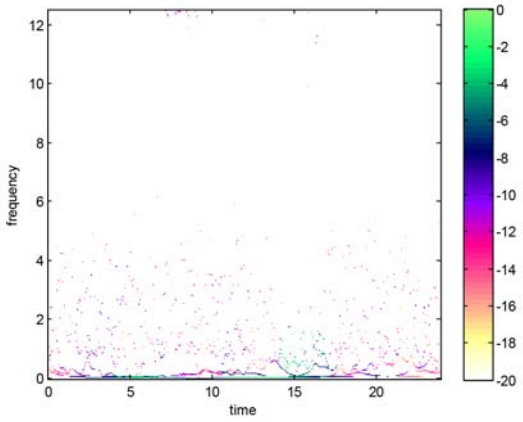

(d) stimulation as in (b)

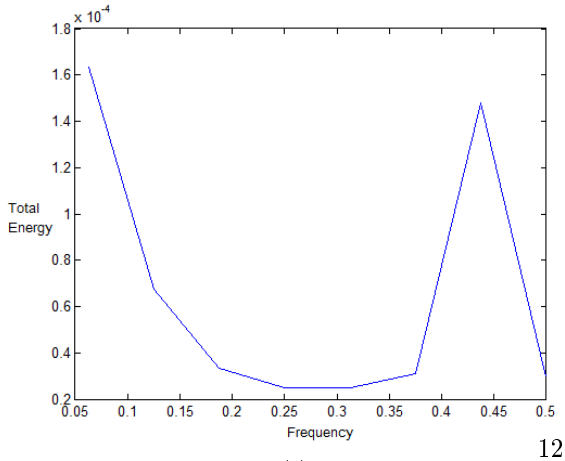

(e)

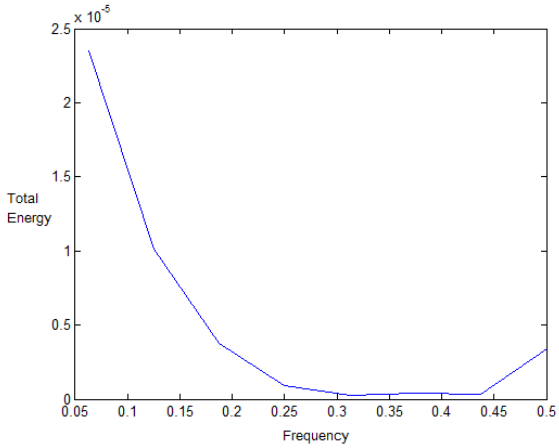

(f)

Figure 76: Results of IS from 14 day denervation group, stimulated at 3.2g/ml. (76a) F-t record of 3.2g/ml ACh stimulation (76b) F-t record (top) and amplitude (A)-t indication of stimulation (bottom) for electrical stimulation post ACh administration (76c) HS of 3.2g/ml ACh stimulation (76d) HS of electrical stimulation post ACh administration (76e) MHS of 3.2g/ml ACh stimulation (76f) MHS of electrical stimulation post ACh administration.

energy, more localised frequency contribution. The MHS showed a small contribution of energy from the 0.44-0.5Hz range, indicating a small/weak response to electrical stimulation post ACh administration. Figure 77 illustrates the results of these tests.

Chemical stimulation at 6.3g/ml of the IG demonstrated the same trend as that of the DS for the same denervation period and concentration. A notable difference between the two is that the IG displayed an increase in force almost immediately post ACh administration (in comparison to the DS in which a delay in force increase was noted). Further, the muscle (IG) appears to reach unfused tetanus at around 700s on the F-t graph (Figure 78a). No clear gradual increase in force or tetanus was apparent in the DG stimulated at the same concentration. No large frequency scatter was noted, as was the case with the DS. High energy contributions in the signal occurred between 0.18-0.31Hz (peak at about 0.25Hz), as indicated by the MHS. (An increase in gradual force generation seemed to occur *pari passu* with a lower frequency range of energy contribution). Note however, that the energy contribution in the 0.18-0.31Hz frequency range was large (higher than that of the initial lowest frequency contributions). The HS of the electrical check test indicates frequency localised, high energy activity corresponding to the stimulation period of 4-7sec. No energy spreading was visible, but high energy components were noted to appear in the low frequency range. A small energy contribution from the 0.44-0.5Hz range was noted from the MHS.

The DS differs from the lower concentrations in the high concentration range in that it displays an additional increase in force post administration. This force increase was only noted to occur about 620s after injection of 6.3g/ml of ACh (800s on graph, Figure 79a) and does not appear to reach tetanus of any mode. The MHS displayed a relatively high energy distribution between the low frequency components of 0.13-0.25Hz (peak at +-0.18Hz). This energy distribution occurred in a lower frequency range than the lower chemical stimulation concentrations of the same muscle type for the same denervation period (but the energy contribution is comparatively substantial). The HS of the electrical test displayed no locality, nor did the MHS display any significant energy contribution in the 0.44-0.5Hz frequency range of the signal. This may be indicative of either undetectable (and hence negligible) reaction, or no reaction of the muscle to electrical stimulation. A consideration of the force trace of the electrical stimulation test confirms this hypothesis, as a barely discernable response to electrical stimulation was noted (see Figure 79b).

The IS stimulated by 6.3g/ml displayed an increase in fluctuation (around the same pretensioned force value). This was supported by the MHS displaying an energy contribution lying within the 0.06-0.18Hz frequency range (which is the same as baseline noise range) but the contribution was notably higher and peaked at 0.13Hz. This may be indicative of a combined energy contribution from both inherent noise contribution as well as the muscles' generated energy contribution. The HS of the electrical test showed neither clear locality in frequency, nor any higher energy contributions. The MHS of the electrical test displayed an increased energy contribution in 0.44-0.5Hz range as well as a larger contribution from the 0.13-0.25Hz frequency range. Further chemical stimulation

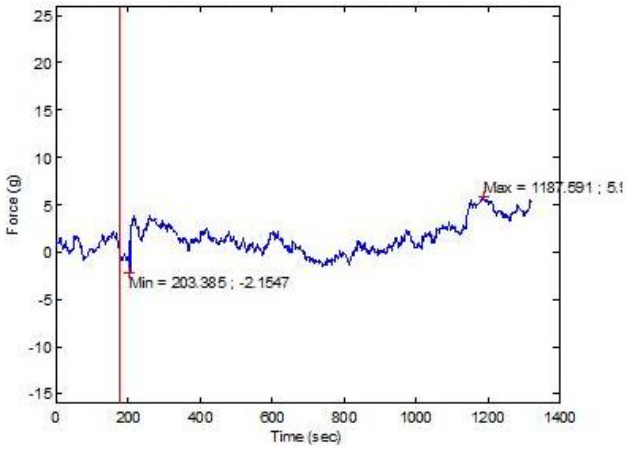

(a)

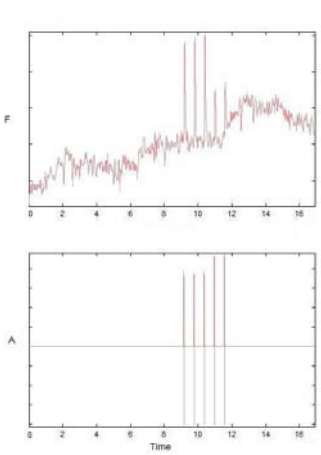

(b)

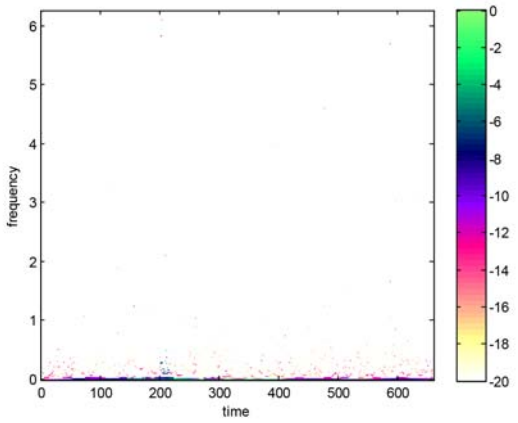

(c) injection at 180 sec

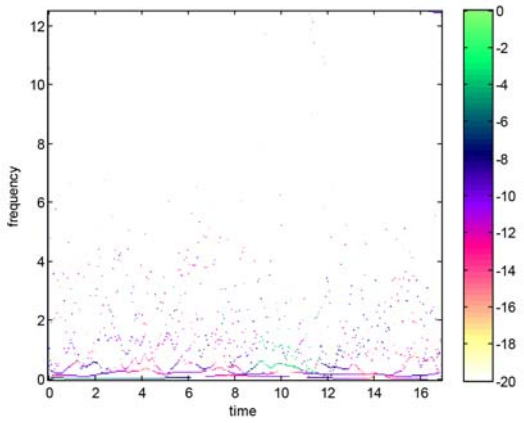

(d) stimulation as in (b)

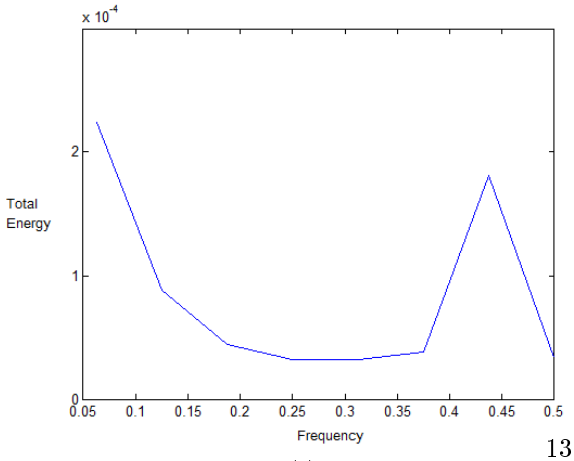

(e)

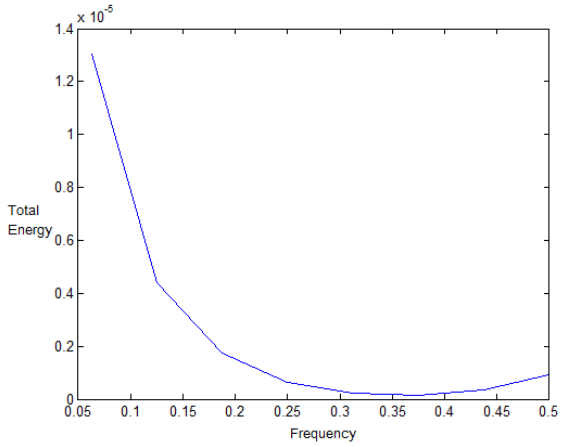

(f)

Figure 77: Results of 14 day DG stimulated at 6.3g/ml. (77a) F-t record of 6.3g/ml ACh stimulation (77b) F-t record (top) and amplitude (A)-t indication of stimulation (bottom) for electrical stimulation post ACh administration (77c) HS of 6.3g/ml ACh stimulation (77d) HS of electrical stimulation post ACh administration (77e) MHS of 6.3g/ml ACh stimulation (77f) MHS of electrical stimulation post ACh administration.

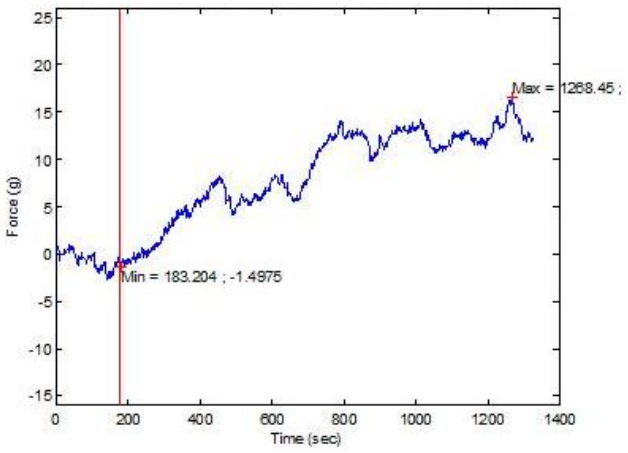

(a)

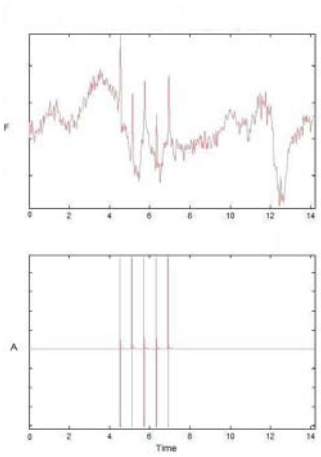

(b)

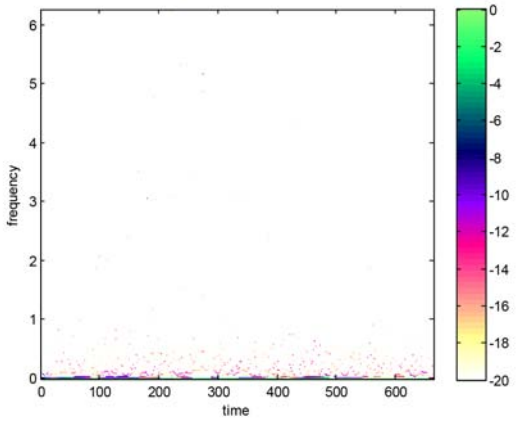

(c) injection at 180 sec

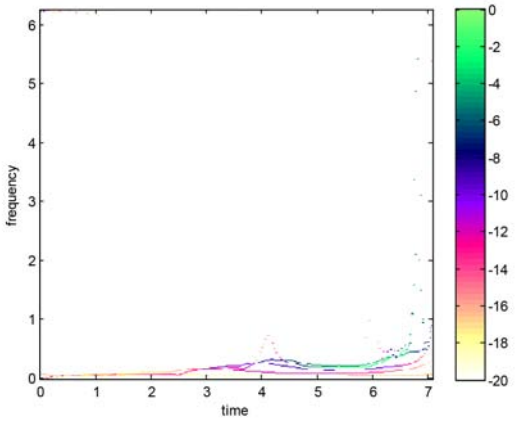

(d) stimulation as in (b)

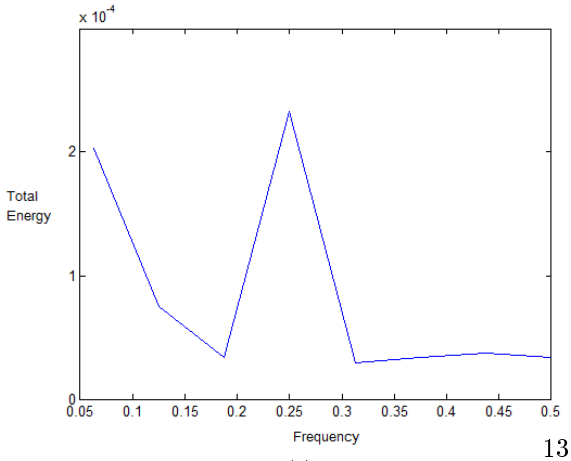

(e)

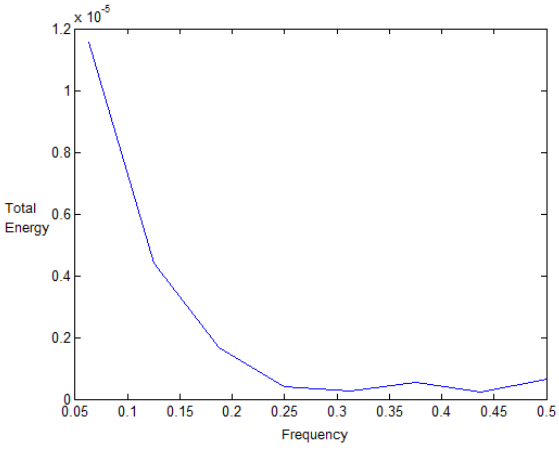

(f)

Figure 78: Results of IG from 14 day denervation group, stimulated at 6.3g/ml. (78a) F-t record of 6.3g/ml ACh stimulation (78b) F-t record (top) and amplitude (A)-t indication of stimulation (bottom) for electrical stimulation post ACh administration (78c) HS of 6.3g/ml ACh stimulation (78d) HS of electrical stimulation post ACh administration (78e) MHS of 6.3g/ml ACh stimulation (78f) MHS of electrical stimulation post ACh administration.

resulted in a large increase in force with time (see F-t graph in Figure 81), with possible occurrence of unfused tetanus after 1020sec (1200s on graph) post injection. The MHS of this test illustrated a large energy contribution in the 0.25-0.37Hz range.

In general, frequency bands of energy contribution were higher for innervated solei than denervated solei at 7 days post-denervation for concentrations up to $550\mu g/ml$ and *vice versa* for the high concentration range up to 6.3g/ml, with the most notable difference in energy contribution observed between IS and DS at 6.3g/ml. The opposite trend was observed for 14 days post-denervation where the range was greater for DS in the low concentration range (except at $96\mu g/ml$, but this was accounted for by energy spread through the full range of frequencies) and less than or equal to that of the IS in the high concentration range. The frequency bands of energy contribution for the DG were always greater for DG than IG, for both denervation periods and all concentrations. Additionally, low frequency energy contributions were always present, representing preferential altered fibre recruitment (in this case slow twitch), followed by recruitment of original fibres (in this case fast twitch fibres).

4.3 Histology

The results of the ATPase staining for fast twitch muscle fibres are presented. Muscles from each denervation period were stained and are compared here to their innervated controls. One example of each group is depicted in Table 7 which are representative of the overall features characteristic of each denervation period.

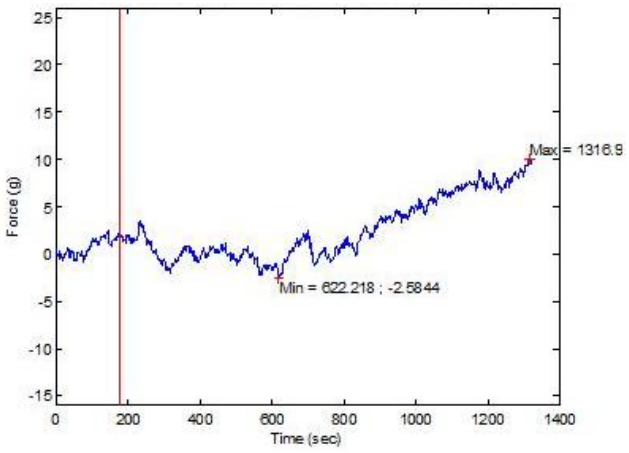

(a)

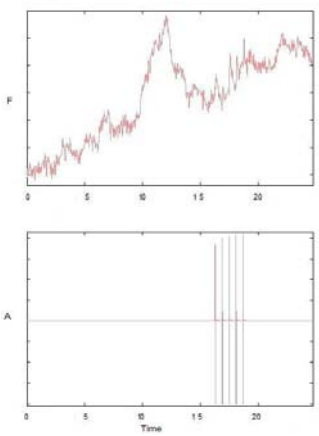

(b)

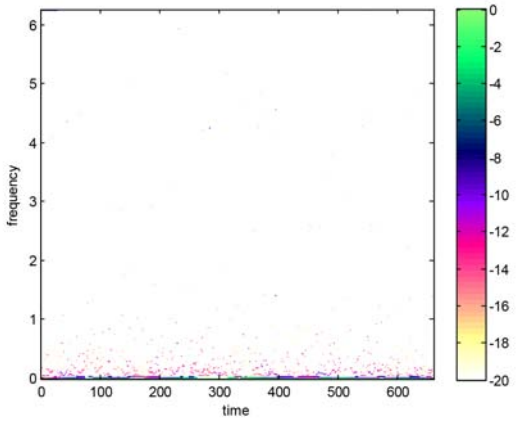

(c) injection at 180 sec

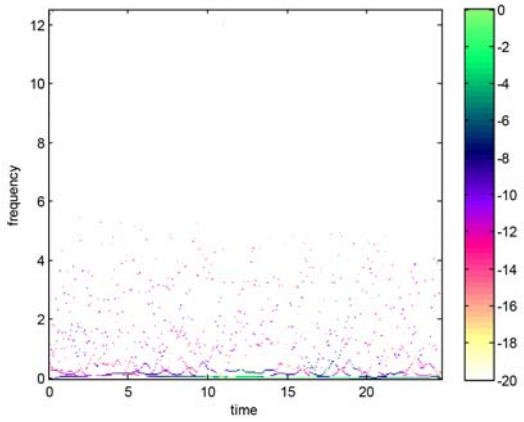

(d) stimulation as in (b)

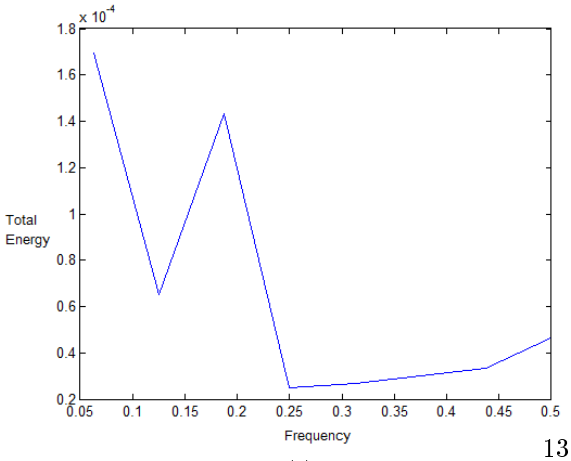

(e)

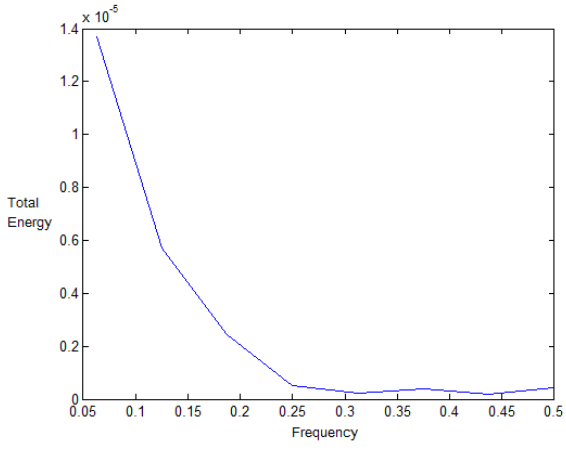

(f)

Figure 79: Results of 14 day DS stimulated at 6.3g/ml. (79a) F-t record of 6.3g/ml ACh stimulation (79b) F-t record (top) and amplitude (A)-t indication of stimulation (bottom) for electrical stimulation post ACh administration (79c) HS of 6.3g/ml ACh stimulation (79d) HS of electrical stimulation post ACh administration (79e) MHS of 6.3g/ml ACh stimulation (79f) MHS of electrical stimulation post ACh administration.

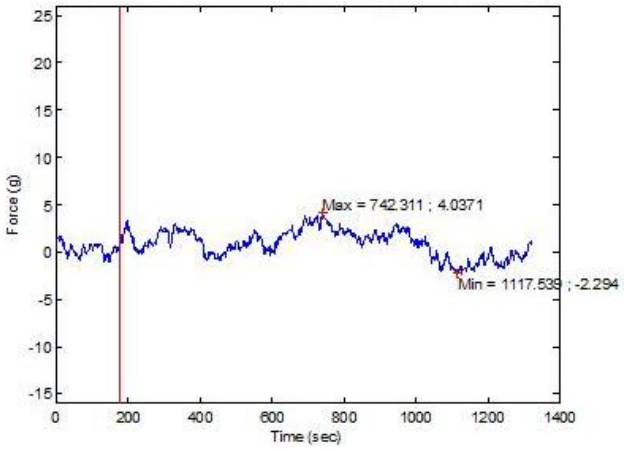

(a)

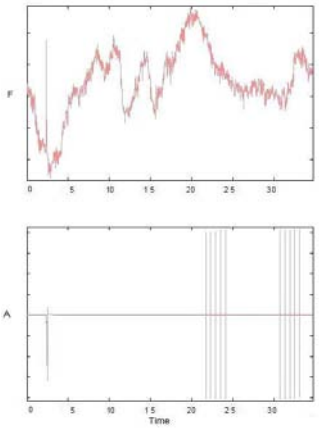

(b)

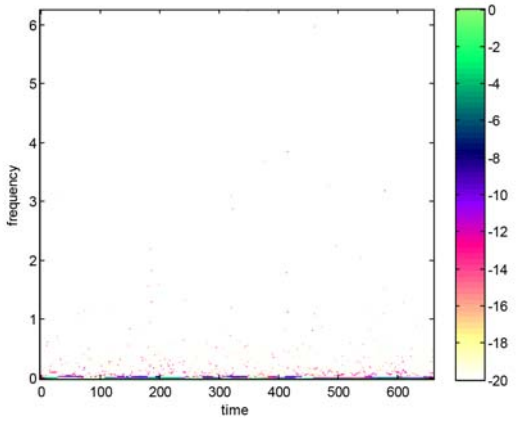

(c) injection at 180 sec

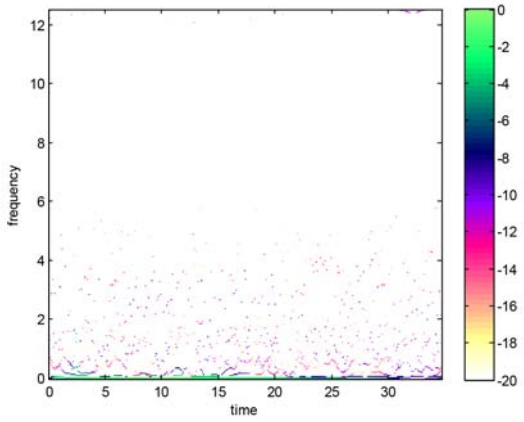

(d) stimulation as in (b)

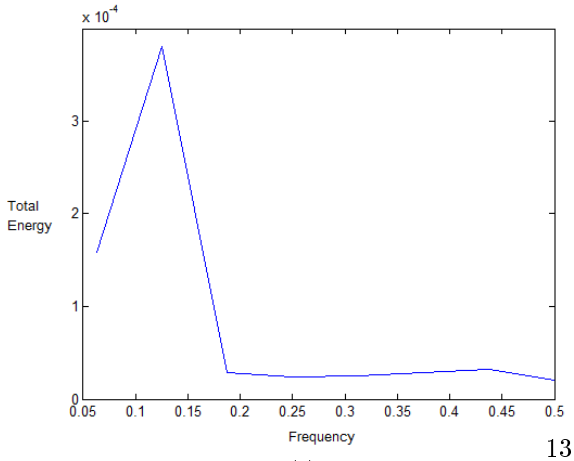

(e)

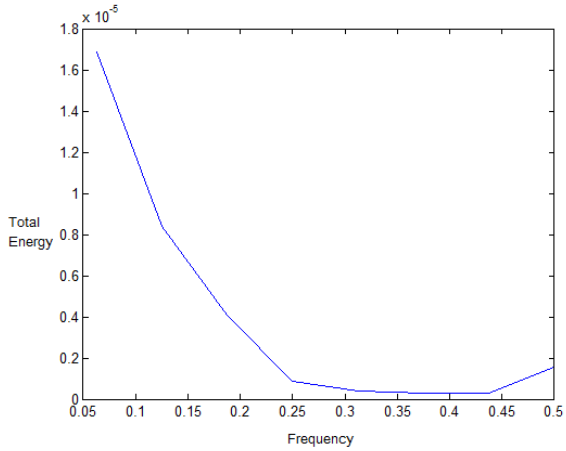

(f)

Figure 80: Results of IS from 14 day denervation group, stimulated at 6.3g/ml. (80a) F-t record of 6.3g/ml ACh stimulation (80b) F-t record (top) and amplitude (A)-t indication of stimulation (bottom) for electrical stimulation post ACh administration (80c) HS of 6.3g/ml ACh stimulation (80d) HS of electrical stimulation post ACh administration (80e) MHS of 6.3g/ml ACh stimulation (80f) MHS of electrical stimulation post ACh administration.

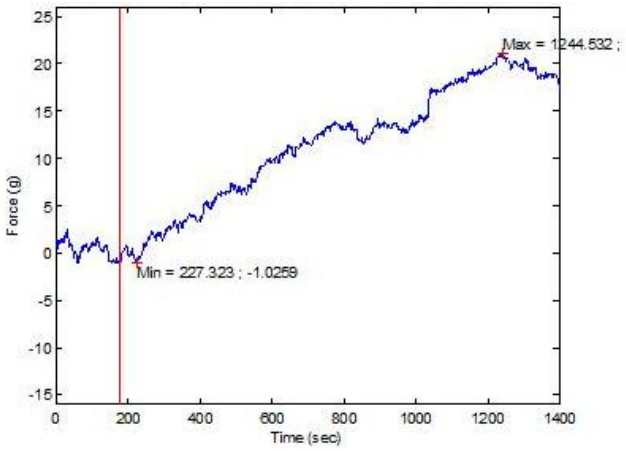

(a)

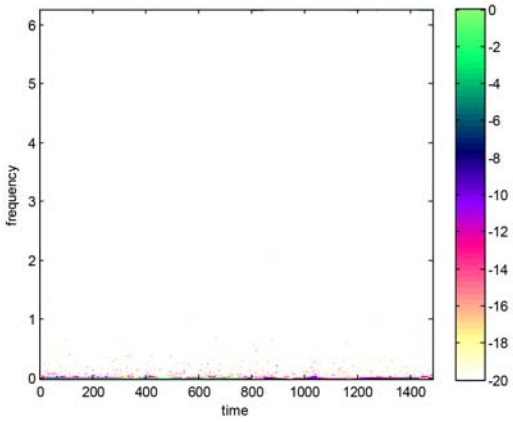

(b) injection at 180 sec

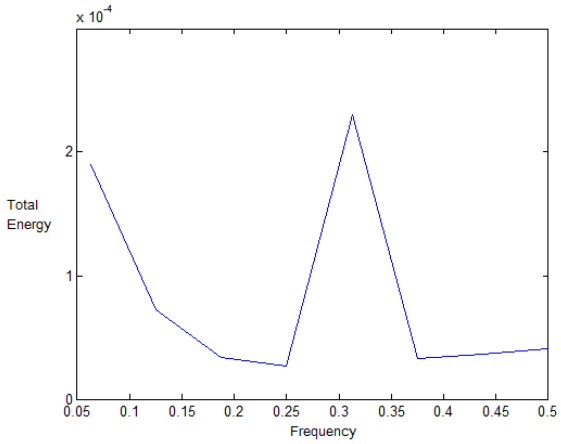

(c)

Figure 81: Results of further chemical stimulation of IS from a 14 day denervation period group, initially stimulated at 6.3g/ml (see Figure 80). (81a) F-t record of stimulation by large dose of ACh (81b) HS of large dose ACh stimulation (81c) MHS of large dose ACh stimulation.

Table 7: Histological sections of fast twitch fibres as demonstrated by ATPase staining for various denervation periods, all shown at 40x magnification

Denervation period	Gastrocnemii	Solei
0 days (innervated)	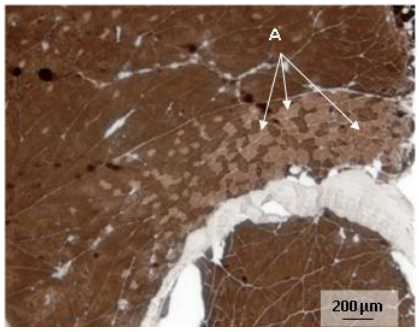	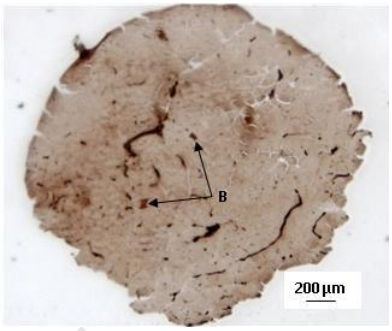
0 days (innervated)	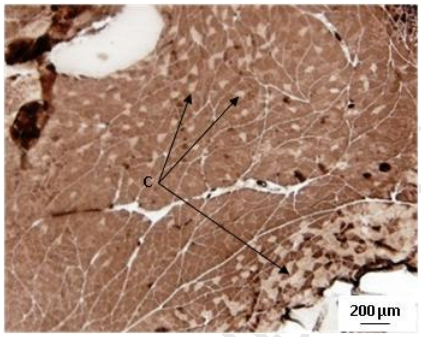	
14 days	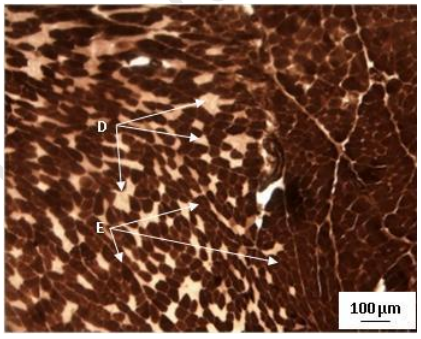	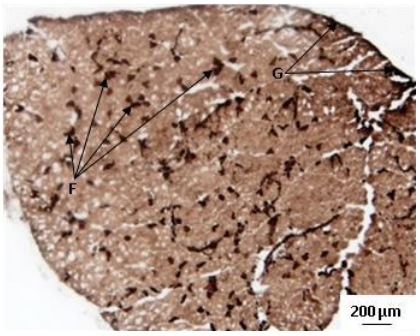

Denervation period	Gastrocnemii	Solei
22 days	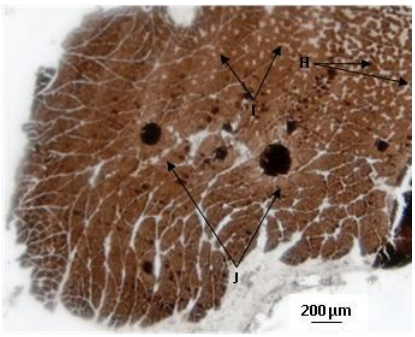	
204 days	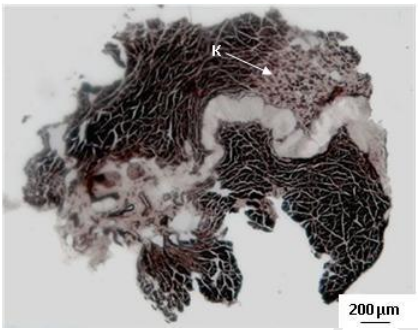	

The labels in Table 7 are indicative of the following:

A and C - slow twitch fibres present in the IG

B - fast twitch fibres present in the IS

D - slow twitch fibres from a 14 day DG

E - fast twitch fibres from a 14 day DG

F - fast twitch fibres from a 14 day DS

G - freezing artefact (not to be mistaken for fast twitch fibres)

H - fast twitch fibres from a 22 day DG

I - slow twitch fibres from a 22 day DG

J - freezing artefact

K - slow twitch fibres present in a 204 day DG

ATPase staining for fast twitch fibres in both gastrocnemii as well as solei produced results consistent with literature [Bakou et al., 1996]. The denervated gastrocnemii muscles demonstrated an increase in slow twitch fibres with an increase in denervation period and the denervated soleus demonstrated an increase in the number of fast twitch fibres 14 days post-denervation. For reasons previously explained, sample sizes were small and solei are only presented for select denervation

periods to demonstrate that the observed changes comply with literature, although further histological ATPase fibre staining would be ideal for the denervation periods not included here. The fibre type changes as observed here are supportive of the muscle responses (as previously discussed as functions of tension, sensitivity and time to peak tension).

5 Overview of Results/Summary

This section presents a brief overview of the results presented and discussed in section 4 and serves as a comprehensive summary before conclusions are drawn in section 6.

A consideration of F-t traces of all muscles as functions of denervation periods and concentration, demonstrated that 7 day DG showed greater slow contracture responses than IG. The IG and 7 day DS displayed the same pattern in slow contracture response as 7 day DG with an increase in concentration, but these patterns initiated at higher concentrations than 7 day DG. This phenomenon was termed a 'concentration lag' (as defined in the Glossary of Terms, page xix).

Larger slow contractures were noted in 14 day DG than 7 day DG in response to low concentrations (4-550μg/ml) of ACh. This observation was not made when these groups were tested with high (1.6-6.3g/ml) concentrations of ACh. IG displayed increased force variation for all concentrations of ACh used in this study at 14 days post-denervation compared to 7 days post-denervation. In general, a reduced response in both force variation as well as in the development of slow contracture, was observed for the two long term denervation periods of 50-55 days and 204-208 days in comparison to the short term denervation periods of 7 and 14 days for gastrocnemii.

DS displayed greater force variation than IS at 7 days probably due to an increase in the number of fast twitch fibres (compared to its pre denervation state). Such fibre type changes were observed post-denervation by histological ATPase staining. At 14 days post-denervation, slow contractures occurred at lower concentrations but the increase in force was observed to be more gradual and has been attributed to fibre type changes, (increased type II fibres), demonstrated to have occurred by histological ATPase staining. No slow contractures were noted for DS from long term denervation periods of 50-55 days and 204-208 days, compared to IS which did display slow contractures.

A consideration of peak forces produced by all tested muscles illustrated that denervated muscles were more sensitive to developing peak forces than their innervated counterparts for all investigated periods of denervation as well as for all concentrations. Greater peak forces were outputted by innervated muscles compared to their denervated contralaterals only as an exception to this observation; and occurred at a combination of high concentrations (1.6-6.3g/ml) and short denervation periods (7 and 14 days) for the gastrocnemii. This was supported by literature reporting a depressed response from muscles at high dosages of ACh.

The highest percentage differences in peak force occurred at 14 days post-denervation for solei (supportive of the high sensitivity to ACh for this period) and increased with increasing periods of denervation (7, 50-55 and 204-208 days) thereafter.

The data indicate that physiological changes either occur, or peak later (i.e. develop at a slower rate and with higher sensitivity to ACh) for the DS than the DG muscles. This was explained by timing in receptor proliferation (noted in literature to occur sooner in gastrocnemii than solei post-denervation), fibre type changes occurring sooner in gastrocnemii than solei (reported by literature

to initiate from 3 days for gastrocnemii and 1 week post-denervation for solei [Bakou et al., 1996, Dhoot and Perry, 1982]) as well as later sensitivity in gastrocnemii for later denervation periods due to an impeded mitochondrial ability to manufacture ATP. The DS displayed the highest sensitivity (generated the largest forces) at 14 days post-denervation, consistent with literature on nAChR proliferation of mammalian slow twitch skeletal fibres [Hartzell and Fambrough, 1972].

In order of decreasing sensitivity to ACh, muscles ranked as follows: DS, IS, DG, IG. In terms of this ranking, a consideration of the fibre types and receptor proliferation suggest that the greatest output force response is obtained from muscles with a combination of slow and fast twitch fibres (although predominantly slow) and most likely a large number of receptors, as occurs in DS. Whilst DG exhibit changes from fast to slow twitch fibres, the possible lack of ATP production may render receptor proliferation inconsequential, thus reducing fibre type influence. The lowest peak forces were produced by IG muscles, containing the least amount of slow twitch fibres and no receptor proliferation since they were not denervated.

An increase in concentration within the low concentration range (4-550μg/ml) was observed with a simultaneous decrease in output force for both solei and gastrocnemii for denervation periods longer than 7 days. This may be due to potential neuromuscular blocking effects similar to those reported by Brown [1950]. The DS however, appeared to demonstrate a threshold concentration such that stimulation with concentrations beyond it were able to cause the reappearance of slow contractures and a consequent increase in force with further increase in concentration. Further testing would be required to establish whether this trend exists for muscles denervated for periods longer than 7 days. Gastrocnemii showed no signs of such a concentration threshold. It may well be that such a trend would be visible in muscles denervated for periods shorter than 7 days, given the time differences in physiological changes between solei and gastrocnemii (with gastrocnemii reacting more quickly to denervation than solei).

An observance of the time to peak force responses of all muscles tested as functions of concentration and denervation period demonstrated that IG reached peak forces faster than IS. This would be expected since IG are comprised primarily of fast twitch fibres and IS are comprised primarily of slow twitch fibres. DG were slower to reach peak force than IG for all denervation periods. This was also expected since DG have been reported, and were observed in this study, by histological ATPase staining, to develop an increased number of slow twitch fibres. All DG follow the same time to peak force response trend as IG from a 7 day denervation period group, but they did so at a time lag. DS followed the opposite trend to DG in terms of time to peak force response. That is, the DS reached peak forces sooner than their innervated contralaterals. This too, is supported by literature as well as by histological ATPase staining conducted in this study, showing an increase in the number of fast twitch fibres in DS post-denervation. DS thus contained more type II fibres than IS, as well as a larger number of nAChR's due to receptor proliferation post-denervation and were thus more likely to display comparatively faster responses.

There were however, similarities in time to peak force responses of DG and DS which were noted by denervation period grouping, where the respective responses (although different for solei and gastrocnemii), were similar for 7 and 14 day groups and followed the trends of their respective innervated contralaterals from the 7 day denervation period. Long term denervation periods of 50-55 days and 204-208 days too, each followed the same trend. The highest forces for the DS occurred at (the most sensitive) 14 day post-denervation period, for which the longest time to peak force was recorded.

The time to peak force measurements demonstrated the possibility that different concentration thresholds exist for different denervation periods at which DS would be more likely to respond faster than IS. The highest concentration dependency was demonstrated at 14 days post-denervation (also the period of highest force generation). Since DG were observed to take longer to reach peak tension than IG, optimisation of shorter time differences are important. Such small time differences occurred between DG and IG with administration of high concentrations (1.6-6.3g/ml) of ACh for short denervation periods (7 and 14 days). It would thus be appropriate to note the effects of high concentrations on the time to peak tension of longer term denervated muscles in potential future studies. Further, DG contracted faster than IG at the lowest concentration ($4\mu g/ml$) for long term denervation periods and at the highest concentration for short term denervation periods.

Fibre type is an important consideration of muscle response to ACh doses. The alteration of fibre type post-denervation, affects the muscle response to ACh, such that either slow contracture responses or fast twitch responses can be obtained. The greatest (in terms of force) fast twitch responses were obtained for gastrocnemii (predominantly comprised of type II fibres) at high concentrations of ACh which allowed for saturation of the fast twitch fibre receptors. Similarly, slow contracture responses were obtained for solei (predominantly comprised of type I fibres) at high concentrations of ACh which allowed for saturation of the slow twitch fibre receptors.

Alternate chemical and electrical stimulation provided further observations supportive of those previously discussed in terms of post-denervation fibre type changes and sensitivity to ACh (observed by the relative degree of change in peak force with increase in concentration). Contractile responses with high energy outputs within a relatively low frequency range were considered to be indicative of slow contracture responses, and such observations were supported by muscle fibre type composition. Energy outputs within higher frequency ranges were considered to be contributions from fast twitch fibres and or from local high energy contractions of fibre bundles. Large energy contributions from frequency bands illustrated in the MHS were represented by little or no scatter in the corresponding HS plots.

In general, visible contractions due to electrical stimulation (as observed by local increases in force at the time of stimulation, or 'spikes' in the F-t traces) were larger and hence more evident in denervated muscles in comparison to their innervated contralaterals. This could well be a further result of the increased sensitivity of denervated muscles. Moreover, the proliferated receptors are

unlikely to have been saturated by low concentrations, thus eliminating the known effect of high concentrations of ACh blocking depolarisation and action potential conduction along the fibre, allowing for further electrical stimulation.

After stimulation at very high concentrations of ACh, contractions due to electrical stimulation were more visible (larger and produced higher energy outputs) in the IS than the DS. The energy output from the DS generally occurred across the full range of frequencies with additional localisations, compared to the energy components of the IS which were more localised in frequency. Frequency 'scatter' was more evident for denervated muscles in comparison to their innervated counterparts, indicating large energy contributions from wider frequency ranges. This could be indicative of localised contractions of fibre bundles occurring at different rates (hence not as well localised in frequency) as their innervated controls.

Muscles tested chemically with large doses of ACh after electrical stimulation demonstrated a reduced energy response and a shift in frequency bands of energy contribution. For denervated muscles, this meant that if the energy was spread throughout the frequency range before, they were more localised in frequency in their response to large doses of ACh administration post electrical stimulation. This suggests that fewer local contractions of fibre bundles were likely to occur and smaller contractures evolved. IG contributed energy from the same frequency range, but outputted a reduced energy response. IS displayed an increased energy contribution from the full frequency range but an overall reduction in energy and a shift to lower frequency band energy contribution, reported in literature as an inhibition of conduction ability due to a block produced by large doses of ACh [Brown, 1950].

Tables 8, 9, 10 and 11 provide summaries of the main findings. The following key applies:
DS: denervated solei
IS: innervated solei
DG: denervated gastrocnemii
IG: innervated gastrocnemii
↑: increase
↓: decrease
[c]: concentration
[low]: low concentration range (4-550μg/ml)
[high]: high concentration range (1.6-6.3g/ml)
- : not applicable

Table 8: Summary of experimental results pertaining to peak force and time to peak force for soleus muscles

DP	Peak Force (contractures)			Time to peak force		
	[low ACh]	[high ACh]	Response	[low ACh]	[high ACh]	Response
7				DS<IS	DS<IS	DS same trend as IS
14			slow contractures initiated at lower concentrations	DS<IS	DS<IS	DS same trend as IS; 14 days same trend as 7 days; DS longest time to peak tension
	↑[c]↓IS		DS displayed threshold concentration beyond which ↑[c]↑DS			
50-55	DS=0, <IS	-		DS<IS	-	DS same trend as IS
	↑[c]↓IS	-	DS displayed threshold concentration beyond which ↑[c]↑DS		-	
204-208	DS=0, <IS	-		DS<IS	-	DS same trend as IS; 204-208 days same trend as 50-55 days
	↑[c]↓IS	-	DS displayed threshold concentration beyond which ↑[c]↑DS		-	

Table 9: Summary of experimental results pertaining to peak force, time to peak force and force variation for gastrocnemii muscles

DP	Peak Force (contractures)		Time to peak force			Force variation (contractions)	
	[low ACh]	[high ACh]	[low ACh]	[high ACh]	Response	[low ACh]	[high ACh]
7	DG7>IG7		IG<IS, IG<DG	IG<IS, IG<DG	Exception: DG<IG at 6.3g/ml		
					DG same trend as IG		
14	DG14>DG7	DG14<DG7	IG<IS, IG<DG	IG<IS, IG<DG	Exception: DG<IG at 6.3g/ml		IG14>IG7
					DG same trend as IG; 14 days same trend as 7 days		
	↑[c]↓IG, DG						
50-55	IG(50-55+204-208)<IG(7+14)	-	IG<IS, IG<DG	-	Exception: DG<IG at 4ug/ml	IG(50-55+204-208)<IG(7+14)	-
	DG(50-55+204-208)<DG(7+14)					DG(50-55+204-208)<DG(7+14)	
					DG same trend as IG		
	↑[c]↓IG, DG	-		-			
204-208	IG(50-55+204-208)<IG(7+14)	-	IG<IS, IG<DG	-	Exception: DG<IG at 4ug/ml	IG(50-55+204-208)<IG(7+14)	-
	DG(50-55+204-208)<DG(7+14)					DG(50-55+204-208)<DG(7+14)	
	↑[c]↓IG, DG	-		-			
					DG same trend as IG; 204-208 days same trend as 50-55 days		

Table 10: Summary of results pertaining to alternate chemical and electrical stimulation for solei and gastrocnemii denervated for 7 days

Test	Gradual increase in F-t p.i.	Large freq. Variation p.i.	Visible elec stim contractions (f-t)	Large relative energy HSA (chem)	Clear elec HS
dg4,7d	N	Y	N	Y	N
ds4,7d	N	Y	Y	Y	Y
is4,7d	Y (slight)	Y (slight)	Y	>1/2	Y
dg96,7d	Y (large)	Y	Y	>1/2	Y
ds96,7d	N	Y	Y	>1/2	Y
is96,7d	Y	Y (slight)	N	N <1/2	N
dg550,7d	Y (slight)	Y	Y	Y	Y
ig550,7d	N	Y	Y	Y	Y
ds550,7d	Y	Y	Y	Y (w/in low energy range but 10^{-3})	Y
is550,7d	Y (large)	Y (slight)	Y	Y (w/in low energy range but 10^{-3})	Y
is1.6,7d	Y (slight)	Y (after time)	Y	Y	Y
is3.2,7d	Y (slight)	Y (slight)	na	N <1/2	Y
ds3.2,7d	Y (initially but decreases after)	Y	Y	>1/2	Y
ig3.2,7d	Y (after time)	N	Y	Y	Y
dg6.3,7d	Y	N	Y	Y (w/in low energy range but 10^{-3})	Y
ds6.3,7d	Y (large)	Y (slight)	Y (tiny)	Y (w/in low energy range but 10^{-3} + 2ranges)	na
is6.3,7d	Y (initially but decreases after)	N	Y (tiny)	Y	N

Table 11: Summary of results pertaining to alternate chemical and electrical stimulation for solei and gastrocnemii denervated for 14 days

Test	Gradual increase in F-t p.i.	Large freq. Variation p.i.	Visible elec stim contractions (f-t)	Large relative energy HSA (chem)	Clear elec HS	High ACh grad increase (f-t)	Visible further elec stim	Further large relative energy HSA (chem)
dg4,14d	Y	Y (slight)	N	>1/2	N			
ds4,14d	Y	Y	Y	Y	Y	Y	Y	>1/2
is4,14d	Y (after time)	Y (slight)	N	>1/2	Y			
dg96,14d	Y	Y	Y	Y	N			
ig96,14d	N	Y (initially)	N	Y	Y	N	N	N
ds96,14d	Y	N	Y	N	N			
is96,14d	Y (slight)	Y (slight)	Y	>1/2	N	N	na	<1/2
ds550,14d	Y	Y (slight)	Y	N	Y			
is550,14d	Y	Y (slight)	Y	>1/2	Y			
ig550,14d	Y (initially but decreases after)	Y (slight)	N	na	N	Y (initially but decreases after)	Y (tiny)	>1/2
dg550,14d	Y	N	N	N	N	N	Y	<1/2
dg1.614d	Y	N	N	>1/2	Y			
ig1.6,14d	Y (slight)	Y	N	Y	N			
ds1.6,14d	N	Y	N	>1/2	N			
is1.6,14d	Y (after time)	Y (slight)	Y	Y	Y			
ds3.2,14d	Y (slight)	Y	Y	Y	Y	N	N	<1/2
is3.2,14d	Y (slight)	Y	Y	>1/2	Y			
dg6.3,14d	Y (slight)	N	Y	>1/2	Y			
ig6.3,14d	Y	Y	Y	Y	Y			
ds6.3,14d	Y (after time)	Y	Y (tiny)	>1/2	N			
is6.3,14d	N	Y	N	Y (w/in low energy range but 10^{-4})	N	Y (large)	na	Y

6 Conclusions

This section draws conclusions following from the results, discussion and overview presented in sections 4 and 5 and highlights the essential deductions relating to the three-fold objectives. The conclusions presented are novel contributions deduced from this study, except where conformation with the literature is explicitly stated.

The investigation involved examining two fundamental parameters (time taken to peak force and maximum force of contraction) under a variation of three conditions (ACh concentration, muscle type and denervation period), the combination of which has not been reported in literature. Forces were examined both in terms of slow contracture or gradual force increase as well as local force variation observed over the full time period of contraction. Data was further analysed by the novel application and combined approach of EMD, HSA and MHS. This allowed for a more thorough and detailed representation of information in terms of energy distribution resulting from muscle stimulation by ACh application. Resultant analysis allowed for the following observations.

6.1 Deductions based on analysis of F-t traces

- Changes in fibre composition post-denervation, for both fast twitch and slow twitch muscles, occurred in a manner consistent with reports in the literature. It can thus be asserted that denervated fast twitch muscles experience an increase in slow twitch fibres post-denervation and similarly denervated slow twitch muscles experience an increase in fast twitch fibres post-denervation.

- Slow twitch muscles denervated for long time periods appear to lose all potential for slow contracture (i.e. even if slow twitch fibres still exist in the muscle, they are not sensitive enough for low concentrations of ACh to initiate contraction).

Slow contractures were still visible in long term denervated muscles which were originally predominantly fast twitch. Additionally, the fast twitch fibre response of originally predominantly fast twitch muscles was still visible (noted by force variation) after long denervation periods (50-55 days and 204-208 days) (note that fast twitch fibres are known to be more sensitive in their contractile response than slow twitch fibres [Gaster et al., 2001, Ploug et al., 1984]).

This observation leads to a number of deductions: (1) either all the fibres of originally slow twitch muscles change to fast twitch fibres, or to a combination of fast and slow twitch fibres in which the post-denervation slow twitch fibres are less sensitive (or likely unable to produce ATP) than the original slow twitch fibres (literature supports the latter [Patterson et al., 2006] by noted differences in phenotypes) and (2) originally slow twitch fibres either deteriorate at a faster rate or are less sensitive than slow twitch fibres which appear post-denervation in originally predominantly fast twitch muscles. The deduction made in '(2)' is supported by Tomanek and Lund [1973] who reported that slow twitch fibres of predominantly fast twitch muscles were less affected than those of slow twitch muscles when compared at the same post-denervation periods, suggesting varying

degrees of neural dependence despite similar histochemical configuration.

- Although beyond the scope of this study, the results indicate that it would be worthwhile to investigate if a preferential change in fast twitch fibre type occurs post-denervation (such that a certain fast twitch fibre type is more likely to convert to a slow twitch fibre).

- Low ACh concentrations produce large contractures (slow/gradual contractions) in slow twitch fibres. Higher concentrations are needed to produce the same effects in the presence of predominantly fast twitch fibre muscles.

- The slow contracture response (and thus greater presentation of force summation) is more prominent in originally fast twitch muscles at 7 days post-denervation compared to the slow contracture response of originally slow twitch muscles of the same denervation period. The slow contracture response of originally predominantly slow twitch muscles is most prominent at 14 days post-denervation compared to other denervation periods as well as to originally predominantly fast twitch muscles of the same denervation period. This is not attributed to receptor proliferation, but rather due to phenotype differences between slow twitch fibres developed post-denervation in originally fast twitch fibres and those from originally slow twitch muscles. Fibre type changes occurred sooner in fast twitch muscles than slow twitch muscles once denervated, as supported by histological evidence.

- Innervated fast twitch muscles appear to display an increase in force variation for short periods of denervation (7 and 14 days), which is taken to indicate an increase in fast twitch fibre activity. This may be due to the increased movement and effort required from the innervated limb to support the animal due to the impaired function of the denervated contralateral.

- For fast twitch muscles: Longer term denervation periods (50-55 days and 204-208 days) displayed a decrease in slow contracture as well as force variation in comparison to short term denervation periods. This demonstrates a reduced response to stimulation with an increase in denervation period, as is consistant with literature.

6.2 Deduction based on analysis of peak force recordings

- High concentrations of ACh cause high peak force fast twitch responses in fast twitch muscles and high peak force contractures in slow twitch muscles, as is to be expected based on theory.

- In general, denervated muscles produced greater peak forces than their innervated contralaterals. This was true for all periods of denervation and all concentrations reported in this study. The only exceptions to occur were related to the concentration of ACh, such that innervated fast twitch muscles produced greater peak forces than short term denervated muscles (7 and 14 days) when stimulated with high concentrations of ACh. Receptor proliferation is considered the primary underlying cause for this observation. It is suggested that the concentration threshold which results in a depressed response is lower for denervated muscles than for their innervated contralaterals due

to the increased sensitivity by way of receptor proliferation after short periods of denervation. It is further suggested that this effect is more prominant in originally fast twitch muscles since, once denervated, fast twitch fibres tend to alter in preference to slow twitch fibres [Gauthier and Dunn, 1973, Tomanek and Lund, 1973]. It is postulated that this effect was not observed for longer denervation periods due to a reduction in receptor proliferation which occurs after the initial increase post-denervation. As a result, fibre type becomes a predominant factor in the contractile response of long term denervated muscle. The significantly larger ratio of slow to fast twitch fibres after long denervation periods in comparison to the innervated contralaterals (fast twitch muscles), surpasses the fast twitch fibre peak force capacity even at high concentrations. The gradual force increase due to contraction of slow twitch fibres is taken to govern the value of the peak force.

- The largest percentage difference in peak force between denervated and innervated slow twitch muscles was observed at 14 days post-denervation, thus further confirming the receptor proliferation peak and conforming to literature.

- In order of decreasing sensitivity, muscles were ranked as follows: denervated slow twitch, innervated slow twitch, denervated fast twitch, innervated fast twitch. This indicates a rank by original predominant fibre type (slow twitch more responsive than fast twitch) and a sub-split by denervation such that denervated muscles are more responsive than their innervated contralaterals, as is supported by literature. It is worth mentioning that the peak response measured was a combined contribution of both slow contracture as well as localised (in time) contractions. Over the testing time of 19 minutes, the slow contracture force is thus the primary contributor to the measured output, explaining why slow twitch fibres were found to outrank fast twitch fibres in their force output. Had only contractions been considered, fast twitch muscles would outrank slow twitch fibres in their measurable contractile ability. Moreover, fibre type influence is reduced due to inhibition of ATP production and the consequent reduction in the effect of proliferated receptors.

- An increase in concentration within the low concentration range of 4-550μg/ml resulted in a simultaneous decrease in output force for all muscles denervated for periods longer than 7 days, suggesting a potential neuromuscular block, as supported by literature. Results suggest that a threshold condition in denervation period in slow twitch muscles exists, such that a subsequent increase in concentration results in an increase in force beyond the suggested threshold denervation period. It is suggested that this is likely due to timing of, and changes in, receptor proliferation. Further testing would be required to confirm this.

Additional testing at shorter denervation periods for a wide concentration range (as used in this study) would allow for further clarification of the threshold denervation period. It could be hypothesised that such an observation (of a threshold denervation period) can be made with denervated fast twitch muscles as well, for shorter time periods of denervation (less than 7 days, based on observation and theory).

6.3 Deductions based on analysis of time to peak force responses

- Innervated fast twitch muscles were found to respond faster than innervated slow twitch muscles, which is to be expected and complies with theory and literature.

- Denervated fast twitch muscles were slower to reach peak force than innervated fast twitch muscles for all denervation periods considered. This is likely due to a reduction in the fast to slow twitch fibre ratio.

- All denervated fast twitch muscles followed the same time response trend as innervated fast twitch muscles from a 7 day denervation period group. This time frame suggests a point of denervation "stability" beyond the peak of receptor proliferation.

- Denervated slow twitch muscles reached peak tension sooner than their innervated contralaterals. This is likely due to a combination of increased sensitivity and an increase in fast to slow twitch fibre ratio (as supported by histological ATPase staining and existing theory).

- Denervated muscles followed the same trend in time to contraction for varying concentrations of ACh as their innervated contralaterals for both fast and slow twitch muscles (although different between twitch types). Further grouping was noted according to denervation period, where short term denervation groups (7 and 14 days) displayed the same trend and simarlarly long term denervation groups (50-55 and 204-208 days) displayed the same trend. This indicates that both fast and slow twitch muscles can be grouped into denervation period categories such that the properties change accordingly with an increase in denervation period. This information can be implemented in later applications of ACh administration where time to contraction can be estimated by the investigator when stimulating muscles of known denervation period and muscle type with a given concentration or concentration range.

- For slow twitch muscles, different concentration dependencies exist for different denervation periods such that denervated muscles tend to react faster than their innervated contralaterals. The highest concentration dependency appears to occur at the height of the receptor proliferation phase (observed at 14 days).

- Small differences in time to contraction occur between innervated and denervated fast twitch muscles denervated for short periods when stimulated with high concentrations of ACh. Further testing is required to determine high concentration effects on long term denervated fast twitch muscles.

- For long term denervation periods and low concentrations, denervated fast twitch muscles were found to contract sooner than their innervated contralaterals. The same was found true in the converse situation of short term denervation periods and high concentrations.

6.4 Deductions based on alternate chemical and electrical stimulation and novel application of signal analysis methods

This thesis made use of EMD and HSA as a novel approach in determining differences in muscle contraction dynamics under various parameters (muscle type, denervation period and concentration strength). Application of ACh to denervated muscles *in vivo* produced raw force-time data which is considered non-stationary and non-linear, thus appropriating the use of these techniques. To the best of my knowledge, no literature has hitherto approached the analysis of muscle contraction dynamics as described in the context of this thesis. Results were analysed in terms of energy distributions in varying frequency ranges of fibre contractions. This approach allowed for a more in depth determination of fibre activity whilst maintaining the perspective of whole muscle contraction.

Based on this approach, the following deductions could be made:

- Direct electrical stimulation of the muscle was used post ACh administration in order to determine the effects of ACh on muscle contractility and measure the response against a known stimulus (electrical). The general result indicated that denervated muscles produced a larger contractions than their innervated contralaterals, suggesting receptor proliferation to account for supersenstivity of denervated muscle.

- The effect of electrical stimulation was more prominant in innervated slow twitch muscles than their denervated contralaterals when stimulated at high concentrations of ACh. This may be due to the saturation of innervated muscle receptors and the known 'priming' effect of electrical stimulation prior to chemical stimulation [Bach-y Rita and Ito, 1966] for contraction, although further experimentation would be required to confirm this hypothesis.

- Large energy contributions from a wider frequency range were noted for denervated muscles compared to their innervated contralaterals. It is suggested that this is due to fibre bundles contracting at different frequencies due to varying fibre type composition of the muscle (where denervated muscle composition is more varied due to physiological post-denervation changes).

- A reduced energy response and change in frequency bands of energy contribution was noted in denervated muscles tested with large doses of ACh post-electrical stimulation. This may indicate a specific fibre type reaction, inferring that some fibre type receptors become saturated in preference to others and/or that fast twitch fibres present in the denervated muscles were easily fatigued - a known property of fast twitch fibres and a likelihood when considering the reduced ability for ATP production in denervated fibres.

- The reduced energy output whilst remaining in the same frequency range from innervated fast twitch muscles stimulated by high doses of ACh post-electrical stimulation, indicates that a number of the fast twitch fibres may have been fatigued.

- The reduced energy output and contractions occurring within a lower frequency range produced by innervated slow twitch muscles stimulated by high doses of ACh post-electrical stimulation,

further indicates slow fibre predominance, fatigue of any existing fast twitch fibres and potential block of conduction ability.

6.5 Overall conclusion

Based on these deductions, it can be surmised that application of ACh in a manner consistent with the methods reported here would be less efficient than the use of electrical stimulation. Times taken to reach peak force were significantly longer than those caused by electrical stimulation as reported in literature. Nevertheless, the breadth of the parameters investigated (large denervation period ranges, large concentration ranges and various muscle types) provide a comparitive basis and valuable documentation of the varying responses of innervated and denervated muscles of various types (type I and II) to application of ACh. These findings can be applied to possible further studies involving i.a. ACh administration, leading up to the eventual administration of ACh by potential implementation of implantable microfluidic devices. In addition, the novel application of the analytical approach presented herein to stochastic F-t signals, allowed for the energy-frequency-time distribution to be depicted in a previously uncharted manner.

7 Recommendations for future studies

This sections provides recommendations for further research pertaining to this topic.

1. The first improvement relates to administration of ACh in the explanted preparation. *In vivo* experiments or alternatively, experiments which involve explantation of the muscle with an artery, could be conducted. This would allow for the ACh to be administered i.a. as done by Sanghvi and Smith [1969], presumably resulting in shorter lag and rise times and increased responses due to improved localisation.

2. In this study it has been demonstrated that slow twitch soleus fibres convert to fast twitch fibres post-denervation, it is hypothesized that intermediate stimulation would result in a reversion of the altered fibres to their original state, dependent on denervation time periods. Consequently, the preparation could be stimulated at a set rate for a set time period (AChE will be required to relax muscle in between stimulations). Subsequently perform an ATPase stain on the tested muscle to determine any change in fibre composition.

3. To further explore physiological compensation for denervated limbs, conduct histological ATPase stains of innervated contralaterals to note fibre type changes which may occur.

4. Conduct tests at shorter denervation periods (1-2 days) before receptors have proliferated. The aim of this would be to test if the physiological changes known to occur after muscle denervation can be intercepted and the muscle made to contract as though it still maintained full functionality. This would most likely work best with tests conducted with i.a. injection where whole muscle contractions will be more visible and easily distinguishable than slow contractures, hence paving the way for more practical device implantation which could release ACh at set periods to cause contraction. The overall picture to keep in mind is (a) fast acting treatment for patients paralysed 1-2 days earlier, (b) rehabilitation for patients in the intermediate stages of denervation and (c) treatment to combat muscle atrophy for patients who have been paralysed for long periods of time.

5. Differences in force trends between low and high concentration ranges of ACh should be further investigated to establish threshold periods for changes in trends. Further, longer denervation periods could be tested at higher concentrations, as data pertaining to these parameters were not recorded in this study.

6. Larger groups of test subjects should be used to attest to statistical significance. Exceptions to trends should be further investigated with larger sample sizes.

7. In order to fully inform device design for furthering the idea of effective stimulation in range of the natural state, a comprehensive investigation into the change in the number of receptors

between fast and slow twitch muscles for various denervation periods should be conducted. This would allow for a better understanding of the force generation with respect to muscle sensitivity based on nAChR proliferation. More often than not, the literature leans towards investigations based on mixed fibre types, or predominantly fast twitch muscles, leaving a gap in the knowledge of slow twitch muscles. In terms of future implementations in practical applications, these gaps need to be filled for device design to eventually effectively simulate the natural state of the human body.

References

Y.O. Adu-Gyamfi, N.O. Attoh-Okine, and A.Y. Ayenu-Prah. Critical analysis of different hilbert-huang algorithms for pavement profile evaluation. *Journal of Computing in Civil Engineering*, 24:514, 2010.

E.X. Albuquerque and S. Thesleff. A comparative study of membrane properties of innervated and chronically denervated fast and slow skeletal muscles of the rat. *Acta Physiologica Scandinavica*, 73(4):471, 1968. ISSN 0001-6772.

A.O. Andrade, S. Nasuto, P. Kyberd, C.M. Sweeney-Reed, and F.R. Van Kanijn. EMG signal filtering based on Empirical Mode Decomposition. *Biomedical Signal Processing and Control*, 1 (1):44–55, 2006. ISSN 1746-8094.

J. Axelsson and S. Thesleff. A study of supersensitivity in denervated mammalian skeletal muscle. *The Journal of Physiology*, 147(1):178, 1959. ISSN 0022-3751.

P. Bach-y Rita and F. Ito. In vivo studies on fast and slow muscle fibers in cat extraocular muscles. *The Journal of General Physiology*, 49(6):1177, 1966.

E. Bajusz. "red" skeletal muscle fibers: Relative independence of neural control. *Science*, 145 (3635):938, 1964.

S. Bakou, Y. Cherel, B. Gabinaud, L. Guigand, and M. Wyers. Type-specific changes in fibre size and satellite cell activation following muscle denervation in two strains of turkey (meleagris gallopavo). *Journal of Anatomy*, 188(Pt 3):677, 1996.

R. Balocchi, D. Menicucci, E. Santarcangelo, L. Sebastiani, A. Gemignani, B. Ghelarducci, and M. Varanini. Deriving the respiratory sinus arrhythmia from the heartbeat time series using empirical mode decomposition. *Chaos, Solitons & Fractals*, 20(1):171–177, 2004. ISSN 0960-0779.

B.M. Battista, C. Knapp, T. McGee, and V. Goebel. Application of the empirical mode decomposition and Hilbert-Huang transform to seismic reflection data. *Geophysics*, 72(2):H29, 2007. ISSN 0016-8033.

F. Benedetti, S. Vighetti, C. Ricco, M. Amanzio, L. Bergamasco, C. Casadio, R. Cianci, R. Giobbe, A. Oliaro, and B. Bergamasco. Neurophysiologic assessment of nerve impairment in posterolateral and muscle-sparing thoracotomy. *The Journal of Thoracic and Cardiovascular Surgery*, 115(4): 841–847, 1998. ISSN 0022-5223.

D. Boutana, M. Benidir, and B. Barkat. On the selection of intrinsic mode function in emd method: Application on heart sound signal. In *Applied Sciences in Biomedical and Communication Technologies (ISABEL), 2010 3rd International Symposium*, pages 1–5. IEEE, 2010.

S.V. Brooks and J.A. Faulkner. Contractile properties of skeletal muscles from young, adult and aged mice. *The Journal of Physiology*, 404(1):71, 1988.

G.L. Brown. The actions of acetylcholine on denervated mammalian and frog's muscle. *The Journal of Physiology*, 89(4):438, 1937.

G.L. Brown. Excitatory and inhibitory effects of the chemical mediators. *Proceedings of the Royal Society of London. Series B, Biological Sciences*, 137(888):303–307, 1950.

L.A. Burnes, S.J. Kolker, J.F. Danielson, R.Y. Walder, and K.A. Sluka. Enhanced muscle fatigue occurs in male but not female asic3–/–mice. *American Journal of Physiology-Regulatory, Integrative and Comparative Physiology*, 294(4):R1347–R1355, 2008.

J.H. Burridge, P.N. Taylor, S.A. Hagan, D.E. Wood, and I.D. Swain. The effects of common peroneal stimulation on the effort and speed of walking: a randomized controlled trial with chronic hemiplegic patients. *Clinical Rehabilitation*, 11(3):201, 1997. ISSN 0269-2155.

A. Bye, M.A. Hoydal, D. Catalucci, M. Langaas, O.J. Kemi, V. Beisvag, L.G. Koch, S.L. Britton, U. Ellingsen, and U. Wisloff. Gene expression profiling of skeletal muscle in exercise-trained and sedentary rats with inborn high and low vo2max. *Physiological Genomics*, 35(3):213–221, 2008.

Walke W. Chahine, K.G. and D. Goldman. A 102 base pair sequence of the nicotinic acetylcholine receptor delta sub-unit gene confers regulation by muscle electrical activity. *Development*, 115: 213–219, 1992.

A.S. Cornachione, P.C.O. Benedini-Elias, J.C. Polizello, L.C. Carvalho, and A.C. Mattiello-Sverzut. Characterization of fiber types in different muscles of the hindlimb in female weanling and adult wistar rats. *Acta histochemica et cytochemica*, 44(2):43, 2011.

H.H. Dale, W. Feldberg, and M. Vogt. Release of acetylcholine at voluntary motor nerve endings. *The Journal of Physiology*, 86(4):353, 1936. ISSN 0022-3751.

J.A. David and R.M. Pitman. The effects of axotomy upon the extrasynaptic acetylcholine sensitivity of an identified motoneurone in the cockroach periplaneta americana. *Journal of Experimental Biology*, 98(1):329, 1982.

E.R. de Lima, A.O. Andrade, J.L. Pons, P. Kyberd, and S.J. Nasuto. Empirical mode decomposition: a novel technique for the study of tremor time series. *Medical and Biological Engineering and Computing*, 44(7):569–582, 2006. ISSN 0140-0118.

G.K. Dhoot and S.V. Perry. The effect of denervation on the distribution of the polymorphic forms of troponin components in fast and slow muscles of the adult rat. *Cell and Tissue Research*, 225 (1):201–215, 1982.

A. Eberstein and S. Eberstein. Electrical stimulation of denervated muscle: is it worthwhile? *Medicine & Science in Sports & Exercise*, 28(12):1463, 1996. ISSN 0195-9131.

T. Eken and K. Gundersen. Electrical stimulation resembling normal motor-unit activity: effects on denervated fast and slow rat muscles. *The Journal of Physiology*, 402(1):651, 1988. ISSN 0022-3751.

C.R. Ethier and C.A. Simmons. *Introductory biomechanics: from cells to organisms*. Cambridge texts in biomedical engineering. Cambridge University Press, 2007. ISBN 9780521841122.

D.M. Fambrough. Acetylcholine receptors. *The Journal of General Physiology*, 64(4):468–472, 1974.

M. Farge. Wavelet transforms and their applications to turbulence. *Annual Review of Fluid Mechanics*, 24(1):395–458, 1992.

W. Feindel, J.R. Hinshaw, and G. Weddell. The pattern of motor innervation in mammalian striated muscle. *Journal of Anatomy*, 86(Pt 1):35, 1952.

A. Feltz, A. Mallart, R. Kahn, and A. Le Yaouanc. An analysis of acetylcholine responses of junctional and extrajunctional receptors of frog muscle fibres. With an Appendix. *The Journal of Physiology*, 218(1):85, 1971. ISSN 0022-3751.

S.I. Fox. *Human Physiology*. McGraw-Hill, 2003. ISBN 9780072440829.

A.B. Fulton and W.B. Isaacs. Titin, a huge, elastic sarcomeric protein with a probable role in morphogenesis. *Bioessays*, 13(4):157–161, 1991.

P.F. Gardiner, R. Michel, and G. Iadeluca. Previous exercise training influences functional sprouting of rat hindlimb motoneurons in response to partial denervation. *Neuroscience Letters*, 45(2):123–127, 1984.

H.S. Gasser. Contractures of skeletal muscle. *Physiological Reviews*, 10(1):35, 1930.

M. Gaster, P. Staehr, H. Beck-Nielsen, H.D. Schrøder, and A. Handberg. Glut4 is reduced in slow muscle fibers of type 2 diabetic patients. *Diabetes*, 50(6):1324, 2001.

G.F. Gauthier and R.A. Dunn. Ultrastructural and cytochemical features of mammalian skeletal muscle fibres following denervation. *Journal of Cell Science*, 12(2):525, 1973.

E. Gutmann and L. Guttmann. The effect of galvanic exercise on denervated and re-innervated muscles in the rabbit. *Journal of Neurology and Psychiatry*, 7(1-2):7, 1944.

H. Hartzell and D.M. Fambrough. Acetylcholine receptors. *The Journal of General Physiology*, 60 (3):248, 1972. ISSN 0022-1295.

A. Hess and G. Pilar. Slow fibres in the extraocular muscles of the cat. *The Journal of Physiology*, 169(4):780, 1963.

N.E. Huang, Z. Shen, S.R. Long, M.C. Wu, H.H. Shih, Q. Zheng, N.C. Yen, C.C. Tung, and H.H. Liu. The empirical mode decomposition and the Hilbert spectrum for nonlinear and non-stationary time series analysis. *Proceedings of the Royal Society of London. Series A: Mathematical, Physical and Engineering Sciences*, 454(1971):903, 1998. ISSN 1364-5021.

C.C. Hunt and S.W. Kuffler. Motor innervation of skeletal muscle: multiple innervation of individual muscle fibres and motor unit function. *The Journal of Physiology*, 126(2):293, 1954. ISSN 0022-3751.

J.P.K. Hyatt, R.R. Roy, K.M. Baldwin, A. Wernig, and V.R. Edgerton. Activity-unrelated neural control of myogenic factors in a slow muscle. *Muscle & Nerve*, 33(1):49–60, 2006.

E.A. Jeckel-Neto, Y. Ito, T. Sato, and H. Tauchi. Quantitative immunohistochemistry of parvalbumin expression in the rat diaphragm. *Analytical and quantitative cytology and histology/the International Academy of Cytology [and] American Society of Cytology*, 15(3):201, 1993.

B. Katz. *Nerve, muscle, and synapse*. New Biology Series. McGraw-Hill, 1966.

B. Katz and R. Miledi. The development of acetylcholine sensitivity in nerve-free segments of skeletal muscle. *The Journal of Physiology*, 170(2):389, 1964a.

B. Katz and R. Miledi. Further observations on the distribution of acetylcholine-reactive sites in skeletal muscle. *The Journal of Physiology*, 170(2):379, 1964b.

B. Katz and S. Thesleff. A study of the 'desensitization' produced by acetylcholine at the motor end-plate. *The Journal of Physiology*, 138(1):63, 1957.

M.S.Z. Kellermayer, S.B. Smith, H.L. Granzier, and C. Bustamante. Folding-unfolding transitions in single titin molecules characterized with laser tweezers. *Science*, 276(5315):1112, 1997.

H. Kern, C. Hofer, M. Strohhofer, W. Mayr, W. Richter, H. Stohr, et al. Standing up with denervated muscles in humans using functional electrical stimulation. *Artificial Organs*, 23:447–452, 1999.

H. Kern, C. Hofer, M. Modlin, C. Forstner, D. Raschka-Hogler, W. Mayr, and H. Stohr. Denervated muscles in humans: limitations and problems of currently used functional electrical stimulation training protocols. *Artificial organs*, 26(3):216–218, 2002. ISSN 1525-1594.

W. Kilarski and M. Sjostrom. Systematic distribution of muscle fibre types in the rat and rabbit diaphragm: a morphometric and ultrastructural analysis. *Journal of Anatomy*, 168:13, 1990.

J.N. Langley and T. Kato. The physiological action of physostigmine and its action on denervated skeletal muscle. *The Journal of Physiology*, 49(5):410, 1915.

T.A. Levitt-Gilmour and M.M. Salpeter. Gradient of extrajunctional acetylcholine receptors early after denervation of mammalian muscle. *The Journal of Neuroscience*, 6(6):1606, 1986.

R.L Lieber. *Skeletal muscle structure and function - implications for rehabilitation and sports medicine*. Williams and Wilkins, 1992.

O. Loewi. Uber humorale ubertragbarkeit der herznervenwirkung. *Pflugers Archiv European Journal of Physiology*, 189(1):239–242, 1921.

T. Lømo and J. Rosenthal. Control of ach sensitivity by muscle activity in the rat. *The Journal of Physiology*, 221(2):493, 1972.

S.R. Long, R.J. Lai, N.E. Huang, and G.R. Spedding. Blocking and trapping of waves in an inhomogeneous flow. *Dynamics of Atmospheres and Oceans*, 20(1-2):79–106, 1993.

E. Marder and D. Paupardin-Tritsch. The pharmacological profile of the acetylcholine response of a crustacean muscle. *The Journal of Experimental Biology*, 88:147–159, 1980.

P.T. Martin, R. Xu, L.R. Rodino-Klapac, E. Oglesbay, M. Camboni, C.L. Montgomery, K. Shontz, L.G. Chicoine, K.R. Clark, Z. Sahenk, et al. Overexpression of galgt2 in skeletal muscle prevents injury resulting from eccentric contractions in both mdx and wild-type mice. *American Journal of Physiology-Cell Physiology*, 296(3):C476, 2009.

J. Mendez and A. Keys. Density and composition of mammalian muscle. *Metabolism*, 9(2):184, 1960.

M.O. Mendez, J. Corthout, S.V. Huffel, M. Matteucci, T. Penzel, S. Cerutti, and A.M. Bianchi. Automatic screening of obstructive sleep apnea from the ECG based on empirical mode decomposition and wavelet analysis. *Physiological Measurement*, 31:273, 2010.

P.A. Merton, H.B. Morton, D.K. Hill, and C.D. Marsden. Scope of a technique for electrical stimulation of human brain, spinal cord, and muscle. *The Lancet*, 320(8298):597–600, 1982. ISSN 0140-6736.

M. Midrio. The denervated muscle: facts and hypotheses. A historical review. *European Journal of Applied Physiology*, 98(1):1–21, 2006. ISSN 1439-6319.

R. Miledi. The acetylcholine sensitivity of frog muscle fibres after complete or partial denervation. *The Journal of Physiology*, 151(1):1, 1960a. ISSN 0022-3751.

R. Miledi. Junctional and extra-junctional acetylcholine receptors in skeletal muscle fibres. *The Journal of Physiology*, 151(1):24, 1960b. ISSN 0022-3751.

J.G. Nicholls. *From Neuron to Brain*. Sinauer Associates, 2001. ISBN 9780878934393.

N. Ørtenblad and D.G. Stephenson. A novel signalling pathway originating in mitochondria modulates rat skeletal muscle membrane excitability. *The Journal of Physiology*, 548(1):139, 2003.

M.F. Patterson, G.M.M. Stephenson, and D.G. Stephenson. Denervation produces different single fiber phenotypes in fast-and slow-twitch hindlimb muscles of the rat. *American Journal of Physiology-Cell Physiology*, 291(3):518, 2006.

Z.K. Peng, P.W. Tse, and F.L. Chu. An improved hilbert-huang transform and its application in vibration signal analysis. *Journal of Sound and Vibration*, 286(1-2):187–205, 2005.

T. Ploug, H. Galbo, and E.A. Richter. Increased muscle glucose uptake during contractions: no need for insulin. *American Journal of Physiology-Endocrinology And Metabolism*, 247(6):E726, 1984.

D. Prodanov, M.A. Thil, E. Marani, J. Delbeke, and J. Holsheimer. Three-dimensional topography of the motor endplates of the rat gastrocnemius muscle. *Muscle & Nerve*, 32(3):292–302, 2005.

J.P. Quilliam. The action of hypnotic drugs on frog skeletal muscle. *British Journal of Pharmacology and Chemotherapy*, 10(2):133, 1955.

A. Robinson, N. Tufft, and D.M. Lewis. A comparison of fibrillation in denervated skeletal muscle of the anaesthetized rat and guinea-pig. *Journal of Muscle Research and Cell Motility*, 12(3): 271–280, 1991.

J. Rosenthal. Trophic interactions of neurons. *Comprehensive Physiology*, 1977.

J.I. Salisbury and Y. Sun. Assessment of chaotic parameters in nonstationary electrocardiograms by use of empirical mode decomposition. *Annals of Biomedical Engineering*, 32(10):1348–1354, 2004. ISSN 0090-6964.

I.S. Sanghvi and C.M. Smith. Characterization of stimulation of mammalian extraocular muscles by cholinomimetics. *Journal of Pharmacology and Experimental Therapeutics*, 167(2):351, 1969. ISSN 0022-3565.

M. Schwartz, W.R. Bennett, and S. Stein. *Communication systems and techniques*. Wiley-IEEE Press, 1995.

R.C. Sharpley and V. Vatchev. Analysis of the intrinsic mode functions. *Constructive Approximation*, 24(1):17–47, 2006.

L.R. Sheffler and J. Chae. Neuromuscular electrical stimulation in neurorehabilitation. *Muscle & Nerve*, 35(5):562–590, 2007. ISSN 1097-4598.

D. Shier, J. Butler, R. Lewis, M. Shier, and R. Terry. Hole's Human Anatomy and Physiology Laboratory Manual. 1996.

T. Shimizu, J.E. Dennis, T. Masaki, and D.A. Fischman. Axial arrangement of the myosin rod in vertebrate thick filaments: immunoelectron microscopy with a monoclonal antibody to light meromyosin. *The Journal of Cell Biology*, 101(3):1115–1123, 1985.

C.M. Sweeney-Reed, A.O. Andrade, and S.J. Nasuto. Empirical mode decomposition of EEG signals for synchronisation analysis. In *IEEE EMBSS UKRI Postgraduate Conference on Biomedical Engineering and Medical Physics, Southampton*, 2004.

P.N. Taylor. The use of electrical stimulation for correction of dropped foot in subjects with upper motor neuron lesions. *Advances in Clinical Neuroscience & Rehabilitation*, 2(1):16–8, 2002.

R.G. Taylor, R.T. Abresch, J.S. Lieberman, W.M. Fowler Jr, and M.M. Portwood. Effect of pentobarbital on contractility of mouse skeletal muscle. *Experimental Neurology*, 83(2):254–263, 1984.

R.J. Tomanek and D.D. Lund. Degeneration of different types of skeletal muscle fibres. i. denervation. *Journal of Anatomy*, 116(Pt 3):395, 1973.

N. ur Rehman and D.P. Mandic. Empirical mode decomposition for trivariate signals. *IEEE Transactions on signal processing*, 58(3):1059–1068, 2010.

K. Wang, J. McClure, and A. Tu. Titin: major myofibrillar components of striated muscle. *Proceedings of the National Academy of Sciences*, 76(8):3698, 1979.

J.E. Watson, T. Gordon, R. Jones, and M.E. Smith. The effect of muscle extracts on the contracture response of skeletal muscle to acetylcholine. *Pflugers Archiv European Journal of Physiology*, 363 (2):161–166, 1976.

A Ethics Proposal, Approval and Reports

This Appendix comprises all correspondence with the AEC, including proposal submissions, protocol amendments, protocol approvals and reports.

A.1 Ethics proposal application

UNIVERSITY OF CAPE TOWN

Faculty of Health Sciences
Department of Human Biology

Anzio Road
Observatory 7925
South Africa
Tel: +27 21 406 6235
Fax: +27 21 448 7226

9 March 2010

University of Cape Town
Animal Ethics Committee

Re: Changes to HSFAEC proposal 010/002 entitled "Response of denervated muscle to electrical and chemical stimulation"

Dear Committee

Please find an attached list of the changes that were made to our proposed research study, based on its initial review.

Many thanks for the useful feedback.

Kind regards

Nicholas A Sachs, PhD
Lecturer
Department of Human Biology
University of Cape Town
e-mail: nicholas.sachs@uct.ac.za

Page number	Section	Change
1	1	Title changed to contain name of rat species to be used in the study
2	7	Asterix (*) included to indicate relevant people who are going to complete the AEC accreditation course in April 2010
4	12	Total number of animals changed to 35
4	13	Third paragraph changed to begin "Ethically and legally this research cannot..."
4	14	A pilot study was introduced and the number of animals per group reduced.
5	16	10mg/kg of meloxicam to be administered every 24 hours for 3 days instead of the original 0.04mg/kg buprenorphine every 12 hours for 2 days
5	16	paragraph 3 changed to start with "Using aseptic technique a 2cm skin incision..."
5	16	under post op care, use of antibiotic changed to intramuscular administration of antibiotic
5	16	paragraph 5: once the wound has healed the animals reflexes will be tested
5	16	paragraph 5: 200 mg/kg of sodium pentobarbital instead of 250mg/kg
7	21.2	caging conditions specified for pre and post-op conditions, dependent on pilot study indications of communal housing and on observation for signs of distress
7	21.3	0.04mg/kg buprenorphine changed to 10mg/kg meloxicam
7	21.5	additional monitoring criteria added
7	21.6	conditions for immediate euthanasia added
8	22	added monitoring critera: animals will be weighed every three days
9	26	10 mg/kg meloxicam replaces buprenorphine every 24 hours for 3 days
9	26	200mg/kg sodium pentobarbital instead of 250mg/kg
9	26	added antibiotic lentrax
14	animal monitoring sheet	animals to be weighed every 3 days
		Discomfort and stress criteria further modified
		Distress criteria further modified

FHS003: Animal Research Ethics Committee - Application Form

Faculty of Health Sciences - University of Cape Town

This application must be typed and 19 completed copies submitted to:	For office use only
The Administrative Officer Pre-Award Unit Research Ethics Office Faculty of Health Sciences E52-24 Old Main Building Groote Schuur Hospital **Phone: (021) 406 6338** **Email:** Lamees.emjedi@uct.ac.za	Application No. Date received Date approved

Category (select one)

This is a first submission	☒		
This is a resubmission	☐	Previous application number	

1. TITLE OF APPLICATION	Response of denervated muscle in Long Evans rats to electrical and chemical stimulation.
2. DETAILS OF APPLICANT	Dr
a. Title (e.g. Professor, Dr, Mr):	
b. Surname:	Sachs
c. Forenames:	Nicholas Alexander
d. Qualifications (e.g. PhD):	PhD
e. Position or appointment:	Lecturer
3. CONTACT DETAILS	UCT Faculty of Health Sciences, Anatomy Building, Room 7.17
a. Address for correspondence:	
b. Telephone number, extension:	021 404 7613 (ext. 7613)
c. Fax number:	021 448 7226
d. E-mail address:	Nicholas.Sachs@uct.ac.za

4. DEPARTMENTAL RESEARCH COMMITTEE REVIEW

I declare that this research protocol has been **peer-reviewed** by the Research Committee of the Department of ..... and has been judged to be relevant, **necessitates the use of animals to achieve its aims,** designed in accordance with accepted scientific practices and norms and is in the opinion of the reviewers to be likely to be successful in achieving its objective's.

Signature		Print name		Date	

5. DURATION OF APPLICATION

Period for which the application is required (must not exceed three years)	Years	1	Months	0
Start date	March 2010	End date	March 2011	

6. PURPOSE (select category)

Research	X	Teaching/training		Other (specify)	

7. RESEARCH PARTICIPANTS

Include all staff involved (principal investigator, associate and assistant research staff) Clearly indicate who will perform any procedures/treatments on, and who will monitor/care for the animals. **Note:** Those individuals employed to perform the work of laboratory animal technologists must be registered or authorised by the SA Veterinary Council to perform these duties.

It is imperative that you indicate which staff will be available for after hours emergencies.

Name Position & Dept. Signature	Contact details	Duties/Procedures to be performed on the animals List Appropriate protocol numbers	Appropriate training and experience in such procedures/duties	Registration with /authorisation from *SAVC, HPCSA or NSCSA*	UCT AEC accredited Yes/No
Prof Graham Louw, Human Biology	Anatomy Bldg. 4.05 ext. 6302	**Legally responsible for prescribing and directing the administration of the controlled Schedule 3-6 medicinal substances**	Veterinarian	SAVC 76/1324	No
Simon Dingalibaba, Human Biology	Anatomy Bldg. 1.01 ext. 6277	Feeding and monitoring of animals daily and **over the weekend**	UCT trained	N/A	Yes
*Dr. Nicholas Sachs, Lect. Human Biology	Anatomy Bldg. 7.17 ext. 7613 0725796900	Will perform animal surgeries and drug administration as well as supervise muscle stimulation experiments and provide surgical training. Available after hours.	4 years experience with small animal surgery, including PhD and postdoc training	N/A	No
Dr. Lester John, Lect. Human Biology	Anatomy Bldg. 7.05 ext. 6548	Will consult on and assist with muscle stimulation procedures.	7 years experience in bioinstrumentation and neural/muscular interfacing	N/A	No
A/Prof Laurie Kellaway, HOD Human Biology	Anatomy Bldg. 5.14 ext. 6271	Will consult on and assist with animal surgery and muscle stimulation procedures.	>25 years experience with small animal surgery and muscle physiology studies	N/A	No
*Ghabiba Modak, MSc Student Human Biology	Anatomy Bldg. 7.07 0732810926	Will perform muscle stimulation experiments (chemical) and receive supervised training in animal surgery.	BS in Mech. Eng. Current MSc (Med) Biomedical Eng. Student	N/A	No
*Nielen Ventner, MSc Student Human Biology	Anatomy Bldg. 7.12 0835567889	Will perform muscle stimulation experiments (electrical) and receive supervised training in animal surgery.	BS in Mechatronics Current MSc (Med) Biomedical Eng. Student	N/A	No

* the AEC accreditation course will be completed by the respective participants

8. STUDY INFORMATION: Background

Provide a brief introductory statement **in non-technical terms** that explains what problems, questions, needs, observations, or new ideas have led to the planning of this experiment. (**Note**: Must be understandable to those outside of the field)

Certain types of injuries and diseases (such as spinal cord injury, stroke, and multiple sclerosis) result in damage to the nervous system. If such damage affects motor neurons, which synapse with muscles and signal them to contract, it will often lead to paralysis. Depending on the type of injury, the motor neuron itself may still be alive and functional, but just disconnected from the brain. In such cases, the use of applied electrical currents (similar to those provided by a pacemaker), has allowed researchers and clinicians to artificially stimulate these nerves and cause the muscles they innervate to contract. This has been an effective means of restoring simple movement and primitive function to paralyzed muscle and has been an active area of research for the past 50 years.

A more complicated problem occurs when the motor neurons actually die, as is the case in peripheral nerve injuries. When this happens, the muscle fibers they had synapsed with become denervated. Denervated muscle fibers can be directly stimulated by electrical currents, in much the same way as motor neurons can be, however it is much more difficult. The difference is that a single nerve synapses with a very large number of muscle fibers, so stimulating a single small nerve can generate a large contraction, whereas each denervated muscle fiber must be activated by the injected electrical currents directly. Because the muscle itself occupies such a large volume compared to the nerve that innervates it, much more current is required to activate the entire denervated muscle than to simply activate the nerve that used to innervate that muscle. Injecting large amounts of current will often cause unwanted side effects, most notably the activation of pain fibers in the surrounding area that may still be connected to the brain. Thus, while technically possible, electrically reactivating denervated muscles in most cases turns out to be impractical.

It has been anecdotally reported that it takes less electrical current to directly activate a denervated muscle fiber than to directly activate an innervated muscle fiber (not via its motor neuron). If this is indeed true, it means that something has happened to the fiber's membrane as a result of denervation that has sensitized it to electrical currents. A thorough understanding of the mechanism of this sensitization would increase our understanding of muscle denervation and could potentially be exploited to improve electrical methods of reactivating denervated muscle fibers. Otherwise it is clear that pursuing alternative (such as chemical) methods of stimulating denervated muscle fibers is warranted. Once muscle fibers have been denervated, changes to the membranes occur which distinguish them from the membranes of innervated muscle fibers. The topography of the receptors which aid neurotransmitter function changes and lack of stimulation results in muscle atrophy. It takes time for the changes which draw the distinction between innervated and denervated muscle fibers to occur. Investigations involving denervation generally allow for a period of 1 to 2 weeks for these changes to take place.

The normal method of communication between the motor neuron and the muscle is via neurotransmitter, specifically acetylcholine (ACh). An alternative method of activating denervated muscle could be to artificially administer ACh directly to the muscle fiber's membrane, activating the ACh receptors and causing contraction in much the same way an incoming signal from the motor neuron would. If this is effective, recent advances in technology (particularly in the field of microfluidics) could potentially enable a prosthetic device to be developed that would chemically stimulate denervated muscle fibers for specific applications where electrical stimulation may not be viable (such as reactivating the muscles in the eyelids to enable eyelid closure following facial paralysis). Not nearly enough is currently known about the interaction between denervated muscle fibers and extracellular ACh to design such a device, let alone confirm its feasibility, however. An investigation of the dynamics of muscle contraction due to controlled amounts of extracellularly delivered ACh is a logical first step along this path.

9. AIMS OF THE STUDY

Please be brief and succinct.

The aims of this study are

- to confirm the anecdotally reported electrical sensitization of denervated muscle fibers through controlled experiments
- to investigate possible mechanisms of electrical sensitization of denervated muscle fibers
- to examine the dynamics of muscle contraction elicited by administration of extracellular ACh, particularly in denervated muscle
- to investigate means of controlling muscle relaxation after extracellular ACh elicited contraction
- to histologically examine the effects of artificially administered ACh on denervated muscle.

10. HYPOTHESIS

If a hypothesis is being tested (explanatory research) please state what it is.

The following hypotheses are being tested:

- Denervation causes muscle fibers to become sensitized to electrical stimulation.
- Extracellularly injected ACh is an effective means of eliciting artificial contraction of denervated muscle.

11. POTENTIAL BENEFITS OF THE RESEARCH FINDINGS

These are required to aid the reviewing committee in performing a harms/benefit assessment of the research/teaching proposal.

This research would increase our understanding of denervated muscle physiology and could be a major first step toward the development of a prosthetic device that could restore muscle function in patients that have experienced paralysis due to muscle denervation.

12. ANIMALS REQUIRED

Species/ Strain	Sex	Age/Mass	Total numbers	Source
Rat/ Long Evans	Both	6 months/ 300-450g	35	UCT Animal Research Facility

13. FOCUS ON REPLACEMENT: JUSTIFICATION FOR THE USE OF SENTIENT ANIMALS

Please provide justification for the use of animals rather than an in-vitro model. Which alternatives to the use of animals have you considered? Also provide justification for the need to use the specified species.

This study requires the use of muscle fibers, which cannot be artificially generated. The physiological changes that occur as a result of denervation require a natural biological environment to develop, and are not well enough understood to be adequately modelled.

Finite element modelling of the electrical properties of muscle fiber membranes both before and after denervation has been considered to address the electrical sensitivity issue, however the sensitization of denervated fibers contradicts what would naturally be expected based on gross morphological changes consistent with muscle atrophy. Therefore, empirical evidence is needed to validate results of newly developed models that might account for more subtle changes to the membrane properties.

Ethically and legally this research cannot be performed on humans, as it requires the denervation of muscle and the harvesting of tissue.

Rats are the most common model for muscle denervation studies and are used widely in the literature. The, triceps surae muscles (soleus and gastrocnemius) in particular are common sites of denervation, with an easily accessible nerve supply (sciatic), simple and reliable way of testing for persistent denervation (drop induced toe spread reflex), and limited adverse effects when paralyzed unilaterally (impaired mobility but no other effects on general health).

The use of the Long Evans strain will provide easy differentiation from Wistar rats that are being held in the same facility and used by researchers for other experiments.

14. FOCUS ON REDUCTION AND REFINEMENT

Please provide justification for:

(a) the number of animals required.

An initial pilot study using 5 animals will be conducted to develop the skills involved with the surgical technique and to monitor the behaviour of the animals and identify potential complications in the post-operative period, especially in term of self-mutilation of the denervated limb. This is essential to test the feasibility and productive outcome of the study. Upon success of the pilot study, the main study will involve 3 separate groups of animals, each of which will undergo muscle denervation for a different duration of time (1 week, 4 weeks, 8 weeks). 30 animals will be used in the main study, which provides for 10 animals per group, a sufficient number for statistical comparison. 35 animals will be used in total (including the pilot study).

(b) sex, if a single sex is required.

N/A

15. OVERVIEW OF EXPERIMENTAL DESIGN

In a flow diagram, summarise how the animals will be allocated to experimental and control groups, indicating the schedule for treatment, sampling and endpoint.

See attachment.

16. DETAILS OF EXPERIMENTAL PROCEDURES AND STATEMENT OF COMPETENCE

Provide a detailed description of all procedures, treatments, tissue sampling that the animals will undergo, and the method of euthanasia. Indicate in **7** who will perform each procedure, and their appropriate competence for the tasks.

Briefly outline parameters to be measured/final tissue analysis to be performed in order to achieve the aims of the study.

Denervation Procedure:

Each animal will be placed in a chamber with halothane (4%) to induce anesthesia. Once the animal is unconscious, a mask will be affixed to the animal through which vaporized halothane (1.5%) will be continuously administered for the duration of the procedure in order to maintain anesthesia. 10mg/kg of meloxicam will be administered subcutaneously every 24 hours for three days following an initial dose, which will be administered one hour pre-operatively in order to provide pre-emptive analgesia.

The right hindlimb will be shaved. A sterile drape will be used to isolate the limb. The hindlimb will be sterilized with iodine, applied three times using sterile gauze and a hemostat from the center of the surgical site outward. Body temperature will be maintained using a temperature controlled base plate.

Using aseptic technique a 2-cm skin incision will be made along the hindlimb, moving distally from the hip. The sciatic nerve will be identified visually and through the use of an electrical stimulator / nerve locator. A 1-cm section of the sciatic nerve will be removed above the knee. The remaining nerve stump will be ligated and fixed to the quadriceps muscles using 6-0 silk suture. Complete denervation of the lower hindlimb will be confirmed using electrical stimulation. The skin will be sutured closed in a single layer using 4-0 silk sutures.

Postoperative Care:

The animal will be monitored until it wakes from anesthesia, at which time it will be returned to the animal facility and kept in isolation until the surgical wound has healed. Meloxicam (10mg/kg) will be administered every 24 hours for 3 days in order to maintain analgesia. Animal monitoring sheets (as shown on page 13) will be filled in daily for the remainder of the experiment. Antibiotic administration will include a once-off intramuscular injection of 0.1ml/kg of Lentrax containing procaine penicillin (150mg/ml) and benzathine penicillin (112.5mg/ml) which is effective for a five day interval. After the wound has healed, each animal will be held in the air and lowered at a rapid rate to test for the existence of the toe spread reflex (lack of the toe spread reflex on the previously denervated side will confirm paralysis).

Muscle Fiber Harvesting / Euthanasia:

At the end of the animal's group-dependent denervation period (1 week, 4 weeks, or 8 weeks post surgery), the reflex test will be repeated to confirm paralysis. The animal will then be placed in a chamber with halothane (4%) to induce anesthesia. Once the animal is unconscious, a mask will be affixed to the animal

through which vaporized halothane (1.5%) will be continuously administered for the duration of the procedure in order to maintain anesthesia. A skin incision will be made along the length of the hindlimb to expose the underlying muscles. An electrical stimulator / nerve locator will be used to confirm denervation of the triceps surae (soleus and gastrocnemius) muscles on the previously operated side. While under anesthesia, a lethal intraperitoneal dose of sodium pentobarbital (200mg/kg) will be administered to euthanize the animal. The lower hindlimb will be detached on both sides and the soleus and gastrocnemius muscles will be harvested for further study.

17. END-POINT FOR EXPERIMENTS THAT, BY NECESSITY OR UNAVOIDABLY, INDUCE ILLNESS/DISTRESS/DEATH

If the experimental procedures/treatments will inevitably cause, illness, loss of weight, and/or increasing pain or distress to the animals, clearly indicate at what endpoint the objectives of the study will be reached, and provide adequate justification for this endpoint. If death is the endpoint, provide additional justification for this requirement.

The denervation procedure will cause discomfort to the animal due to impaired movement. Anaesthesia will be administered during the surgery and analgesia will be administered pre- and post-operatively to avoid the animal from experiencing any pain. Some weight loss is expected but will be monitored – a 20% weight loss is considered significant and will result in euthanasia. For details on distress factors resulting in euthanasia, please refer to section 21.6. Further than the distress factors, there are 3 explicit endpoints to the study at 1 week, 4 weeks and 8 weeks post-denervation, at which times the animals will be euthanized depending on their respective groups. It would be inhumane to keep the animals alive when their movement is impaired by a paralyzed limb.

18. STATISTICAL ANALYSIS

Describe briefly how data obtained from this study will be analysed statistically, and by whom.

Rheobase values will be recorded and chronaxie values will be calculated for all electrical stimulation experiments. These will be compared among groups using a t-test and ANOVA by Nielen Ventner.

Onset times and maximum force outputs of muscle contraction for varied concentrations of ACh delivery will be recorded and compared among groups using a t-test and ANOVA by Ghabiba Modak.

The healthy contralateral muscle will be used as a control for all experiments.

19. RECEPTION

Is this study a repetition of previous work performed by yourself or others?
If yes, explain why it is being repeated.

If no, is it part of ongoing research being conducted by your group.

No, this study is not a repeat of previous work. It is the first study in a developing research direction for our group, but is informed by previous work that has been done on electrical stimulation of denervated muscle (specifically in the rabbit eyelid).

20. PUBLICATIONS

Highlight any publications stemming from your research involving the use of animals thus far.

N. A. Sachs, E. L. Chang, N. Vyas, B. N. Sorensen, and J. D. Weiland, "Electrical stimulation of the paralyzed orbicularis oculi in rabbit," IEEE Trans. Neur. Sys. Rehab. Eng., vol. 15, pp. 67-75, 2007.

N. A. Sachs, E. L. Chang, V. Pradeep and J. D. Weiland, "Restoration of blink symmetry following unilateral facial paralysis," in Proc. 12th Ann. Conf. IFESS, Philadelphia, PA, Nov. 10-14, 2007.

N. A. Sachs, E. L. Chang, and J. D. Weiland, "Contralateral EMG-triggered electrical stimulation of the

eyelid," in Proc. 11th Ann. Conf. IFESS, Miyagi-Zao, Japan, Sept. 12-15, 2006.

N. A. Sachs, E. L. Chang, and J. D. Weiland, "Kinematics of electrically elicited eyelid movement," in Proc. 28th Ann. Intl. Conf. IEEE-EMBS, New York, NY, Aug. 30-Sept. 3, 2006.

N. A. Sachs, E. L. Chang, N. Vyas, and J. D. Weiland, "Electrical stimulation of the paralyzed orbicularis oculi," in Proc. 10th Ann. Conf. IFESS, Montreal, Canada, July 5-10, 2005.

21. ANIMAL CARE AND HOUSING

21.1 Location
Where will the animals be housed (specify pre- and post-treatment if different)?
Where will the experiments be performed?

(For both of the above, if not at the Animal Unit, explain why not)

Animals will be housed in the Department of Human Biology's Animal Satellite Facility.

Experiments will be performed in the Anatomy Building on the UCT Faculty of Health Sciences, room 4.13.

21.2 Caging and social requirements

Describe how the animals will be caged and what provisions have been made for their physical and psychological well-being i.e. comfort, socialisation, behavioural needs and enrichment of their cage environment.

Animals will be housed in plastic cages with wire grids and a built in food hopper. Food and water will be provided *ad lib*. Wood shavings will be used as bedding material. The animals will be housed in groups of three per cage. This requires 10 cages and allows for them to maintain their social environment.

Animals will be isolated during the recovery period following surgery in order to ensure proper wound healing and to avoid cannibalism from other rats before being returned to standard caging conditions. If however, the pilot study indicates that it would be more feasible to keep the animals in isolation to prevent inflicting harm on one another then they will be kept in isolation for the remainder of the study until euthanized.

21.3 Measures to be taken to minimise pain/distress caused by the experimental procedures

What negative effects will the experimental procedures/treatments have on study animal well-being (e.g. fear, deprivation, pain and distress). Give details of preventative measures taken pre-, intra- and post-procedure/treatment, as well as during transportation and restraint of the animals, that may minimize these effects. Indicate in **7** who will implement these measures, and their appropriate competence for the tasks.

A single dose of pre-emptive analgesia will be provided via intramuscular injection of 10mg/kg of meloxicam 1 hour prior to surgery.

21.4 Expected/unavoidable effects of the procedures on animal well-being

Describe how the experimental procedures may unavoidably impact on the animals' welfare, irrespective of the measures taken as indicated in **21.3** (e.g. paralysis due to nerve transection; post-op social deprivation of animals if justified).

Animals will undergo unilateral nerve transection, resulting in paralysis of the right hindlimb. This is an unavoidable result corresponding to the muscle denervation that is the focus of this study.

21.5. Potential adverse effects of the experimental procedures

State what specific signs (physical and behavioural e.g. not eating) will be monitored for as an indication of unexpected but potential adverse events (e.g. septicaemia) caused by the procedure/treatment.

The condition of the surgical wound will be monitored as an indication of localized infection following surgery. Additionally, animals will be monitored for lethargy, hyperactivity, isolation from the social group (after the wound has healed), signs of self-mutilation when in isolation, limb injury due to movement restriction induced by paralysis and weight loss (animals will be weighed every three days) as indications of poor health and/or distress (see Animal Monitoring Sheet on page 13). Further observation of communal interaction will be made when the rats are placed back in groups of 3 again after wound healing. Cannibalism from other rats in communal cages will result in animal separation or, if severe, in euthanasia.

21.6 Euthanasia

Under what conditions will euthanasia be performed prior to the determined experimental end-point defined in **16** above?

Animals will be euthanized if they are observed to be in distress (see Animal Monitoring Sheet on page 13). A 20% weight loss will serve as the limit which, if reached, will result in the respective animal being euthanized. Severe self-mutilation or mutilation by cannibalism will be an indication for immediate euthanasia.

22. DISTRESS AND DISCOMFORT SEVERITY (Please tick where appropriate)

Category A	Experiments involving non-living materials, plants, bacteria, or non-sentient species of animals.	
Category B **(mild)**	Experiments on sentient animal species expected to produce little or no discomfort, e.g. blood sampling, injections, or procedures on anaesthetised animals that do not regain consciousness.	
Category C **(moderate)**	Experiments that involve some discomfort to sentient animals, e.g. surgical procedure under anaesthesia and some postoperative discomfort.	
Category D **(severe)**	Experiments that involve significant but unavoidable distress or discomfort to sentient animals.	X

23. ANIMAL MONITORING AND STATEMENT OF ANIMAL CARE COMPETENCE

How often will the animal subjects in this study be monitored (pre-, intra- and post-procedure/treatment) to ensure their comfort, health and humane treatment? Indicate in **7** who will do this for each stage, and their appropriate competence for the task.

NOTE: Alleviation of pain: POSTOPERATIVE CARE MONITORING

As a manifestation of pain in animals is not always easily recognised the internationally accepted principle is that any procedure which is liable to cause pain in humans will cause at least a similar level of pain in animals. A reasoned scientific justification for the decision to withhold the use of anaesthetics and analgesics will be required, if any invasive procedure is to be performed.

Animals will be monitored daily and weighed every 3 days. Frequency of monitoring may be increased to twice daily at any time in cases of animal discomfort or stress. Animal monitoring sheets will be completed (see page 13).

24. FATE OF THE ANIMALS AND METHOD OF DISPOSAL

Will the animals be killed at the end of the experiment? If so, please explain why, if it is not obvious from the experimental design.

Animals will be euthanized immediately prior to muscle fiber harvesting. This is necessary because they will be paralyzed during the surgical procedures and muscles from both hindlimbs will be harvested for analysis. It would be inhumane to keep them alive following such procedures.

25. METHOD OF KILLING (Please tick category, and give details in *16*)

Inhalation (specify agent and system used in **26** below)		Exsanguination under anaesthesia (specify who will ensure death in **16** above)	
Fatal dose of anaesthetic agent (specify agent and dose in **26** below)	X	Lethal injection whilst under anaesthesia (specify agent and dose in **26** below)	
Other (specify here and in **26** as required, and justify in **16** above)			

26: DRUGS AND SUBSTANCES TO BE ADMINISTERED

List **all substances** administered to the animals. Indicate the route of administration and dosage per body mass for each substance. Include anaesthetics, analgesics and killing agents.

Note: It is imperative that you state in **7** above who is legally authorised to prescribe, and direct the administration of Schedule 3-6 medicinal substances.

Item	Route/Site	Dose	Frequency	Name and Signature of person administering the substance
Halothane	**Inhalation**	**4.0%**	**To induce anesthesia**	**Nicholas Sachs**
Halothane	**Inhalation**	**1.5%**	**Throughout surgery in order to maintain anesthesia**	**Nicholas Sachs**
Meloxicam	**Subcutaneous**	**10mg/kg**	**Once one hour prior to surgery, every 24 hours for 3 days following the first administration (4 total doses)**	**Nicholas Sachs**
Sodium pentobarbital	**Intraperitoneal**	**200mg/kg**	**Once for euthanasia**	**Nicholas Sachs**
Lentrax Antiobiotic: procaine penicillin (150mg/ml) Benzathine penicillin (112.5mg/ml)	**Intramuscular**	**0.1ml/kg**	**Once post-operatively**	**Nicholas Sachs**

Person taking legal responsibility for the schedule 3-6 drugs listed above:

Name	**Dr. Graham Louw**		
Signature		Date	

27. BIOHAZARD STATEMENT

Is this a requirement for this project? If yes, please append proof of approval

No

28. REFERENCES

Give a brief list of references to support the information in 8, 13 and 14.

Note: Provide references/sources to support the manner in which you will perform the procedures, treatments and monitoring of the study animals.

28. REFERENCES

Give a brief list of references to support the information in 8, 13 and 14.

Note: Provide references/sources to support the manner in which you will perform the procedures, treatments and monitoring of the study animals.

A. Feltz and A. Mallart, "An analysis of Acetylcholine responses of junctional and extrajunctional receptors of frog muscle fibres," J. Physiol. vol. 218, pp. 85-100, 1971.

D.B. Drachman, E.F. Stanley, A. Pestronk, J.W. Griffin and D.L. Price, "Neurotrophic regulation of two properties of skeletal muscle by impulse-dependent and spontaneous Acetylcholine transmission," The Journal of Neuroscience, vol. 2, no. 2, pp. 232-243, 1982.

G. Bezakova, I. Rabben, I. Sefland, G. Fumagalli and T. Lømo, "Neural agrin controls Acetylcholine receptor stability in skeletal muscle fibres," Neurobiology, vol. 98, no.17, pp. 9924-9929, 2001.

H.C Hartzell and D.M. Fambrough, "Acetylcholine receptors – Distribution and extrajunctional density in rat diaphragm after denervation correlated with acetylcholine sensitivity," The Journal of General Physiology, vol.60, pp. 248-262, 1972.

J.C. Jay and K.F. Barald, "Denervated single myofibers: neurite interactions and synaptic molecules," Muscle and Nerve, vol. 12, pp. 981-992, 1989.

J.H. Steinbach, J. Merlie, S. Heinemann and R. Bloch, "Degradation of junctional and extrajunctional Acetylcholine receptors by developing rat skeletal muscle," Neurobiology, vol. 76, no.7, pp. 3547-3551, 1979.

J.J. McArdle and E.X. Albuquerque, "A study of the reinnervation of fast and slow mammalian muscles," Journal of General Physiology, vol.61, pp. 1-23, 1973.

J.M. Nooney, J.A. Peters and J.J. Lambert, "A patch clamp study of the nicotinic acetylcholine receptor of bovine adrenomedullary chromaffin cells in culture," Journal of Physiology, vol.455, pp. 503-527, 1992.

L.L. Rubin, "Increases in muscle Ca2+ mediate changes in acetylcholinesterase and acetylcholine receptors caused by muscle contraction," Neurobiology, vol. 82, pp. 7121-7125, 1985.

R. Miledi and C.R. Slater, "Electrophysiology and electron-microscopy of rat neuromuscular junctions after nerve degeneration," Proceedings of the Royal Society of London. Series B, Biological Sciences, vol. 169, No. 1016, pp. 289-306, 1968.

S. Rotzler and H.R. Brenner, "Metabolic stabilisation of acetylcholine receptors in vertebrate neuromuscular junction by muscle activity," The Journal of Cell Biology, vol. 111, pp. 655-661, 1990.

T.A. Levitt-Gilmour and M.M. Salpeter, "Gradient of extrajunctional acetylcholine receptors early after denervation of mammalian muscle," The Journal of Neuroscience, vol. 6, no. 6, pp. 1606-1612, 1986.

T. Lømo and C.T. Slater, "Control of Acetylcholine sensitivity and synapse formation by muscle activity," J. Physiol., vol.275, pp. 391-402, 1978.

T. Lømo and R.H Westgaard, "Further studies on the control of ACh sensitivity by muscle activity in the rat," J. Physiol., vol. 252, pp. 603-626, 1975.

V. Witzemann, H.R. Brenner and B. Sakmann, "Neural factors regulate AChR subunit mRNAs at rat muscular synapses," The Journal of Cell Biology, vol. 114, pp. 125-141, 1991.

PRINCIPLES

Animal Welfare

Ethical review of proposed experiments on sentient animals is necessary because such animals have moral standing. Accordingly, there are restrictions on how such animals may be treated. Although there is disagreement on whether animals may be used *at all* in experiments that cause deprivation, fear, discomfort, distress, pain or death, there is now widespread agreement that animals used in scientific experiments:

- May not be used in studies that are methodologically unsound, frivolous, trivial, or which unnecessarily duplicate earlier studies.
- May not be subjected to unnecessary hunger, thirst, disease, parasitism, injury, discomfort, pain fear, or social deprivation.

Therefore, animals held for, and used in, scientific experiments:

- Must be kept comfortable under conditions that are suitable to their species, enabling them to express normal behaviour. These include adequate space, company of conspecifics, and adequate stimulation.
- Must be monitored for ill-health and distress, and, where necessary, enjoy rapid diagnosis and either treatment or other alleviation of their condition.
- Must be handled and treated in ways that either avoid or at least minimize distress, pain and suffering.

The Three 'R's

Proposals for research on sentient animal subjects must satisfy three principles:
Replacement: Sentient animals may not be used if they can be replaced by non-sentient subjects or systems.
Reduction: The number of animals used must be reduced to the minimum that will allow the objectives of the study to be attained.
Refinement: Experimental methodology and procedures should be refined in a way that minimizes the causation of pain, discomfort, fear and social deprivation to the experimental animal.

Responsibility

Everyone using animals, whether for experimentation, testing or provision of tissues or body fluids is responsible in their personal capacity for assuring that they are afforded the highest levels of welfare and protection from abuse.

Responsibilities of the Principal Investigator:

a. To read and comply with the University's "Code of Ethics and Procedures for the Use of Animals in Teaching and Research".
b. To maintain records of all procedures performed on the animals.
c. To ensure that all animals used are clearly identified with the allocated authorisation number by means of labels on cages, pens or rooms.
d. To ensure that all the designated associate and assistant personnel are qualified and competent to perform the allocated procedures and that no other personnel will be allowed to perform any procedures without written authorisation from the Animal Ethics Committee.
e. To ensure that there will be no deviation from any of the procedures as specified in the application without the prior written approval of the Animal Ethics Committee.
f. To ensure that, in the event of a situation arising during the course of the experiment whereby an animal is found to be suffering from severe pain or distress, a veterinarian will be consulted for advice. In the event that the pain or distress cannot be alleviated, the experiment will be terminated, the animal immediately euthanased and the Animal Ethics Committee informed.

DECLARATION

1. I, ..., as **Principal Investigator** in this application hereby declare that I am familiar with the ideas, principles and responsibilities outlined in **Section L** and will ***personally*** undertake to see that these are upheld in the conduct of this study, should it be approved.
2. I understand that I am **legally responsible** for all aspects of the study.
3. In my opinion, all persons named and working under my supervision have the **appropriate training and skills required** to carry out their responsibilities as indicated.
4. I undertake not to deviate from the approved protocol without **first** obtaining approval for such amendments from the UCT Health Sciences Faculty Animal Ethics Committee.
5. I undertake to **report** to the Animal Ethics Committee on the outcome of the study at its conclusion, and to furnish the AEC office with copies of all publications that result from this study
6. Should the study take longer than 1 year, I undertake to submit an **annual progress report** to the AEC. This will be submitted 12 monthly from the month of the initial approval by the Committee.
7. If a **biohazard declaration** is necessary, this has been submitted to the Faculty Bio safety Committee, and proof of their approval of the safety practices stipulated in this application appended.

I have read and accept the declaration.

.....	.....	...../...../.....
Signature of applicant	**Print name**	**Date**

Support from Head of Department

Note: Your attention is drawn to the responsibilities of the Head of Department as specified in the University's "Code of Ethics and Procedures for the Use of Animals in Teaching and Research".

In my opinion, the researcher is competent to perform the experiment and I support this application

.....	.....	...../...../.....
Signature of Head of Department	**Print name**	**Date**

Animal Monitoring Sheet

Name of monitor(s):

Animal Identification	Date		Date		Date		Date		Date		Date		Date		Date		Date		Date		Date	
Weight (at 3 day intervals)																						
	am	pm	am	pm	am	pm	am	pm	am	pm	am	pm	am	pm	am	pm	am	pm	am	pm	am	pm
Behaviour: No Visible Discomfort or Stress																						
Discomfort and Stress Score 1 (mild) or 2 (moderate)																						
Distress																						

ACTION

Discomfort and Stress (*Score 1:* Monitor daily; **Score 2:** Monitor twice daily)

Distress (Kill animal)

No Visible Discomfort or Stress

Criteria: Animals active and inquisitive when disturbed and hair coat clean and groomed)

Discomfort and Stress

Criteria: Hyperactivity and avoidance behaviour; Hypoactivity and depressive behaviour; Physical signs of poor coat grooming, ocular discharge; Isolation of animal from the group; Weight loss; wound inspection for indications of localised injury/infection post-operatively; lethargy; signs of self-mutilation; signs of cannibalism when in communal cages; signs of skin injury/lesions to denervated limb (affected rat will immediately be placed alone in new cage).

Score 1 (mild) or 2 (moderate)

Distress

Criteria: Severe limb injury/self-mutilation; animals unresponsive to being disturbed or to touch; animals unconscious; animals judged to be moribund and dying; 20% body weight loss

A.2 Ethics addenda

UNIVERSITY OF CAPE TOWN

Faculty of Health Sciences
Department of Human Biology

Anzio Road
Observatory 7925
South Africa
Tel: +27 21 406 6235
Fax: +27 21 448 7226

16 August 2010

University of Cape Town
Animal Ethics Committee

Re: Changes to HSFAEC proposal 010/002 entitled "Response of denervated muscle to electrical and chemical stimulation"

Dear Committee

Unfortunately, the group of animals that we have used (originally allocated as five rats) was inadequate to refine our data collection procedures. One of these rats died during surgery and of the four remaining, only one gave useful data. In order to properly develop our data collection procedure we will require the use of more rats. We will begin by drawing these from the remaining allocation for the study, but in order to maintain appropriate numbers for statstical significance within our study groups we may need to draw additional rats beyond the original study allocation of 35. This additional cohort will be capped at 10, giving a new total allocation of 45 animals. Please advise if this change is acceptable.

Kind regards

Nicholas A Sachs, PhD
Lecturer
Department of Human Biology
University of Cape Town
e-mail: nicholas.sachs@uct.ac.za

UNIVERSITY OF CAPE TOWN

Faculty of Health Sciences
Department of Human Biology

Anzio Road
Observatory 7925
South Africa
Tel: +27 21 406 6235
Fax: +27 21 448 7226

30 August 2010

University of Cape Town
Animal Ethics Committee

Re: Changes to HSFAEC proposal 010/002 entitled "Response of denervated muscle to electrical and chemical stimulation"

Dear Committee

The original application detailed a muscle explantation procedure which was to be done whilst the rats were anaesthetised with halothane. We have subsequently found that the use of halothane affects muscle contractility. The muscle response to stimulation decreased substantially towards the end of the explantation procedure (ie the longer the rats remained on halothane, the greater the effect on the muscle contractility). We therefore propose that decapitation be used instead.

The muscle fibre harvesting procedure will thus be as follows:

At the end of the animal's group-dependent denervation period, the reflex test will be repeated to confirm paralysis. The animal will then be decapitated. A skin incision will be made at the base of the leg along the length of the hindlimb to expose the underlying muscles. The denervated muscles will be removed and the procedure repeated on the innervated hindlimb.

Please advise if this change is acceptable.

Kind regards

Nicholas A Sachs, PhD
Lecturer
Department of Human Biology
University of Cape Town
e-mail: nicholas.sachs@uct.ac.za

A.3 Ethics reports and accreditation course certificate

Two reports based on the addenda were submitted to the AEC, one presenting the differences in results between rats which were euthanised with halothane and those which were decapitated and one which detailed animal numbers at various periods throughout the duration of the study. (In addition to these reports, annual reports were submitted but are not included in the appendices as they would serve only as repetitive summaries of what has been presented in the body of the dissertation).

AEC REPORT

UNIVERSITY OF CAPE TOWN

DEPARTMENT OF BIOMEDICAL ENGINEERING

RONDEBOSCH, CAPE TOWN, SOUTH AFRICA

Report on the effects of halothane versus decapitation on skeletal muscle contractility of Long Evans rats when stimulated *in vitro*

Prepared for:

Animal Ethics Committee

University of Cape Town

Prepared by:

Surname, Initial: Modak, G

Venter, N

Student Number: mdkgha001

vntnic001

January 2011

TABLE OF CONTENTS

LIST OF FIGURES

1 INTRODUCTION

This report details the effects of halothane versus decapitation as a means of euthanasia of Long Evans rats with the purpose of subsequent use of skeletal muscle fibres for *in vitro* stimulation. The skeletal muscle fibres are stimulated both chemically (by means of the neurotransmitter Acetylcholine (ACh)) as well as electrically.

1.1 Subject of report

Two methods of euthanasia will be discussed with direct application to their effects on skeletal muscle contraction dynamics.

1.2 Background to report

An original application was submitted for two studies which detailed the *in vitro* electrical and chemical stimulation of denervated and innervated (as a control) skeletal muscle fibres which were to be explanted from Long Evans rats. This application stipulated the use of halothane as a means of anaesthetic during the explantation procedure. Muscle fibres were explanted and tested on whilst the rat was under anaesthetic. This was a validated method in literature and was thus deemed acceptable at the time of the application. It subsequently became evident that halothane had a substantial effect on the skeletal muscle contractility. Literature cited shorter time periods of halothane usage. As this was compromising the study, it was decided that an amendment to the original protocol would be submitted for ethical approval where decapitation would be used as a means of euthanasia instead of halothane. This application was approved and a report of the results (as requested by the AEC) is as follows.

1.3 Objectives of report

The objectives of the report are therefore to:

- Outline the effects of halothane on skeletal muscle contractility over time
- Demonstrate the differences between halothane and decapitation on skeletal muscle contractility

1.4 Scope and limitations of report

This report will focus on the skeletal muscle explantation procedure of the first five decapitated rats, as requested by the AEC upon approval of the amendment for decapitation.

1.5 Plan of development

This report relates to the effects of halothane over time on skeletal muscle contractility. The comparative effects of decapitation are presented. The plan for the most viable option for the results of this study is then provided.

2 METHODOLOGY

Both innervated and denervated muscle fibres were tested. Fast and slow type fibres were used, from the soleus and gastrocnemius muscles respectively.

The information for halothane and decapitation tests was gathered in the following way:

2.1 Muscles explanted under halothane anaesthesia

Muscles were explanted from the rats whilst under anaesthesia. One muscle at a time was explanted into a special chamber containing Krebs Ringer buffer solution and separated into fibre bundles before being tested. This procedure was repeated for each of the four muscles which were tested (innervated soleus, denervated soleus, innervated gastrocnemius and denervated gastrocnemius). For chemical stimulation, the muscle fibre bundles were stimulated with a number of different concentrations of ACh over a time period of 20 minutes per test.

2.2 Muscles explanted after decapitation

Rats were rapidly decapitated using a specific small animal guillotine and all four muscles removed immediately and placed in a Krebs Ringer buffer solution. As previously described, stimulation tests were conducted immediately after the explantation procedure. Tests were done successively and the muscles were kept in solution at 4 °C until tested on.

All procedures adhered to protocols approved by the AEC for application 001/004.

3 COMPARISON OF THE EFFECTS OF HALOTHANE AND DECAPITATION ON SKELATAL MUSCLE CONTRACTION OVER TIME

Halothane is a volatile anaesthetic and has been shown to affect skeletal muscle contraction dynamics in both cases of direct as well as indirect stimulation by depressing the post-synaptic response to the neurotransmitter, ACh [1]. Literature cites dependencies on exposure duration (of skeletal muscle to halothane), halothane concentration and temperature control. Complete block has been shown to occur at with administration of halothane at 4% and 5.6% under varying conditions [1]. The tests pertaining to this report were conducted under the following conditions:

- Controlled body and testing temperature of 37°C.
- Concentration maintained at 1.5%.
- All exposure durations exceeded 40 minutes.

3.1 Stimulation by means of ACh

Three concentrations of ACh were used to stimulate contractions. These were 4µg/ml, 96µg/ml and 550µg/ml.

3.1.1 Decapitation and Halothane effects on contraction times

Figures 1 depicts the time to contraction and time to peak tension (PT) for decapitated rats and rats under halothane anaesthetic.

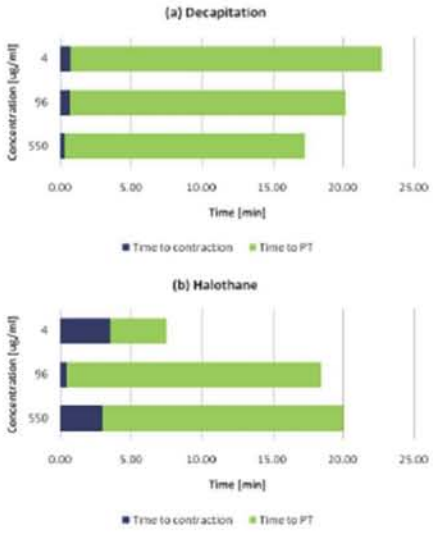

Figure 1: Time to contraction and time to taken to reach peak tension for innervated soleus muscle from (a) decapitated model and (b) halothane model.

For the decapitation model, an increase in concentration is shown to cause a decrease in the time to contraction as well as time to peak tension. The halothane model does not display this trend. This could be attributed to the duration of exposure of the muscle to halothane. The soleus muscle stimulated with 4µg/ml of ACh was exposed to halothane for 45 minutes before the test was conducted. The soleus muscle stimulated with 550µg/ml of ACh was exposed to halothane for 25 minutes before the test was conducted.

Figures 2 displays a more direct comparison between decapitation and halothane models for time to contraction and time to peak tension.

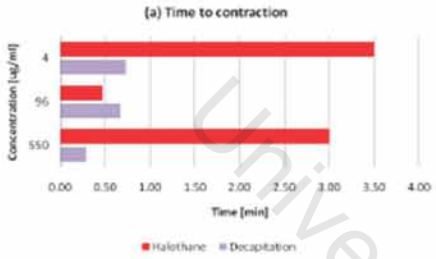

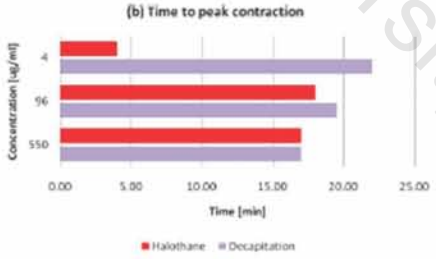

Figure 2: Direct comparison between decapitation and halothane models for (a) time to contraction and (b) time taken to reach peak tension.

Time taken to contraction is significantly higher for halothane than decapitation models (Figure 2(a)) at stimulation concentrations of 4µg/ml and 550µg/ml and slightly less for 96µg/ml. The soleus muscle tested stimulated at 96µg/ml was exposed to halothane for less than 5 minutes whereas those tested at 4µg/ml and 550µg/ml were exposed for 45 minutes and 25 minutes respectively.

Figure 2(b) indicates that halothane affected tests reach peak tension faster than decapitation models. The lower concentration of ACh, the greater the effect of halothane (shorter time to peak tension).

Figure 3 illustrates the effect on contraction force of exposure time to halothane.

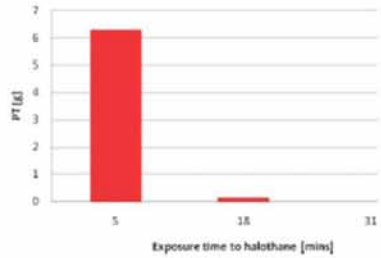

Figure 3: Influence on PT of exposure time to halothane on denervated gastrocnemius muscle, stimulated with 4µg/ml ACh.

A significant decrease in force with an increase in exposure time is depicted in Figure 3. Results display ACh stimulation concentration of 4µg/ml (the lowest used concentration). After half an hour of exposure time to halothane, the denervated gastrocnemius was unable to be stimulated with the lowest concentration.

3.1.2 Decapitation and Halothane effects on force generation

Figure 4 illustrates the differences in peak tension obtained at the three stimulating concentrations for both halothane and decapitation models.

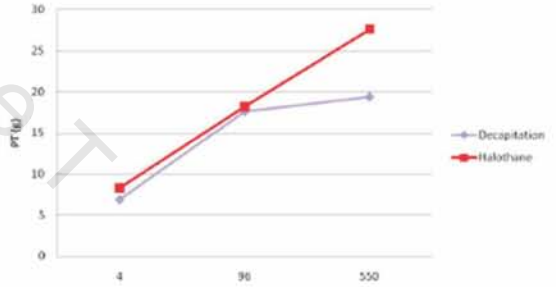

Figure 4: Differences in PT between halothane and decapitation test models at 3 tested concentrations. Results from innervated soleus muscles.

From Figure 4 it is evident that halothane increases peak tension in comparison to no anaesthetic use. This conforms to literature [1].

3.2 Electrical stimulation

The purpose of the electrical stimulation project is to model the specific parameters of skeletal muscles by observing the muscle's overall response to electrical stimulation. If any of the experimental conditions alter the state of the measured parameters, the results will be futile.

Halothane has been found to affect membrane events, excitation-contraction coupling steps, time to peak tension as well as peak tension in isolated muscles [2].

The method of euthanasia that leaves the muscle in as natural a state as possible is decapitation. This procedure is clearly best suited to the experimental conditions.

3.2.1 Results from decapitation experiments

The strength-duration curves of soleus muscles (explanted after decapitation) from two seperate rats are shown below in Fig. 5 (other results are similar). In these graphs red represents the threshold values for denervated soleus and blue represents the threshold values for innervated soleus.

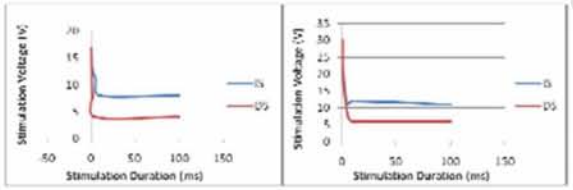

Figure 5: Strength duration curves of soleus muscles

While these graphs could benefit from improved curve fitting techniques, this initial comparison suggests confirmation of the literature, in this case the fact that the denervated muscle contracts at a lower voltage level (due to the higher resting membrane potential after denervation [3]).

4 CONCLUSION

The data presented indicates that halothane affects muscle contractility over time. Whilst literature cites frequent use of halothane as an anaesthetic, long test durations make it unfeasible for the purposes of this study. Test results from decapitated rats conform to literature and thus add further validation to results shown here and thus warrant amendment to the original procedure.

5 REFERENCES

[1] Waud BE, Waud DR. Effects of Volatile Anesthetics on Directly and Indirectly Stimulated Skeletal Muscle. Anesthesiology 50:103-110, 1979.

[2] Rosenberg H. Sites and Mechanisms of Action of Halothane on Skeletal Muscle Function in Vitro. Anesthesiology 50:331-335, 1979.

[3] S. Thesleff. The physiological effects of denervation on muscle. Annals of the New York Academy of Sciences. Volume 228, Issue 1.

AEC REPORT

UNIVERSITY OF CAPE TOWN

DEPARTMENT OF BIOMEDICAL ENGINEERING

RONDEBOSCH, CAPE TOWN, SOUTH AFRICA

Breakdown of number of animals used to date for Project 010/004

Prepared for:

Animal Ethics Committee

University of Cape Town

Prepared by:

Surname, Initial: Modak, G

Student Number: mdkgha001

January 2011

Attached is a breakdown of the testing dates and number of rats used. The first number of 25 was the amount of rats denervated by the date of that application. 23 was the number killed/explanted from by the hand-in date of the final application (we handed the form in by the 26 November but started the letters etc by the 22 November (by the 22 we had killed 20). The final row in the last table indicates the totals to show where the extra 3 came from). 32 is thus the amount used to date.

Group	Animal number	Denervation date	Explantation date	Notes
Pilot study	1	27/05/2010	6/08/2010	
	2	28/5/2010	-	Rat died coming out of anaesthesia
	3	31/05/2010	11/08/2011	
	4	2/06/2010	12/08/2010	
	5	4/06/2010	13/08/2010	
Pilot study extension	1	14/06/2010	29/10/2010	
	2	14/06/2010	-	Euthenised on 12/07/2010 due to foot infection
	3	15/06/2010		Died on 16/06/2010
	4	15/06/2010	-	Died on 16/06/2010
	5	16/06/2010	30/10/2010	
	6	16/06/2010	2/11/2010	
	7	17/06/2010	19/08/2010	
	8	17/06/2010	20/08/2010	
	9	18/06/2010	23/08/2010	
	10	18/06/2010	23/08/2011	
Long term	1	19/07/2010	-	Muscle not yet explanted -> rat alive
	2	19/07/2010	-	Muscle not yet explanted -> rat alive
	3	20/07/2010	16/08/2010	
	4	20/07/2010	-	Died on 21/07/2010
	5	20/07/2010	18/08/2010	
	6	21/07/2010	-	Muscle not yet explanted -> rat alive
	7	21/07/2010	-	Muscle not yet explanted -> rat alive
	8	21/07/2010	-	Muscle not yet explanted -> rat alive
	9	23/07/2010	-	Muscle not yet explanted -> rat alive
	10	23/07/2010	-	Muscle not yet explanted -> rat alive
Middle term	1	11/10/2010	29/11/2010	
	2	11/10/2010	30/11/2010	
	3	12/10/2010	3/11/2010	Done early since foot was starting to become infected and didn't want him to suffer
	4	12/10/2010	1/12/2010	
	5	13/10/2010	2/12/2010	
	6	13/10/2010	3/12/2010	
	7	13/10/2010	6/12/2010	
	8	13/10/2010	7/12/2010	
	9	18/10/2010	8/12/2010	
	10	18/10/2010	10/12/2010	
Short term	1	19/10/2010	4/11/2010	
	2	20/10/2010	4/11/2010	
	3	21/10/2010	5/11/2010	
	4	22/10/2011	-	Died whilst being put under with halothane
	5	25/10/2012	6/11/2010	
	6	25/10/2013	8/11/2010	
	7	26/10/2014	9/11/2010	
	8	26/10/2015	24/11/2010	
	9	27/10/2016	25/11/2010	
	10	28/10/2017	26/11/2010	

	Totals				
	Ordered	Denervated	Explanted (killed)	Died (causes other than explantation)	Alive
First ammendment application 16/08/2010	25	**25**	5	5	15
Second ammendment application 30/08/2010	25	25	10	5	10
Third ammendment application process start date 22/11/2010	45	45	20	6	19
Third ammendment application handed in by 26/11/2010	45	45	**23**	6	16
As of 20/12/2010	45	45	**32**	6	7

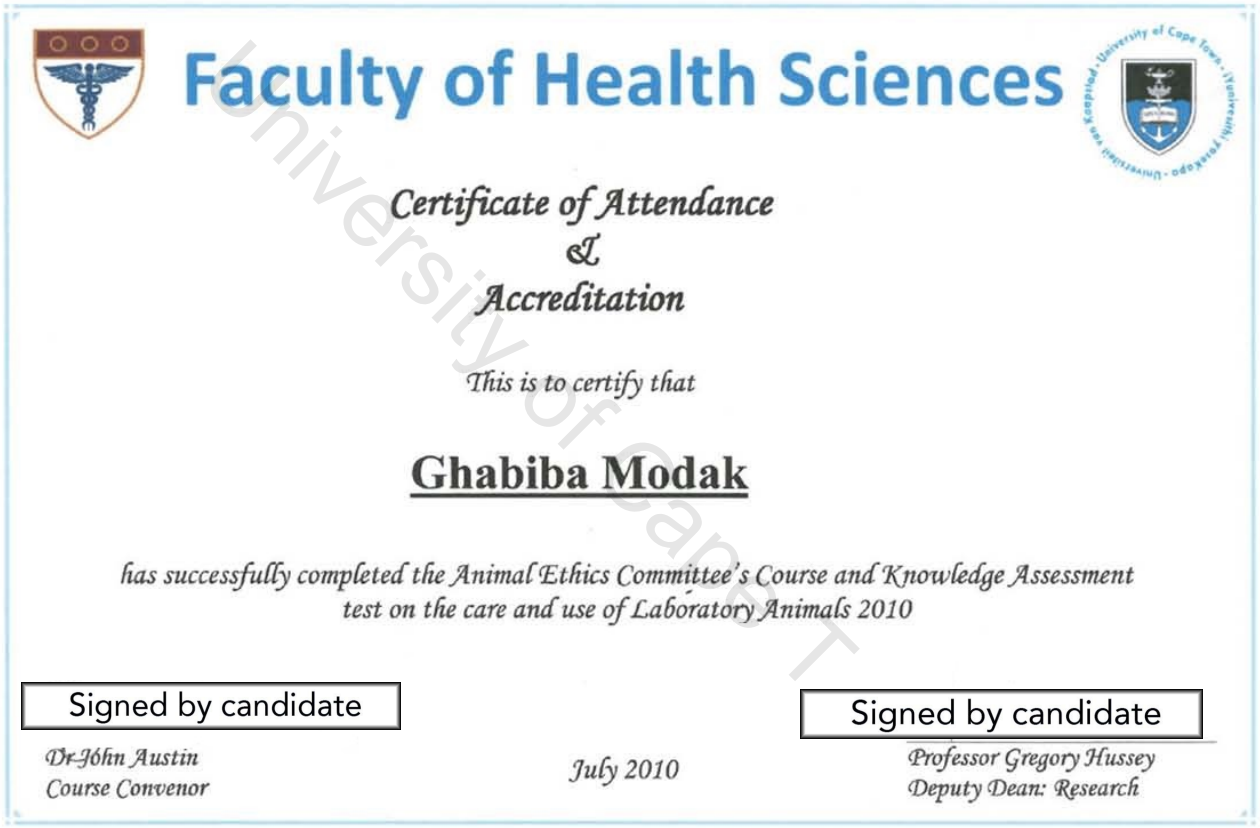

Faculty of Health Sciences

Certificate of Attendance
&
Accreditation

This is to certify that

Ghabiba Modak

has successfully completed the Animal Ethics Committee's Course and Knowledge Assessment test on the care and use of Laboratory Animals 2010

Signed by candidate

Dr John Austin
Course Convenor

July 2010

Signed by candidate

Professor Gregory Hussey
Deputy Dean: Research

B Equipment Design and Specifications

This Appendix includes the workshop drawings for the tissue bath used in the chemical stimulation procedure. All drawings were done in ProEngineer Wildfire 5.0. Drawings are presented as component parts and an additional final exploded assembly. All component parts were manufactured from acrylic with the exception of the central heating tubes which were made of glass.

The experimental set-up was designed for practicality and ease of use. Descriptions of such design implementation are given for further clarification.

The bath was designed to be horizontal to ensure ease of access to the muscle, for both chemical as well as electrical stimulation. The bath was fixed into a cupboard with all necessary pipes and leads passed through side connections. A sliding glass front enabled the cupboard to be closed during testing. The fan and temperature probe were thus able to operate at maximum efficiency and fewer disturbances were introduced from external factors.

In the bath itself, the two glass tubes were fitted into tapered brass connectors and the connection sealed with non-reactive sealant. The ends of the brass connectors attached to the tissue bath were threaded for a secure interference fit into the endcaps of the tissue bath. The opposite ends of the connectors were tapered, allowing for ease of use of flexible pipes, the ends of which were attached to the heating circulator, thus forming a closed circulation loop.

The entry point for the bubbled carbogen gas was placed at the lowest possible position in one of the endcaps. A thin perspex sheet was slightly distended into the bathing solution during testing at the entry point of the gases to detract from the formation of large bubbles which might burst against the strain gauge attachment and cause spurious results. These features also allowed for minimum disturbance of the muscle by movement of the bathing solution due to bubbling.

Prior to the commencement of recording, a small circulator was placed in the bath to circulate the carbogen gas and ensure homogeneity in the pH of the solution. The circulator was made from a simple round rubber stopper attached to the connecting shaft of a small motor, and was powered by a 2V battery. The circulator was removed before AChCl administration to prevent circulating the chemical stimulant away from the muscle.

A suction pump was used to remove bathing and flushing solutions between tests.

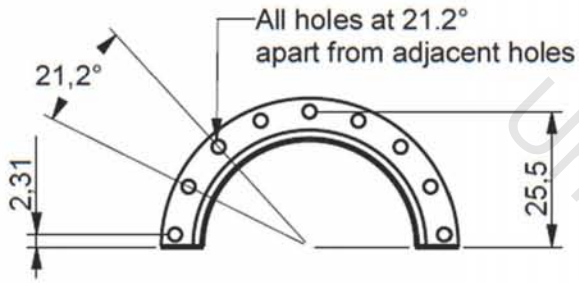

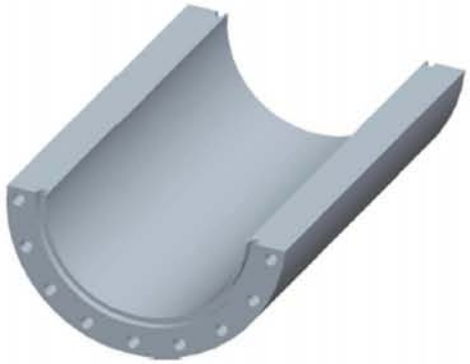

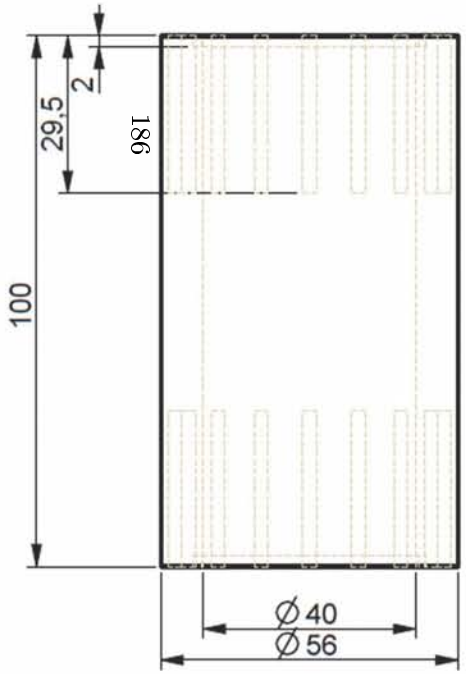

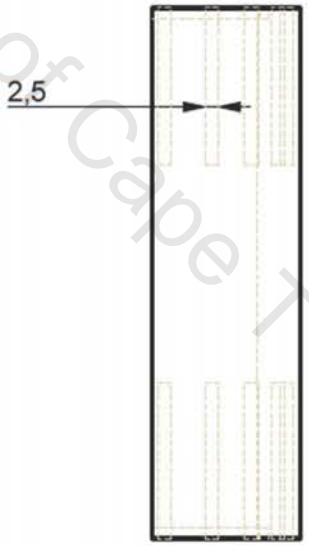

All dimesions in mm.

UCT BME
Ghabiba Modak
April 2010
Tissue Bath Base
Scale: 0,850

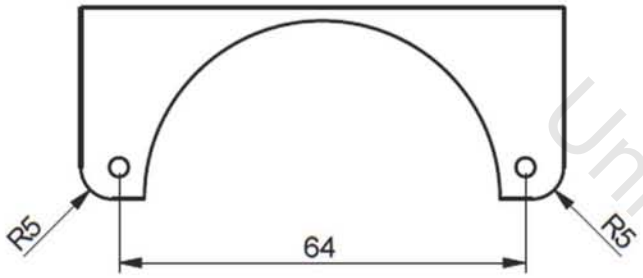

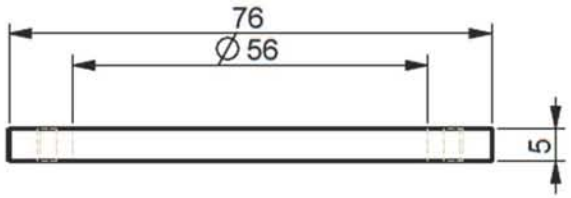

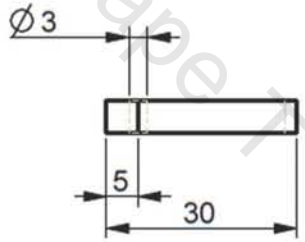

All dimensions in mm.

UCT BME
Ghabiba Modak
April 2010
Tissue Bath Stand
Quantity: 2
Scale: 1,000

All chamfers R5.

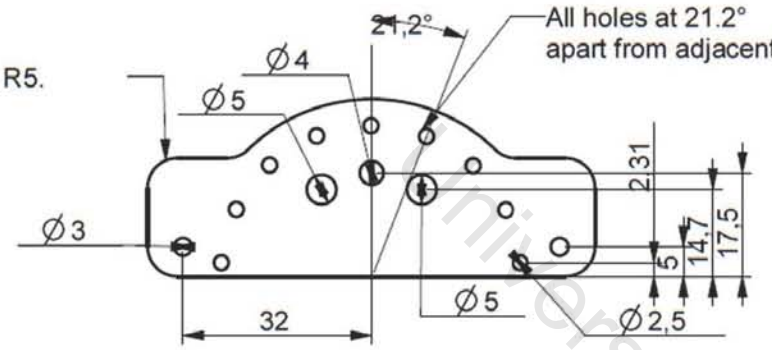

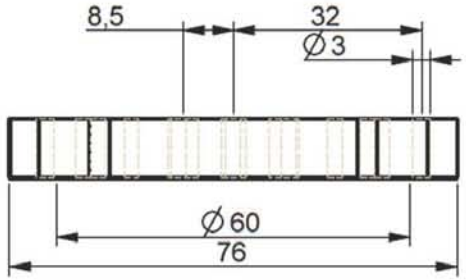

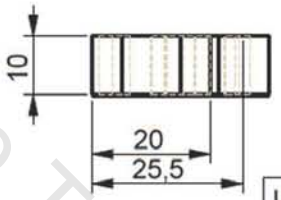

All dimensions in mm.

UCT BME
Ghabiba Modak
April 2010
Tissue Bath Stopper1
Scale: 1,000

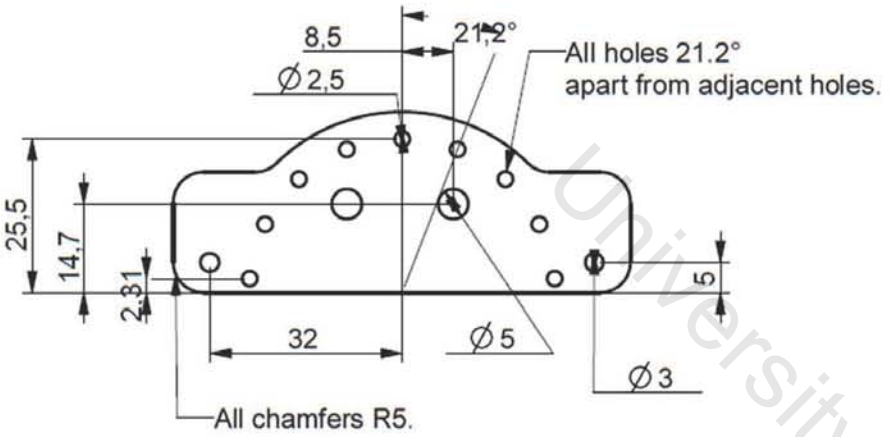

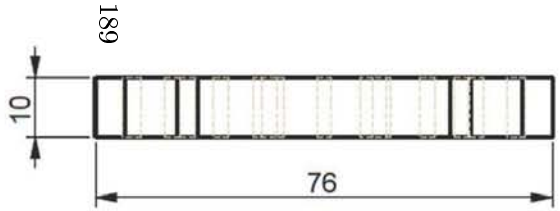

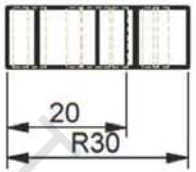

All dimension in mm.

UCT BME
Ghabiba Modak
April 2010
Tissue Bath Stopper2
Scale: 1,000

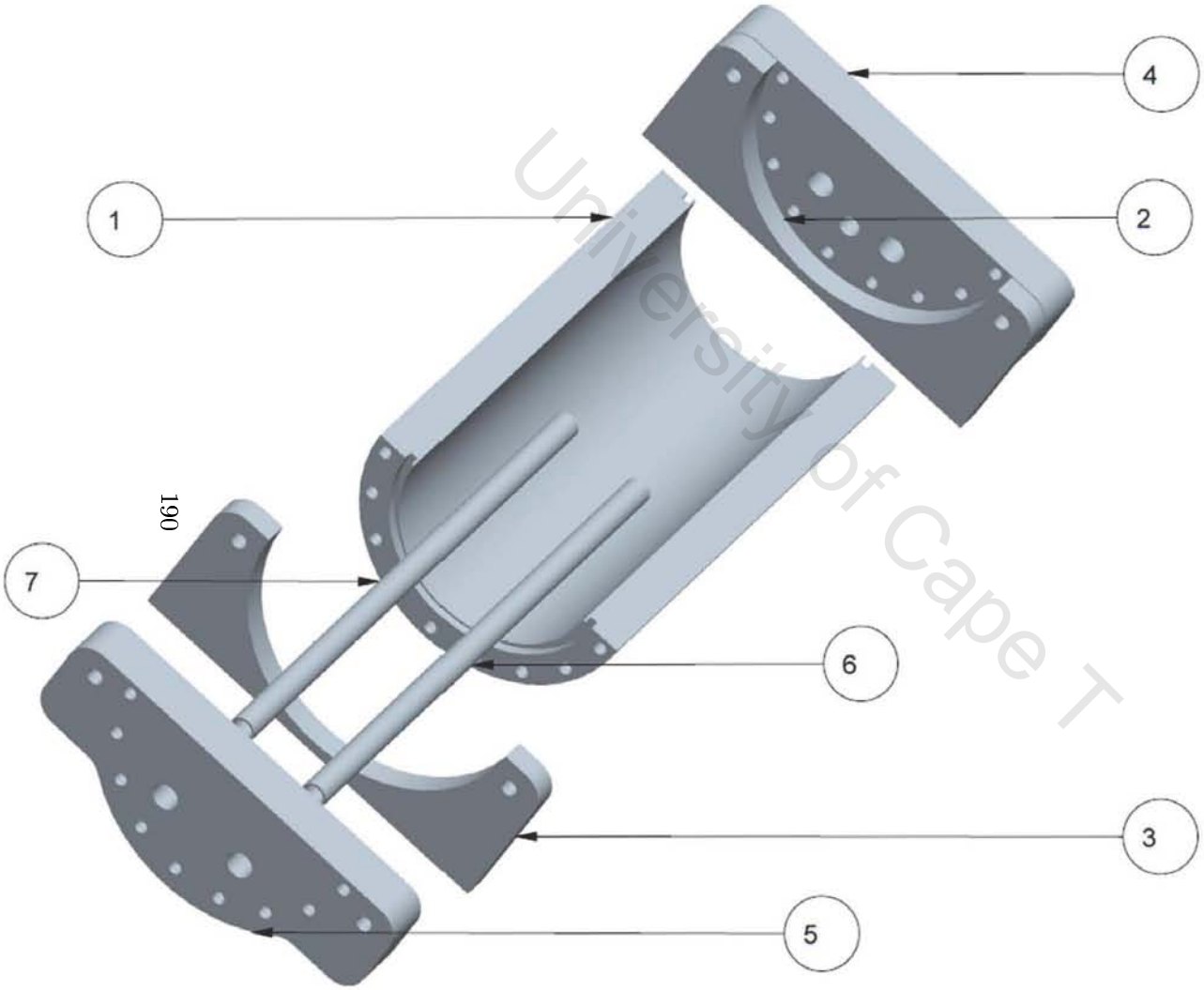

Index	Part Name
1	BASE
2	STAND
3	STAND
4	STOPPER
5	STOPPER_2
6	GLASS_ROD
7	GLASS_ROD

UCT BME
Ghabiba Modak
April 2010
Tissue Bath Assembly

C Chemical Dose Calculations and Specifications

C.1 Calculations of AChCl doses to be administered

This study implemented the use of 6 different concentrations of AChCl which were injected onto skeletal muscle held within a tissue bath containing Krebs Ringer buffer solution. The 6 concentrations were known, predetermined values. In order to ensure that the muscle was exposed to the proper concentration, the dilution principle was employed. The method undertaken is presented as follows.

The concentrations used could be separated into a low concentration range and a high concentration range. The first step in the process was to mix stock solutions from which the necessary doses could be obtained. Two stock solutions were thus prepared, namely that of 1mM and 0.56M concentrations. The former was chosen based on similar concentration use reported in literature and the latter was chosen based on the solubility of AChCl (as provided by Sigma-Aldrich). Further information on the chemical specifications is presented later in this Appendix. The molecular weight of AChCl, as provided by Sigma-Aldrich is 181.66g/mol.

Given that

$$(stock\,solution\,concentration)\,(molecular\,weight) = mass\,per\,unit\,volume$$

and the known molecular weight of AChCl, the amount (in g/L) of AChCl which is required to obtain a stock solution of given concentration can thus be determined.

Thus for a 1mM[11] stock solution

$$\left(1x10^{-3}\right)\left[\frac{mol}{L}\right](181.66)\left[\frac{g}{mol}\right] = 0.1817g/L \tag{C.1}$$

and for a 0.56M stock solution

$$(0.56)\left[\frac{mol}{L}\right](181.66)\left[\frac{g}{mol}\right] = 101.7230g/L \tag{C.2}$$

Measured on a scale sensitive to 4 decimal units, the following amounts of AChCl were dissolved in the specified volume to obtain the two stock solutions (based on equations C.1 and C.2):

0.1mM stock solution: 0.1817g dissolved in 1000ml of double distilled water

0.56M stock solution: 40.6918g dissolved in 400ml of double distilled water (calculated by ratio)

Once the stock solutions were mixed, it was necessary to determine the volumes of stock solution which needed to be added to the 63ml tissue bath (the detailed design of which is presented in Appendix B) to obtain the concentrations given in section 3.3, Table 2. The dilution principle, given by equation 3.1 in section 3.3 was thus applied here as follows

[11] $1mM = 1x10^{-3}M$ and the unit $M = \frac{mol}{L}$

Table 12: Application of the dilution principle in determination of stock solution volumes (**V*start***) to be added to tissue bath solution

C*start*	**V*start*** $[\mu l]$ =	C*final*	V*final [ml]*
1 [mM]	1.39	4 $[\mu g/ml]$	63
1 [mM]	33.3	96 $[\mu g/ml]$	63
1 [mM]	190.7	550 $[\mu g/ml]$	63
0.56 [M]	100	1.6 [g/ml]	63
0.56 [M]	200	3.2 [g/ml]	63
0.56 [M]	400	6.3 [g/ml]	63

and the required volumes of stock solution are presented alongside the concentrations in Table 2.

C.2 Chemical specifications and material safety data sheets

Specification Sheet

SIGMA-ALDRICH

Product Name	Acetylcholine chloride, ≥99% (TLC)
Product Number	A6625
Product Brand	SIGMA
CAS Number	60-31-1
Molecular Weight	181.66

TEST	SPECIFICATION
APPEARANCE	WHITE TO WHITE WITH A FAINT YELLOW CAST POWDER
SOLUBILITY	CLEAR COLORLESS SOLUTION AT 400 MG PLUS 4 ML WATER
IR SPECTRUM	CONSISTENT WITH STRUCTURE
PURITY BY THIN LAYER CHROMATOGRAPHY	NOT LESS THAN 99%
	APPROVED HAM 6/16/92

Specification Sheet

SIGMA-ALDRICH

Product Name	Krebs-Ringer Bicarbonate Buffer, With 1800 mg/L glucose, without calcium chloride and sodium bicarbonate, powder, cell culture tested
Product Number	K4002
Product Brand	SIGMA

TEST	SPECIFICATION
ORIGIN	ANIMAL DERIVED COMPONENT FREE
APPEARANCE	WHITE TO OFF-WHITE POWDER
SOLUBILITY	CLEAR SOLUTION AT 9.5 G/L IN WATER
WATER BY KARL FISCHER	NMT 2.0%
PH TEST	6.1 - 6.7
PH TEST WITH NAHCO3	7.0 - 7.6
OSMOLALITY	235 - 260 MOSM/KG H2O
OSMOLALITY WITH NAHCO3	253 - 280 MOSM/KG H2O
GLUCOSE	17.1 - 20.9%
ENDOTOXIN ASSAY	NMT 1.0 EU/ML AT 1X
KEY ELEMENTS BY ICP	CONSISTENT WITH FORMULA
CELL CULTURE TEST	PASS
EXPIRATION DATE	24 MONTHS
	K4002:09/06-12

SIGMA-ALDRICH

SAFETY DATA SHEET

according to Regulation (EU) No. 1907/2006
Version 3.0 Revision Date 26.06.2007
Print Date 01.08.2010
GENERIC EU MSDS - NO COUNTRY SPECIFIC DATA - NO OEL DATA

1. IDENTIFICATION OF THE SUBSTANCE/PREPARATION AND OF THE COMPANY/UNDERTAKING

Product name : **Acetylcholine chloride**

Product Number : A6625
Brand : Sigma

Company : Sigma-Aldrich (Pty.) Ltd.
17 Pomona Street
Aviation Park, Unit 4
KEMPTON PARK
1619 SOUTH AFRICA
Telephone : +27119791188
Fax : +27119791119
Emergency Phone # :

2. HAZARDS IDENTIFICATION

Risk advice to man and the environment
Irritating to eyes, respiratory system and skin.

3. COMPOSITION/INFORMATION ON INGREDIENTS

Synonyms : ACh

Formula : C7H16NO2Cl
Molecular Weight : 181,66 g/mol

CAS-No.	EC-No.	Index-No.	Classification	Concentration [%]
Acetylcholine chloride				
60-31-1	200-468-8	-	Xi, R36/37/38	-

4. FIRST AID MEASURES

General advice
Consult a physician. Show this safety data sheet to the doctor in attendance.

If inhaled
If breathed in, move person into fresh air. If not breathing give artificial respiration Consult a physician.

In case of skin contact
Wash off with soap and plenty of water. Consult a physician.

In case of eye contact
Rinse thoroughly with plenty of water for at least 15 minutes and consult a physician.

If swallowed
Never give anything by mouth to an unconscious person. Rinse mouth with water. Consult a physician.

5. FIRE-FIGHTING MEASURES

Suitable extinguishing media
Use water spray, alcohol-resistant foam, dry chemical or carbon dioxide.

Special protective equipment for fire-fighters
Wear self contained breathing apparatus for fire fighting if necessary.

6. ACCIDENTAL RELEASE MEASURES

Personal precautions
Use personal protective equipment. Avoid dust formation. Avoid breathing dust. Ensure adequate ventilation.

Environmental precautions
Do not let product enter drains.

Methods for cleaning up
Pick up and arrange disposal without creating dust. Keep in suitable, closed containers for disposal.

7. HANDLING AND STORAGE

Handling
Avoid contact with skin and eyes. Avoid formation of dust and aerosols.
Provide appropriate exhaust ventilation at places where dust is formed. Normal measures for preventive fire protection.

Storage
Store in cool place.Keep container tightly closed in a dry and well-ventilated place.

strongly hygroscopic Store under inert gas.

8. EXPOSURE CONTROLS / PERSONAL PROTECTION

Personal protective equipment

Respiratory protection
Where risk assessment shows air-purifying respirators are appropriate use a dust mask type N95 (US) or type P1 (EN 143) respirator. Use respirators and components tested and approved under appropriate government standards such as NIOSH (US) or CEN (EU).

Hand protection
Handle with gloves. The selected protective gloves have to satisfy the specifications of EU Directive 89/689/EEC and the standard EN 374 derived from it.

Eye protection
Safety glasses

Skin and body protection
Choose body protection according to the amount and concentration of the dangerous substance at the work place.

Hygiene measures
Handle in accordance with good industrial hygiene and safety practice. Wash hands before breaks and at the end of workday.

9. PHYSICAL AND CHEMICAL PROPERTIES

Appearance

Form	crystalline
Colour	white

Safety data

pH	no data available
Melting point	148 °C
Boiling point	no data available
Flash point	no data available
Ignition temperature	no data available
Lower explosion limit	no data available
Upper explosion limit	no data available
Water solubility	no data available

10. STABILITY AND REACTIVITY

Storage stability
Stable under recommended storage conditions.

Conditions to avoid
Avoid moisture.

Materials to avoid
Strong oxidizing agents

Hazardous decomposition products

Hazardous decomposition products formed under fire conditions.
Carbon oxides, nitrogen oxides (NOx), Hydrogen chloride gas

11. TOXICOLOGICAL INFORMATION

Acute toxicity

LD50 Orai - rat - 2.500 mg/kg

Irritation and corrosion

no data available

Sensitisation

no data available

Chronic exposure

no data available

Signs and Symptoms of Exposure

Spastic paralysis

Potential Health Effects

Inhalation	May be harmful if inhaled. Causes respiratory tract irritation.
Skin	May be harmful if absorbed through skin. Causes skin irritation.
Eyes	Causes eye irritation.
Ingestion	May be harmful if swallowed.
Target Organs	Vascular system., Heart, Central nervous system, Smooth muscle., Skeletal muscle., Adrenal medulla.,

12. ECOLOGICAL INFORMATION

Elimination information (persistence and degradability)

no data available

Ecotoxicity effects

no data available

Further information on ecology

no data available

13. DISPOSAL CONSIDERATIONS

Product
Observe all federal, state, and local environmental regulations.Contact a licensed professional waste disposal service to dispose of this material. Dissolve or mix the material with a combustible solvent and burn in a chemical incinerator equipped with an afterburner and scrubber.

Contaminated packaging
Dispose of as unused product.

14. TRANSPORT INFORMATION

ADR/RID
Not dangerous goods

IMDG
Not dangerous goods

IATA
Not dangerous goods

15. REGULATORY INFORMATION

Labelling according to EC Directives

Hazard symbols	
Xi	Irritant
R-phrase(s)	
R36/37/38	Irritating to eyes, respiratory system and skin.
S-phrase(s)	
S26	In case of contact with eyes, rinse immediately with plenty of water and seek medical advice.

16. OTHER INFORMATION

Further information

The above information is believed to be correct but does not purport to be all inclusive and shall be used only as a guide. The information in this document is based on the present state of our knowledge and is applicable to the product with regard to appropriate safety precautions. It does not represent any guarantee of the properties of the product. Sigma-Aldrich Co., shall not be held liable for any damage resulting from handling or from contact with the above product. See reverse side of invoice or packing slip for additional terms and conditions of sale.

SIGMA-ALDRICH

Material Safety Data Sheet

Date Printed: 01/AUG/2010
Date Updated: 14/FEB/2006
Version 1.2
Regulation (EC) No 1907/2006

1 - Product and Company Information

Product Name	KREBS-RINGER BICARBONATE BUFFER, WITH 1800 MG/L GLUCOSE, WITHOUT CALCIUM CHLORIDE AND SODIUM BICARBONATE. CELL CULTURE TESTED
Product Number	K4002
Company	Sigma-Aldrich (Pty.) Ltd. Aviation Park, Unit 4 1619 Kempton Park South Africa
Technical Phone #	27 11 979 1188
Fax	27 11 979 1119

2 - Hazards Identification

SPECIAL INDICATION OF HAZARDS TO HUMANS AND THE ENVIRONMENT
Not hazardous according to Directive 67/548/EEC.

3 - Composition/Information on Ingredients

Product Name	CAS #	EC no	Annex I Index Number
KREBS-RINGER BICARBONATE BUFFERW/1800 MG GLUCOSE/L W/O	None	None	None

4 - First Aid Measures

AFTER INHALATION
If inhaled, remove to fresh air. If breathing becomes difficult, call a physician.

AFTER SKIN CONTACT
In case of contact, immediately wash skin with soap and copious amounts of water.

AFTER EYE CONTACT
In case of contact with eyes, flush with copious amounts of water for at least 15 minutes. Assure adequate flushing by separating the eyelids with fingers. Call a physician.

AFTER INGESTION
If swallowed, wash out mouth with water provided person is conscious. Call a physician.

5 - Fire Fighting Measures

EXTINGUISHING MEDIA
Suitable: Water spray. Carbon dioxide, dry chemical powder, or appropriate foam.

SPECIAL RISKS
Specific Hazard(s): Emits toxic fumes under fire conditions.

SPECIAL PROTECTIVE EQUIPMENT FOR FIREFIGHTERS
Wear self-contained breathing apparatus and protective clothing to prevent contact with skin and eyes.

6 - Accidental Release Measures

PROCEDURE(S) OF PERSONAL PRECAUTION(S)
Exercise appropriate precautions to minimize direct contact with skin or eyes and prevent inhalation of dust.

METHODS FOR CLEANING UP
Sweep up, place in a bag and hold for waste disposal. Avoid raising dust. Ventilate area and wash spill site after material pickup is complete.

7 - Handling and Storage

HANDLING
Directions for Safe Handling: Avoid inhalation. Avoid contact with eyes, skin, and clothing. Avoid prolonged or repeated exposure.

STORAGE
Conditions of Storage: Keep tightly closed.
Store at 2-8°C

8 - Exposure Controls / Personal Protection

ENGINEERING CONTROLS
Safety shower and eye bath. Mechanical exhaust required.

GENERAL HYGIENE MEASURES
Wash thoroughly after handling.

PERSONAL PROTECTIVE EQUIPMENT
Respiratory Protection: Use respirators and components tested and approved under appropriate government standards such as NIOSH (US) or CEN (EU). Respiratory protection is not required. Where protection from nuisance levels of dusts are desired, use type N95 (US) or type P1 (EN 143) dust masks.
Hand Protection: Protective gloves.
Eye Protection: Chemical safety goggles.

9 - Physical and Chemical Properties

pH	N/A
BP/BP Range	N/A
MP/MP Range	N/A
Flash Point	N/A
Flammability	N/A
Autoignition Temp	N/A
Oxidizing Properties	N/A
Explosive Properties	N/A
Explosion Limits	N/A
Vapor Pressure	N/A
Partition Coefficient	N/A
Viscosity	N/A
Vapor Density	N/A
Saturated Vapor Conc.	N/A

Evaporation Rate	N/A
Bulk Density	N/A
Decomposition Temp.	N/A
Solvent Content	N/A
Water Content	N/A
Surface Tension	N/A
Conductivity	N/A
Miscellaneous Data	N/A
Solubility	N/A

10 - Stability and Reactivity

STABILITY
Stable: Stable.
Materials to Avoid: Strong oxidizing agents.

HAZARDOUS DECOMPOSITION PRODUCTS
Hazardous Decomposition Products: Carbon monoxide, Carbon dioxide.

HAZARDOUS POLYMERIZATION
Hazardous Polymerization: Will not occur

11 - Toxicological Information

SIGNS AND SYMPTOMS OF EXPOSURE
To the best of our knowledge, the chemical, physical, and toxicological properties have not been thoroughly investigated.

ROUTE OF EXPOSURE
Skin Contact: May cause skin irritation.
Skin Absorption: May be harmful if absorbed through the skin.
Eye Contact: May cause eye irritation.
Inhalation: Material may be irritating to mucous membranes and upper respiratory tract. May be harmful if inhaled.
Ingestion: May be harmful if swallowed.

12 - Ecological Information

No data available.

13 - Disposal Considerations

SUBSTANCE DISPOSAL
Contact a licensed professional waste disposal service to dispose of this material. Dissolve or mix the material with a combustible solvent and burn in a chemical incinerator equipped with an afterburner and scrubber. Observe all federal, state, and local environmental regulations.

14 - Transport Information

RID/ADR
Non-hazardous for road transport.

IMDG
Non-hazardous for sea transport.

IATA
Non-hazardous for air transport.

15 - Regulatory Information

Not hazardous according to Directive 67/548/EEC.

Caution: Substance not yet fully tested (EU).

COUNTRY SPECIFIC INFORMATION

Germany
WGK: 3
Self-Classification

16 - Other Information

WARRANTY
The above information is believed to be correct but does not purport to be all inclusive and shall be used only as a guide. The information in this document is based on the present state of our knowledge and is applicable to the product with regard to appropriate safety precautions. It does not represent any guarantee of the properties of the product. Sigma-Aldrich Inc., shall not be held liable for any damage resulting from handling or from contact with the above product. See reverse side of invoice or packing slip for additional terms and conditions of sale.

DISCLAIMER
For R&D use only. Not for drug, household or other uses.

D MATLAB Code

```
% Reference (file sequence):
% http://matlab.wikia.com/wiki/FAQ#How_can_I_process_a_sequence_of_files.3F

clear all
close all
clc

date_now = clock;
date_now = strcat(num2str(date_now(1)),'_',num2str(date_now(2)),'_',
num2str(date_now(3)), num2str(date_now(4)), num2str(date_now(5)));
diary(strcat('log', date_now,'.log'));
diary on

myFolder = 'G:\lab results\mat files';
filePattern = fullfile(myFolder, '*.mat');
matFiles = dir(filePattern);

for k = 1:length(matFiles)
    s = 180;
    try     %try-catch: allows for code to jump to next loop (ie test) if error occurs
        baseFileName = matFiles(k).name;
        fullFileName = fullfile(myFolder, baseFileName);
        fprintf(1, 'Now reading %s\n', fullFileName);

        %Load individual data sets into workspace to downsample
        load(baseFileName)


        % Downsample data
        ticktimes_block2_ds = downsample(ticktimes_block2, 20);
        clear ticktimes_block2
        T = ticktimes_block2_ds;
        clear ticktimes_block2_ds
        data_block2_ds = downsample(data_block2(1,:), 20);
        clear data_block2
        F = (data_block2_ds/(-0.1*10^-6))*0.551;        %Converts mV to Force -> -2.5*10^-
6 for tests before 29Nov2010, -0.1*10^-6 for after
        clear data_block2_ds
        %         F0 = (F - (F(1)-0.551))*-1 + 0.551;            %Brings pretensioned
(start value) to F0 = 0.551g, no inversion needed
        F0 = F - F(1) + 0.551;
        clear F
        con = conv(F0, ones(1, 1000)*(1/1000));
        CCC = (con - con(1) + 0.551);
        clear con

        % PLOTS
        injT = min(round(((s/max(T)))*length(T)),length(T)-501);   %finds injection time
at 30sec
        %NOTE: comment out injT2 if only one injection
%       injT2 = min(round(((238/max(T)))*length(T)),length(T)-501);   %finds second
injection time if applicable

        %find index of max and min points:
        iFmax = find(max(CCC(injT+500:length(T))) == CCC(injT+500:length(T)))+injT+500-1;
        iFmin = find(min(CCC(injT:length(T))) == CCC(injT:length(T)))+injT-1;

        %finds max and min amplitudes
        dmax = ((F0(iFmax))-F0(1));
        dmin = ((F0(iFmin))-F0(1));
        clear iFmax iFmin

        % Determine by means of amplitude if graph should be inverted or not
         if abs(dmax)<abs(dmin)
            iFmax = find(max(CCC(injT+500:length(T))) ==
CCC(injT+500:length(T)))+injT+500-1;
            iFmin = find(min(CCC(injT:length(T))) == CCC(injT:length(T)))+injT-1;
             p = plot(T, CCC(1:length(CCC)-999));
        else
            iFmax = find(max(-1*CCC(injT+500:length(T))) ==
-1*CCC(injT+500:length(T)))+injT+500-1;
            iFmin = find(min(-1*CCC(injT:length(T))) == -1*CCC(injT:length(T)))+injT-1;
            p = plot(T, CCC(1:length(CCC)-999)*-1 +0.551*2) ;              % invert data
plot
        end

%         m = ((F0(length(F0)-100))-F0(1))/(T(length(T)-T(1)));          %gradient bet.
first and last point
%
%         %Determine by means of gradient if graph should be inverted or not
%         if m >0
%             iFmax = find(max(CCC(injT+500:length(T))) ==
CCC(injT+500:length(T)))+injT+500-1;
%             iFmin = find(min(CCC(injT:length(T))) == CCC(injT:length(T)))+injT-1;
%             p = plot(T, CCC(1:length(CCC)-999));
%         else
%             iFmax = find(max(-1*CCC(injT+500:length(T))) ==
-1*CCC(injT+500:length(T)))+injT+500-1;
%             iFmin = find(min(-1*CCC(injT:length(T))) == -1*CCC(injT:length(T)))+injT-1;
%             p = plot(T, CCC(1:length(CCC)-999)*-1 +0.551*2) ;              % invert data
plot
%         end

        title(regexprep(baseFileName, '_', ' '))

        e = regexpi(baseFileName, 'elec');
        if e > 0;
            axis([0 1000 -5 5])
        else
            % injection line plot
            %ylim=get(gca,'ylim');
            ylim=[-12, 26];
            line([T(injT);T(injT)],ylim.', 'linewidth',0.5, 'color',[1,0,0]);
            %NOTE: comment out next line if only 1 injection
%           line([T(injT2);T(injT2)],ylim.', 'linewidth',0.5, 'color',[1,0,0]);
            axis([0 1400 -12 26])  %[0 800 -12 26] for tests before 29Nov2010
        end

        axis(axis)

        xlabel('Time (sec)')
        ylabel('Force (g)')
        x = get(p, 'XData');
        y = get(p, 'YData');

        % Min and Max labels
        text(x(iFmin), y(iFmin), ['Min = ',num2str(x(iFmin)), ' ; ', num2str(y(iFmin))],
'VerticalAlignment','top', 'HorizontalAlignment','left', 'FontSize',10)
        text(x(iFmax), y(iFmax), ['Max = ',num2str(x(iFmax)), ' ; ', num2str(y(iFmax))],
'VerticalAlignment','bottom', 'HorizontalAlignment','left', 'FontSize',10)
        hold on
        plot(x(iFmin), y(iFmin),'r+', x(iFmax), y(iFmax),'r+');
        hold off
```

```
        % Output maximum force Fmax and time to maximum force Tmax and copy
        % into excel

        xlswrite('cellwrite.xls', y(iFmax), 'Statistics', ['G' num2str(k)]);

        % Alter 'filename' to save looped datasets:
        % Saves plot from each data set as .emf to working directory, 'gcf' refers
        % to current figure
        % saveas(gcf, 'filename denervation period.jpg')
        saveas(gcf, strcat(baseFileName,'.emf'));

    catch ME
        display(strcat(baseFileName,' FAILED'));
        display(ME.message);% ME is a structure with info on the error
    end
end

diary off
```

```
% Reference (file sequence):
% http://matlab.wikia.com/wiki/FAQ#How_can_I_process_a_sequence_of_files.3F

date_now = clock;
date_now = strcat(num2str(date_now(1)),'_',num2str(date_now(2)),'_',
num2str(date_now(3)), num2str(date_now(4)), num2str(date_now(5)));
diary(strcat('log', date_now,'.log'));
diary on

clear all
close all
clc

myFolder = 'G:\lab results\mat files';
filePattern = fullfile(myFolder, '*.mat');
matFiles = dir(filePattern);

% Value of k based on tests to be concatenated

for k = 490 %1:length(matFiles)
    s = 180;          %times marker for later determination of injection time
    try     %try-catch: allows for code to jump to next loop (ie test) if error occurs
        baseFileName = matFiles(k).name;
        fullFileName = fullfile(myFolder, baseFileName);
        fprintf(1, 'Now reading %s\n', fullFileName);

        %Load individual data sets into workspace to downsample
        load(baseFileName)


        % Downsample data
        ticktimes_block1_ds = downsample(ticktimes_block1, 20);
        clear ticktimes_block1
        T = ticktimes_block1_ds;
        clear ticktimes_block1_ds
        data_block1_ds = downsample(data_block1(1,:), 20);
        clear data_block1
        F = (data_block1_ds/(-0.1*10^-6))*0.551;        %Converts mV to Force -> -2.5*10^-
6 for tests before 29Nov2010, -0.1*10^-6 for after
        clear data_block1_ds
        %         F0 = (F - (F(1)-0.551))*-1 + 0.551;           %Brings pretensioned
(start value) to F0 = 0.551g, no inversion needed
        F0 = F - F(1) + 0.551;
        clear F
        con = conv(F0, ones(1, 1000)*(1/1000));
        CCC = detrend(con - con(1) + 0.551);
        clear con

        % PLOTS
        injT = min(round(((s/max(T)))*length(T)),length(T)-501);   %finds injection time
at 30sec
        %NOTE: comment out injT2 if only one injection
        %         injT2 = min(round(((238/max(T)))*length(T)),length(T)-501);   %finds
second injection time if applicable
        injT2 = length(T);                                                      %end of
first test and injection and hence start of ach check test

        %find index of max and min points:
        iFmax = find(max(CCC(injT+500:length(T))) == CCC(injT+500:length(T)))+injT+500-1;
        iFmin = find(min(CCC(injT:length(T))) == CCC(injT:length(T)))+injT-1;

        %finds max and min amplitudes
        dmax = ((F0(iFmax))-F0(1));
        dmin = ((F0(iFmin))-F0(1));
        clear iFmax iFmin
        % Determine by means of amplitude if graph should be inverted or not
        if dmax<dmin
            iFmax = find(max(CCC(injT+500:length(T))) ==
CCC(injT+500:length(T)))+injT+500-1;
            iFmin = find(min(CCC(injT:length(T))) == CCC(injT:length(T)))+injT-1;
            p = plot(T, CCC(1:length(CCC)-999));
        else
            iFmax = find(max(-1*CCC(injT+500:length(T))) == -
1*CCC(injT+500:length(T)))+injT+500-1;
            iFmin = find(min(-1*CCC(injT:length(T))) == -1*CCC(injT:length(T)))+injT-1;
            p = plot(T, CCC(1:length(CCC)-999)*-1 +0.551*2) ;             % invert data
plot
        end

        %         m = ((F0(length(F0)-100))-F0(1))/(T(length(T)-T(1)));
%gradient bet. first and last point
        %
        %         % Determine by means of gradient if graph should be inverted or not
        %         if m >0
        %             iFmax = find(max(CCC(injT+500:length(T))) ==
CCC(injT+500:length(T)))+injT+500-1;
        %             iFmin = find(min(CCC(injT:length(T))) == CCC(injT:length(T)))+injT-
1;
        %             p = plot(T, CCC(1:length(CCC)-999));
        %         else
        %             iFmax = find(max(-1*CCC(injT+500:length(T))) == -
1*CCC(injT+500:length(T)))+injT+500-1;
        %             iFmin = find(min(-1*CCC(injT:length(T))) == -
1*CCC(injT:length(T)))+injT-1;
        %             p = plot(T, CCC(1:length(CCC)-999)*-1 +0.551*2) ;             %
invert data plot
        %         end

        title(regexprep(baseFileName, '_', ' '))

        e = regexpi(baseFileName, 'elec');
        if e > 0;
            axis([0 50 -5 5])
        else
            % Injection line plot
            %ylim=get(gca,'ylim');
            ylim=[-12, 26];
            line([T(injT);T(injT)],ylim.', 'linewidth',0.5, 'color',[1,0,0]);
            line([T(injT2);T(injT2)],ylim.','linewidth',0.5, 'color',[1,0,0]);
            %NOTE: comment out next line if only 1 injection
            %             line([T(injT2);T(injT2)],ylim.', 'linewidth',0.5,
'color',[1,0,0]);
            %axis([0 2000 -12 26])  %[0 800 -12 26] for tests before 29Nov2010
        end

        %axis(axis)

        xlabel('Time (sec)')
        ylabel('Force (g)')
        x = get(p, 'XData');
        y = get(p, 'YData');

        % Min and Max labels
```

```
        text(x(iFmin), y(iFmin), ['Min = ',num2str(x(iFmin)), ' : ', num2str(y(iFmin))],
'VerticalAlignment','top', 'HorizontalAlignment','left', 'FontSize',10)
        text(x(iFmax), y(iFmax), ['Max = ',num2str(x(iFmax)), ' : ', num2str(y(iFmax))],
'VerticalAlignment','bottom', 'HorizontalAlignment','left', 'FontSize',10)
        hold on
        plot(x(iFmin), y(iFmin),'r+', x(iFmax), y(iFmax),'r+');
        %hold off
        clear p

        % Output maximum force Fmax and time to maximum force Tmax and copy
        % into excel

        xlswrite('callwrite.xls', y(iFmax), 'test', ['G' num2str(k)]);

        % Alter 'filename' to save looped datasets:
        % Saves plot from each data set as .emf to working directory, 'gcf' refers
        % to current figure
        %
        saveas(gcf, strcat(baseFileName,'.emf'));

    catch ME
        display(strcat(baseFileName,' FAILED'));
        display(ME.message);% ME is a structure with info on the error
    end
end

%%% ELECTRICAL CHECK %%%

for k = 482 %1:length(matFiles)
    try         %try-catch: allows for code to jump to next loop (ie test) if error occurs
        baseFileName = matFiles(k).name;
        fullFileName = fullfile(myFolder, baseFileName);
        fprintf(1, 'Now reading %s\n', fullFileName);

        %Load individual data sets into workspace to downsample
        load(baseFileName)

        % Downsample data
        ticktimes_block1_ds = downsample(ticktimes_block1, 20);
        clear ticktimes_block1
        Te = ticktimes_block1_ds;
        clear ticktimes_block1_ds
        data_block1_ds = downsample(data_block1(1,:), 20);
        clear data_block1
        Fe = (data_block1_ds/(-0.1*10^-6))*0.551;       %Converts mV to Force -> -
2.5*10^-6 for tests before 29Nov2010, -0.1*10^-6 for after
        clear data_block1_ds
        %       F0 = (F - (F(1)-0.551))*-1 + 0.551;           %Brings pretensioned
(start value) to F0 = 0.551g, no inversion needed
        F0e = Fe - Fe(1) + 0.551; % + F0(length(T));
        clear Fe
        con = conv(F0e, ones(1, 1000)*(1/1000));
        CCOe = con - con(1) + 0.551;
        clear con
```

```
%PLOTS

        iFmaxe = find(max(CCOe(1:length(Te))) == CCOe(1:length(Te)))+1+500-1;
        iFmine = find(min(CCOe(1:length(Te))) == CCOe(1:length(Te)))+1-1;

        dmaxe = (F0e(iFmaxe)-F0e(1));           %amplitude bet. first and last point
        dmine = (F0e(iFmine)-F0e(1));
        clear iFmaxe iFmine
        % Determine by means of gradient if graph should be inverted or not
        if dmaxe < dmine
            iFmaxe = find(max(CCOe(1:length(Te))) == CCOe(1:length(Te)))+1+500-1;
            iFmine = find(min(CCOe(1:length(Te))) == CCOe(1:length(Te)))+1-1;
            p = plot(T(length(T))+Te, CCOe(1:length(CCOe)-999));
        else
            iFmaxe = find(max(-1*CCOe(1+500:length(Te))) ==
1*CCOe(1+500:length(Te)))+1+500-1;
            iFmine = find(min(-1*CCOe(1:length(Te))) == -1*CCOe(1:length(Te)))+1-1;
            p = plot(T(length(T))+Te, CCOe(1:length(CCOe)-999)*-1 +F0(length(T))*2) ;
% invert data plot
        end

        xe = get(p, 'XData');
        ye = get(p, 'YData');

%       Min and Max labels
        text(xe(iFmine), ye(iFmine), ['Min = ',num2str(xe(iFmine)), ' : ',
num2str(ye(iFmine))], 'VerticalAlignment','top', 'HorizontalAlignment','left',
'FontSize',10)
        text(xe(iFmaxe), ye(iFmaxe), ['Max = ',num2str(xe(iFmaxe)), ' : ',
num2str(ye(iFmaxe))], 'VerticalAlignment','bottom', 'HorizontalAlignment','left',
'FontSize',10)
        hold on
        plot(xe(iFmine), ye(iFmine),'r+', xe(iFmaxe), ye(iFmaxe),'r+');
        %hold off
         catch ME
        display(strcat(baseFileName,' FAILED'));
        display(ME.message);% ME is a structure with info on the error
    end
end

%%% CHEMICAL CHECK %%%

for k = 489 %1:length(matFiles)
    try         %try-catch: allows for code to jump to next loop (ie test) if error occurs
        baseFileName = matFiles(k).name;
        fullFileName = fullfile(myFolder, baseFileName);
        fprintf(1, 'Now reading %s\n', fullFileName);

        %Load individual data sets into workspace to downsample
        load(baseFileName)

        % Downsample data
        ticktimes_block1_ds = downsample(ticktimes_block1, 20);
        clear ticktimes_block1
        T2 = ticktimes_block1_ds;
        clear ticktimes_block1_ds
        data_block1_ds = downsample(data_block1(1,:), 20);
        clear data_block1
        F2 = (data_block1_ds/(-0.1*10^-6))*0.551;       %Converts mV to Force -> -
2.5*10^-6 for tests before 29Nov2010, -0.1*10^-6 for after
        clear data_block1_ds
```

```
        %         F0 = (F - (F(1)-0.55))*-1 + 0.55;            %brings pretensioned
(start value) to F0 = 0.55lg, no inversion needed
        F02 = F2 - F2(1) + 0.55; % - F0(length(T));
        clear F2
        con = conv(F02, ones(1, 1000)*(1/1000));
        CCC2 = con - con(1) + 0.55;
        clear con
        %PLOTS

        iFmax2 = find(max(CCC2(1:length(T2))) == CCC2(1:length(T2)))+1+500-1;
        iFmin2 = find(min(CCC2(1:length(T2))) == CCC2(1:length(T2)))+1-1;

        dmax2 = (F02(iFmax2)-F02(1));           %gradient bet. first and last point
        dmin2 = (F02(iFmin2)-F02(1));
        clear iFmax2 iFmin2
        % Determine by means of gradient if graph should be inverted or not
        if dmax2 > dmin2
            iFmax2 = find(max(CCC2(1:length(T2))) == CCC2(1:length(T2)))+1+500-1;
            iFmin2 = find(min(CCC2(1:length(T2))) == CCC2(1:length(T2)))+1-1;
            p = plot(T(length(T))+Te+T2, CCC2(1:length(CCC2)-999), 'r');
        else
            iFmax2 = find(max(-1*CCC2(1+500:length(T2))) == -
1*CCC2(1+500:length(T2)))+1+500-1;
            iFmin2 = find(min(-1*CCC2(1:length(T2))) == -1*CCC2(1:length(T2)))+1-1;
            p = plot(T(length(T))+Te+T2, CCC2(1:length(CCC2)-999)*-1 +F0(length(T))*2,
'r') ;
                % invert data plot
        end

        x2 = get(p, 'XData');
        y2 = get(p, 'YData');

        % Min and Max labels
        text(x2(iFmin2), y2(iFmin2), ['Min = ',num2str(x2(iFmin2)), ' ; ',
num2str(y2(iFmin2))], 'VerticalAlignment','top', 'HorizontalAlignment','left',
'FontSize',10)
        text(x2(iFmax2), y2(iFmax2), ['Max = ',num2str(x2(iFmax2)), ' ; ',
num2str(y2(iFmax2))], 'VerticalAlignment','bottom', 'HorizontalAlignment','left',
'FontSize',10)
        hold on
        plot(x2(iFmin2), y2(iFmin2),'r+', x2(iFmax2), y2(iFmax2),'r+');
        %hold off

        % Output maximum force Fmax and time to maximum force Tmax and copy
        % into excel

        xlswrite('cellwrite.xls', y2(iFmax), 'test', ['H' num2str(k)]);

        % Alter 'filename' to save looped datasets:
        % Saves plot from each data set as .emf to working directory, 'gcf' refers
        % to current figure

        saveas(gcf, strcat(baseFileName,'.emf'));

    catch ME
        display(strcat(baseFileName,' FAILED'));
        display(ME.message);% ME is a structure with info on the error
    end
end
diary off
```

```
date_now  = clock;
date_now = strcat(num2str(date_now(1)), '_', num2str(date_now(2)), '_',
num2str(date_now(3)), num2str(date_now(4)), num2str(date_now(5)));
diary(strcat('log', date_now, '.log'));
diary on

clear all
close all
clc

myFolder = 'G:\transfer to mikis laptop\hht';
filePattern = fullfile(myFolder, '*mat');
matFiles = dir(filePattern);

for k = 1: length(matFiles)
    try
        baseFileName = matFiles(k).name;
        fullFileName = fullfile(myFolder, baseFileName);
        fprintf(1, 'Now reading %s\n', fullFileName);

        % Script to run hhspectrum.m, toimage.m and disp_hhs.m

        %Run hhspectrum.m
        load(baseFileName)
        data_block1_ds = downsample(data_block1, 20);
        clear data_block1
        x = data_block1_ds(1:124:length(data_block1_ds));
        clear data_block1_ds
        imf = emd(x);

        [A,f,tt] = hhspectrum(imf(1:end-1,:));

        clear x

        %Run toimage.m
        t = 1:length(f);
        % splx = length(t);
        % sply = length(t);

        % [im,tt] = toimage(A,f,t);
        [im,tt,ff] = toimage(A,f,t);

        %Run disp_hhs
        ticktimes_block1_ds = downsample(ticktimes_block1, 20);
        clear ticktimes_block1
        disp_hhs(im,ticktimes_block1_ds)
        % disp_hhs(im,t)
        colorbar
        saveas(gcf, strcat(baseFileName, '.emf'));
    catch ME
        display(strcat(baseFileName, 'FAILED'));
        display(ME.message); %ME is a sructure with info on the error
    end
end

diary off
```

```
date_now  = clock;
date_now = strcat(num2str(date_now(1)), '_', num2str(date_now(2)), '_',
num2str(date_now(3)), num2str(date_now(4)), num2str(date_now(5)));
diary(strcat('log', date_now, '.log'));
diary on

clear all
close all
clc

myFolder = 'F:\transfer to mikis laptop\hht';
filePattern = fullfile(myFolder, '*mat');
matFiles = dir(filePattern);

for k = 1: length(matFiles)
    try
        baseFileName = matFiles(k).name;
        fullFileName = fullfile(myFolder, baseFileName);
        fprintf(1, 'Now reading %s\n', fullFileName);

        % Script to run hhspectrum.m, mhs.m

        %Run hhspectrum.m
        load(baseFileName)
        data_block1_ds = downsample(data_block1, 20);
        clear data_block1
        x = data_block1_ds(1:124:length(data_block1_ds));
        clear data_block1_ds
        imf = emd(x);

        [A,f,tt] = hhspectrum(imf(1:end-1,:));

        clear x

        %Run mhs.m
        HS = A';
        freq = f;
        flag = 0;
        fres = 0.05;
        fs = 20;%(20000/20)/124;

        [a F] = mhs(HS,freq,flag,fres,fs);
        plot(F, a)

        saveas(gcf, strcat(baseFileName, '.emf'));

    catch ME
        display(strcat(baseFileName, 'FAILED'));
        display(ME.message); %ME is a sructure with info on the error
    end
end

diary off
```

```
%HHSPECTRUM  compute Hilbert-Huang spectrum
%
% [A,f,tt] = HHSPECTRUM(x,t,l,aff) computes the Hilbert-Huang spectrum
%
% inputs:
%   - x   : matrix with one signal per row
%   - t   : time instants
%   - l   : estimation parameter for instfreq (integer >=1 (1:default))
%   - aff : if 1, displays the computation evolution
%
% outputs:
%   - A   : instantaneous amplitudes
%   - f   : instantaneous frequencies
%   - tt  : truncated time instants
%
% calls:
%   - hilbert  : computes the analytic signal
%   - instfreq : computes the instantaneous frequency
%   - disprog : displays the computation evolution
%
%Examples:
%
%s = randn(1,512);
%imf = emd(s);
%[A,f,tt] = hhspectrum(imf(1:end-1,:));
%
%s = randn(10,512);
%[A,f,tt] = hhspectrum(s,1:512,2,1);
%
% rem: need the Time-Frequency Toolbox (http://tftb.nongnu.org)
%
% See also
%  emd, toimage, disp_hhs
%
% REFERENCE: G. Rilling, last modification 3.2007
% gabriel.rilling@ens-lyon.fr

function [A,f,tt] = hhspectrum(x,t,l,aff)

error(nargchk(1,4,nargin));

if nargin < 2

  t=1:size(x,2);

end

if nargin < 3

  l=1;

end

if nargin < 4

  aff = 0;

end

if min(size(x)) == 1
    if size(x,2) == 1
        x = x';
        if nargin < 2
            t = 1:size(x,2);
        end
    end
    Nmodes = 1;
else
    Nmodes = size(x,1);
end

lt=length(t);

tt=t((l+1):(lt-l));

for i=1:Nmodes

  an(i,:)=hilbert(x(i,:)')';
  f(i,:)=instfreq(an(i,:)',tt,l)';
  A=abs(an(:,l+1:end-l));

  if aff
    disprog(i,Nmodes,max(Nmodes,100))
  end

end
```

```
%TOIMAGE  transforms a spectrum made of 1D functions in an 2D image
%
% [im,tt,ff] = TOIMAGE(A,f,t,splx,sply) transforms a spectrum made
% of 1D functions (e.g., output of "hhspectrum") in an 2D image
%
% inputs :   - A    : amplitudes of modes (1 mode per row of A)
%            - f    : instantaneous frequencies
%            - t    : time instants
%            - splx : number of columns of the output im (time resolution).
%                     If different from length(t), works only for uniform
%                     sampling.
%            - sply : number of rows of the output im (frequency resolution).
% outputs :  - im   : 2D image of the spectrum
%            - tt   : time instants in the image
%            - ff   : centers of the frequency bins
%
% Examples : [im,tt,ff] = toimage(A,f);[im,tt] = toimage(A,f,t);[im,tt,ff] =
toimage(A,f,sply);
%            [im,tt,ff] = toimage(A,f,splx,sply);[im,tt,ff] = toimage(A,f,t,splx,sply);
%
%
% See also
%  emd, hhspectrum, disp_hhs
%
% REFERENCE: G. Rilling, last modification 3.2007
% gabriel.rilling@ens-lyon.fr

function [im,tt,ff] = toimage(A,f,varargin)


DEFSPL = 400;

error(nargchk(2,5,nargin));

switch nargin
  case 2
    t = 1:size(A,2);
    sply = DEFSPL;
    splx = length(t);
  case 3
    if isscalar(varargin{1})
      t = 1:size(A,2);
      splx = length(t);
      sply = varargin{1};
    else
      t = varargin{1};
      splx = length(t);
      sply = DEFSPL;
    end
  case 4
    if isscalar(varargin{1})
      t = 1:size(A,2);
      sply = varargin{1};
      splx = varargin{2};
    else
      t = varargin{1};
      sply = varargin{2};
      splx = length(t);
    end
  case 5
    t = varargin{1};
    splx = varargin{2};
    sply = varargin{3};
end
if isvector(A)
  A = A(:)';
  f = f(:)';
end


if issparse(A) || ~isreal(A) || length(size(A)) > 2
  error('A argument must be a real matrix')
end
if issparse(f) || ~isreal(f) || length(size(f)) > 2
  error('f argument must be a real matrix')
end
if any(size(f)~=size(A))
  error('A and f matrices must have the same size')
end
if issparse(t) || ~isreal(t) || ~isvector(t) || length(t)~=size(A,2)
  error('t argument must be a vector and its length must be the number of columns in A
and f inputs')
end
if ~isscalar(splx) || ~isreal(splx) || splx ~= floor(splx) || splx <= 0
  error('splx argument must be a positive integer')
end
if ~isscalar(sply) || ~isreal(sply) || sply ~= floor(sply) || sply <= 0
  error('splx argument must be a positive integer')
end

if any(diff(diff(t))) && splx ~= length(t)
  warning('toimage:nonuniformtimeinsants','When splx differs from length(t), the function
only works for equally spaced time instants. You may consider reformating your data
(using e.g. interpolation) before using toimage.')
end

f = min(f,0.5);
f = max(f,0);

indf = round(2*f*(sply-1)+1);
indt = repmat(round(linspace(1,length(t),splx)),size(A,1),1);
im = accumarray([indf(:),indt(:)],A(:),[sply,splx]);

indt = indt(1,:);
tt = t(indt);
ff = (0:sply-1)*0.5/sply+1/(4*sply);

end
```

```
%DISP_HHS  display Hilbert-Huang spectrum
%
% DISP_HHS(im,t,inf)
% displays in a new figure the spectrum contained in matrix "im"
% (amplitudes in dB).
%
% inputs:  - im: image matrix (e.g., output of "toimage")
%          - t (optional): time instants (e.g., output of "toimage")
%          - inf (optional): -dynamic range in dB (wrt max)
%            default: inf = -20
%          - fs: sampling frequency
%
% use:  disp_hhs(im) ; disp_hhs(im,t) ; disp_hhs(im,inf)
%       disp_hhs(im,t,inf) ; disp_hhs(im,inf,fs) ; disp_hhs(im,[],fs)
%       disp_hhs(im,t,[],fs) ; disp_hhs(im,t,inf,fs)
%
%
% See also
%  emd, hhspectrum, toimage
%
% REFERENCE: G. Rilling, last modification 3.2007
% gabriel.rilling@ens-lyon.fr

function disp_hhs(varargin)

error(nargchk(1,3,nargin));
fs = 20;
inf = -20;
im = varargin{1};
t = 1:size(im,2);
switch nargin
  case 1
    %raf
  case 2
    if isscalar(varargin{2})
      inf = varargin{2};
    else
      t = varargin{2};
    end
  case 3
    if isvector(varargin{2})
      t = varargin{2};
      inf = varargin{3};
    else
      inf = varargin{2};
      fs = varargin{3};
    end
  case 4
    t = varargin{2};
    inf = varargin{3};
    fs = varargin{4};
end

if isempty(inf)
  inf = -20;
end

if inf > 0
  inf = -inf;
elseif inf == 0
  error('inf must be nonzero')
end

M=max(max(im));

warning off
im = 10*log10(im/M);
warning on

figure

if fs == 0
  imagesc(t, [0,0.5],im, [inf,0]);
  %colormap(colorcube)
  ylabel('normalized frequency')
else
  imagesc(t, [0,0.5*fs],im, [inf,0]);
  %colormap(colorcube)
  ylabel('frequency')
end
set(gca,'YDir','normal')
xlabel('time')
title('Hilbert-Huang spectrum')
```

```
% find the maginal Hilbert Spectrum
function [a F] = mhs(HS,freq,flag,fres,fs)
%-------------------------------JDSA-----------------------------------------
% 'a' is the sum of the contribution of each frequency component in the freq
% vector for all time points.
%
% F is the vector with the frequency axis, use it as x axis to plot the mhs
%
% HS is the Hilbert spectrum amplitudes, one imf per coulmn
%
% freq is the instantaneous frequency, one instantaneous frequency per
% column
%
% flag (1 or 0) flag=1 is used to quantize the values of the instantaneous
% frequency, then values inside a unit of the resolution ar counted as as
% the same frequency. for instance if you have 2 frequencies 10,34 and
% 10,45 and the resolution is .25, those 2 frequencies are counted each one
% as 10.5 and the mhs sum the amplitude related to each frequency as if
% they belong to the same frequency value, this produces smoothed graphs
% fs is the sample rate of the original signal.
% flag = 0 dont quantize the vectors of instantaneous frequency

%NOTE:TAKE ON COUNT THAT THE FREQUENCY AXIS IS NOT EQUALLY EESPACED, FROM
%THE INSTANTANEOUS FREQUENCY SOME VALUES OF F ARE NEVER REACHED, THE IF CAN
%CHANGE FOR INSTANCE FROM 12.5 TO 14.5 AND 13 AND 13.5 DO NOT APPEAR AS
%HAVING 0 (ZERO) CONTRIBUTION

% REFERENCE: Jaime Delgado Saa

HS = reshape(HS,1,[])';
freq = reshape(freq,1,[])';

if flag==1
    if (fres > 1 || fres <= 0)
        disp('The value of resolution should be > 0 and <= 1Hz')
        return
    end
    fraction = log(1/fres)/log(2);
    wordlength = nearest(log((fs/2-fraction)*2^(fraction))+1)/log(2));
    q = quantizer('ufixed', 'nearest', 'saturate', [wordlength fraction]);
    freq = quantize(q,freq);

end


i=1;
while isempty(freq)==0
    indx = find(freq==freq(1));
    ftemp(i)= freq(1);
    Atemp(i)=sum(HS(indx));
    freq(indx)=0;
    HS(indx)=0;
    freq = freq(freq~=0);
    HS=HS(HS~=0);
    i = i + 1;
end

[F indx] = sort(ftemp);
a = Atemp(indx);
end
```

E Raw Data

This Appendix presents the raw data obtained from the experimental procedures. Additional data may be obtained in soft copy from the disc accompanying this submission.

Muscle	Conc	Denervation	Fmax	Mass	Length	CSA	F(csa)	Time to F(csa)
	[ug/ml] [g/ml]	[days]	[g]	[g]	[mm]	[mm^2]	[g]	[s]
ds	96	50	2.64	0.072	15	4.53	0.58	1025.09
is	96	50	7.01	0.301	19	14.95	0.47	1140.54
ds	4	53	1.04	0.175	19	8.69	0.12	217.66
ig	4	53	2.12	2.105	20	99.29	0.02	850.04
is	4	53	0.23	0.309	20	14.58	0.02	921.60
dg	25	50	1.99	0.742	25	28.00	0.07	1267.40
ds	25	50	61.72	0.190	20	8.96	6.89	1106.40
ig	2.5	50	3.67	0.789	25	29.77	0.12	912.98
ig	25	50	3.67	0.789	25	29.77	0.12	912.98
is	25	50	6.14	0.362	18	18.97	0.32	1284.55
dg	4	54	4.79	1.006	20	47.45	0.10	1005.53
ds	4	54	3.10	0.129	16	7.61	0.41	1379.00
ig	4	54	13.50	2.183	22	93.61	0.14	1099.69
is	4	54	7.86	0.386	19	19.17	0.41	1314.90
dg	550	55	1.63	0.657	19	32.62	0.05	933.80
ds	550	55	1.23	0.144	25	5.43	0.23	1321.60
ig	550	55	1.84	2.377	22	101.93	0.02	246.65
is	550	55	3.67	0.503	17	27.91	0.13	1330.50
dg	96	51	16.44	0.988	24	38.84	0.42	1313.30
ds	96	51	6.54	0.152	20	7.17	0.91	489.45
ig	96	51	9.90	2.562	25	96.68	0.10	600.58
is	96	51	2.81	0.300	17	16.65	0.17	821.99

Muscle	Conc	Denervation	Fmax	Mass	Length	CSA	F(csa)	Time to F(csa)
is	na	29	0.32	0.252	12	19.81	0.02	47.85
dg	150	50	2.69	0.620	26	22.50	0.12	1388.02
ds	150	50	1.74	0.076	19	3.77	0.46	908.47
is	150	50	3.66	0.245	19	12.16	0.30	839.22
dg	550	104	1.03	0.815	27	28.48	0.04	186.80
ds	550	104	1.77	0.085	10	8.02	0.22	354.05
ig	550	104	8.07	2.492	25	94.04	0.09	1301.76
is	550	104	8.91	0.424	13	30.77	0.29	1307.90
dg	550	104	3.25	0.817	25	30.83	0.11	574.39
ds	550	104	2.01	0.090	9	9.43	0.21	354.01
ig	550	104	7.64	2.522	26	91.51	0.08	1299.70
is	550	104	8.35	0.418	11	35.85	0.23	1306.40
dg	96	105	1.85	0.627	23	25.72	0.07	1314.40
ds	96	105	4.34	0.133	15	8.36	0.52	684.82
ig	96	105	6.89	2.924	22	125.39	0.05	625.82
is	96	105	6.45	0.340	13	24.67	0.26	1321.00
dg	96	105	1.84	0.633	22	27.14	0.07	1313.10
ds	96	105	4.20	0.140	15	8.81	0.48	686.31
ig	96	105	8.17	3.010	21	135.22	0.06	623.71
is	96	105	5.46	0.340	13	24.67	0.22	1303.24
dg	4	104	3.20	0.812	29	26.42	0.12	826.72
ds	4	104	2.08	0.085	13	6.17	0.34	576.26
ig	4	104	3.78	2.194	25	82.79	0.05	1278.00
is	4	104	4.22	0.377	18	19.76	0.21	1271.38
dg	4	104	3.09	0.874	27	30.54	0.10	824.64
ds	4	104	2.22	0.070	12	5.50	0.40	570.25

Muscle	Conc	Denervation	Fmax	Mass	Length	CSA	F(csa)	Time to F(csa)
ig	4	104	4.54	2.054	24	80.74	0.06	1281.12
is	4	104	4.49	0.387	16	22.82	0.20	1269.46
dg	550	105	11.67	0.876	25	33.06	0.35	917.93
ds	550	105	4.44	0.166	14	11.19	0.40	1257.48
ig	550	105	2.32	1.242	27	43.40	0.05	447.84
is	550	105	6.42	0.336	12	26.42	0.24	1212.67
dg	96	108	4.81	1.126	22	48.28	0.10	1014.16
ds	96	108	8.04	0.118	19	5.86	1.37	1296.04
ig	96	108	5.93	2.666	22	114.32	0.05	460.62
is	96	108	4.19	0.416	15	26.16	0.16	1261.99
dg	4	107	17.52	0.692	26	25.11	0.70	1229.00
ds	4	107	5.06	0.035	14	2.36	2.15	1212.08
is	4	107	1.52	0.216	20	10.19	0.15	1211.03
dg	3.2	7	12.28	1.470	17	81.58	0.15	1293.74
ds	3.2	7	12.26	0.238	15	14.97	0.82	1288.97
ig	3.2	7	6.95	2.031	18	106.45	0.07	1216.87
is	3.2	7	4.67	0.220	10	20.75	0.23	908.21
dg	3.2	7	21.70	1.899	15	119.43	0.18	1199.69
ds	3.2	7	5.28	0.170	19	8.44	0.63	191.11
ig	3.2	7	21.40	1.735	22	74.40	0.29	967.15
is	3.2	7	34.30	0.227	18	11.90	2.88	880.26
dg	3.2	7	22.88	1.954	15	122.89	0.19	1212.66
ds	3.2	7	4.74	0.164	18	8.60	0.55	190.72
ig	3.2	7	21.01	1.712	20	80.75	0.26	976.17
is	3.2	7	34.33	0.225	18	11.79	2.91	874.19
dg	1.6	7	16.93	1.184	16	69.81	0.24	1262.28

Muscle	Conc	Denervation	Fmax	Mass	Length	CSA	F(csa)	Time to F(csa)
ds	1.6	7	7.57	0.161	17	8.93	0.85	873.79
is	elec	7	1.64	0.220	11	18.87	0.09	NA
ig	1.6	7	6.89	1.588	20	74.91	0.09	1028.32
is	1.6	7	2.88	0.220	11	18.87	0.15	1309.55
dg	3.2	7	2.11	1.917	20	90.42	0.02	1250.14
ds	elec	7	1.89	0.177	14	11.93	0.16	NA
ds	3.2	7	10.52	0.177	14	11.93	0.88	580.90
ig	elec	7	1.86	1.420	23	58.24	0.03	NA
ig	3.2	7	13.08	1.420	23	58.24	0.22	1001.12
is	elec	7	1.42	0.257	19	12.76	0.11	NA
is	3.2	7	6.24	0.257	19	12.76	0.49	1164.58
dg	3.2	7	1.26	1.917	20	90.42	0.01	1250.14
dg	elec	7	3.24	1.521	20	71.75	0.05	NA
dg	6.3	7	13.43	1.521	20	71.75	0.19	1248.11
ds	elec	7	0.30	0.200	19	9.93	0.03	NA
ds	6.3	7	37.80	0.200	19	9.93	3.81	999.19
ig	6.3	7	11.24	1.746	25	65.89	0.17	207.36
ig	elec	7	0.71	1.746	25	65.89	0.01	NA
ig	6.3	7	55.73	1.746	25	65.89	0.85	1288.63
is	elec	7	2.73	0.202	13	14.66	0.19	NA
is	6.3	7	5.69	0.202	13	14.66	0.39	428.06
dg	elec	7	3.89	1.929	20	90.99	0.04	NA
dg	550	7	7.21	1.929	20	90.99	0.08	984.33
ds	elec	7	1.97	0.214	15	13.46	0.15	NA
ds	550	7	8.70	0.214	15	13.46	0.65	1082.05
ig	elec	7	1.23	1.958	25	73.89	0.02	NA

Muscle	Conc	Denervation	Fmax	Mass	Length	CSA	F(csa)	Time to F(csa)
ig	550	7	4.44	1.958	25	73.89	0.06	643.30
is	elec	7	0.50	0.288	22	12.35	0.04	NA
is	550	7	34.28	0.288	22	12.35	2.78	1322.00
ig	high	14	5.31	1.594	25	60.15	0.09	149.45
dg	550	14	3.19	0.714	18	37.42	0.09	1004.92
ds	elec	14	1.31	0.116	20	5.47	0.24	NA
ds	550	14	3.13	0.116	20	5.47	0.57	762.16
ig	high	14	5.48	1.594	25	60.15	0.09	186.83
ig	elec	14	1.30	1.594	25	60.15	0.02	NA
ig	elec	14	0.53	1.594	25	60.15	0.01	NA
ig	550	14	10.63	1.594	25	60.15	0.18	738.25
is	elec	14	1.20	0.155	17	8.60	0.14	NA
is	550	14	10.43	0.155	17	8.60	1.21	1166.62
dg	elec	7	0.63	1.601	21	71.92	0.01	NA
dg	96	7	25.00	1.601	21	71.92	0.35	1185.25
ds	elec	7	1.32	0.157	17	8.71	0.15	NA
ds	96	7	4.58	0.157	17	8.71	0.53	845.06
ig	96	7	6.68	1.509	22	64.71	0.10	922.76
is	elec	7	1.44	0.219	15	13.77	0.10	NA
is	96	7	8.96	0.219	15	13.77	0.65	1273.93
dg	96	7	25.19	1.601	20	75.52	0.33	1180.01
ds	elec	7	1.37	0.157	17	8.71	0.16	NA
ds	96	7	3.80	0.157	17	8.71	0.44	844.86
ig	96	7	6.63	1.509	22	64.71	0.10	919.83
is	elec	7	0.31	0.219	16	12.91	0.02	NA
is	96	7	9.16	0.219	16	12.91	0.71	1316.40

Muscle	Conc	Denervation	Fmax	Mass	Length	CSA	F(csa)	Time to F(csa)
dg	0.56	14	3.91	1.322	25	49.89	0.08	931.88
ds	elec	14	1.49	0.134	19	6.65	0.22	NA
ds	elec	14	1.09	0.134	19	6.65	0.16	NA
ds	high	14	3.60	0.134	19	6.65	0.54	185.05
ds	0.56	14	6.17	0.134	19	6.65	0.93	997.41
ig	0.56	14	6.73	1.538	25	58.04	0.12	1178.42
is	elec	14	1.51	0.234	22	10.03	0.15	NA
is	0.56	14	5.36	0.234	22	10.03	0.53	1324.50
dg	elec	7	1.93	1.676	20	79.06	0.02	NA
dg	4	7	4.06	1.676	20	79.06	0.05	1260.40
ds	elec	7	1.26	0.177	20	8.35	0.15	NA
ds	4	7	4.76	0.177	20	8.35	0.57	585.84
ig	4	7	16.74	1.934	23	79.33	0.21	1276.94
is	elec	7	2.73	0.173	15	10.88	0.25	NA
is	4	7	4.55	0.173	15	10.88	0.42	1301.88
dg	elec	14	0.64	1.305	25	49.25	0.01	NA
dg	6.3	14	5.91	1.305	25	49.25	0.12	1187.59
ds	elec	14	1.28	0.114	17	6.33	0.20	NA
ds	6.3	14	10.11	0.114	17	6.33	1.60	1316.90
ig	elec	14	-0.07	2.359	30	74.18	0.00	NA
ig	6.3	14	16.64	2.359	30	74.18	0.22	1268.45
is	elec	14	0.27	0.297	20	14.01	0.02	NA
is	high	14	21.10	0.297	20	14.01	1.51	1244.53
is	6.3	14	4.04	0.297	20	14.01	0.29	742.31
dg	elec	7	0.88	1.670	21	75.02	0.01	NA
dg	1.6	7	16.90	1.670	21	75.02	0.23	1227.99

Muscle	Conc	Denervation	Fmax	Mass	Length	CSA	F(csa)	Time to F(csa)
ds	1.6	7	53.07	0.153	14	10.31	5.15	1317.30
ig	1.6	7	11.98	1.767	25	66.68	0.18	1205.78
is	elec	7	1.28	0.239	20	11.27	0.11	NA
is	1.6	7	16.09	0.239	20	11.27	1.43	763.67
dg	elec	14	1.18	1.498	25	56.53	0.02	NA
dg	1.6	14	18.37	1.498	25	56.53	0.32	1326.60
ds	elec	14	0.37	0.112	20	5.28	0.07	NA
ds	1.6	14	5.67	0.112	20	5.28	1.07	1182.79
ig	elec	14	0.53	1.142	25	43.09	0.01	NA
ig	1.6	14	6.77	1.142	25	43.09	0.16	1193.23
is	elec	14	1.29	0.198	15	12.45	0.10	NA
is	1.6	14	8.61	0.198	15	12.45	0.69	1304.67
is	elec	7	0.12	0.133	18	6.97	0.02	NA
dg	elec	7	0.45	1.550	25	58.49	0.01	NA
dg	6.3	7	2.74	1.550	25	58.49	0.05	1224.51
ds	elec	7	0.32	0.121	16	7.13	0.05	NA
ds	6.3	7	6.91	0.121	16	7.13	0.97	536.56
ig	6.3	7	47.34	1.326	22	56.86	0.83	1303.73
is	high	7	3.61	0.133	18	6.97	0.52	60.80
is	6.3	7	28.45	0.133	18	6.97	4.08	1272.62
dg	elec	14	1.32	1.456	23	59.72	0.02	NA
dg	96	14	15.97	1.456	23	59.72	0.27	1087.32
ds	elec	14	1.14	0.070	13	5.08	0.22	NA
ds	96	14	20.36	0.070	13	5.08	4.01	461.22
ig	elec	14	1.80	1.975	25	74.53	0.02	NA
ig	elec	14	1.69	1.975	25	74.53	0.02	NA

Muscle	Conc	Denervation	Fmax	Mass	Length	CSA	F(csa)	Time to F(csa)
ig	96	14	9.14	1.975	25	74.53	0.12	413.28
ig	high	14	0.12	1.975	25	74.53	0.00	122.55
is	elec	14	2.62	0.224	21	10.06	0.26	NA
is	96	14	14.57	0.224	21	10.06	1.45	916.52
dg	elec	14	1.07	0.937	25	35.36	0.03	NA
dg	4	14	11.74	0.937	25	35.36	0.33	971.53
ds	elec	14	0.40	0.087	20	4.10	0.10	NA
ds	elec	14	2.20	0.087	20	4.10	0.54	NA
ds	high	14	6.23	0.087	20	4.10	1.52	261.66
ds	4	14	15.91	0.087	20	4.10	3.88	1032.25
ig	4	14	6.64	1.414	20	66.70	0.10	491.68
is	elec	14	1.21	0.141	11	12.09	0.10	NA
is	4	14	11.37	0.141	11	12.09	0.94	1115.07
ds	elec	14	0.98	0.090	17	4.99	0.20	NA
ds	96	14	12.41	0.090	17	4.99	2.49	1320.10
ig	96	14	25.12	1.777	28	59.87	0.42	1191.97
is	elec	14	0.55	0.238	15	14.97	0.04	NA
is	elec	14	0.28	0.238	15	14.97	0.02	NA
is	high	14	1.60	0.238	15	14.97	0.11	294.28
is	96	14	4.57	0.238	15	14.97	0.31	1258.79
dg	elec	14	1.10	1.368	25	51.62	0.02	NA
dg	elec	14	0.31	1.368	25	51.62	0.01	NA
dg	elec	14	1.30	1.368	25	51.62	0.03	NA
dg	high	14	1.50	1.368	25	51.62	0.03	214.35
dg	550	14	6.75	1.368	25	51.62	0.13	1296.67
ds	elec	14	-0.12	0.087	18	4.56	-0.03	NA

Muscle	Conc	Denervation	Fmax	Mass	Length	CSA	F(csa)	Time to F(csa)
ds	550	14	4.58	0.087	18	4.56	1.00	1271.81
ig	elec	14	0.27	1.483	25	55.96	0.00	NA
ig	550	14	14.48	1.483	25	55.96	0.26	1319.40
is	elec	14	0.08	0.224	20	10.57	0.01	NA
is	550	14	3.66	0.224	20	10.57	0.35	1172.85